MAGNETOHYDRODYNAMIC NATURAL CONVECTION FLOW WITH TEMPERATURE DEPENDENT PHYSICAL PROPERTIES ALONG A VERTICAL WAVY SURFACE

by

NAZMA PARVEEN
Student No.: P10050901P
Registration No. 961877, Session: October-2005

DOCTOR OF PHILOSOPHY
IN
MATHEMATICS

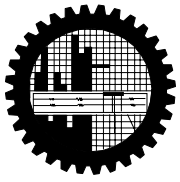

Department of Mathematics
BANGLADESH UNIVERSITY OF ENGINEERING AND TECHNOLOGY, DHAKA-1000, BANGLADESH
October – 2011

The thesis entitled "**Magnetohydrodynamic Natural Convection Flow with Temperature Dependent Physical Properties along a Vertical Wavy Surface**", submitted by **Nazma Parveen**, Roll No.: P10050901P, Registration No. 961877, Session: October-2005 has been accepted as satisfactory in partial fulfillment of the requirement for the degree of **Doctor of Philosophy in Mathematics** on October 08, 2011.

Board of Examiners

1. _____

Dr. Md. Abdul Alim — Chairman
Associate Professor — (Supervisor)
Department of Mathematics
BUET, Dhaka-1000

2. _____

Head — Member
Department of Mathematics — (Ex-Officio)
BUET, Dhaka-1000

3. _____

Dr. Md. Mustafa Kamal Chowdhury — Member
Professor
Department of Mathematics
BUET, Dhaka-1000

4. _____

Dr. Md. Abdul Hakim Khan Member
Professor
Department of Mathematics
BUET, Dhaka-1000

5. _____

Dr. Gazi Md. Khalil Member
Professor
Department of Naval Architecture and Marine Engineering
BUET, Dhaka-1000

6. _____

Dr. S. Reaz Ahmed Member
Professor
Department of Mechanical Engineering
BUET, Dhaka-1000

7. _____

Dr. Amal Krishna Halder Member
Professor (External)
Department of Mathematics
University of Dhaka

DEDICATION

This work is dedicated

to

My Late Father, **Md. Abul Hashem Bhuiyan**

Candidate’s declaration

It is hereby declared that this thesis or any part of it has not been submitted elsewhere (Universities or Institutions) for the award of any degree or diploma.

_____

Nazma Parveen

October - 2011

Acknowledgements

At first all praise belongs to Almighty Allah, the most merciful, benevolent to mankind and his action.

I would like to express my profound gratitude and appreciation to Dr. Md. Abdul Alim, Associate Professor, Department of Mathematics, Bangladesh University of Engineering and Technology, BUET, Dhaka, for his continuous guidance and indefatigable assistance at all stages of my research work. I am also grateful to him for his earnest feeling and helps in matters concerning my research affairs.

I express my deep regards to my entire respectable teachers, Professor Dr. Md. Mustafa Kamal Chowdhury, Department of Mathematics, BUET, Dhaka, Professor Dr. Md. Abdul Hakim Khan, Department of Mathematics, BUET, Dhaka and Professor & Head Dr. Md. Elias, Department of Mathematics, BUET, Dhaka for their generous help and continuous encouragement. I also express my gratitude to all my teachers and colleagues, Department of Mathematics, BUET, Dhaka.

I express my gratitude to all members of the doctoral committee, Professor Dr. Gazi Md. Khalil, Department of Naval Architecture and Marine Engineering, BUET, Dhaka, Professor Dr. S. Reaz Ahmed, Department of Mechanical Engineering, BUET, Dhaka and external member Professor Dr. Amal Krishna Halder, Department of Mathematics, University of Dhaka, Dhaka.

It is not possible to express in words my deepest indebtedness to my husband Engr. Md. Waz Uddin Wazed, Executive Engineer, Dhaka WASA for his continuous cooperation, valuable suggestion and inspiration during the preparation of thesis work.

Finally, express my deepest gratitude to my parents for whom I able to see the beautiful sights and sounds of the world.

Abstract

A steady two-dimensional laminar magnetohydrodynamic (MHD) natural convection flow of viscous incompressible fluid with temperature dependent viscosity and thermal conductivity along a uniformly heated vertical wavy surface has been investigated. The governing boundary layer equations with associated boundary conditions are converted to non-dimensional form using a suitable transformation. The resulting nonlinear system of partial differential equations are mapped into the domain of a vertical flat plate and then solved numerically employing the implicit finite difference method, known as the Keller-box scheme. Depending on different flow conditions the abstract of the work are as follows:

Firstly, the effect of magnetohydrodynamic natural convection boundary layer flow along a vertical wavy surface with a temperature dependent viscosity (linear function and inversely proportional to linear function of temperature) has been analyzed. The results of the numerical solution are shown graphically in the form of skin friction coefficient, the rate of heat transfer, the velocity and temperature profiles, the streamlines and the isotherms over the whole boundary layer for different values of temperature dependent viscosity, magnetic parameter, the amplitude-to-length ratio of the wavy surface and Prandtl number. The skin friction coefficient and the rate of heat transfer are also displayed in tables showing the effects of viscosity, Prandtl number and the intensity of magnetic field.

Secondly, the effect of temperature dependent thermal conductivity on magnetohydrodynamic natural convection flow of viscous incompressible fluid along a uniformly heated vertical wavy surface has been studied numerically. The effects of temperature dependent thermal conductivity, magnetic field, Prandtl number and the amplitude-to-length ratio of the wavy surface on the surface shear stress in terms of the skin friction coefficient C_{fx}, the rate of heat transfer in terms of Nusselt number Nu_x, the velocity and temperature profiles, the streamlines and the isotherms over the whole boundary layer are displayed graphically. Numerical results of the local skin friction coefficient and the rate of heat transfer for different values of thermal conductivity, Prandtl number and magnetic parameter have also been presented in tabular forms.

Thirdly, steady two-dimensional viscous incompressible fluid on magnetohydrodynamic free convection laminar flow with combined effects of temperature dependent viscosity and thermal conductivity of the fluid are taken to be proportional to a linear function of temperature along a uniformly heated vertical wavy surface have been considered. The numerical results of the surface shear stress in terms of skin friction coefficient C_{fx} and the rate of heat transfer in terms of local Nusselt number Nu_x, the stream lines and the isotherms have been presented graphically for a selection of parameters set consisting of temperature dependent viscosity, temperature dependent thermal conductivity, magnetic field, the amplitude-to-length ratio of the wavy surface and Prandtl number.

Finally, the effect of Joule heating on MHD natural convection flow with viscosity and thermal conductivity variation owing to temperature along a uniformly heated vertical wavy surface has been studied. Here, the attention are focused on the surface shear stress in terms of the skin friction coefficient, the rate of heat transfer in terms of Nusselt number, the velocity, the temperature profiles, the streamlines and the isotherms for the effects of Joule heating, temperature dependent viscosity, temperature dependent thermal conductivity, the intensity of magnetic field, the amplitude-to-length ratio of the wavy surface and Prandtl number. In tabular form the numerical results of the local skin friction coefficient C_{fx} and the rate of heat transfer in terms of local Nusselt number Nu_x for different values of Joule heating parameter are also represented.

Comparisons with previously reported investigations are performed and the results show excellent agreement.

CONTENTS

Nomenclature

$\vec{B}$	Magnetic induction vector
C_{fx}	Local skin friction coefficient [-]
C_p	Specific heat at constant pressure [$Jkg^{-1}K^{-1}$]
$\vec{D}$	Electron displacement vector [m]
$\vec{E}$	Electric field vector [-]
$\vec{F}$	Body force per unit volume [$kgms^{-2}$]
f	Dimensionless stream function [$f(x, \eta)$]
g	Acceleration due to gravity [ms^{-2}]
Gr	Grashof number [$g \beta (T_w - T_\infty) L^2 / \nu^2$]
$\vec{J}$	Current density vector [kgm^{-3}]
J	Joule heating parameter [$\sigma_0 \beta_0^2 \nu Gr^{1/2} / \rho C_p (T_w - T_\infty)$]
k	Thermal conductivity of the fluid [$Wm^{-1}K^{-1}$]
k_∞	Thermal conductivity of the ambient fluid [$Wm^{-1}K^{-1}$]
L	Wavelength associated with the wavy surface [m]
M	Magnetic parameter [$\sigma_0 \beta_0^2 L^2 / \mu Gr^{1/2}$]
n	Wave number indicator
$\bar{n}$	Unit vector normal to the wavy surface [$\frac{\bar{i} f_x + \bar{j} f_y}{\sqrt{f_x^2 + f_y^2}}$]
Nu_x	Local Nusselt number [$-(\partial \theta / \partial y)_{y=0}$] [-]
P	Dimensional pressure of the fluid [Nm^{-2}]
P_∞	Pressure of the ambient fluid [Nm^{-2}]
p	Dimensionless pressure of the fluid [-]
Pr	Prandtl number [$\mu C_P / k$]
$\vec{q}$	Velocity vector field [ms^{-1}]
q_w	Heat flux at the surface [$-k(\bar{n}.\nabla T)_{y=0}$] [$Wm^{-2}$]
T	Temperature of the fluid in the boundary layer [^0K or ^0C]

T_w Temperature at the surface [^{0}K or ^{0}C]

T_∞ Temperature of the ambient fluid [^{0}K or ^{0}C]

U, V Velocity component in X, Y direction [ms^{-1}]

u , v Dimensionless velocity components in x, y direction [-]

X, Y Cartesian co-ordinates [m]

x , y Dimensionless Cartesian co-ordinates [-]

Greek symbols

α Amplitude-to-length ratio of the wavy surface

β Volumetric coefficient of thermal expansion [K^{-1}]

β_0 Applied magnetic field strength [-]

γ Thermal conductivity variation parameter [$\gamma = \gamma^* (T_w - T_\infty)$]

γ^* Thermal conductivity gradient due to film temperature [$\frac{1}{k_f}\left(\frac{\partial k}{\partial T}\right)_f$]

∇ Vector differential operator [-]

ε Viscosity variation parameter [$\varepsilon = \varepsilon^* (T_w - T_\infty)$]

ε' Electric permeability of the medium [-]

ε^* Viscosity gradient due to film temperature [$\frac{1}{\mu_f}\left(\frac{\partial \mu}{\partial T}\right)_f$]

η Dimensionless similarity variable [$y\, x^{-1/4}$]

θ Dimensionless temperature function [$\theta(x, \eta)$] [-]

μ Dynamic coefficient of viscosity [kgm^{-1}s^{-1}]

μ_∞ Dynamic viscosity of the ambient fluid [kgm^{-1}s^{-1}]

μ_e Magnetic permeability of the medium [-]

ν Kinematic coefficient of viscosity [m^2 s^{-1}]

ρ Density of the fluid [kgm^{-3}]

ρ_e Charge density [kgm^{-3}]

σ_0 Electrical conductivity of the fluid

τ_w Shearing stress [$(\mu \bar{n}.\nabla U)_{y=0}$]

ψ Stream function $[x^{3/4} f(x, \eta)]$ $[m^2 s^{-1}]$

σ_x Non dimensional surface profile function

$\bar{\sigma}$ Surface profile function

Subscripts

w Wall conditions

∞ Ambient conditions

x Differentiation with respect to x

Superscripts

Prime ($'$) Differentiation with respect to η

List of tables

List of figures

CHAPTER 1

Introduction

The characteristics of natural convection flow of electrically conducting fluid in the presence of magnetic field along a wavy surface is important from the technical point of view and such type of problems have received much attention of many researchers. Natural convection occurs due to the variations in density, which is caused by the non-uniform distribution of temperature or/and concentration of a dissolved substance. The natural convection procedures are governed essentially by three features namely the body force, the temperature difference in the flow field and the fluid density variations with temperature. The manipulation of natural convection heat transfer can be deserted in the case of large Reynolds number and very small Grashof number. Alternately, the natural convection should be the governing aspect for large Grashof number and small Reynolds number. The analysis of natural convection has been considerable interest to engineers and scientists since it is important in many industrial and natural problems. There are many physical processes in which buoyancy forces resulting from thermal diffusion play an important role in the convective transfer of heat. Few examples of the heat transfer by natural convection can be found in geophysics and energy related engineering problems such as natural circulation in geothermal reservoirs, refrigerator coils, hot radiator used for heating a room, transmission lines, porous insulations, solar power collectors, spreading of pollutants etc. A very common industrial application of natural convection is free air cooling without the aid of fans, this can happen on small scales (computer chips) to large scale process equipment.

It is necessary to study the heat transfer from an irregular surface. If the surface is roughened the flow is disturbed by the surface and this alters the rate of heat transfer. Irregular surfaces are often present in many applications. It is often encountered in heat transfer devices to enhance heat transfer. Laminar natural convection flow from irregular surfaces can be used for transferring heat in several heat transfer devices, for examples, flat-plate solar collectors, flat-plate condensers in refrigerators, heat exchanger, functional clothing design, geothermal reservoirs and other industrial applications. They are widely used in space heating, refrigeration, air conditioning,

power plants, chemical plants, petrochemical plants, petroleum refineries and natural gas processing. One common example of a heat exchanger is the radiator used in car/vehicles, in which the heat generated from engine transferred to air flowing through the radiator. Heat exchanger also widely used in industry both for cooling and heating large scale industrial processes. Another industrial application of wavy surface is injection molding system. Injection molding is used to create many things such as wire spools, packaging, bottle caps, automotive dashboards, pocket combs and plastic products available now a days.

In heat transfer sinusoidal wavy surface can be shown approximately in practical geometries. A good example is a cooling fin. Since cooling fins have a larger area than a flat surface, they are better heat transfer devices. Another example is a machine-roughened surface for heat transfer enhancement. The interface between concurrent or countercurrent two-phase flow is another example remotely related to this problem. Such an interface is always wavy and momentum transfer across is by no means similar to that across a smooth, flat surface, and neither is the heat transfer. Also a wavy interface can have an important effect on the condensation process.

The word magnetohydrodynamics (MHD) is derived from magneto- meaning magnetic field, hydro-meaning liquid and dynamics meaning–movement. Magnetohydrodynamics (MHD) is the branch of continuum mechanics, which deals with the flow of electrically conducting fluids in electric and magnetic fields. Probably the advance towards an understanding of such phenomena comes from the field of astrophysics and geophysics. It has long been assumed that most of the matter in the universe is in the plasma or highly ionized state and much of the basic knowledge in the area of electromagnetic fluid dynamics evolved from these studies. It has long been suspected that most of the matter in the universe is in the plasma or highly ionized gaseous state.

The motion of the conducting fluid across the magnetic field induced electric currents which change the magnetic field and the action of the magnetic field on these currents give rise to mechanical forces, which modify the fluid. The interaction of the magnetic field and the moving electric charge carried by the flowing fluid induces a force, which tends to oppose the fluid motion and near the leading edge.

The velocity is very small, so that the magnetic force that is proportional to the magnitude of the longitudinal velocity and acts in the opposite direction is also very small. Consequently, the influence of the magnetic field on the boundary layer is exerted only through induced forces within the boundary layer itself without additional effects arising from the free stream pressure gradient. Thus there is a two-way interaction between the flow field and the magnetic field, the magnetic field exerts force on the fluid by producing induced currents and induced currents change the original magnetic field.

Many natural phenomena and engineering problems are susceptible to MHD analysis. It is useful in astrophysics. Geophysical encounter MHD phenomena in the interactions of conducting fluids and magnetic fields those are present in and around heavenly bodies. Engineers employ MHD principles in the design of heat exchanger, pumps and flow meters, in space vehicle propulsion, control and re-entry, in creating novel power generating systems and developing confinement schemes for controlled fusion. The most important application of MHD are in the generation of electrical power with the flow of an electrically conducting fluid through a transverse magnetic field, electromagnetic pump, the MHD generator using ionized gas as an armature, electromagnetic pumping of liquid metal coolants in nuclear reactors. Other potential applications for MHD include electromagnets with fluid conductors, various energy conversion or storage devices and magnetically controlled lubrication by conducting fluids etc.

As a branch of plasma physics, the field of magnetohydrodynamics consists of the study of a continuous electrically conducting under the influence of electromagnetic fields. A related application is the use of MHD acceleration to shoot plasma into fusion devices or to produce high-energy wind tunnels for simulating hypersonic flight. Originally, MHD included only the study of strictly incompressible fluid, but today the terminology is applied to studies of partially ionized gases as well.

Most of the liquids and gases are poor conductors of electricity. In the case when the conductor is either a liquid or gas, electromagnetic forces will be generated which may be of the same order of magnitude as the hydrodynamical and inertial forces.

Thus the equation of motion as well as the other forces will have to take these electromagnetic forces into account.

Joule heating is the heating effect of conductors carrying currents. Joule heating occurs when an electrical current is passed through a material and material's resistivity to the current cause's heat generation. When current flows in an electrical conductor such as wire, electrical energy is lost due to the resistance of the electrical conductor. This lost electrical energy is converted into thermal energy called Joule heating. One common example of Joule heating is light which electrical energy converts to thermal energy.

Joule heating is caused by interactions between the moving particles that form the current (usually, but not always, electrons) and the atomic ions that make up the body of the conductor. Joule heating is also referred to as Ohmic heating or Resistive heating because of its relationship to Ohm's law.

It was first studied by James Prescott Joule in 1841. It is the process by which the passage of an electric current through a conductor releases heat. Joule's first law is also known as Joule effect. It states that heat generated by a constant current through a resistive conductor for a time whose unit is joule. It is also related to Ohm's first law. The SI unit of energy was subsequently named the Joule and given the symbol *J*. The commonly known unit of power, the watt, is equivalent to one joule per second.

Physical properties like viscosity and thermal conductivity may be changed significantly with temperature. The viscosity of liquids decreases and the viscosity of gases increases with temperature. The viscosity of air is 1.3289 kg $m^{-1}s^{-1}$, 2.671 kg $m^{-1}s^{-1}$ and 3.625 kg $m^{-1}s^{-1}$ at 100^0C, 500 ^{0}C and 800^0C temperature respectively. The viscosity of water is 1006.523 kg $m^{-1}s^{-1}$, 471.049 kg $m^{-1}s^{-1}$, 282.425 kg $m^{-1}s^{-1}$ and 138.681 kg $m^{-1}s^{-1}$ at 20^0C, 60^0C, 100^0C and 200^0C temperature respectively (see Cebeci and Bradshow (1984)). For a liquid, it has been found that the thermal conductivity *k* varies with temperature in an approximately linear manner in the range from 0 to 400^0F (see Kays (1966)). To predict accurately the flow behavior, it is necessary to take into account viscosity and thermal conductivity.

A scalar function whose contour lines define the streamlines is known as the stream function. The stream function ψ is constant along a streamline.

Fluids, which obey Newton's law of viscosity, are called as Newtonian fluids. Common fluids like water, air, and mercury are all Newtonian fluids. Fluids, which do not obey Newton's law of viscosity, are called as non-Newtonian fluids. For such fluids the shear stress is not proportional to the velocity gradient. Fluids like blood, Paints, coal tar, liquid plastics and polymer solution are all non-Newtonian fluids.

Taking the x-axis to be horizontal and the y-axis to be vertically upwards, a motion in which the equation of the vertical section of the free surface is of the form $y = \alpha sinnx$. When $\alpha = 0$, the profile is $y = 0$ which is the mean level. The maximum value of y, namely α, is known as the amplitude-to-length ratio of the wave. The elevation is known as crest. The distance between two consecutive crests is known as the wavelength and is denoted by $L = 2\pi/n$, where n is the wave number.

1.1 Literature review

Natural convection heat transfer has gained considerable attention because of its numerous applications in the areas of energy conservations, cooling of electrical and electronic components, design of solar collectors, heat exchangers and many others. The most important application of MHD is in the generation of electrical power with the flow of an electrically conducting fluid through a transverse magnetic field. In case of natural convection flows, now a days, MHD analysis is playing a vital role. Sparrow and Cess (1961) investigated the effect of magnetic field on free convection heat transfer. Kuiken (1970) investigated MHD free convection in a strong cross field. Gebhart and Pera (1971) investigated the nature of vertical natural convection flows resulting from the combined buoyancy effects of thermal and mass diffusion. They indicated that buoyancy effects from concentration gradients could be as important as those from temperature gradients. There are applications of interest in which combined heat and mass transfer by natural convection, such as design of chemical processing equipment, design of heat exchangers, formation and dispersion of fog, distributions of temperature and moisture over agricultural fields, pollution of the environments and thermoprotection systems. Wilks (1976) presented MHD free convection about a semi-infinite vertical plate in a strong cross field. Ingham (1978)

investigated free convection boundary layer on an isothermal horizontal cylinder. Raptis and Kafoussius (1982) analyzed MHD free convection flow and mass transfer through a porous medium bounded by an infinite vertical porous plate with constant heat flux. Pozzi and Lupo (1988) explored the coupling of conduction with laminar convection along a flat plate. By means of two expansions, the entire thermo-fluid dynamic field was studied. The first one, describing the field in the lower part of the plate, was a regular series. The radius of convergence of which was determined by means of approximant techniques. The second expansion, an asymptotic one required a different analysis because of the presence of eigensolutions. Hossain and Ahmed (1990) considered MHD forced and free convection boundary layer flow near the leading edge. Hossain (1992) analyzed the viscous and Joule heating effects on MHD free convection flow with variable plate temperature and found that temperature varied linearly with the distance from the leading edge in presence of uniformly transverse magnetic field. The equations governing the flow were solved and the numerical solutions were obtained for small Prandtl numbers, appropriate for coolant liquid metal, in the presence of a large magnetic field. Hossain et al. (1997) considered MHD forced and free convection boundary layer flow along a vertical porous plate. Hossain et al. (1998) studied heat transfer response of MHD free convection flow along a vertical plate to surface temperature oscillation. Al-Nimr and Hader (1999) studied MHD free convection flow in open-ended vertical porous channels. Chowdhury and Islam (2000) presented MHD free convection flow of visco-elastic fluid past an infinite porous plate. The conjugate conduction-natural convection heat transfer along a thin vertical plate with non-uniform internal heat generation presented by Mendez and Trevino (2000). El-Amin (2003) analyzed combined effect of viscous dissipation and Joule heating on MHD forced convection over a non isothermal horizontal cylinder embedded in a fluid saturated porous medium. Ahmed and Zaidi (2004) presented magnetic effect on overback convection through vertical stratum. Molla et al. (2006) also investigated MHD natural convection flow on a sphere with uniform heat flux in presence of heat generation. Viscous dissipation effects on MHD natural convection flow over a sphere in the presence of heat generation have been investigated by Alam et al. (2007). Alim et al. (2007) investigated Joule heating effect on the coupling of conduction with MHD

free convection flow from a vertical flat plate. Combined effects of viscous dissipation and Joule heating on the coupling of conduction and free convection along a vertical flat plate have also studied by Alim et al. (2008). Entropy generation during fluid flow in a channel under the effect of transverse magnetic field presented by Damseh et al. (2008). Mamun et al. (2007) studied combined effect of conduction and viscous dissipation on MHD free convection flow along a vertical flat plate. Parveen and Chowdhury (2009) considered stability analysis of the laminar boundary layer flow.

1.1.1 Temperature dependent physical properties

The viscosity and thermal conductivity of the fluid to be proportional to a linear function of temperature two semi-empirical formulae were proposed by Charraudeau (1975). Arunachalam and Rajappa (1978) studied thermal boundary layer in liquid metals with variable thermal conductivity. Gray et al. (1982) studied the effect of significant viscosity variation on convective heat transfer in water–saturated porous media. Transient free convection flow with temperature dependent viscosity in a fluid saturated porous media has shown by Mehta and Sood (1992). As per their investigation the flow characteristics substantially change when the effect of temperature dependent viscosity considered. Mehta and Sood (1993) extended their works by considering effect of temperature dependent viscosity on the free convective flow across an impermeable partition. The effect of temperature dependent viscosity on the free convective laminar boundary layer flow past a vertical isothermal flat plate in the region near the leading edge have been studied by Kafoussius and Williams (1995). Kafoussius and Rees (1995) also studied numerical study of the combined free and forced convective laminar boundary layer flow past a vertical isothermal flat plate with temperature dependent viscosity. Hady, Bakier and Gorla (1996) studied mixed convection boundary layer flow on a continuous flat plate with variable viscosity. Chaim (1998) investigated heat transfer in a fluid with variable thermal conductivity over a linearly stretching sheet. Elbashbeshy (2000) analyzed the free convection flow along a vertical plate, taking into account the variation of the viscosity and thermal diffusivity with temperature in the presence of the magnetic field. Hossain et al. (2000) investigated the natural convection flow past a permeable wedge with uniform surface heat flux for the fluid having temperature

dependent viscosity and thermal conductivity. They considered the various configurations of wedge from Blasius flow to Hiemenz flow. They obtained three distinct methodologies; namely, the perturbation method for small values of the transpiration parameter ξ, the asymptotic solutions for large values ξ and an implicit finite difference method for all values of ξ for solved the equations. They concluded that the dimensionless dynamic viscosity as well as the thermal conductivity of the fluid approach unity at the outer edge of the boundary layer for values of all the pertinent parameters, which was trivial. Hossain and Munir (2000) presented mixed convection flow from a vertical flat plate with temperature dependent viscosity. Unsteady flow of viscous incompressible fluid with temperature dependent viscosity due to a rotating disc in presence of transverse magnetic field and heat transfer studied by Hossain and Wilson (2001). Hossain and Munir (2001) have studied numerically natural convection flow of a viscous fluid about a truncated cone with temperature dependent viscosity and thermal conductivity. They used the perturbation method to obtain the solution in the regimes near and far away from the point of truncation. They also used the implicit finite difference method for solving the governing equations numerically. They compared the perturbation solutions with the finite difference solutions and found to be in excellent agreement. Hossain et al. (2001) investigated the effect of radiation on the free convection flow of fluid with variable viscosity from a porous vertical plate. Munir et al. (2001) studied natural convection of a viscous fluid with viscosity inversely proportional to linear function of temperature from a vertical wavy cone. They considered the boundary-layer regime when the Grashof number was very large and assumed that the wavy surfaces have O(1) amplitude and wavelength. They also considered the buoyancy forces assist the flow for various values of the viscosity variation parameter ε, with the Prandtl number Pr = 0.7 and 7.0 which are appropriate for air and water respectively. They found the difference between the flow and heat transfer characteristics over a flat cone and a wavy one, respectively. For a wavy cone the isotherms showed a sinusoidal behavior, while for a flat cone these are parallel lines. Considering natural convection with variable viscosity and thermal conductivity from a vertical wavy cone Munir et al. (2001) extended their works using the Kellar box method. The problem of natural convection of fluid with temperature dependent viscosity from a

heated vertical wavy surface have been studied by Hossain et al. (2002). Mamun et al. (2005) investigated natural convection flow from an isothermal sphere with temperature dependent thermal conductivity. Molla et al. (2005) considered natural convection flow from an isothermal horizontal circular cylinder with temperature dependent viscosity. They considered the effects of viscosity variation parameter ε and Prandtl number Pr on the velocity and viscosity distribution of the fluid as well as on the local rate of heat transfer in terms of the local Nusselt number Nu and the local skin-friction for fluids having Prandtl number, Pr ranging from 1.0 to 30.0. They concluded that the assumption of the constant fluid properties might introduce severe errors in the prediction of surface friction factor and heat transfer rate. Rahman et al. (2008) investigated the effects of temperature dependent thermal conductivity on MHD free convection flow along a vertical flat plate with heat conduction. The numerical calculation was proceeding in finite-difference method and the velocity, temperature, local skin friction co-efficient and surface temperature profiles were shown by the effect of various parameters. Rahman and Alim (2009) considered numerical study of magnetohydrodynamic free convective heat transfer flow along a vertical plate with temperature dependent thermal conductivity. Nasrin and Alim (2009) investigated MHD free convection flow along a vertical flat plate with thermal conductivity and viscosity depending on temperature. Numerical study on a vertical plate with variable viscosity and thermal conductivity has been investigated by Palani and Kim (2009). They assumed that the viscosity of the fluid is an exponential function and the thermal conductivity is a linear function of the temperature. They considered the unsteady boundary layer equations. They observed that neglecting the viscosity and thermal conductivity variation found substantial errors and concluded that considered the effects of the variation viscosity and thermal conductivity to predict more accurate results.

1.1.2 Flow on wavy surfaces

Natural convection from wavy surfaces can be used for transferring heat in several heat transfer devices, such as flat-plate solar collectors and flat-plate condensers in refrigerators. Surfaces are sometimes intentionally roughened to enhance heat transfer. Yao (1983) first investigated the natural convection heat transfer from an isothermal vertical wavy surface and used an extended Prantdl's transposition

theorem and a finite-difference scheme. He proposed a simple transformation to study the natural convection heat transfer for an isothermal vertical sinusoidal surface. These simple coordinate transformations method to change the wavy surface into a flat plate. The advantage of this transformation is that the form of the boundary layer equations remains invariant and the surface conditions can therefore, be applied on a transformed flat surface. Although the transformation itself is quite simple, it can handle very complex geometries. Yao (1988) also considered Prantdl's transposition theorem. Saidi et al. (1987) presented numerical and experimental results of flow over and heat transfer from a sinusoidal cavity. They reported that the total heat exchange between the wavy wall of the cavity and flowing fluid was reduced by the presence of vortex. Vortex plays the role of a thermal screen, which creates a large region of uniform temperature in the bottom of the cavity. Moulic and Yao (1989) investigated mixed convection along wavy surface and they showed that the force convection component of the heat transfer contains two harmonics. The amplitude of the first harmonic is proportional to the amplitude of the wavy surface and the natural convection component is a second harmonic, with a frequency twice that of the wavy surface. Moulic and Yao (1989) also investigated natural convection along a wavy surface with uniform heat flux. Bhavnani and Bergles (1991) investigated natural convection heat transfer from sinusoidal wavy surfaces. Chiu and Chou (1993) considered free convection in the boundary layer flow of a micropolar fluid along a vertical wavy surface. Chiu and Chou (1994) extended their works by considering transient analysis of natural convection along a vertical wavy surface in micropolar fluids. They found that the frequency of the local heat transfer rate and the skin friction on the wall are twice that of the wavy surface irrespective of whether the fluid is a Newtonian fluid or micropolar fluid. A note on free convection along a vertical wavy surface in a porous medium has investigated by Rees and Pop (1994). Rees and Pop (1994) also investigated free convection induced by a horizontal wavy surface in a porous medium. Rees and Pop (1995) considered the natural convection boundary layer induced by vertical wavy surface in a porous medium. They found that wavy surface exhibiting small amplitude waves embedded in a porous medium. In this research, they assumed that when the Rayleigh number is high, the amplitude of a wave has a close order with a wavelength. Hossain and Pop

(1996) investigated MHD boundary layer flow and heat transfer on a continuous moving wavy surface. Pop et al. (1996) studied laminar boundary layer flow of power-law fluids over wavy surfaces. They found that the skin-friction coefficient decreases with the power-law index increased. Furthermore, the rise and fall of the skin-friction coefficient was shown to follow the change of the surface contour. Yang et al. (1996) presented natural convection of non-Newtonian fluids along a wavy vertical plate including the magnetic field effect. Alam et al. (1997) have also studied the problem of free convection from a wavy vertical surface in presence of a transverse magnetic field using Keller box method. They used a sinusoidal surface to elucidate the effects of magnetic field and the amplitude of the wavy surface on the velocity and temperature fields as well as on the local rate of heat transfer. They found that the effect of the magnetic parameter was to decrease the velocity profiles and to increase the temperature profiles and the amplitude of the sinusoidal surface results in decreasing the heat transfer rate. Kim (1997) studied natural convection along a wavy vertical plate to non-Newtonian fluids. Kumari et al. (1997) analyzed free-convection boundary-layer flow of a non-Newtonian fluid along a vertical wavy surface. Murthy et al. (1997) studied natural convection heat transfer from a horizontal wavy surface in a porous enclosure. Kumar et al. (1998) investigated free convection heat transfer from an isothermal wavy surface in a porous enclosure. They performed a series of studies about the natural convection heat transfer in porous enclosures. They found that the effects of the phase of the wavy surface on the flow and temperature fields are important. Hadjadj and Kyal (1999) numerically investigated the effect of sinusoidal protuberances on heat transfer and fluid flow inside an annular space using a non-orthogonal coordinate transformation. They reported that both local and average heat transfer increase with the increase of protuberances amplitude and Grashof number and decreasing Prandtl number. The combined effects of thermal and mass diffusion on the natural convection flow of a viscous incompressible fluid along a vertical wavy surface has been investigated by Hossain and Rees (1999). The effects of waviness of the surface on the heat and mass flux distributions in combination with the species concentration for a fluid having Prandtl number equal to 0.7 have been studied in that paper. Kumar (2000) presented parametric results of flow and thermal field inside a vertical wavy

enclosure with porous media. He concluded that the surface temperature was very sensitive to the drifts in the surface undulations, phase of the wavy surface and number of the wave. Rahman (2000) analyzed natural convection along vertical wavy surfaces. Chen and Wang (2000) considered transient analysis of force convection along a wavy surface in micropolar fluids. Cheng (2000) investigated natural convection heat and mass transfer near a vertical wavy surface with constant wall temperature and concentration in a porous medium. He found the effects of the buoyancy ratio, the Lewis number and the dimensionless amplitude of wavy surface on the local Sherwood number and the local Nusselt number. He showed the amplitudes of the local Nusselt number and the local Sherwood number increases with the amplitude wavelength ratio of the wavy surface. Cheng (2000) also investigated natural convection heat and mass transfer near a wavy cone with constant wall temperature and concentration in a porous medium. Cheng (2006) extended his works by considering the effect of temperature dependent viscosity on natural convection heat transfer from a horizontal isothermal cylinder of elliptic cross section. Mahmud et al. (2001) presented numerical prediction of fluid flow and heat transfer in a wavy pipe. Mahmud et al. (2002) presented the flow and heat transfer characteristics inside a vertical wavy walled enclosure. They also reported that the decrease of average heat transfer with the increase of surface waviness. Wang and Chen (2001) numerically studied transient force and free convection along a vertical wavy surface in micropolar fluid. Wang and Chen (2002) extended their works by considering forced convection in a wavy wall channel. Jang et al. (2003) has studied numerically on natural convection heat and mass transfer along a vertical wavy surface with Newtonian fluids. However, this study only pertains to steady flow. They showed the effects of amplitude–wavelength ratio, buoyancy ratio and Schmidt number on momentum and heat and mass transfer. Jang and Yan (2004a) presented mixed convection heat and mass transfer along a vertical wavy surface. They examined numerically the mixed convection heat and mass transfer along a vertical wavy surface by using Prandtl’s transposition theorem and investigated the effect of irregular surfaces on the characteristics of mixed convection heat and mass transfer. They have shown that the influence of Richardson number, the buoyancy ratio and the wavy amplitude–wavelength ratio on the local Nusselt number and Sherwood

number including local skin-friction coefficient. They concluded that the properties of the flow field for the wavy surface show a periodical variation and the amplitude of variation decrease gradually downstream. Jang and Yan (2004b) also analyzed the transient natural convection heat and mass transfer in Newtonian fluid flow along a vertical wavy surface numerically by using Prandtl's transposition theorem. They found that the flow field takes more time to reach steady condition for a higher amplitude-wavelength ratio a, small buoyancy ratio and large Schmidt number. Kumar and Shalini (2004) considered Non-Darcy free convection induced by a vertical wavy surface in a thermally stratified porous medium. In this study they found that natural convection heat transfer in a thermally stratified fluid saturated porous medium with the effects of wave phase. Molla et al. (2004) investigated natural convection flow along a vertical wavy surface with uniform surface temperature in presence of heat generation/absorption. They found the effect of varying the heat generation/absorption on the heat transfer rate in terms of local Nusselt number as well as on the streamlines and isotherm patterns for very small Prandtl number Pr ranging from 0.001 to 1.0. They concluded that the velocity and temperature distributions for the case of heat generation higher than that of the heat absorption case. Tashtoush and Al-Odat (2004) presented magnetic field effect on heat and fluid flow over a wavy surface with a variable heat flux. Yao (2006) also studied numerically natural convection flow along a vertical complex wavy surface. He showed that the enhanced total heat transfer rate seems to depend on the ratio of amplitude and wavelength of a surface. Ahmed (2008) investigated MHD free convection flow along a heated vertical wavy surface with heat generation. Parveen and Alim (2010a) investigated natural convection of fluid with variable thermal conductivity along a uniformly heated vertical wavy surface. Parveen and Alim (2010b) considered effect of temperature dependent viscosity inversely proportional to linear function of temperature on magnetohydrodynamic natural convection flow along a vertical wavy surface. Very recently, Parveen and Alim (2011a) analyzed Joule heating effect on Magnetohydrodynamic natural convection flow of fluid with temperature dependent viscosity inversely proportional to linear function of temperature along a vertical wavy surface. Parveen and Alim (2011b) studied effect of temperature dependent thermal conductivity on magnetohydrodynamic natural

convection flow along a vertical wavy surface. Parveen and Alim (2011c) also studied effect of temperature dependent variable viscosity on magnetohydrodynamic natural convection flow along a vertical wavy surface. At the same time Parveen and Alim (2011d) considered Joule heating effect on MHD natural convection flow along a vertical wavy surface with viscosity dependent on temperature.

From the above investigations it is found that variation of viscosity and thermal conductivity with temperature of magnetic field is an interesting macroscopic physical phenomenon in fluid dynamics. Main objective of the present study is detailed investigation of the effect of temperature dependent physical properties like viscosity and thermal conductivity on magnetohydrodynamic natural convection flow along a vertical wavy surface.

1.2 Importance of the present study

Laminar natural convection boundary layer flow and heat transfer problem from a vertical wavy surface get a great deal of attention in various branches of engineering. Free convection boundary layer flow of an electrically conducting fluid in the presence of magnetic field and Joule heating are very important because of their applications in nuclear engineering in connection with the cooling of reactors. The heat transfer rate can be controlled using a magnetic field. One of the ways of studying magnetohydrodynamic heat transfer field is the electromagnetic field, which is used to control the heat transfer as in the convection flows and aerodynamic heating. The prediction of heat transfer from irregular surfaces is a topic of fundamental importance for some heat transfer devices, such as, flat plate solar collectors, flat plate condensers in refrigerators, double-wall thermal insulation, underground cable systems, electric machinery, cooling system of micro-electronic devices, natural circulation in the atmosphere, geophysical applications e.g. flows in the earth’s crust etc. In case of wavy surface, more heat transfer area is available compared to plane surface. That is why heat transfer increases in case of wavy surface. However, it is necessary to take into account the variation of viscosity and thermal conductivity to obtain a better estimation of the flow and heat transfer behavior, because these properties must have a significant change with temperature.

1.3 Objectives of the present study

The objective of this study is to numerically investigate the effects of temperature dependent physical properties like viscosity and thermal conductivity on magnetohydrodynamic natural convection flow of viscous incompressible fluid along a uniformly heated vertical wavy surface. The stream is assumed to flow in the upward vertical direction. Here the surface temperature T_w is higher than the ambient temperature T_∞. Using the appropriate transformations, the basic boundary layer equations are reduced to non-linear partial differential forms. The transformed boundary layer equations are solved numerically using the implicit finite difference method known as the Keller box scheme. Solutions are obtained and analyzed for the surface shear stress in terms of the local skin friction coefficient, the rate of heat transfer in terms of local Nusselt number, the velocity and temperature profiles, the streamlines and isotherms patterns over the whole boundary layer for a set of parameters namely viscosity parameter, thermal conductivity parameter, magnetic parameter, the amplitude-to-length ratio of the wavy surface, Prandtl number and Joule heating parameter. Numerical results of the local skin friction coefficient and the rate of heat transfer for different values are presented in tabular form.

The major objectives of this study are:

- To develop a suitable mathematical model and the corresponding numerical scheme for the solution of magnetohydrodynamic natural convection flow heat transfer problem.
- To assess the effect of heat transfer from a heated vertical wavy surface to the surrounding fluid.
- To investigate the local skin friction and the local rate of heat transfer from the wavy surface in presence of a magnetic field and temperature dependent physical properties like, viscosity and thermal conductivity.
- To study the effects of the strength of magnetic field, Joule heating, the amplitude-to-length ratio of the wavy surface, viscosity, thermal conductivity and Prandtl number on the velocity and temperature.

- To investigate the effects of the viscosity, thermal conductivity, the magnetic field, the amplitude-to-length ratio of the wavy surface, Joule heating and Prandtl number on the streamlines and isotherms.
- To compare the results of the present investigation with similar available works in the literature.

1.4 Outline of the thesis

In chapter 1, a brief introduction is presented with aim and objective. This chapter also consists a literature review of the past studies regarding free convection, MHD and Joule heating on fluid flow, temperature dependent physical properties like viscosity and thermal conductivity and heat transfer in various irregular surfaces.

The basic governing equations for MHD heat transfer flow are shown in standard vector form and mathematical modeling of the problem for various cases are discussed in chapter 2. The numerical procedures for solving nonlinear dimensionless governing equations are also presented in this chapter.

In chapter 3, MHD natural convection boundary layer flow of viscous incompressible fluid along a vertical wavy surface maintained at a uniform surface temperature immersed in a fluid with a temperature dependent viscosity (linear function and inversely proportional to linear function of temperature) has been considered. The skin friction coefficient C_{fx}, the rate of heat transfer in terms of Nusselt number Nu_x, the velocity and temperature profiles as well as the streamlines and the isotherms have been exhibited graphically for temperature dependent viscosity, the intensity of magnetic field, the amplitude-to-length ratio of the wavy surface and for fluids having large Prandtl number Pr ranging from 0.73 to 100. Also in tabular form numerical results of the local skin friction coefficient and the rate of heat transfer for different values of viscosity parameter ε, magnetic parameter M and Prandtl number Pr have been represented whose are depicted in Appendix. The effect of viscosity is vary small when it is inversely proportional to linear function of temperature that has been shown in this chapter.

In chapter 4, the effect of temperature dependent thermal conductivity on MHD natural convection flow of viscous incompressible fluid along a uniformly heated vertical wavy surface has been described. The numerical results of the surface shear

stress in terms of skin friction coefficient C_{fx} and the rate of heat transfer in terms of local Nusselt number Nu_x, the velocity and temperature profiles, the stream lines and the isotherms have been presented graphically for a selection of parameters set consisting of temperature dependent thermal conductivity, magnetic field, Prandtl number Pr ranging from 0.73 to 13.5 and the amplitude-to-length ratio of the wavy surface. Some numerical results of the local skin friction coefficient and the rate of heat transfer for different values of thermal conductivity parameter, Prandtl number Pr and the intensity of magnetic field have also been presented in tabular form as well.

In chapter 5, we studied a steady two-dimensional viscous incompressible fluid on MHD free convection laminar flow with combined effects of temperature dependent viscosity and thermal conductivity of the fluid are taken to be proportional to a linear function of temperature along a uniformly heated vertical wavy surface. The effects of the temperature dependent viscosity, temperature dependent thermal conductivity, the intensity of magnetic field, the amplitude-to-length ratio of the wavy surface and Prandtl number Pr on the surface shear stress in terms of the skin friction coefficient C_{fx}, the rate of heat transfer in terms of Nusselt number Nu_x, the streamlines and the isotherms over the whole boundary layer are shown graphically.

In chapter 6, the effect of magnetic field and Joule heating natural convection flow with viscosity and thermal conductivity variation owing to temperature along a uniformly heated vertical wavy surface has been analyzed. Numerical results of the surface shear stress in terms of the skin friction coefficient C_{fx}, the rate of heat transfer in terms of Nusselt number Nu_x, the velocity and temperature profiles as well as the streamlines and the isotherms for Joule heating, temperature dependent viscosity, temperature dependent thermal conductivity, the intensity of magnetic field, the amplitude-to-length ratio of the wavy surface α and Prandtl number Pr ranging from 0.73 to 9.45 have been presented graphically. Numerical results of the local skin friction coefficient C_{fx} and the rate of heat transfer Nu_x for different values of Joule heating parameter are also presented in tabular form.

In chapter 7, the comparisons of the numerical results of the skin friction coefficient, the rate of heat transfer, the velocity and temperature as well as the streamlines and

the isotherms for the effects of temperature dependent viscosity, temperature dependent thermal conductivity, the intensity of magnetic field, Prandtl number and Joule heating are presented graphically and also in tabular form. The comparisons of the present numerical results of the skin friction coefficient, the rate of heat transfer, the velocity and temperature in tabular form and graphically with those obtaintd by Hossain et al. (2002) and Alam et al. (1997) are also presented.

The above problems have been solved numerically by employing the implicit finite difference method, known as the Keller-box scheme Keller (1978).

A summary of major outcome and some ideas of further work are expressed in chapter 8. Tables related to chapters 3, 4 and 6 are displayed in Appendix.

CHAPTER 2

Mathematical modeling of the problem

2.1 Governing equations

Magnetohydrodynamic equations are the ordinary electromagnetic and hydrodynamic equations modified to take account of the interaction between the motion of the fluid and electromagnetic field. Formulation of electromagnetic theory in mathematical form is known as Maxwell's equations. Maxwell's basic equations show the relation of basic field quantities and their production. But it is assumed that all velocities are small in comparison with the speed of light. Before writing down the MHD equations it is essential to know about the ordinary electromagnetic equations and hydromagnetic equations, which are as follows (see Cramer and Pai (1974)).

Charge Continuity: $$\nabla.\vec{D} = \rho_e \tag{2.1}$$

Current Continuity: $$\nabla.\vec{J} = -\frac{\partial \rho_e}{\partial t} \tag{2.2}$$

Magnetic field continuity: $$\nabla.\vec{B} = 0 \tag{2.3}$$

Ampere's Law: $$\nabla \wedge \beta_0 = \vec{J} + \frac{\partial \vec{D}}{\partial t} \tag{2.4}$$

Faraday's Law: $$\nabla \wedge \vec{E} = -\frac{\partial \vec{B}}{\partial t} \tag{2.5}$$

Constitutive equations for D and B: $\vec{D} = \varepsilon' \vec{E}$ and $\vec{B} = \mu_e \beta_0$ (2.6)

Total current density flow: $$\vec{J} = \sigma_0 \left(\vec{E} + \vec{q} \wedge \vec{B}\right) + \rho_e \vec{q} \tag{2.7}$$

The above equations (2.1) to (2.7) are Maxwell's equations where $\vec{D}$ is the electron displacement, ρ_e is the charge density, $\vec{E}$ is the electric field, $\vec{B}$ is the magnetic field, β_0 is the magnetic field strength, $\vec{J}$ is the current density, $\partial\vec{D}/\partial t$ is the displacement current density, ε' is the electric permeability of the medium, μ_e is the

magnetic permeability of the medium, $\vec{q}$ is the vector field and σ_0 is the electric conductivity.

The electromagnetic equations as shown above are not usually applied in their present form and require interpretation and several assumptions to provide the set to be used in MHD. In MHD a fluid is considered that is grossly neutral. The charge density ρ_e in Maxwell's equations must then be interpreted, as an excess charge density, which is generally not large. If it is disregard the excess charge density then it must disregard the displacement current. In most problems the displacement current, the excess charge density and the current due to convection of the excess charge are small. Taking into this effect the electromagnetic equations can be reduced to the following form:

$$\nabla.\vec{D} = 0 \tag{2.8}$$

$$\nabla.\vec{J} = 0 \tag{2.9}$$

$$\nabla.\vec{B} = 0 \tag{2.10}$$

$$\nabla \wedge \beta_0 = \vec{J} \tag{2.11}$$

$$\nabla \wedge \vec{E} = -\frac{\partial \vec{B}}{\partial t} \tag{2.12}$$

$$\vec{D} = \varepsilon' \vec{E} \text{ and } \vec{B} = \mu_e \beta_0 \tag{2.13}$$

$$\vec{J} = \sigma_0 \left(\vec{E} + \vec{q} \wedge \vec{B} \right) \tag{2.14}$$

Below we shall now suitably represent the equations of fluid dynamics to take account of the electromagnetic phenomena.

The continuity equation

The MHD continuity equation for viscous incompressible electrically conducting fluid remains same as that of usual continuity equation

$$\nabla \cdot \vec{q} = 0 \tag{2.15}$$

The Navier-Stokes equation

The motion of the conducting fluid across the magnetic field generates electric currents, which change the magnetic field and the action of the magnetic field on these current give rises to mechanical forces, which modify the flow of the fluid. Thus, the fundamental equation of the magneto-fluid combines the equations of the motion from fluid mechanics with Maxwell's equations from electrodynamics.

Then the Navier-stokes equation for a viscous incompressible fluid may be written in the following form:

$$\rho(\vec{q}\cdot\nabla)\vec{q} = -\nabla P + \mu\nabla^2\vec{q} + \vec{F} + \vec{J}\times\vec{B} \qquad (2.16)$$

Where ρ is the fluid density, μ is the viscosity and P is the pressure. The first term on the right hand side of equation (2.16) is the pressure gradient, second term is the viscosity, third term is the body force per unit volume and last term is the electromagnetic force due to motion of the fluid.

The energy equation

The energy equation for a viscous incompressible fluid is obtained by adding the electromagnetic energy term into the classical gas dynamic energy equation. This equation can be written as

$$\rho C_P(\vec{q}\cdot\nabla)T = \nabla\cdot(k\nabla T) + (\vec{J}\times\vec{q})U \qquad (2.17)$$

Where, k is the thermal conductivity, C_P is the specific heat with constant pressure. The left side of equation (2.17) represents the net energy transfer due to mass transfer, the first term on the right hand side represents conductive heat transfer and second term is Joule heating term due to the resistance of the fluid to the flow of current.

Where $\vec{q} = (U,V)$, U and V are the velocity components along the X and Y axes respectively, $\vec{F}$ is the body force per unit volume which is defined as $-\rho g$, the terms $\vec{J}$ and $\vec{B}$ are respectively the current density and magnetic induction vector and the term $\vec{J}\times\vec{B}$ is the force on the fluid per unit volume produced by the interaction of the current and magnetic field in the absence of excess charges, T is the temperature of the fluid in the boundary layer , g is the acceleration due to gravity, k is the thermal

conductivity and C_P is the specific heat at constant pressure and μ is the viscosity of the fluid.

Here $\vec{B} = \mu_e \beta_0$, μ_e being the magnetic permeability of the fluid, β_0 is the uniformly distributed transverse magnetic field of strength and ∇ is the vector differential operator and is defined for two dimensional case as

$$\nabla = \hat{l}_x \frac{\partial}{\partial x} + \hat{l}_y \frac{\partial}{\partial y}$$

Where $\hat{l}_x$ and $\hat{l}_y$ are the unit vector along x and y axes respectively. When the external electric field is zero and the induced electric field is negligible, the current density is related to the velocity by Ohm's law as follows

$$\vec{J} = \sigma_0 \left(\vec{q} \times \vec{B} \right) \tag{2.18}$$

Where $\left(\vec{q} \times \vec{B} \right)$ is electrical fluid vector and σ_0 denotes the electric conductivity of the fluid. Under the conduction that the magnetic Reynolds number is small, the induced magnetic field is negligible compared with applied field. This condition is well satisfied in terrestrial applications, especially so in (low velocity) free convection flows. So it can be written as

$$\vec{B} = \hat{l}_y \beta_0 \tag{2.19}$$

Bringing together equations (2.18) and (2.19) the force per unit volume $\vec{J} \times \vec{B}$ acting along the x-axis takes the following form

$$\vec{J} \times \vec{B} = -\sigma_0 \beta_0^2 U \tag{2.20}$$

2.2 Physical model of the problem

Steady two dimensional laminar free convection boundary layer flow of a viscous incompressible and electrically conducting fluid along a vertical wavy surface in presence of uniform transverse magnetic field of strength β_0 with temperature dependent physical properties like viscosity and thermal conductivity is considered. It is assumed that the wavy surface is electrically insulated and is maintained at a uniform temperature T_w. Far above the wavy plate, the fluid is stationary and is kept

at a temperature T_∞. The surface temperature T_w is greater than the ambient temperature T_∞ that is $T_w > T_\infty$. A uniform magnetic field of strength β_0 is imposed along the Y-axis i.e. normal direction to the surface and X -axis is taken along the surface.

The flow configuration of the wavy surface and the two-dimensional cartesian coordinate system are shown in figure 2.1.

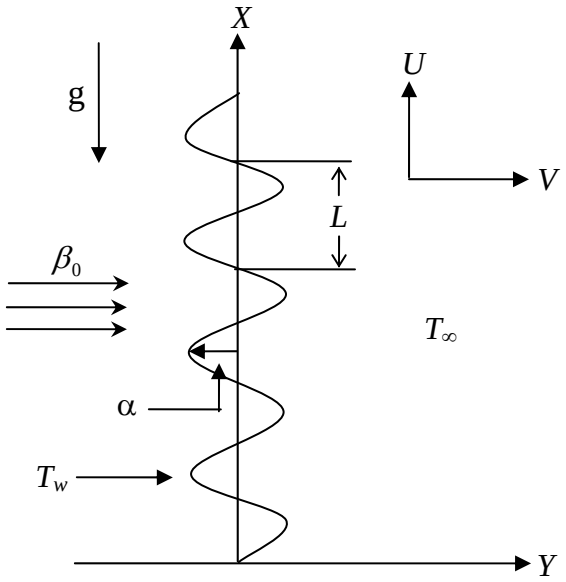

Figure 2.1: Physical model and coordinate system

The boundary layer analysis outlined below allows $\bar{\sigma}(X)$ being arbitrary, but our detailed numerical work assumed that the surface exhibits sinusoidal deformations. The wavy surface may be described by

$$Y_w = \bar{\sigma}(X) = \alpha \sin\left(\frac{n\pi X}{L}\right) \tag{2.21}$$

where α is the amplitude and L is the wave length associated with the wavy surface.

2.3 Formulation of the problem

Case I Viscosity is a linear function of temperature

Consider a steady two-dimensional incompressible magnetohydrodynamic laminar free convection boundary layer flow along a vertical wavy surface. Using the

equations (2.18) to (2.20) into the basic equations (2.15) to (2.17), the steady two-dimensional, laminar free convection boundary layer flow of viscous incompressible, temperature dependent viscosity and conducting fluid through a uniformly distributed transverse magnetic field of strength β_0 take the following form:

Continuity Equation

$$\frac{\partial U}{\partial X}+\frac{\partial V}{\partial Y}=0 \tag{2.22}$$

X-Momentum Equation

$$U\frac{\partial U}{\partial X}+V\frac{\partial U}{\partial Y}=-\frac{1}{\rho}\frac{\partial P}{\partial X}+\frac{1}{\rho}\nabla.(\mu\nabla U)+g\beta(T-T_\infty)-\frac{\sigma_0\beta_0^2}{\rho}U \tag{2.23}$$

Y-Momentum Equation

$$U\frac{\partial V}{\partial X}+V\frac{\partial V}{\partial Y}=-\frac{1}{\rho}\frac{\partial P}{\partial Y}+\frac{1}{\rho}\nabla.(\mu\nabla V) \tag{2.24}$$

Energy Equation

$$U\frac{\partial T}{\partial X}+V\frac{\partial T}{\partial Y}=\frac{k}{\rho C_p}\nabla^2 T \tag{2.25}$$

where (*X*, *Y*) are the dimensional coordinates along and normal to the tangent of the surface and (*U*, *V*) are the velocity components parallel to (*X*, *Y*), $\nabla^2(=\partial^2/\partial x^2+\partial^2/\partial y^2)$ is the Laplacian operator, *T* is the temperature of the fluid in the boundary layer, *g* is the acceleration due to earth gravity , *P* is the dimensional pressure of the fluid, ρ is the density, C_P is the specific heat at constant pressure and $\nu(=\mu/\rho)$ is the kinematic viscosity and $\mu(T)$ is the dynamic viscosity of the fluid in the boundary layer region depending on the fluid temperature, *k* is the thermal conductivity of the fluid, σ_0 is the electrical conductivity of the fluid, β_0 is the strength of magnetic field and β is the volumetric coefficient of thermal expansion.

The boundary conditions for the present problem are

$$U=0, V=0, T=T_w \quad at\ Y=Y_w=\overline{\sigma}(X) \tag{2.26a}$$

$$U=0, \quad T=T_\infty, \quad P=p_\infty \quad as \quad Y\to\infty \tag{2.26b}$$

where T_w is the surface temperature, T_∞ is the ambient temperature of the fluid and P_∞ is the pressure of fluid outside the boundary layer.

There are very few forms of viscosity variation available in the literature. Among them here we consider one which is appropriate for liquid introduced by Hossain et al. (2000) as follows:

$$\mu = \mu_\infty[1+\varepsilon^*(T-T_\infty)] \tag{2.27}$$

where μ_∞ is the viscosity of the ambient fluid and $\varepsilon^* = \frac{1}{\mu_f}\left(\frac{\partial\mu}{\partial T}\right)_f$ is a constant evaluated at the film temperature of the flow $T_f = 1/2\,(T_w + T_\infty)$.

Using Prandtl's transposition theorem to transform the irregular wavy surface into a flat surface as extended by Yao (1983) and boundary layer approximation, the following dimensionless variables are introduced for non-dimensionalizing the governing equations $x = \frac{X}{L}, \quad y = \frac{Y-\overline{\sigma}}{L}Gr^{\frac{1}{4}}, \; p = \frac{L^2}{\rho\nu^2}Gr^{-1}P$

$$u = \frac{\rho L}{\mu_\infty}Gr^{-1/2}U, \quad v = \frac{\rho L}{\mu_\infty}Gr^{-1/4}\left(V-\sigma_x U\right), \quad \theta = \frac{T-T_\infty}{T_w-T_\infty} \tag{2.28}$$

$$\sigma_x = \frac{d\overline{\sigma}}{dX} = \frac{d\sigma}{dx}, \quad Gr = \frac{g\beta(T_w-T_\infty)}{\nu^2}L^3$$

where θ is the dimensionless temperature function and (u, v) are the dimensionless velocity components parallel to (x, y). Here (x, y) are not orthogonal, but a regular rectangular computational grid can be easily fitted in the transformed coordinates. It is also worthwhile to point out that (u, v) are the velocity components parallel to (x, y) which are not parallel to the wavy surface, p is the dimensionless pressure of the fluid, L is the wave length associated with the wavy surface and Gr is the Grashof number.

Introducing the above dimensionless dependent and independent variables into equations (2.22)–(2.25), the following dimensionless form of the governing equations are obtained after ignoring terms of smaller orders of magnitude in Gr, the Grashof number defined in (2.28).

$$\frac{\partial u}{\partial x}+\frac{\partial v}{\partial y}=0 \tag{2.29}$$

$$u\frac{\partial u}{\partial x}+v\frac{\partial u}{\partial y}=-\frac{\partial p}{\partial x}+Gr^{1/4}\sigma_x\frac{\partial p}{\partial y}+\left(1+\sigma_x^2\right)(1+\varepsilon\theta)\frac{\partial^2 u}{\partial y^2}$$
$$+\varepsilon\left(1+\sigma_x^2\right)\frac{\partial\theta}{\partial y}\frac{\partial u}{\partial y}-Mu+\theta \tag{2.30}$$

$$\sigma_x\left(u\frac{\partial u}{\partial x}+v\frac{\partial u}{\partial y}\right)=-Gr^{1/4}\frac{\partial p}{\partial y}+\sigma_x\left(1+\sigma_x^2\right)(1+\varepsilon\theta)\frac{\partial^2 u}{\partial y^2}$$
$$+\varepsilon\sigma_x\left(1+\sigma_x^2\right)\frac{\partial\theta}{\partial y}\frac{\partial u}{\partial y}-\sigma_{xx}u^2 \tag{2.31}$$

$$u\frac{\partial\theta}{\partial x}+v\frac{\partial\theta}{\partial y}=\frac{1}{\mathrm{Pr}}\left(1+\sigma_x^2\right)\frac{\partial^2\theta}{\partial y^2} \tag{2.32}$$

It is worth noting that the σ_x and σ_{xx} indicate the first and second differentiations of σ with respect to x, therefore, $\sigma_x = d\bar{\sigma}/dX = d\sigma/dx$ and $\sigma_{xx} = d\sigma_x/dx$.

In the above equations Pr, ε and M are respectively known as the Prandtl number, the viscosity variation parameter and magnetic parameter, which are defined as

$$\mathrm{Pr}=\frac{C_p\mu_\infty}{k},\quad \varepsilon=\varepsilon^*(T_w-T_\infty),\qquad M=\frac{\sigma_0\beta_0^2L^2}{\mu Gr^{1/2}} \tag{2.33}$$

It can easily be seen that the convection induced by the wavy surface is described by equations (2.29)–(2.32). We further notice that, equation (2.31) indicates that the pressure gradient along the y-direction is $O(Gr^{-1/4})$, which implies that lowest order pressure gradient along x-direction can be determined from the inviscid flow solution. For the present problem this pressure gradient ($\partial p/\partial x = 0$) is zero. Because the pressure along x-direction turns into convective motion of fluid. Equation (2.31) further shows that $Gr^{1/4}\partial p/\partial y$ is $O(1)$ and is determined by the left-hand side of this equation. Thus, the elimination of $\partial p/\partial y$ from equations (2.30) and (2.31) leads to

$$u\frac{\partial u}{\partial x}+v\frac{\partial u}{\partial y}=\left(1+\sigma_x^2\right)(1+\varepsilon\theta)\frac{\partial^2 u}{\partial y^2}-\frac{\sigma_x\sigma_{xx}}{1+\sigma_x^2}u^2+\varepsilon\left(1+\sigma_x^2\right)\frac{\partial u}{\partial y}\frac{\partial\theta}{\partial y}$$
$$-\frac{M}{1+\sigma_x^2}u+\frac{1}{1+\sigma_x^2}\theta \tag{2.34}$$

The corresponding boundary conditions for the present problem then turn into

$$\left.\begin{aligned} &u = v = 0, \quad \theta = 1 \qquad at \quad y = 0 \\ &u = \theta = 0, \quad p = 0 \qquad as \quad y \to \infty \end{aligned}\right\} \tag{2.35}$$

Now we introduce the following transformations to reduce the governing equations to a convenient form:

$$\psi = x^{3/4} f(x,\eta), \quad \eta = yx^{-1/4}, \quad \theta = \theta(x,\eta) \tag{2.36}$$

where $f(\eta)$ is the dimensionless stream function, η is the dimensionless similarity variable and ψ is the stream function that satisfies the continuity equation (2.29) and is related to the velocity components in the usual way as

$$u = \frac{\partial \psi}{\partial y}, \quad v = -\frac{\partial \psi}{\partial x} \tag{2.37}$$

Introducing the transformations given in equation (2.36) and using (2.37) into equations (2.34) and (2.32) are transformed into the new co-ordinate system. Thus the resulting equations are

$$\begin{aligned} &(1+\sigma_x^2)(1+\varepsilon\theta) f''' + \frac{3}{4} ff'' - \left(\frac{1}{2} + \frac{x\sigma_x \sigma_{xx}}{1+\sigma_x^2}\right) f'^2 + \frac{1}{1+\sigma_x^{\,2}}\theta \\ &\qquad - \frac{Mx^{1/2}}{1+\sigma_x^{\,2}} f' + \varepsilon(1+\sigma_x^2)\theta' f'' = x\left(f' \frac{\partial f'}{\partial x} - f'' \frac{\partial f}{\partial x}\right) \end{aligned} \tag{2.38}$$

$$\frac{1}{\Pr}\left(1+\sigma_x^2\right)\theta'' + \frac{3}{4} f\theta' = x\left(f' \frac{\partial \theta}{\partial x} - \theta' \frac{\partial f}{\partial x}\right) \tag{2.39}$$

The boundary conditions (2.35) now take the following form:

$$\left.\begin{aligned} &f(x,o) = f'(x,o) = 0, \qquad \theta(x,o) = 1 \\ &f'(x,\infty) = 0, \qquad \theta(x,\infty) = 0 \end{aligned}\right\} \tag{2.40}$$

In the above equations prime denote the differentiation with respect to η.

However, once we know the values of the functions f and θ and their derivatives, it is important to calculate the values of the rate of heat transfer in terms of local Nusselt number Nu_x and the shearing stress τ_w in terms of the local skin friction coefficient C_{fx} from the following relations:

$$Nu_x = \frac{q_w x}{k(T_w - T_\infty)} \quad \text{and} \quad C_{fx} = \frac{2\tau_w}{\rho U_\infty^2} \tag{2.41}$$

where

$$q_w = -k(\bar{n}.\nabla T)_{y=0}$$

$$= -k \frac{\bar{i}f_x + \bar{j}f_y}{\sqrt{f_x^2 + f_y^2}} . \left(\bar{i} \frac{\partial T}{\partial X} + \bar{j} \frac{\partial T}{\partial Y} \right)_{y=0} \tag{2.42a}$$

$$(\bar{n}.\nabla T) = \frac{\bar{i}f_x + \bar{j}f_y}{\sqrt{f_x^2 + f_y^2}} . \left(\bar{i} \frac{\partial T}{\partial X} + \bar{j} \frac{\partial T}{\partial Y} \right)$$

$$= \frac{\Delta T}{L\sqrt{\sigma_x^2 + 1}} \left[-\sigma_x \frac{\partial \theta}{\partial x} + Gr^{1/4}(\sigma_x^2 + 1) \frac{\partial \theta}{\partial y} \right] \tag{2.421b}$$

$$= \frac{\Delta T}{L} x^{-1/4} Gr^{1/4} \sqrt{\sigma_x^2 + 1} \;\; \theta'(x,0)$$

where $\Delta T = (T_w - T_\infty)$ and $f(X,Y) = Y - \sigma(X)$

and $\tau_w = (\mu \bar{n}.\nabla U)_{y=0}$

$$= \mu_\infty (1+\varepsilon) \frac{\bar{i}f_x + \bar{j}f_y}{\sqrt{f_x^2 + f_y^2}} . \left(\bar{i} \frac{\partial U}{\partial X} + \bar{j} \frac{\partial U}{\partial Y} \right)_{y=0}$$

$$= \frac{\mu_\infty^2}{\rho L^2} Gr^{3/4} x^{1/4} (1+\varepsilon) \sqrt{1+\sigma_x^2} \;\; f''(x,o) \tag{2.42c}$$

Also $U_\infty = \mu_\infty Gr^{1/2} / \rho L$ (2.42d)

Here $\bar{n} = \dfrac{\bar{i}f_x + \bar{j}f_y}{\sqrt{f_x^2 + f_y^2}}$ is the unit normal to the surface. Using the transformation (2.36) and (2.42) into equation (2.41) the rate of heat transfer in terms of the local Nusselt number Nu_x and the local skin friction coefficient C_{fx} take the following forms:

$$Nu_x (Gr/x)^{-1/4} = -\sqrt{1+\sigma_x^2}\,\theta'(x,o) \tag{2.43}$$

$$C_{fx} (Gr/x)^{1/4} / 2 = (1+\varepsilon)\sqrt{1+\sigma_x^2} \;\; f''(x,o) \tag{2.44}$$

Finally it should be mentioned that for the computational purpose the period of oscillations in the waviness of this surface has been considered to be π and the typical values of n have been taken to be 2.

Case II Viscosity is inversely proportional to linear function of temperature

Temperature dependent viscosity inversely proportional to linear function of temperature chosen is this case, which is introduced by Hossain and Munir (2000) as follows:

$$\mu = \frac{\mu_\infty}{1+\varepsilon^*(T-T_\infty)} \tag{2.45}$$

Introducing the transformation given in equation (2.28) and using (2.45) into equations (2.23) and (2.24) the following dimensionless form of the momentum equations are obtained

$$u\frac{\partial u}{\partial x}+v\frac{\partial u}{\partial y} = -\frac{\partial p}{\partial x}+Gr^{1/4}\sigma_x\frac{\partial p}{\partial y}+\frac{(1+\sigma_x^2)}{(1+\varepsilon\theta)}\frac{\partial^2 u}{\partial y^2} -\frac{\varepsilon(1+\sigma_x^2)}{(1+\varepsilon\theta)^2}\frac{\partial\theta}{\partial y}\frac{\partial u}{\partial y}-Mu+\theta \tag{2.46}$$

$$\sigma_x\left(u\frac{\partial u}{\partial x}+v\frac{\partial u}{\partial y}\right) = -Gr^{1/4}\frac{\partial p}{\partial y}+\frac{\sigma_x(1+\sigma_x^2)}{(1+\varepsilon\theta)}\frac{\partial^2 u}{\partial y^2} -\frac{\varepsilon\sigma_x(1+\sigma_x^2)}{(1+\varepsilon\theta)^2}\frac{\partial\theta}{\partial y}\frac{\partial u}{\partial y}-\sigma_{xx}u^2 \tag{2.47}$$

The elimination of variation of pressure in the direction along and normal to the surface from equations (2.46) and (2.47) leads to new momentum equation

$$u\frac{\partial u}{\partial x} + v\frac{\partial u}{\partial y} = \frac{(1+\sigma_x^2)}{(1+\varepsilon\theta)}\frac{\partial^2 u}{\partial y^2}-\frac{\sigma_x\sigma_{xx}}{1+\sigma_x^2}u^2-\frac{\varepsilon(1+\sigma_x^2)}{(1+\varepsilon\theta)^2}\frac{\partial u}{\partial y}\frac{\partial\theta}{\partial y} -\frac{M}{1+\sigma_x^2}u+\frac{1}{1+\sigma_x^2}\theta \tag{2.48}$$

The boundary conditions are same i.e. (2.40).

Substituting the transformations given in equation (2.36) into equation (2.48) the momentum equation takes the following new co-ordinate form

$$\frac{(1+\sigma_x^2)}{(1+\varepsilon\theta)} f''' + \frac{3}{4} ff'' - \left(\frac{1}{2} + \frac{x\sigma_x\sigma_{xx}}{1+\sigma_x^2}\right) f'^2 + \frac{1}{1+\sigma_x^2}\theta - \frac{Mx^{1/2}}{1+\sigma_x^2} f' - \frac{\varepsilon(1+\sigma_x^2)}{(1+\varepsilon\theta)^2}\theta' f'' = x\left(f'\frac{\partial f'}{\partial x} - f''\frac{\partial f}{\partial x}\right) \tag{2.49}$$

Using the transformation (2.36) and equation (2.42) into equation (2.41) the local skin friction coefficient C_{fx} take the following form:

$$C_{fx}(Gr/x)^{1/4}/2 = \frac{\sqrt{1+\sigma_x^2}}{(1+\varepsilon)} f''(x,o) \tag{2.50}$$

Case III Temperature dependent thermal conductivity

The mathematical statement of the basic conservation lows of momentum equation (2.16) and energy equation (2.17) for the steady, two dimensional natural convection flow of an electrically conducting, viscous and incompressible fluid with variable thermal conductivity along a vertical wavy surface after simplifying can be written as:

$$U\frac{\partial U}{\partial X} + V\frac{\partial U}{\partial Y} = -\frac{1}{\rho}\frac{\partial P}{\partial X} + \nu\nabla^2 U + g\beta(T - T_\infty) - \frac{\sigma_0\beta_0^2}{\rho}U \tag{2.51}$$

$$U\frac{\partial V}{\partial X} + V\frac{\partial V}{\partial Y} = -\frac{1}{\rho}\frac{\partial P}{\partial Y} + \nu\nabla^2 V \tag{2.52}$$

$$U\frac{\partial T}{\partial X} + V\frac{\partial T}{\partial Y} = \frac{1}{\rho C_p}\nabla.(k\nabla T) \tag{2.53}$$

where k(T) is the thermal conductivity of the fluid in the boundary layer region depending on the fluid temperature and ν (= μ/ρ) is the kinematics viscosity.

The variable thermal conductivity chosen in this case which was proposed by Charraudeau (1975) and used by Hossain et al. (2000) as follows:

$$k = k_\infty\left[1 + \gamma^*(T - T_\infty)\right] \tag{2.54}$$

where k_∞ is the thermal conductivity of the ambient fluid and $\gamma^* = \frac{1}{k_f}\left(\frac{\partial k}{\partial T}\right)_f$ is a constant evaluated at the film temperature of the flow $T_f = 1/2\,(T_w + T_\infty)$.

Following Yao (1983), we now introduce the following non-dimensional variables

$$x = \frac{X}{L}, \quad y = \frac{Y - \overline{\sigma}}{L} Gr^{\frac{1}{4}}, \quad p = \frac{L^2}{\rho \nu^2} Gr^{-1} P$$

$$u = \frac{L}{\nu} Gr^{-1/2} U, \quad v = \frac{L}{\nu} Gr^{-1/4} (V - \sigma_x U), \tag{2.55}$$

$$\theta = \frac{T - T_\infty}{T_w - T_\infty}, \quad \sigma_x = \frac{d\overline{\sigma}}{dX} = \frac{d\sigma}{dx}, \quad Gr = \frac{g\beta(T_w - T_\infty)}{\nu^2} L^3$$

Introducing the above dimensionless dependent and independent variables into equations (2.51)–(2.53), the following dimensionless form of the governing equations are obtained after ignoring terms of smaller orders of magnitude in *Gr*, the Grashof number defined in (2.55).

$$u\frac{\partial u}{\partial x} + v\frac{\partial u}{\partial y} = -\frac{\partial p}{\partial x} + Gr^{1/4}\sigma_x \frac{\partial p}{\partial y} + \left(1 + \sigma_x^2\right)\frac{\partial^2 u}{\partial y^2} - Mu + \theta \tag{2.56}$$

$$\sigma_x\left(u\frac{\partial u}{\partial x} + v\frac{\partial u}{\partial y}\right) = -Gr^{1/4}\frac{\partial p}{\partial y} + \sigma_x\left(1 + \sigma_x^2\right)\frac{\partial^2 u}{\partial y^2} - \sigma_{xx}u^2 \tag{2.57}$$

$$u\frac{\partial \theta}{\partial x} + v\frac{\partial \theta}{\partial y} = \frac{1}{\Pr}\left(1 + \sigma_x^2\right)(1 + \gamma\theta)\frac{\partial^2 \theta}{\partial y^2} + \frac{1}{\Pr}\left(1 + \sigma_x^2\right)\gamma\left(\frac{\partial \theta}{\partial y}\right)^2 \tag{2.58}$$

In the above equations Pr, γ and *M* are respectively known as the Prandtl number, the thermal conductivity variation parameter and magnetic parameter, which are defined as

$$\Pr = \frac{C_p \mu}{k_\infty}, \quad \gamma = \gamma^*(T_w - T_\infty), \quad M = \frac{\sigma_0 \beta_0^2 L^2}{\mu Gr^{1/2}} \tag{2.59}$$

The elimination of variation of pressure in the direction along and normal to the surface from equations (2.56) and (2.57) leads to new momentum equation

$$u\frac{\partial u}{\partial x} + v\frac{\partial u}{\partial y} = \left(1 + \sigma_x^2\right)\frac{\partial^2 u}{\partial y^2} - \frac{\sigma_x \sigma_{xx}}{1 + \sigma_x^2}u^2 - \frac{M}{1 + \sigma_x^2}u + \frac{1}{1 + \sigma_x^2}\theta \tag{2.60}$$

Substituting the transformations given in equation (2.36) into equations (2.60) and (2.58) the momentum and energy equations transformed into the new co-ordinate system. Thus the resulting equations are obtained

$$\left(1+\sigma_x^2\right)f'''+\frac{3}{4}ff''-\left(\frac{1}{2}+\frac{x\sigma_x\sigma_{xx}}{1+\sigma_x^2}\right)f'^2+\frac{1}{1+\sigma_x^2}\theta-\frac{Mx^{1/2}}{1+\sigma_x^2}f' = x\left(f'\frac{\partial f'}{\partial x}-f''\frac{\partial f}{\partial x}\right) \tag{2.61}$$

$$\frac{1}{\Pr}\left(1+\sigma_x^2\right)(1+\gamma\theta)\theta''+\frac{1}{\Pr}\left(1+\sigma_x^2\right)\gamma\theta'^2+\frac{3}{4}f\theta' = x\left(f'\frac{\partial\theta}{\partial x}-\theta'\frac{\partial f}{\partial x}\right) \tag{2.62}$$

In the above equations prime denote the differentiation with respect to η.

The boundary conditions are same i.e. (2.40).

In practical applications, the physical quantities of principle interest are the shearing stress τ_w and the rate of heat transfer in terms of the skin friction coefficient C_{fx} and Nusselt number Nu_x respectively, which can be written as

$$C_{fx}=\frac{2\tau_w}{\rho U^2} \quad \text{and} \quad Nu_x=\frac{q_w x}{k_\infty(T_w-T_\infty)} \tag{2.63}$$

Using the transformation (2.36) and equation (2.42) into equation (2.63), the rate of heat transfer in terms of the local Nusselt number Nu_x and the local skin friction coefficient C_{fx} takes the following form:

$$Nu_x(Gr/x)^{-1/4}=-(1+\gamma)\sqrt{1+\sigma_x^2}\,\theta'(x,o) \tag{2.64}$$

$$C_{fx}(Gr/x)^{1/4}/2=\sqrt{1+\sigma_x^2}\,f''(x,o) \tag{2.65}$$

Finally, it should be mentioned that for the computational purpose the period of oscillations in the waviness of this surface has been considered to be π and the typical values of n have been taken to be 2.

Case IV Temperature dependent viscosity and thermal conductivity

The mathematical statement of the basic conservation lows of momentum equation (2.16) and energy equation (2.17) for the steady, two dimensional natural convection flow of an electrically conducting, viscous and incompressible fluid with combined

effects of temperature dependent physical properties like viscosity and thermal conductivity along a vertical wavy surface after simplifying and using the transformation given in equation (2.28) into equations (2.23), (2.24) and (2.53) the following dimensionless form of the governing equations are obtained

$$u\frac{\partial u}{\partial x}+v\frac{\partial u}{\partial y}=-\frac{\partial p}{\partial x}+Gr^{1/4}\sigma_x\frac{\partial p}{\partial y}+\left(1+\sigma_x^2\right)(1+\varepsilon\theta)\frac{\partial^2 u}{\partial y^2}$$
$$+\varepsilon\left(1+\sigma_x^2\right)\frac{\partial\theta}{\partial y}\frac{\partial u}{\partial y}-Mu+\theta \tag{2.66}$$

$$\sigma_x\left(u\frac{\partial u}{\partial x}+v\frac{\partial u}{\partial y}\right)=-Gr^{1/4}\frac{\partial p}{\partial y}+\sigma_x\left(1+\sigma_x^2\right)(1+\varepsilon\theta)\frac{\partial^2 u}{\partial y^2}$$
$$+\varepsilon\sigma_x\left(1+\sigma_x^2\right)\frac{\partial\theta}{\partial y}\frac{\partial u}{\partial y}-\sigma_{xx}u^2 \tag{2.67}$$

$$u\frac{\partial\theta}{\partial x}+v\frac{\partial\theta}{\partial y}=\frac{1}{\Pr}\left(1+\sigma_x^2\right)(1+\gamma\theta)\frac{\partial^2\theta}{\partial y^2}+\frac{1}{\Pr}\left(1+\sigma_x^2\right)\gamma\left(\frac{\partial\theta}{\partial y}\right)^2 \tag{2.68}$$

In the above equation $\Pr=\dfrac{C_p\mu_\infty}{k_\infty}$ is the Prandtl number, ε, M and γ are defined earlier in equations (2.33) and (2.59) respectively.

The variable viscosity and thermal conductivity chosen in this case which are given in equations (2.27) and (2.54).

The elimination of variation of pressure in the direction along and normal to the surface from equations (2.66) and (2.67) leads to new momentum equation which is same as the equation (2.34).

The boundary conditions are same i.e. (2.40).

Substituting the transformations given in equation (2.36) into equations (2.34) and (2.68) the momentum and energy equations are transformed into the new co-ordinate system which are same as the equations (2.38) and (2.62).

The rate of heat transfer in terms of the local Nusselt number Nu_x and the local skin friction coefficient C_{fx} are same as the above equations (2.64) and (2.44) respectively.

Case V The effect of Joule heating

The continuity and momentum equations are same which was mentioned in case-I and the energy equation (2.17) with Joule heating for the steady, two dimensional natural convection flow of an electrically conducting, viscous and incompressible fluid with variable viscosity and thermal conductivity along a vertical wavy surface after simplifying can be written as:

$$U\frac{\partial T}{\partial X}+V\frac{\partial T}{\partial Y}=\frac{1}{\rho C_p}\nabla.\left(k\nabla T\right)+\frac{\sigma_0\beta_0^2}{\rho C_p}U^2 \tag{2.69}$$

where (X, Y) are the dimensional coordinates along and normal to the tangent of the surface and (U, V) are the velocity components parallel to (X, Y), ρ is the density, β_0 is the strength of magnetic field, σ_0 is the electrical conduction, C_p is the specific heat due to constant pressure and $k(T)$ is the thermal conductivity of the fluid in the boundary layer region depending on temperature T.

The variable viscosity and thermal conductivity chosen in this case which are given in equations (2.27) and (2.54).

Introducing the transformation given in equation (2.28) into equation (2.69) the following dimensionless form of the energy equation is obtained

$$u\frac{\partial\theta}{\partial x}+v\frac{\partial\theta}{\partial y}=\frac{1}{\Pr}\left(1+\sigma_x^2\right)\left(1+\gamma\theta\right)\frac{\partial^2\theta}{\partial y^2}+\frac{1}{\Pr}\left(1+\sigma_x^2\right)\gamma\left(\frac{\partial\theta}{\partial y}\right)^2+Ju^2 \tag{2.70}$$

In the above equation $J=\dfrac{\sigma_0\ \beta_0^2\ \nu\ Gr^{1/2}}{\rho C_p\left(T_w-T_\infty\right)}$ is the Joule heating parameter, $\Pr=\dfrac{C_p\mu_\infty}{k_\infty}$ is the Prandtl number and γ is defined earlier in equation (2.59).

Introducing the transformations given in equation (2.36) into equation (2.70) the following system of non linear equation governing the flow is obtained:

$$\begin{aligned}&\frac{1}{\Pr}\left(1+\sigma_x^2\right)\left(1+\gamma\theta\right)\theta''+\frac{1}{\Pr}\left(1+\sigma_x^2\right)\gamma\theta'^2+\frac{3}{4}f\theta'+J\,x^{3/2}f'^2\\&=x\left(f'\frac{\partial\theta}{\partial x}-\theta'\frac{\partial f}{\partial x}\right)\end{aligned} \tag{2.71}$$

The boundary conditions are same i.e. (2.40).

In the above equations prime denote the differentiation with respect to η.

2.4 Numerical approach

The transformed boundary layer equations solved numerically with the help of implicit finite difference method together with the Keller-Box scheme (1978) and used by Hossain et al. (1996, 1997, 1999, 2000, 2001). To begin with, the partial differential equations are first converted into a system of first order differential equations. Then these equations are expressed in finite difference forms by approximating the functions and their derivatives in terms of the center differences. Denoting the mesh points in the x and η-plane by x_i and η_j where i = 1, 2 ,……, M and j = 1, 2,……,N, central difference approximations are made, such that those equations involving x explicitly are centered at $(x_{i-1/2}, \eta_{j-1/2})$ and the remainder at $(x_i, \eta_{j-1/2})$, where $\eta_{j-1/2} = 1/2(\eta_j + \eta_{j-1})$ etc. The above central difference approximations reduce the system of first order differential equations to a set of non-linear difference equations for the unknown at x_i in terms of their values at x_{i-1}. The resulting set of non-linear difference equations are solved by using the Newton's quasi-linearization method. The Jacobian matrix has a block-tridiagonal structure and the difference equations are efficiently solved using a block-matrix version of the Thomas algorithm. In the program test, a finer axial step size is tried and find to give acceptable accuracy. A uniform grid of 201 points is used in x- direction with Δx = 0.05, while a non-uniform grid of 76 points lying between η = 0.0 and 10.017 is chosen. Grid points are concentrated towards the heated surface in order to improve resolution and the accuracy of the computed values of the surface shear stress and rate of heat transfer. During the program test, the convergent criteria for the relative errors between two iterations are less 10^{-5}. It means that iterative procedure is stopped when the maximum change between successive iterates is less then 10^{-5}.

2.5 Implicit Finite Difference Method (IFDM)

To apply the aforementioned method, equations (2.38) and (2.39) their boundary condition (2.40) are first converted into the following system of first order equations. For this purpose we introduce new dependent variables $u(\xi,\eta)$, $v(\xi,\eta)$, $p(\xi,\eta)$ and $g(\xi,\eta)$ so that the transformed momentum and energy equations can be written as:

$$f' = u \tag{2.72}$$

$$u' = v \tag{2.73}$$

$$g' = p \tag{2.74}$$

$$P_1 T v' + P_2 f v - P_3 u^2 + P_4 g - P_5 u + P_6 p v = \xi(u\frac{\partial u}{\partial \xi} - v\frac{\partial f}{\partial \xi}) \tag{2.75}$$

$$\frac{1}{\Pr} P_1 p' + P_2 f\ p = \xi\ (u\ \frac{\partial g}{\partial \xi} - p\ \frac{\partial f}{\partial \xi}) \tag{2.76}$$

where $x = \xi,\ \theta = g$ and

$$P_1 = (1+\sigma_x^2),\ P_2 = \frac{3}{4},\ P_3 = \frac{1}{2} + \frac{x\sigma_x\sigma_{xx}}{1+\sigma_x^2},\ P_4 = \frac{1}{1+\sigma_x^2},\ P_5 = \frac{Mx^{1/2}}{1+\sigma_x^2},$$

$$P_6 = \varepsilon(1+\sigma_x^2) \text{ and } T = (1+\varepsilon\theta)$$

and the boundary conditions (2.40) are

$$\begin{aligned} &f(\xi,0) = 0,\ u(\xi,0) = 0, g(\xi,0) = 1 \\ &u(\xi,\infty) = 0,\ g\ (\xi,\infty) = 0 \end{aligned} \tag{2.77}$$

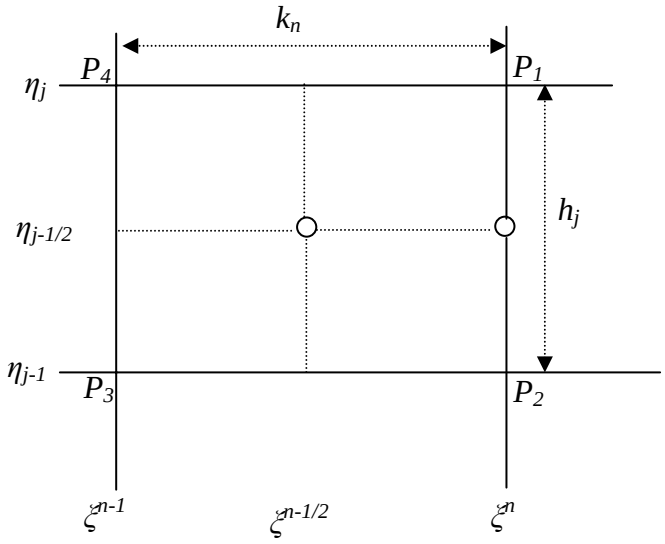

Figure 2.2: Net rectangle of difference approximations for the Box scheme.

Now consider the net rectangle on the (ξ,η) plane shown in the figure 2.2 and denote the net points by

$$\begin{aligned} &\xi^0 = 0,\ \xi^n = \xi^{n-1} + k_n,\ n = 1,2,\cdots\cdots\cdots\cdots, N \\ &\eta_0 = 0,\ \eta_j = \eta_{j-1} + h_j,\quad j = 1,2,\cdots\cdots\cdots\cdots, J \end{aligned} \tag{2.78}$$

Here n and j are just sequence of numbers on the (ξ,η) plane, k_n and h_j are the variable mesh widths. Approximate the quantities f, u, v and p at the points (ξ^n,η_j) of the net by f_j^n, u_j^n, v_j^n, p_j^n which call net function. It is also employed that the notation P_j^n for the quantities midway between net points shown in figure 2.2 and for any net function as

$$\xi^{n-1/2} = \frac{1}{2}(\xi^n + \xi^{n-1}) \tag{2.79}$$

$$\eta_{j-1/2} = \frac{1}{2}(\eta_j + \eta_{j-1}) \tag{2.80}$$

$$g_j^{\,n-1/2} = \frac{1}{2}(g_j^n + g_j^{n-1}) \tag{2.81}$$

$$g_{j-1/2}^n = \frac{1}{2}(g_j^n + g_{j-1}^n) \tag{2.82}$$

The finite difference approximations according to box method to the three first order ordinary differential equations (2.72) – (2.74) are written for the mid point $(\xi^n,\eta_{j-1/2})$ of the segment P_1P_2 shown in the figure 2.2 and the finite difference approximations to the two first order differential equations (2.75) and (2.76) are written for the mid point $(\xi^{n-1/2},\eta_{j-1/2})$ of the rectangle $P_1P_2P_3P_4$. This procedure yields

$$\frac{f_j^n - f_{j-1}^n}{h_j} = u_{j-1/2}^n = \frac{u_{j-1}^n + u_j^n}{2} \tag{2.83}$$

$$\frac{u_j^n - u_{j-1}^n}{h_j} = v_{j-1/2}^n = \frac{v_{j-1}^n + v_j^n}{2} \tag{2.84}$$

$$\frac{g_j^n - g_{j-1}^n}{h_j} = p_{j-1/2}^n = \frac{p_{j-1}^n + p_j^n}{2} \tag{2.85}$$

$$\frac{1}{2}(P_1T)^{n}_{j-1/2}\left(\frac{v^{n}_{j}-v^{n}_{j-1}}{h_j}\right)+\frac{1}{2}(P_1T)^{n}_{j-1/2}\left(\frac{v^{n-1}_{j}-v^{n-1}_{j-1}}{h_j}\right)+(P_2\,fp)^{n-1/2}_{j-1/2}-(P_3u^2)^{n-1}_{j-1/2}$$
$$+(P_4g)^{n-1}_{j-1/2}-(P_5u)^{n-1}_{j-1/2}+(P_6\,pv)^{n-1}_{j-1/2} \qquad (2.86)$$
$$=\xi^{n-1/2}_{j-1/2}\left(u^{n-1/2}_{j-1/2}\frac{u^{n}_{j-1/2}-u^{n-1}_{j-1/2}}{k_n}-v^{n-1/2}_{j-1/2}\frac{f^{n}_{j-1/2}-f^{n-1}_{j-1/2}}{k_n}\right)$$

$$\frac{1}{2\,\mathrm{Pr}}\left\{(P_1)^{n}_{j-1/2}\right\}\left(\frac{p^{n}_{j}-p^{n}_{j-1}}{h_j}\right)+\frac{1}{2\,\mathrm{Pr}}\left\{(P_1)^{n-1}_{j-1/2}\right\}\left(\frac{p^{n-1}_{j}-p^{n-1}_{j-1}}{h_j}\right)+(P_2\,fp)^{n-1/2}_{j-1/2} \qquad (2.87)$$
$$=\xi^{n-1/2}_{j-1/2}\left(u^{n-1/2}_{j-1/2}\frac{g^{n}_{j-1/2}-g^{n-1}_{j-1/2}}{k_n}-p^{n-1/2}_{j-1/2}\frac{f^{n}_{j-1/2}-f^{n-1}_{j-1/2}}{k_n}\right)$$

Now the equation (2.86) can be written as

$$\Rightarrow\frac{1}{2}(P_1T)^{n}_{j-1/2}\left(\frac{v^{n}_{j}-v^{n}_{j-1}}{h_j}\right)+\frac{1}{2}(P_1T)^{n-1}_{j-1/2}\left(\frac{v^{n-1}_{j}-v^{n-1}_{j-1}}{h_j}\right)+\frac{1}{2}\left\{(P_2\,fv)^{n}_{j-1/2}+(P_2\,fv)^{n-1}_{j-1/2}\right\}$$
$$-\frac{1}{2}\left\{(P_3u^2)^{n}_{j-1/2}+(P_3u^2)^{n-1}_{j-1/2}\right\}+\frac{1}{2}\left\{\left(P_4g^{n}_{j-1/2}\right)+\left(P_4g^{n-1}_{j-1/2}\right)\right\}-\frac{1}{2}\left\{\left(P_5u^{n}_{j-1/2}\right)+\left(P_5u^{n-1}_{j-1/2}\right)\right\}$$
$$+\frac{1}{2}\left\{(P_6\,pv)^{n}_{j-1/2}+(P_6\,pv)^{n-1}_{j-1/2}\right\}=\frac{1}{2k_n}\xi^{n-1/2}_{j-1/2}\left(u^{n}_{j-1/2}+u^{n-1}_{j-1/2}\right)\left(u^{n}_{j-1/2}-u^{n-1}_{j-1/2}\right)$$
$$-\frac{1}{2k_n}\xi^{n-1/2}_{j-1/2}\left(v^{n}_{j-1/2}+v^{n-1}_{j-1/2}\right)\left(f^{n}_{j-1/2}-f^{n-1}_{j-1/2}\right)$$
$$\Rightarrow(P_1T)^{n}_{j-1/2}\left(\frac{v^{n}_{j}-v^{n}_{j-1}}{h_j}\right)+(P_1T)^{n-1}_{j-1/2}\left(\frac{v^{n-1}_{j}-v^{n-1}_{j-1}}{h_j}\right)+(P_2)^{n}_{j-1/2}\,(fv)^{n}_{j-1/2}+(P_2)^{n-1}_{j-1/2}\,(fv)^{n-1}_{j-1/2}$$
$$-(P_3)^{n}_{j-1/2}\,(u^2)^{n}_{j-1/2}-(P_3)^{n-1}_{j-1/2}\,(u^2)^{n-1}_{j-1/2}+(P_4)^{n}_{j-1/2}\,g^{n}_{j-1/2}+(P_4)^{n-1}_{j-1/2}\,g^{n-1}_{j-1/2}$$
$$-(P_5)^{n}_{j-1/2}(u)^{n}_{j-1/2}-(P_5)^{n-1}_{j-1/2}(u)^{n-1}_{j-1/2}+(P_6)^{n}_{j-1/2}(pv)^{n}_{j-1/2}+(P_6)^{n-1}_{j-1/2}(pv)^{n-1}_{j-1/2}$$
$$=\alpha_n\left\{(u^2)^{n}_{j-1/2}-(u^2)^{n-1}_{j-1/2}-(fv)^{n}_{j-1/2}+f^{n-1}_{j-1/2}v^{n}_{j-1/2}-f^{n}_{j-1/2}v^{n-1}_{j-1/2}+(fv)^{n-1}_{j-1/2}\right\}$$

$$\Rightarrow(P_1T)^{n}_{j-1/2}\left(\frac{v^{n}_{j}-v^{n}_{j-1}}{h_j}\right)+\left\{(P_2)^{n}_{j-1/2}+\alpha_n\right\}(fv)^{n}_{j-1/2}-\left\{(P_3)^{n}_{j-1/2}+\alpha_n\right\}(u^2)^{n}_{j-1/2}$$
$$+(P_4)^{n}_{j-1/2}\,g^{n}_{j-1/2}-(P_5)^{n}_{j-1/2}(u)^{n}_{j-1/2}+(P_6)^{n}_{j-1/2}(pv)^{n}_{j-1/2}$$
$$=\alpha_n\left[\left\{-(u^2)^{n-1}_{j-1/2}+v^{n}_{j-1/2}\,f^{n-1}_{j-1/2}-f^{n}_{j-1/2}\,v^{n-1}_{j-1/2}+(fv)^{n-1}_{j-1/2}\right\}\right]-(P_2)^{n-1}_{j-1/2}(fv)^{n-1}_{j-1/2}$$
$$+(P_3)^{n-1}_{j-1/2}(u^2)^{n-1}_{j-1/2}-(P_4)^{n-1}_{j-1/2}g^{n-1}_{j-1/2}+(P_5)^{n-1}_{j-1/2}(u)^{n-1}_{j-1/2}-(P_6)^{n-1}_{j-1/2}(pv)^{n-1}_{j-1/2}$$
$$-(P_1T)^{n-1}_{j-1/2}\left(\frac{v^{n-1}_{j}-v^{n-1}_{j-1}}{h_j}\right)$$

$$R^{n-1}_{j-1/2} = \alpha_n \left\{ (fv)^{n-1}_{j-1/2} - (u^2)^{n-1}_{j-1/2} \right\} - L^{n-1}_{j-1/2} \tag{2.88}$$

where $\alpha_n = \frac{1}{k_n} \xi^{n-1/2}_{j-1/2}$ (2.89)

$$\begin{aligned} &\Rightarrow (P_1 T)^n_{j-1/2} h_j^{-1} \left(v^n_j - v^n_{j-1} \right) + \left\{ (P_2)^n_{j-1/2} + \alpha_n \right\} (fv)^n_{j-1/2} \\ &- \left\{ (P_3)^n_{j-1/2} + \alpha_n \right\} (u^2)^n_{j-1/2} + (P_4)^n_{j-1/2} g^n_{j-1/2} - (P_5)^n_{j-1/2} (u)^n_{j-1/2} \\ &+ (P_6)^n_{j-1/2} (pv)^n_{j-1/2} + \alpha_n \left(f^n_{j-1/2} \, v^{n-1}_{j-1/2} - v^n_{j-1/2} \, f^{n-1}_{j-1/2} \right) \\ &= R^{n-1}_{j-1/2} \end{aligned} \tag{2.90}$$

$$\begin{aligned} &\Rightarrow (P_1 T)^{n-1}_{j-1/2} h_j^{-1} \left(v^{n-1}_j - v^{n-1}_{j-1} \right) + (P_2)^{n-1}_{j-1/2} (fv)^{n-1}_{j-1/2} - (P_3)^{n-1}_{j-1/2} (u^2)^n_{j-1/2} \\ &+ (P_4)^{n-1}_{j-1/2} g^n_{j-1/2} - (P_5)^{n-1}_{j-1/2} (u)^n_{j-1/2} + (P_6)^{n-1}_{j-1/2} (pv)^{n-1}_{j-1/2} \\ &= L^{n-1}_{j-1/2} \end{aligned} \tag{2.91}$$

Again from the equation (2.87) then

$$\begin{aligned} &\frac{1}{\mathrm{Pr}} \left[\left\{ (P_1)^n_{j-1/2} \right\} \left(\frac{p^n_j - p^n_{j-1}}{h_j} \right) + \left\{ (P_1)^{n-1}_{j-1/2} \right\} \left(\frac{p^{n-1}_j - p^{n-1}_{j-1}}{h_j} \right) \right] + \left\{ (P_2 \, fp)^n_{j-1/2} + (P_2 \, fp)^{n-1}_{j-1/2} \right\} \\ &= \alpha_n \left[\left(u^n_{j-1/2} + u^{n-1}_{j-1/2} \right) \left(g^n_{j-1/2} - g^{n-1}_{j-1/2} \right) - \left(p^n_{j-1/2} + p^{n-1}_{j-1/2} \right) \left(f^n_{j-1/2} - f^{n-1}_{j-1/2} \right) \right] \end{aligned}$$

$$\begin{aligned} &\Rightarrow \frac{1}{\mathrm{Pr}} \left\{ (P_1)^n_{j-1/2} \right\} \left(\frac{p^n_j - p^n_{j-1}}{h_j} \right) + \frac{1}{\mathrm{Pr}} \left\{ (P_1)^{n-1}_{j-1/2} \right\} \left(\frac{p^{n-1}_j - p^{n-1}_{j-1}}{h_j} \right) + (P_2)^n_{j-1/2} (fp)^n_{j-1/2} \\ &+ (P_2)^{n-1}_{j-1/2} (fp)^{n-1}_{j-1/2} \\ &= \alpha_n \begin{bmatrix} (ug)^n_{j-1/2} - u^n_{j-1/2} \, g^{n-1}_{j-1/2} + g^n_{j-1/2} \, u^{n-1}_{j-1/2} - (ug)^{n-1}_{j-1/2} - (fp)^n_{j-1/2} \\ + p^n_{j-1/2} \, f^{n-1}_{j-1/2} - f^n_{j-1/2} \, p^{n-1}_{j-1/2} + (fp)^{n-1}_{j-1/2} \end{bmatrix} \end{aligned}$$

$$\begin{aligned} &\Rightarrow \frac{1}{\mathrm{Pr}} \left\{ (P_1)^n_{j-1/2} \right\} \left(\frac{p^n_j - p^n_{j-1}}{h_j} \right) + \left\{ (P_2)^n_{j-1/2} + \alpha_n \right\} (fp)^n_{j-1/2} - \alpha_n (ug)^n_{j-1/2} \\ &+ \alpha_n \left[u^n_{j-1/2} \, g^{n-1}_{j-1/2} - g^n_{j-1/2} \, u^{n-1}_{j-1/2} - p^n_{j-1/2} \, f^{n-1}_{j-1/2} + f^n_{j-1/2} \, p^{n-1}_{j-1/2} \right] \\ &= -\frac{1}{\mathrm{Pr}} \left\{ (P_1)^{n-1}_{j-1/2} \right\} \left(\frac{p^{n-1}_j - p^{n-1}_{j-1}}{h_j} \right) - (P_2)^{n-1}_{j-1/2} (fp)^{n-1}_{j-1/2} + \alpha_n \left[(fp)^{n-1}_{j-1/2} - (ug)^{n-1}_{j-1/2} \right] \end{aligned}$$

where $T^{n-1}_{j-1/2} = -M^{n-1}_{j-1/2} + \alpha_n \left\{ (fp)^{n-1}_{j-1/2} - (ug)^{n-1}_{j-1/2} \right\}$ (2.92)

where, $\alpha_n = \frac{1}{k_n}\xi_{j-1/2}^{n-1/2}$ (2.93)

$$M_{j-\frac{1}{2}}^{n-1} = \frac{h_j^{-1}}{\mathrm{Pr}}(P_1)_{j-\frac{1}{2}}^{n-1}\left\{p_j^{n-1} - p_{j-1}^{n-1}\right\} + (P_2)_{j-\frac{1}{2}}^{n-1}(fp)_{j-\frac{1}{2}}^{n-1} \tag{2.94}$$

$$\begin{aligned}\Rightarrow T_{j-1/2}^{n-1} &= \frac{1}{\mathrm{Pr}}(P_1)_{j-1/2}^{n} h_j^{-1}\left(p_j^n - p_{j-1}^n\right) + \left\{(P_2)_{j-1/2}^{n} + \alpha_n\right\}(fp)_{j-1/2}^{n} - \alpha_n (ug)_{j-1/2}^{n} \\ &+ \alpha_n\left(u_{j-1/2}^{n} g_{j-1/2}^{n-1} - g_{j-1/2}^{n} u_{j-1/2}^{n-1}\right) - \alpha_n\left(p_{j-1/2}^{n} f_{j-1/2}^{n-1} - f_{j-1/2}^{n} p_{j-1/2}^{n-1}\right)\end{aligned} \tag{2.95}$$

The boundary condition becomes

$$\begin{aligned} &f_0^n = 0, \quad u_0^n = 0\ , g_0^n = 1 \\ &u_j^n = 0, \quad g_j^n = 0\end{aligned} \tag{2.96}$$

CHAPTER 3

Effect of temperature dependent viscosity on MHD natural convection flow

3.1 Introduction

It is worth pointing out that the MHD flow and heat transfer over a wavy surface is of importance in several heat transfer collectors where the presence of roughness elements disturbs the flow past surfaces and alters the heat transfer rate. The study of the flow of electrically conducting fluid in the presence of magnetic field is also important from the technical point of view so more attention given by many researchers. The specific problem selected for study is the flow and heat transfer in an electrically conducting fluid adjacent to the surface. The surface is maintained at a uniform temperature T_w, which may either exceed the ambient temperature T_∞ or may be less then β_0. When $T_w \geq T_\infty$, an upward flow is established along the surface due to free convection, where as for $T_w \leq T_\infty$, there is a down flow. The interaction of the magnetic field and the moving electric charge carried by the flowing fluid induces a force, which is proportional to the magnitude of the longitudinal velocity and acts in the opposite direction is also very small. Additionally, a magnetic field of strength β_0 acts normal to the surface. Consequently, the influence of the magnetic field on the boundary layer is exerted only through induced forces within the boundary layer itself, with no additional effects arising from the free stream pressure gradient. The action of a magnetic field on the fluid has many practical applications, e.g. metals processing industry, including the control of liquid metals in continuous casting processes, plasma welding, nuclear industry and many others. Mathematical modeling of the magnetohydrodynamic problems is particularly desirable. However, because the property (viscosity) must have a significant change with temperature, it is necessary to take into account the variation of viscosity to obtain a better estimation of the flow and heat transfer behavior.

The present work describes the effect of magnetohydrodynamic natural convection flow of viscous incompressible fluid with temperature dependent viscosity along a uniformly heated vertical wavy surface. The viscosity of the fluid are taken to be

linear function and inversely proportional to linear function of temperature. Using the appropriate transformations the governing equations with associated boundary conditions are converted to non-dimensional boundary layer equations, which are solved numerically by employing the implicit finite difference method, known as the Keller-box scheme.

The effects of the pertinent parameters, such as the viscosity parameter (ε), the magnetic parameter (M), the amplitude-to-length ratio of the wavy surface (α) and Prandtl number (Pr) on the surface shear stress in terms of the skin friction coefficient C_{fx}, the rate of heat transfer in terms of Nusselt number Nu_x, the velocity and temperature profiles, the streamlines and the isotherms over the whole boundary layer are shown graphically. Numerical results of the local skin friction coefficient and the rate of heat transfer for different values are presented in tabular form. From these results it can be observed that the different flow and heat transfer characteristics by varying the relevant parameters. Two different cases have been considered in relation to temperature dependent viscosity, which are,

3.2 Results and discussions

(a) Viscosity is a linear function of temperature

The problem of MHD natural convection flow of a viscous incompressible fluid with variable viscosity along a vertical wavy surface with uniform surface temperature has been investigated. The numerical results obtained from the governing equations (2.38) and (2.39) with the boundary conditions in equation (2.40) are discussed and some of the numerical results are tabulated in Tables A1- A2. Numerical values of the skin friction coefficient C_{fx}, the rate of heat transfer in terms of the Nusselt number Nu_x, velocity, temperature, the streamlines and the isotherms are obtained for different values of the viscosity parameter ε = 0.0 (constant viscosity) to 60.0, the magnetic parameter M = 0.0 (non magnetic field) to 2.0, Prandtl number Pr = 0.73, 3.0, 7.0, 15.5, 100 and the amplitude-to-length ratio of the wavy surface ranging from α = 0.0 (flat plate) to 0.4 and depicted in figures 3.1- 3.16. When Pr = 0.73 which correspond to the air at 2100^0K, Pr = 3.0 and 7.0 which correspond to water at 60^0C and 20^0C respectively and Pr = 15.5, 100 which correspond to calcium chloride

solution. The value of viscosity (ε = 0.0, 5.0, 20.0, 40.0, 60) is used to solve the problem numerically. But practically no fluid is avalible which satisfies these values.

The effect of temperature dependent viscosity (ε = 0.0, 5.0, 20.0, 40.0, 60) on the surface shear stress in terms of the local skin friction coefficient C_{fx} and the rate of heat transfer in terms of the local Nusselt number Nu_x are depicted graphically in figures 3.1(a) and 3.1(b) respectively against the axial distance of x keeping all other parameters amplitude-to-length ratio of wavy surface α = 0.3, magnetic parameter M = 0.5 and Prandtl number Pr = 0.73. Figure 3.1(a) indicates that increasing values of the viscosity, the surface shear stress in terms of the frictional force increases monotonically along the upstream direction of the surface and a decrease in the values of the rate of heat transfer along the wavy surface is observed from figure 3.1(b). Moreover, the maximum values of local skin friction coefficient C_{fx} are 0.86640, 1.54688, 2.20782, 2.60723 and 2.85371 for ε = 0.0, 5.0, 20.0, 40.0 and 60.0 respectively which occurs at x = 0.50 and it is seen that the local skin friction coefficient C_{fx} increases by approximately 70% as the value of viscosity parameter grows up from 0.0 to 60.0. Increasing values of viscosity lead to increase the amplitude of the skin friction coefficient along the upward direction of the surface. Furthermore, maximum values of local the rate of heat transfer are 0.31824 for ε = 0.0 and 0.17258 for ε = 60 respectively. Each of which occurs at different position of x and the rate of heat transfer decreases by approximately 46% as the value of viscosity parameter enhances from 0.0 to 60.0. Here it is concluded that for high viscous fluid the skin friction coefficient is higher and the corresponding rate of heat transfer is slow. When viscosity increases then the skin friction coefficient increases because the skin friction coefficient is directly dependent on temperature dependent viscosity.

The influence of magnetic field, on the reduced local skin friction coefficient and local rate of heat transfer are illustrated in figures 3.2(a) and 3.2 (b) respectively for different values of controlling parameters Pr = 0.73, α = 0.3 and ε = 5.0. As electrically conducting fluid in presence of magnetic field generates electrical current, the magnetic field is changed and the fluid motion is moderated. As a result, the velocity gradient $f''(x, 0)$ decreases with the effect of magnetic field. The same

result is observed on the local rate of heat transfer due to increase value of the intensity of magnetic field at different position of x. The maximum values of local skin friction coefficient C_{fx} and the rate of heat transfer in terms of the local Nusselt number Nu_x are 1.68211, 1.27924 for M = 0.0 and 0.26789, 0.23573 for M = 2.0 respectively. It is shown that the skin friction coefficient decreases by approximately 24% when intensity of magnetic field increases from 0.0 to 2.0. Furthermore, the heat transfer rate decreases by approximately 12% as intensity of magnetic field increases from 0.0 to 2.0. The magnetic field acts against the direction of fluid flow and reduce the skin friction and the rate of heat transfer.

In figures 3.3(a) and 3.3(b), the surface shear stress in terms of the local skin friction coefficient C_{fx} and the rate of heat transfer in terms of Nusselt number Nu_x are depicted graphically for different values of Prandtl number (Pr = 0.73, 3.0, 7.0, 15.5, 100) when the values of amplitude-to-length ratio of wavy surface α = 0.3, magnetic parameter M = 0.5, and viscosity parameter ε = 5.0. From figure 3.3(a), it is observed that the skin friction coefficient decreases monotonically for increasing values of Prandtl number Pr and from figure 3.3(b), the opposite result is observed on the rate of heat transfer due to increase of Prandtl number Pr. Increasing values of Prandtl number Pr, speed up the decay of the temperature field away from the heated surface with a consequent increase in the rate of heat transfer. The maximum values of local skin friction coefficient are 1.54688, 0.53835 and the rate of heat transfer in terms of the local Nusselt number are 0.25070 and 0.99839 for Pr = 0.73 and 100 respectively which occurs at the axial position of x = 0.50. It is seen that the local skin friction coefficient decreases by approximately 65% and the rate of heat transfer increases by approximately 75% as Pr increases from 0.73 to 100.

Figures 3.4(a) and 3.4(b) show that increase in the value of the amplitude-to-length ratio of wavy surface (α = 0.0, 0.1, 0.2, 0.3, 0.4) leads to decrease the value of the skin friction coefficient and the rate of heat transfer in terms of the local Nusselt number while Prandtl number Pr = 0.73, magnetic parameter M = 0.5 and viscosity parameter ε = 5.0. Frictional force depends on the smoothness of the surface, temperature and nature of fluid. Surface becomes more roughened for increasing values of amplitude-to-length ratio of wavy surface. Velocity force decreases at the

local points. However, the maximum values of the skin friction coefficient and the heat transfer rate are 1.65971 and 0.27478 for α = 0.0 which occurs at the surface and 1.53714, 0.25186 for α = 0.4 which occurs at the axial position of x = 0.50. It is seen that the skin friction coefficient and the heat transfer rate decrease by 7.39% and 8.34% respectively as α increases from 0.0 to 0.4.

Numerical values of the velocity $f'(x,\eta)$ and the temperature $\theta(x,\eta)$ are depicted graphically in figure 3.5(a) and figure 3.5(b) respectively against the axial distance of η for different values of temperature dependent viscosity (ε = 0.0, 5.0, 20.0, 40.0, 60.0) for the fluid having α = 0.3, magnetic parameter M = 0.5 and Prandtl number Pr = 0.73. Viscosity is a physical property of the fluid, which controls its rate of flow. When viscosity increases then velocity gradient normal to the wall decreases. For this reason figure 3.5(a), shows that the velocity of the fluid against η decreases quickly for increasing values of temperature dependent viscosity. But for natural convection near the surface of the plate velocity increases and become maximum and then decreases and finally approaches to zero asymptotically. The maximum values of the velocity are found to be 0.49107, 0.31965, 0.20781, 0.15546 and 0.12783 for ε = 0.0, ε = 5.0, ε = 20.0, ε = 40.0 and ε = 60.0 respectively. It is noted that the velocity decreases by approximately 74% as ε increases from 0.0 to 60.0. On the other hand figure 3.5(b), shows that the temperature increases within the boundary layer with the increase value of viscosity parameter. As $\varepsilon = \varepsilon^*(T_w - T_\infty)$. So the increasing values of viscosity increase the temperature difference between the surface and ambient temperature of the fluid. Then heat is transferred rapidly from surface to fluid within the boundary layer. That is why temperature increases with the increasing values of viscosity.

The interaction of the magnetic field and moving electric charge carried by the flowing fluid induces a force, which tends to oppose the fluid motion. In figure 3.6(a), it is observed that the magnetic field acting along the horizontal direction retards the fluid velocity with Prandtl number Pr = 0.73, α = 0.3 and viscosity parameter ε = 5.0. Here position of peak velocity moves toward the interface with the increasing M. From figure 3.6(b), it is evident that when M increases in the region η

$\in$ [0, 10] the temperature increases significantly. At the surface the temperature is maximum and it is decreases away from the surface and finally takes asymptotic values against η. Magnetic field decreases the temperature gradient at the wall and increases the temperature in the flow region due to the interaction.

Figure 3.7(a) and figure 3.7(b) deal with the effect of Prandtl number (Pr = 0.73, 3.0, 7.0, 15.5, 100) with other fixed controlling parameters amplitude-to-length ratio of the wavy surface α = 0.3, magnetic parameter M = 0.5 and viscosity parameter ε = 5.0 on the velocity $f'(x,\eta)$ and the temperature $\theta(x,\eta)$ against the axial distance of η. Prandtl number is the ratio of viscous force and thermal force. Increasing values of Pr increases viscosity and decreases thermal action of the fluid. If viscosity increases, then fluid does not move freely. Because of this fact, it is observed from figure 3.7(a) that the velocity of the fluid decreases quickly along the downward direction of the plate against η for increasing values of Prandtl number. It is seen that the velocity decreases by approximately 85% when Pr increases from 0.73 to 100.0. This is because the highest value of velocity are 0.31965 for Pr = 0.73 and 0.04703 for Pr = 100. From figure 3.7(b), it is noted that the temperature shift downward with the increasing Prandtl number Pr.

Figure 3.8(a) demonstrates the velocity for variation of the amplitude-to-length ratio of the wavy surface (α = 0.0, 0.1, 0.2, 0.3) with Prandtl number Pr = 0.73, magnetic parameter M = 0.5 and viscosity parameter ε = 5.0 and the corresponding temperature $\theta(x,\eta)$ is shown in figure 3.8(b). From figure 3.8(a), it is revealed that the velocity $f'(x,\eta)$ increases slowly against the axial distance of η along the upstream direction of the plate. Figure 3.8(b) shows the small increment on the temperature $\theta(x,\eta)$ for increasing values of the amplitude-to-length ratio of the wavy surface.

Figures 3.9 and 3.10 illustrate the effect of the temperature dependent viscosity on the development of streamlines and isotherms respectively which are plotted for Prandtl number Pr = 0.73, α = 0.3 and M = 0.5. It is noted that for ε = 0.0 the value of ψ_{max} is 6.20, for ε = 5.0 ψ_{max} is 5.23, for ε = 20.0 ψ_{max} is 3.98 and ψ_{max} is 3.09 where ε = 40.0. From figure 3.9, it is seen that the effect of viscosity, the flow rate in the boundary layer decreases. From figure 3.10, it is observed that owing to the effect

of temperature dependent viscosity, the thermal state of the fluid increases, causing the thermal boundary layer becomes thicker.

The effect of variation of the surface roughness on the streamlines and isotherms for the values of intensity of magnetic field equal to 0.0, 0.2, 1.0 and 2.0 are depicted in the figure 3.11 and figure 3.12 respectively while Prandtl number Pr = 0.73, α = 0.3 and ε = 5.0. It is observed from figure 3.12 that as the values of M increases the thermal boundary layer becomes higher gradually. Figure 3.11 depicts that the maximum values of ψ decreases steadily while the values of intensity of magnetic field increases. The maximum values of ψ, that is, ψ_{max} are 8.08, 6.67, 3.87 and 2.58 for M = 0.0, 0.2, 1.0 and 2.0 respectively. Finally it is concluded that for much roughness of the surface with the effect of magnetic field the velocity of the fluid flow decreases in the boundary layer.

Figures 3.13and 3.14 show the effect of Prandtl number (Pr = 0.73, 3.0, 7.0 and 15.5) on the formation of streamlines and isotherms respectively for α = 0.3, magnetic parameter M = 0.5 and viscosity parameter ε = 5.0. It can be seen that for Pr equal to 0.73, 3.0, 7.0, and 15.5 the maximum values of ψ, that is, ψ_{max} are 5.23, 2.85, 1.83 and 1.19 respectively. So it is concluded that for small value of Prandtl number with the effect of magnetic field and temperature dependent viscosity both the momentum and the thermal boundary layer become thicker.

The effect of variation of the surface roughness on the streamlines and isotherms for the values of the amplitude-to-length ratio of the wavy surface equal to 0.0, 0.1, 0.2 and 0.3 are displayed by the figure 3.15 and figure 3.16 respectively with other fixed parameters, Prandtl number Pr = 0.73, M = 0.5 and ε = 5.0. It is observed from figure 3.15 that as the values of the amplitude-to-length ratio of the wavy surface increases, the maximum values of ψ increases slightly. The maximum values of ψ, that is, ψ_{max} are 5.25, 5.29, 5.32 and 5.51 for α = 0.0, 0.1, 0.2 and 0.3 respectively. Figure 3.16 indicates that the increases of the amplitude-to-length ratio of the wavy surface affect the isotherms and leads to thicker thermal boundary layer. Here it is concluded that for much roughness of the surface with the effect of temperature dependent viscosity and magnetic field, the velocity and the temperature of the fluid flow increase in the boundary layer.

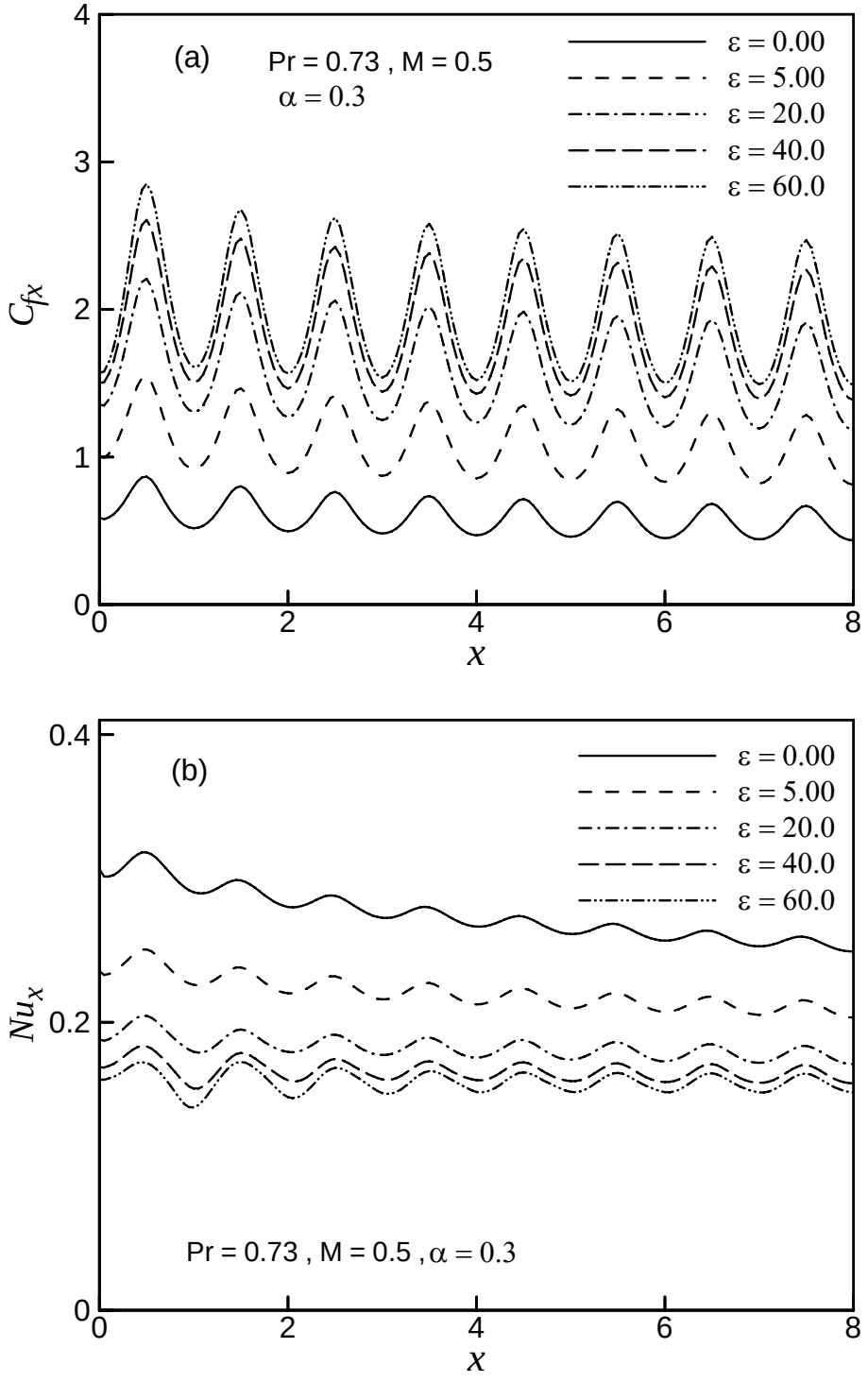

Figure 3.1: Variation of (a) skin friction coefficient C_{fx} and (b) rate of heat transfer Nu_x against dimensionless distance x for different values of viscosity parameter ε while α = 0.3, M = 0.5 and Pr = 0.73.

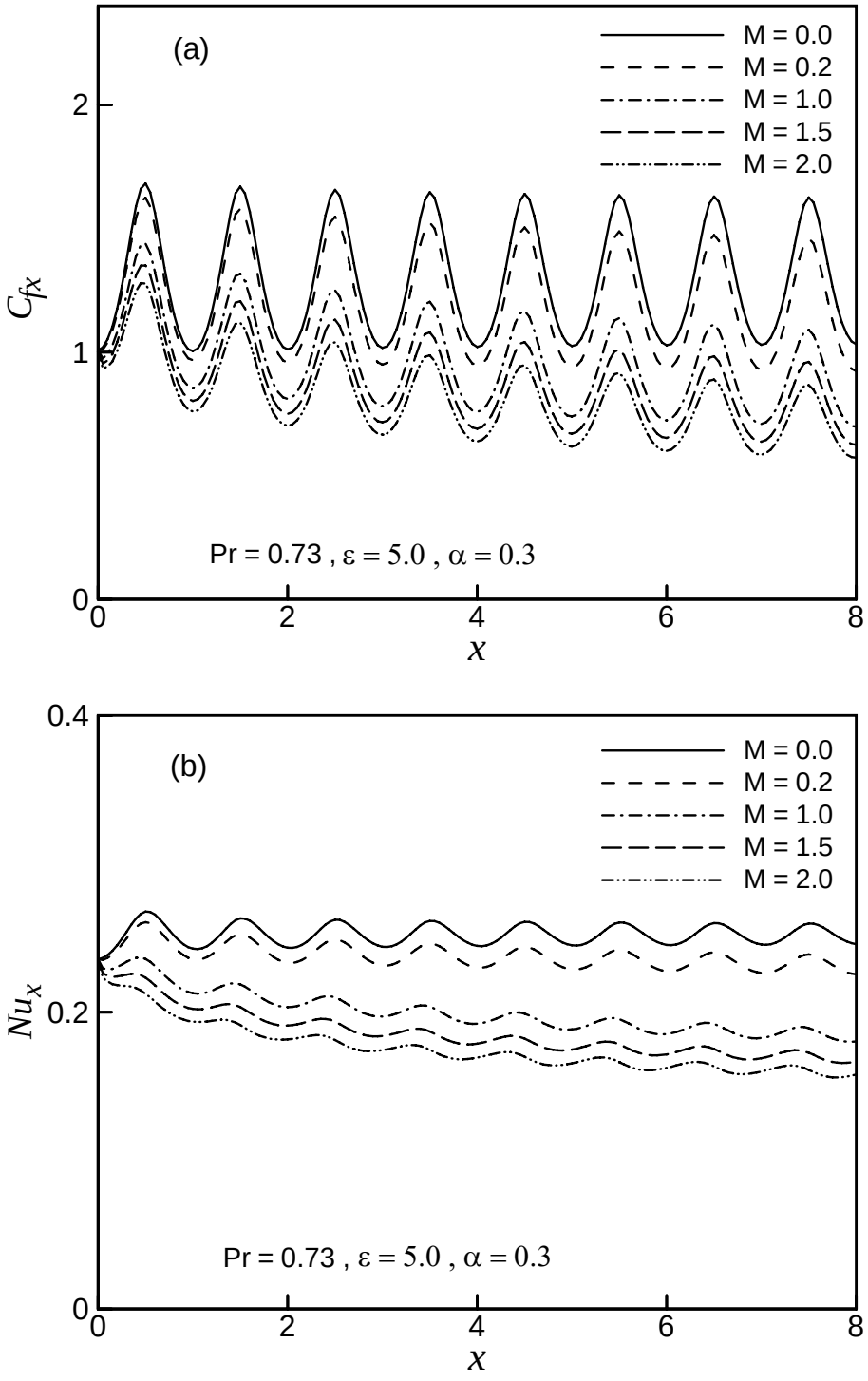

Figure 3.2: Variation of (a) skin friction coefficient C_{fx} and (b) rate of heat transfer Nu_x against dimensionless distance x for different values of magnetic parameter M with Pr = 0.73, α = 0.3 and ε = 5.0.

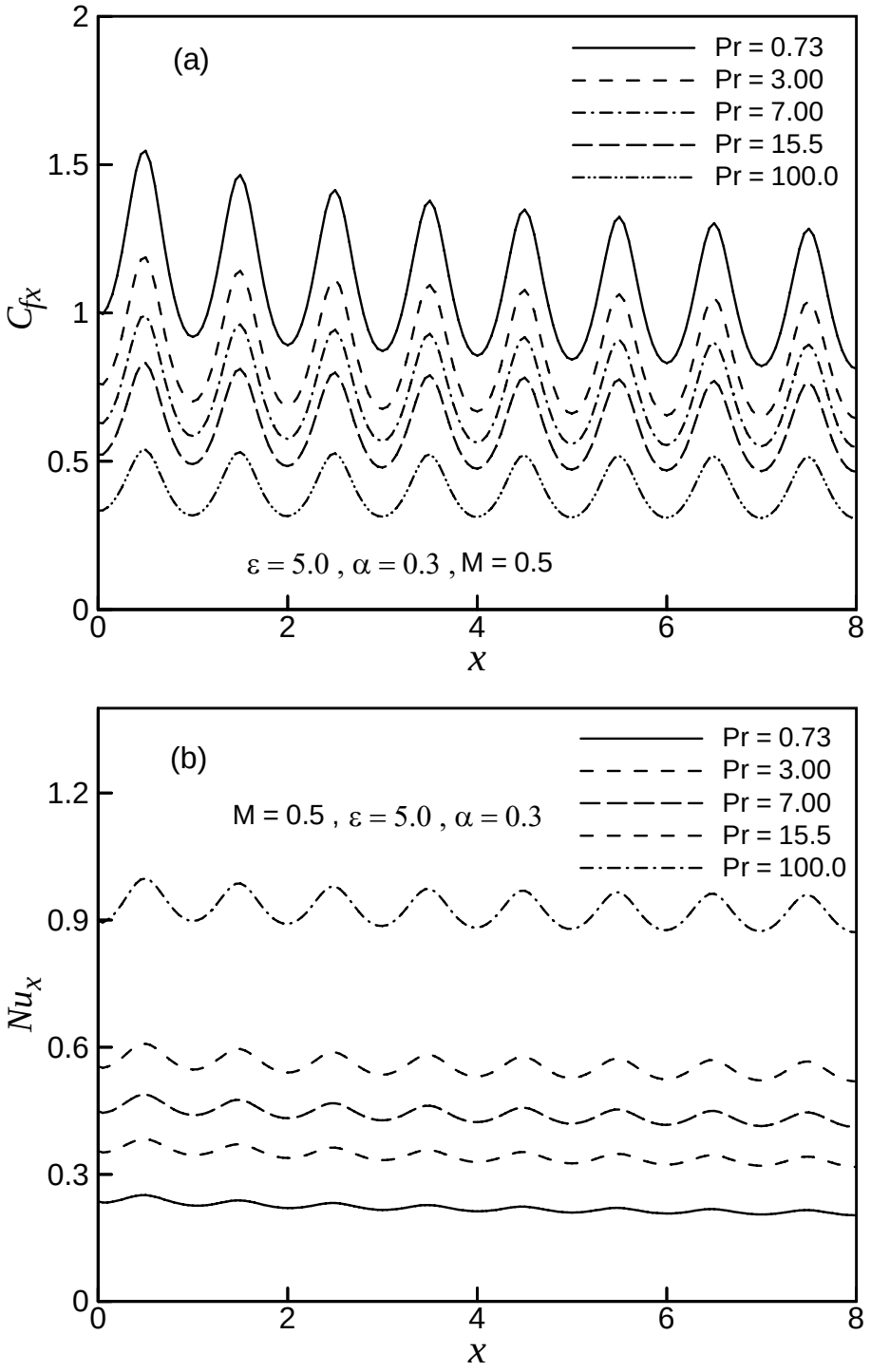

Figure 3.3: Variation of (a) skin friction coefficient C_{fx} and (b) rate of heat transfer Nu_x against dimensionless distance x for different values of Prandtl number Pr while $\alpha = 0.3$, $M = 0.5$ and $\varepsilon = 5.0$.

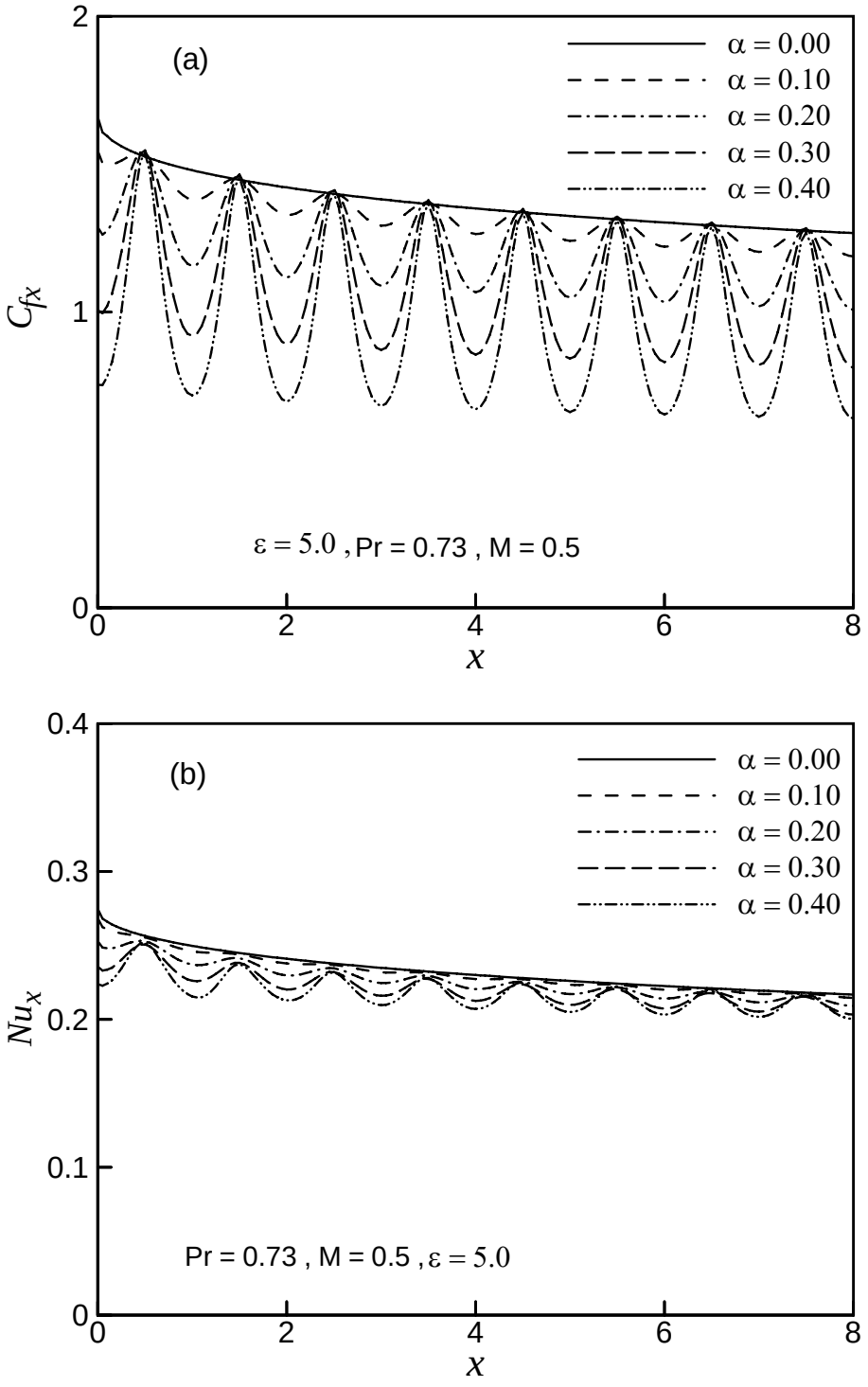

Figure 3.4: Variation of (a) skin friction coefficient C_{fx} and (b) rate of heat transfer Nu_x against dimensionless distance x for different values of the amplitude-to-length ratio of the wavy surface α when Pr = 0.73, M = 0.5 and ε = 5.0.

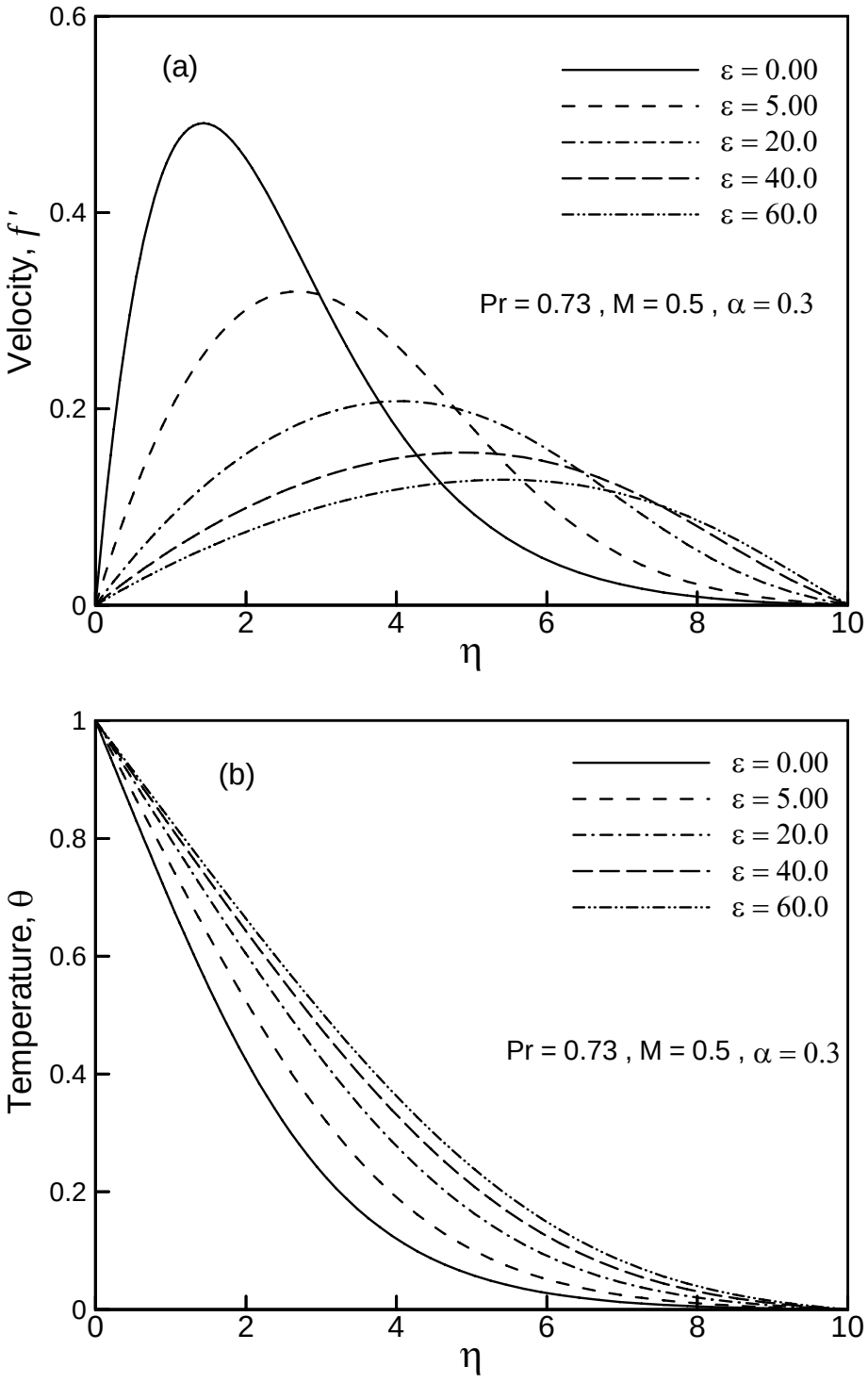

Figure 3.5: (a) Velocity profiles f' and (b) temperature distribution θ against dimensionless distance η for different values of viscosity parameter ε while $\alpha = 0.3$, $M = 0.5$ and Pr = 0.73.

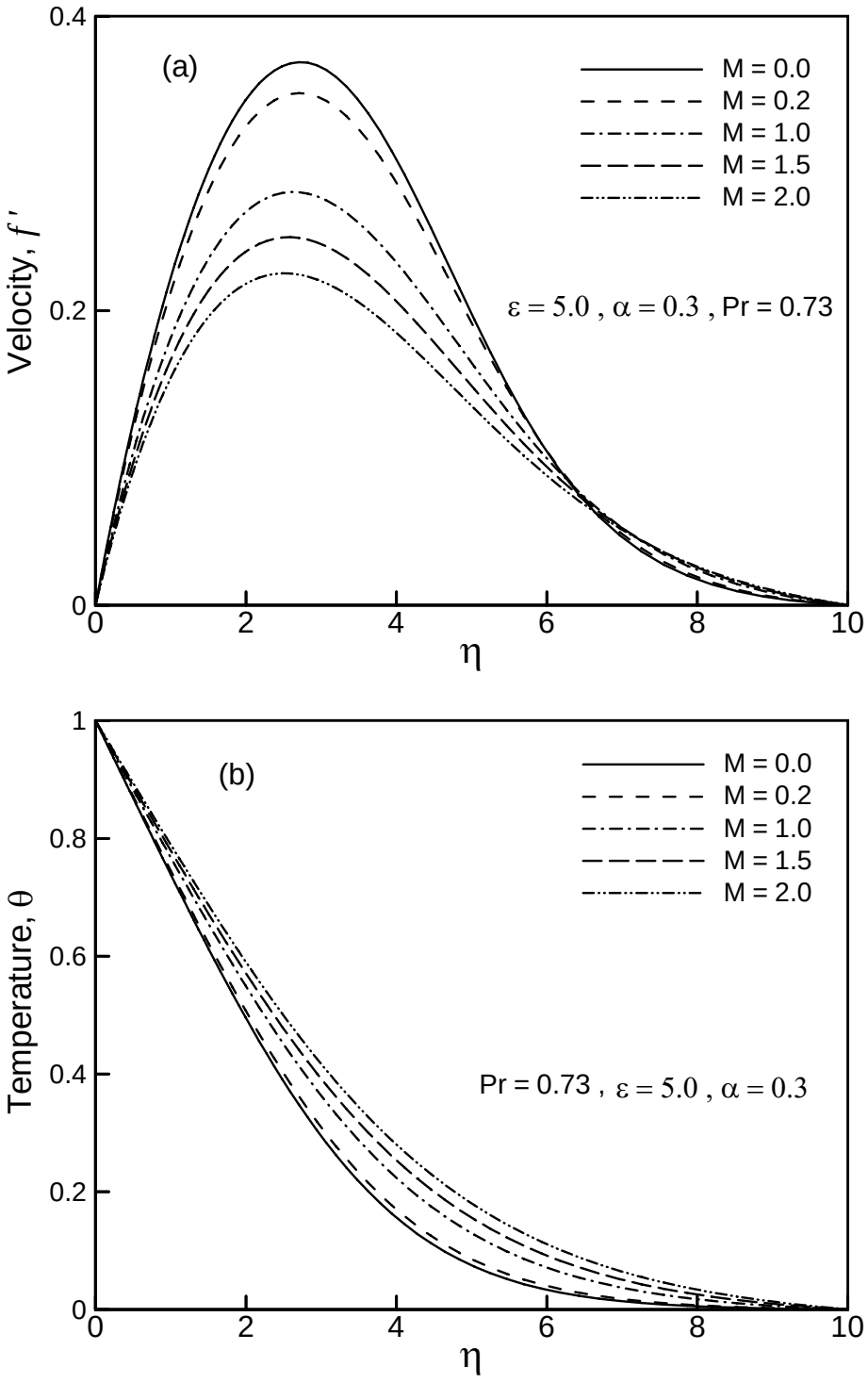

Figure 3.6: (a) Velocity profiles f' and (b) temperature distribution θ against dimensionless distance η for different values of magnetic parameter M with Pr = 0.73, $\alpha = 0.3$ and $\varepsilon = 5.0$.

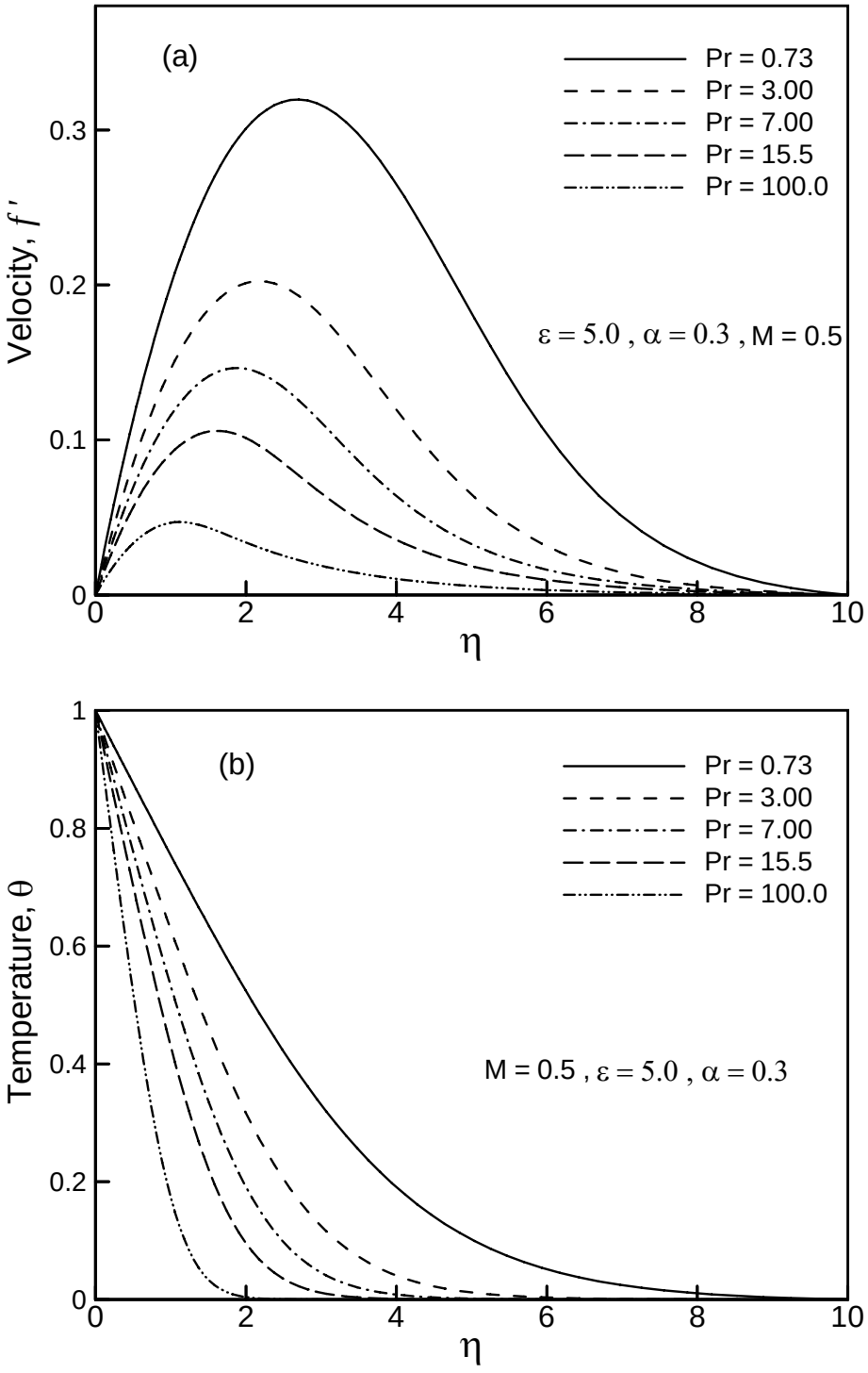

Figure 3.7: (a) Velocity profiles f' and (b) temperature distribution θ against dimensionless distance η for different values of Prandtl number Pr while $\alpha = 0.3$, $M = 0.5$ and $\varepsilon = 5.0$.

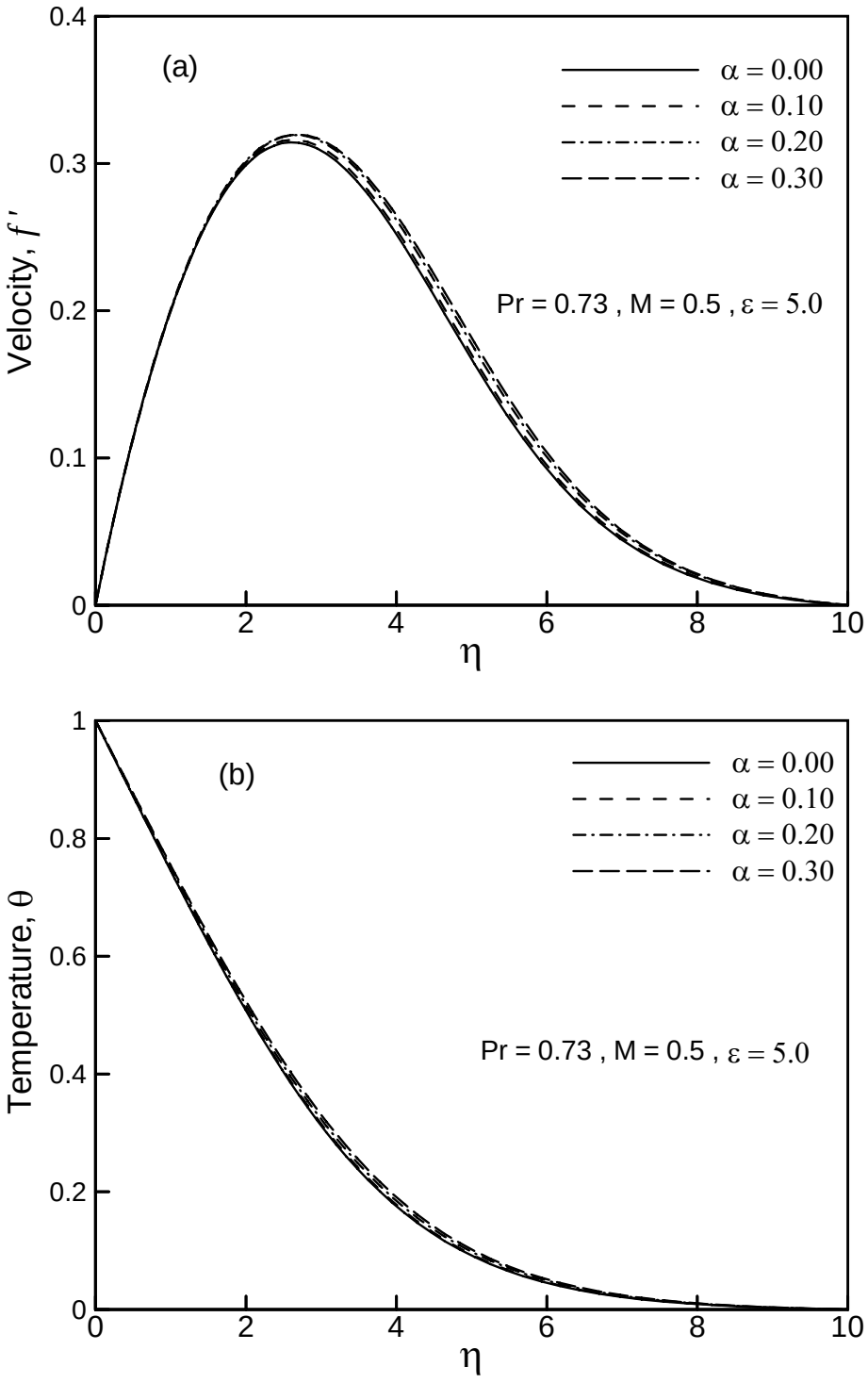

Figure 3.8: (a) Velocity profiles f' and (b) temperature distribution θ against dimensionless distance η for different values of α while Pr = 0.73, M = 0.5 and ε = 5.0.

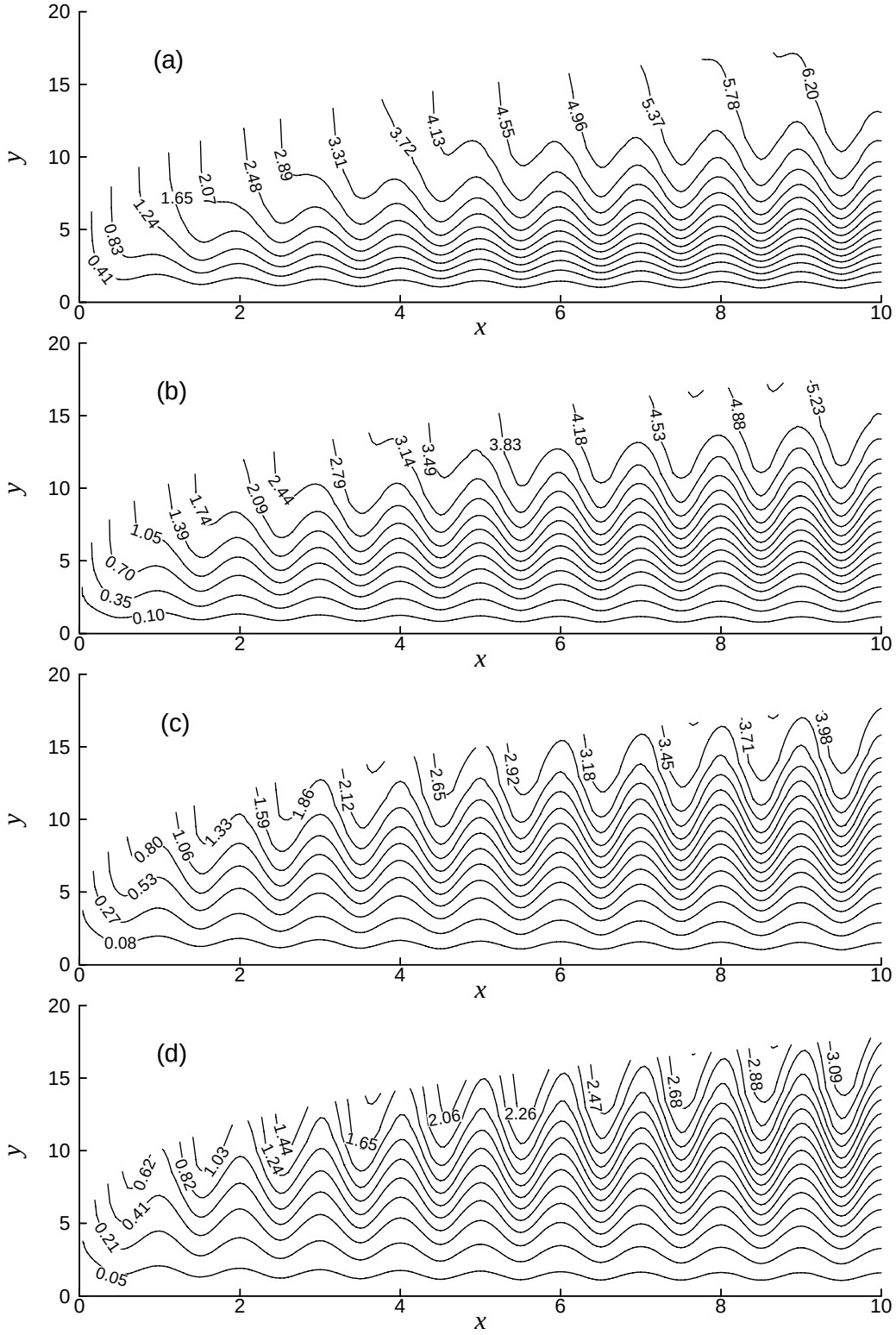

Figure 3.9: Streamlines for (a) $\varepsilon = 0.0$ (b) $\varepsilon = 5.0$ (c) $\varepsilon = 20.0$ (d) $\varepsilon = 40.0$ while Pr = 0.73, $\alpha = 0.3$ and $M = 0.5$.

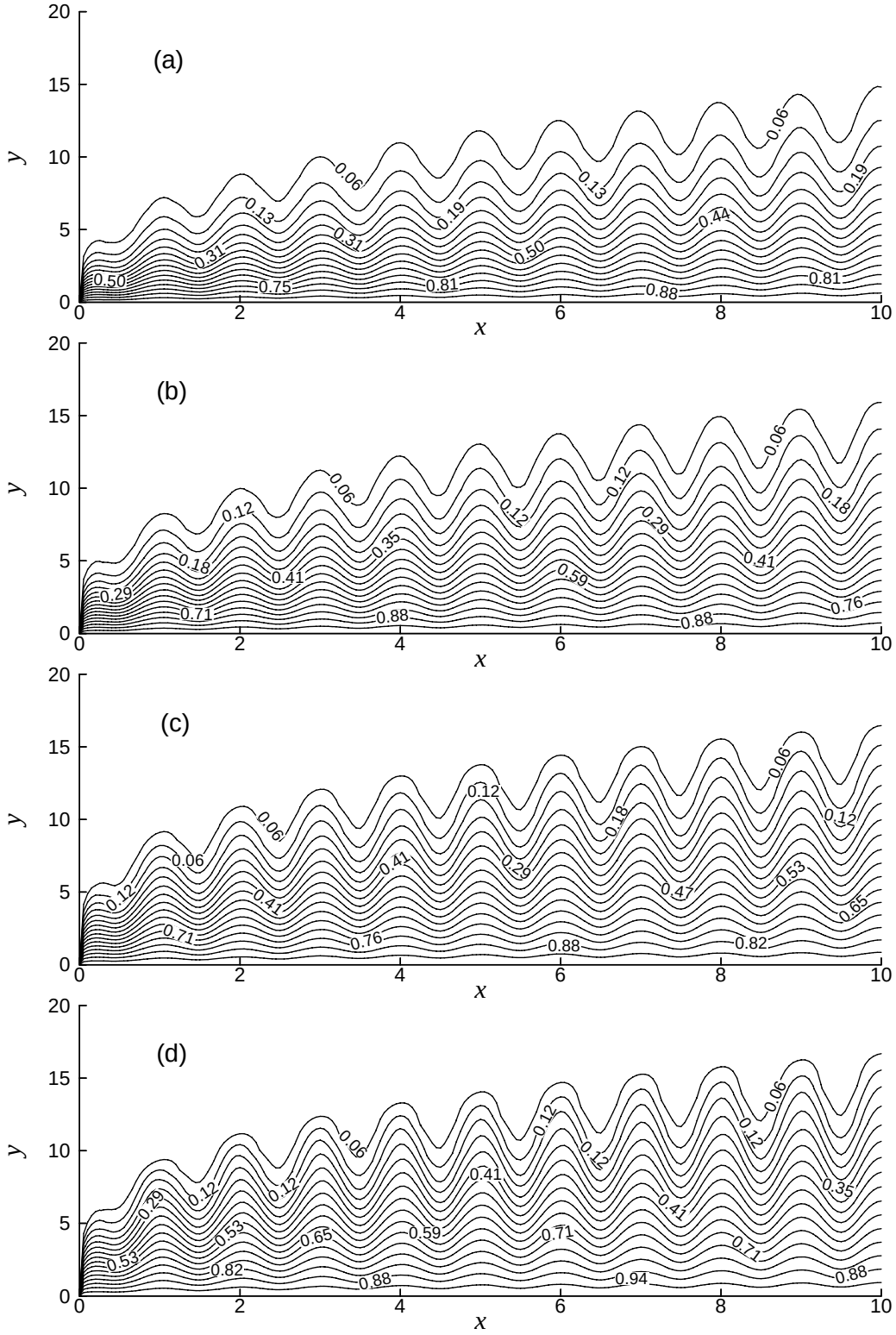

Figure 3.10: Isotherms for (a) $\varepsilon = 0.0$ (b) $\varepsilon = 5.0$ (c) $\varepsilon = 20.0$ (d) $\varepsilon = 40.0$ while Pr = 0.73, $\alpha = 0.3$ and $M = 0.5$.

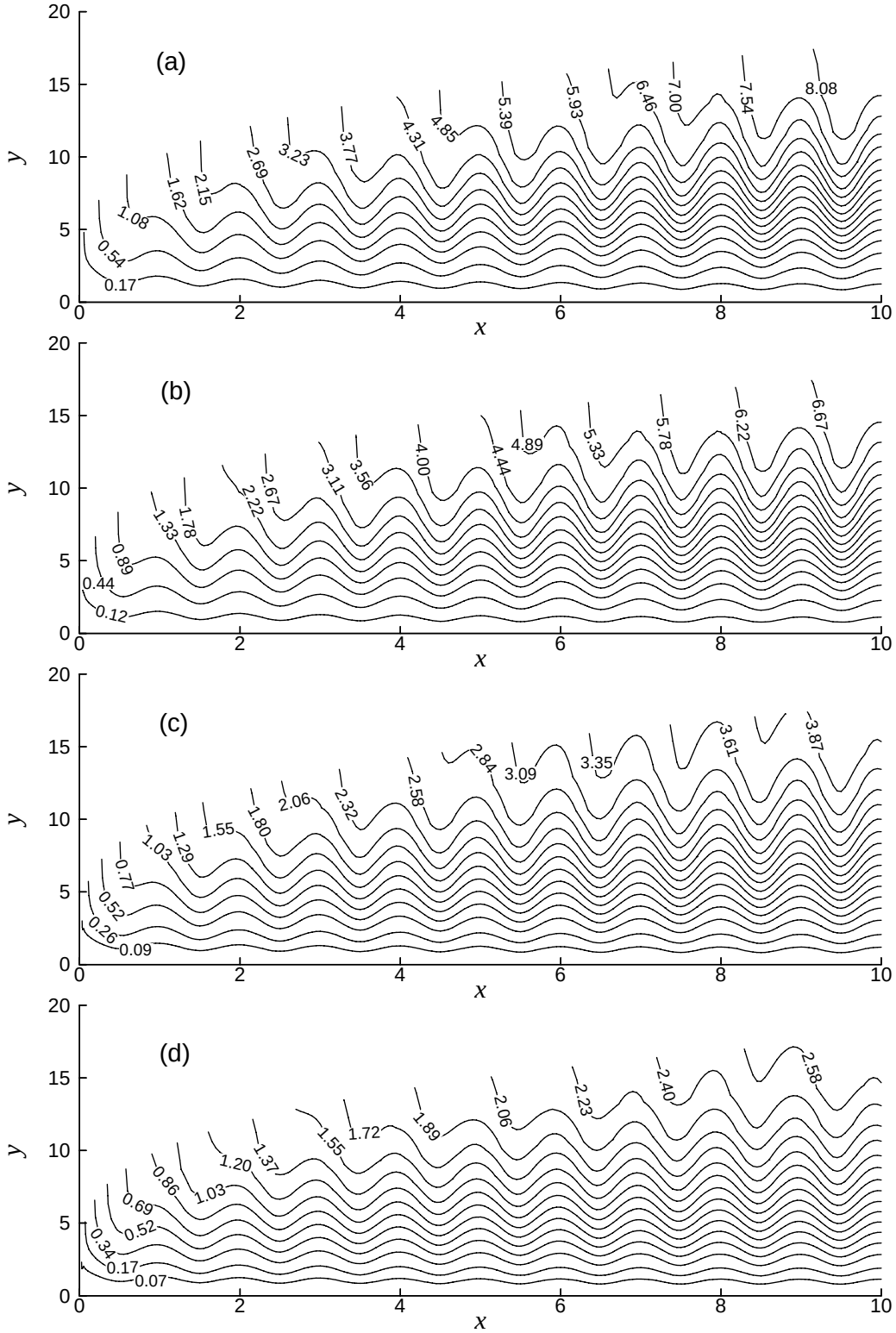

Figure 3.11: Streamlines for (a) M = 0.0 (b) M = 0.2 (c) M = 1.0 (d) M = 2.0 while ε = 5.0, α = 0.3 and Pr = 0.73.

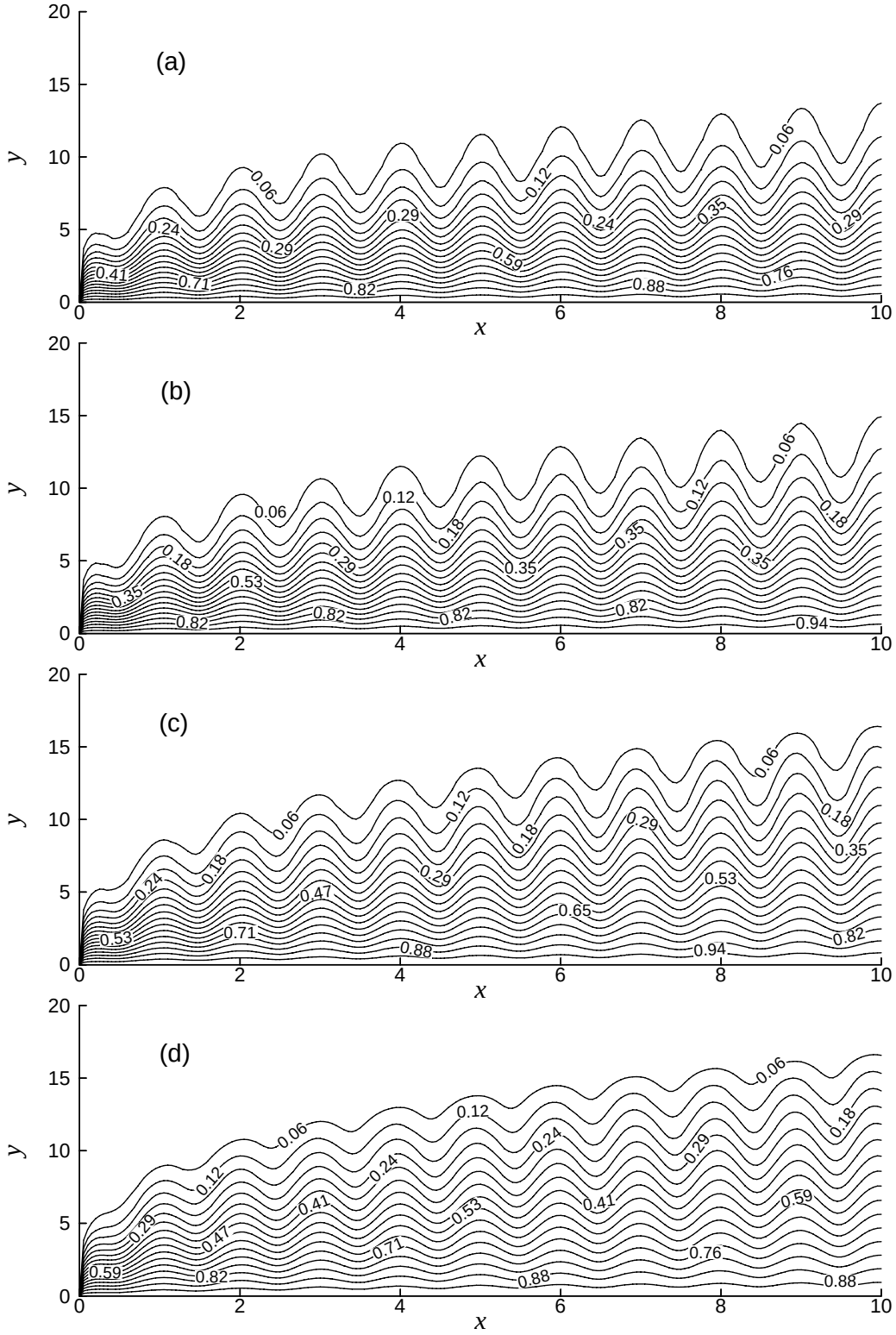

Figure 3.12: Isotherms for (a) M = 0.0 (b) M = 0.2 (c) M = 1.0 (d) M = 2.0 while ε = 5.0, α = 0.3 and Pr = 0.73.

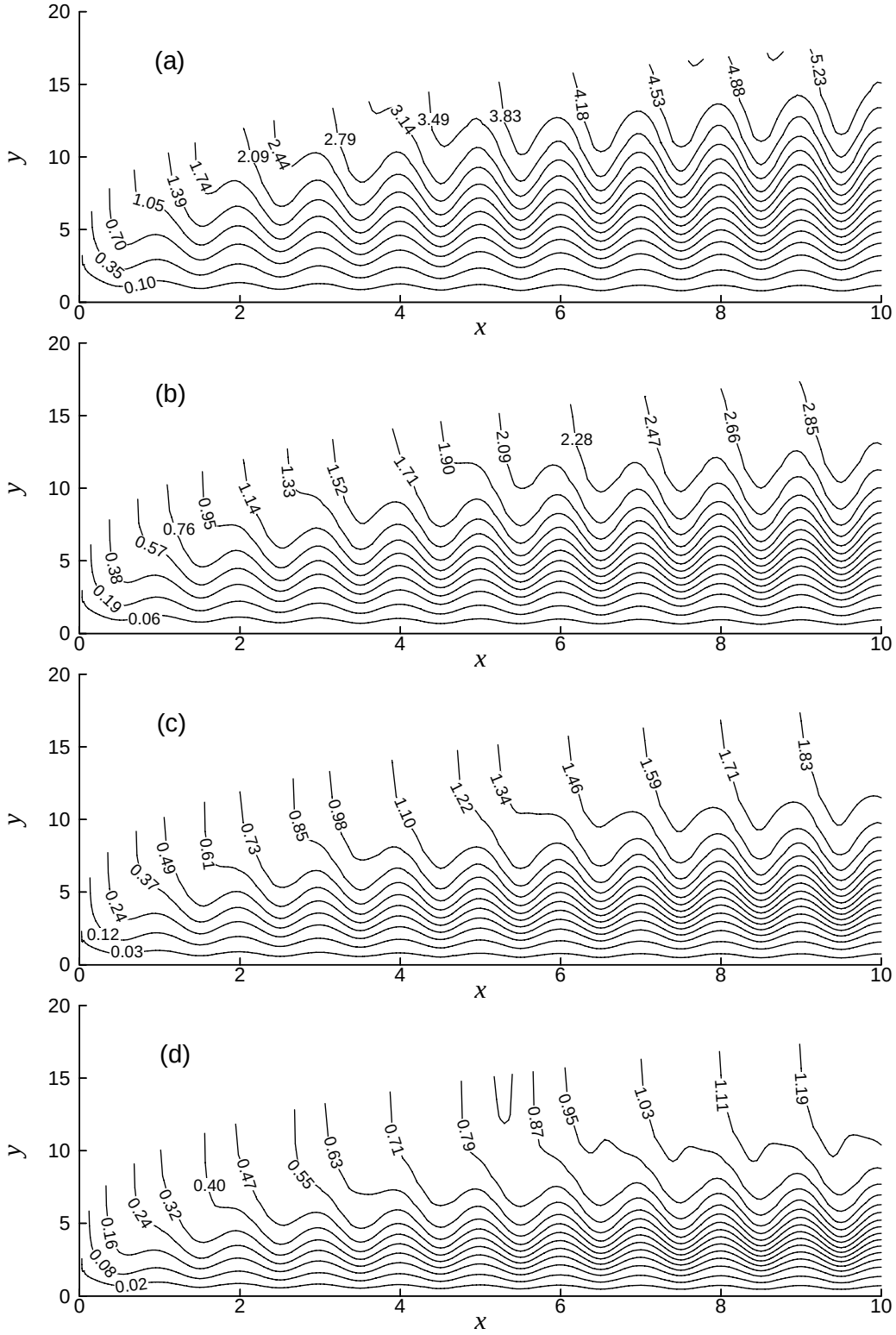

Figure 3.13: Streamlines for (a) Pr = 0.73 (b) Pr = 3.0 (c) Pr = 7.0 (d) Pr = 15.5 while $\varepsilon = 5.0$, $\alpha = 0.3$ and $M = 0.5$.

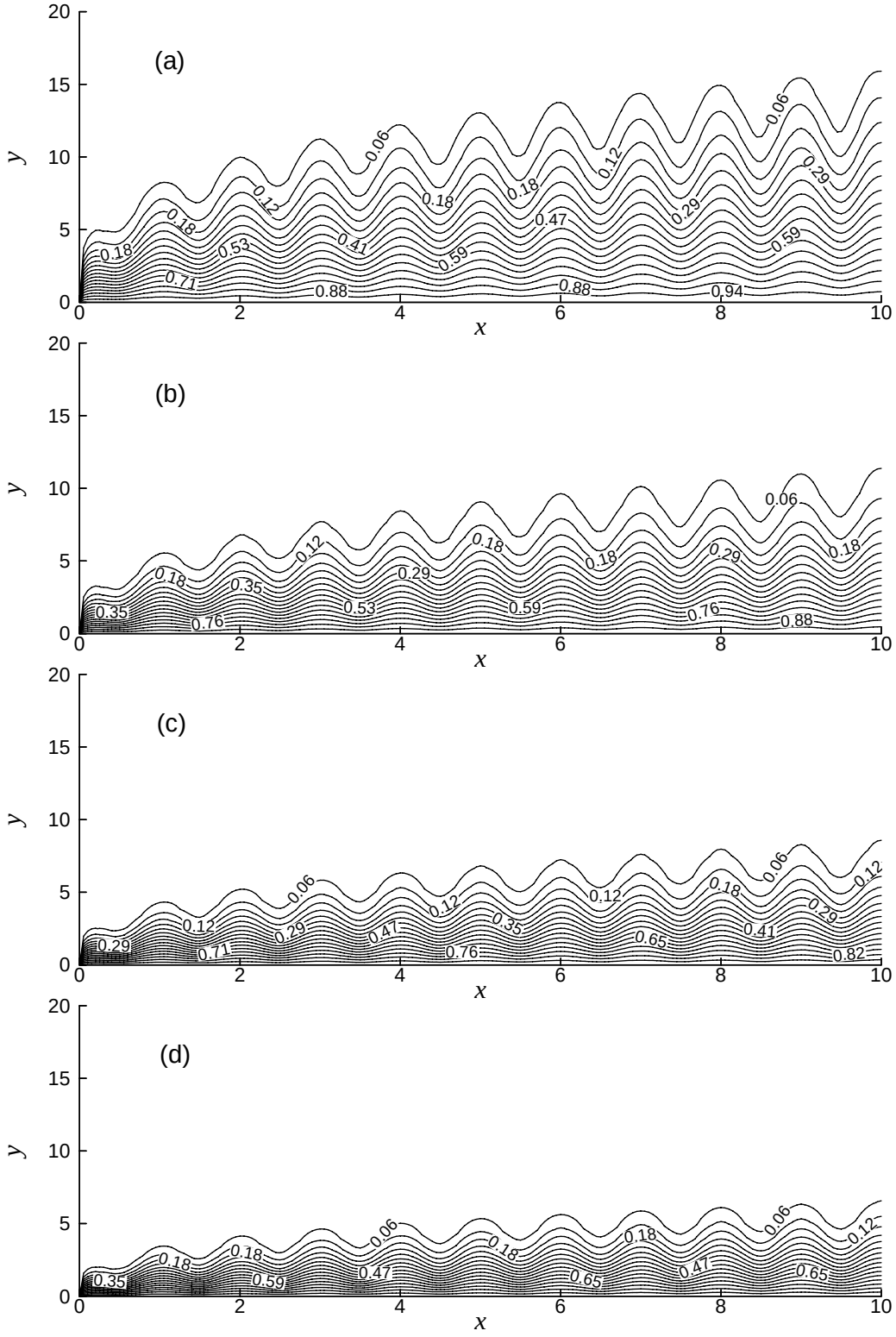

Figure 3.14: Isotherms for (a) Pr = 0.73 (b) Pr = 3.0 (c) Pr = 7.0 (d) Pr = 15.5 while $\varepsilon = 5.0$, $\alpha = 0.3$ and $M = 0.5$.

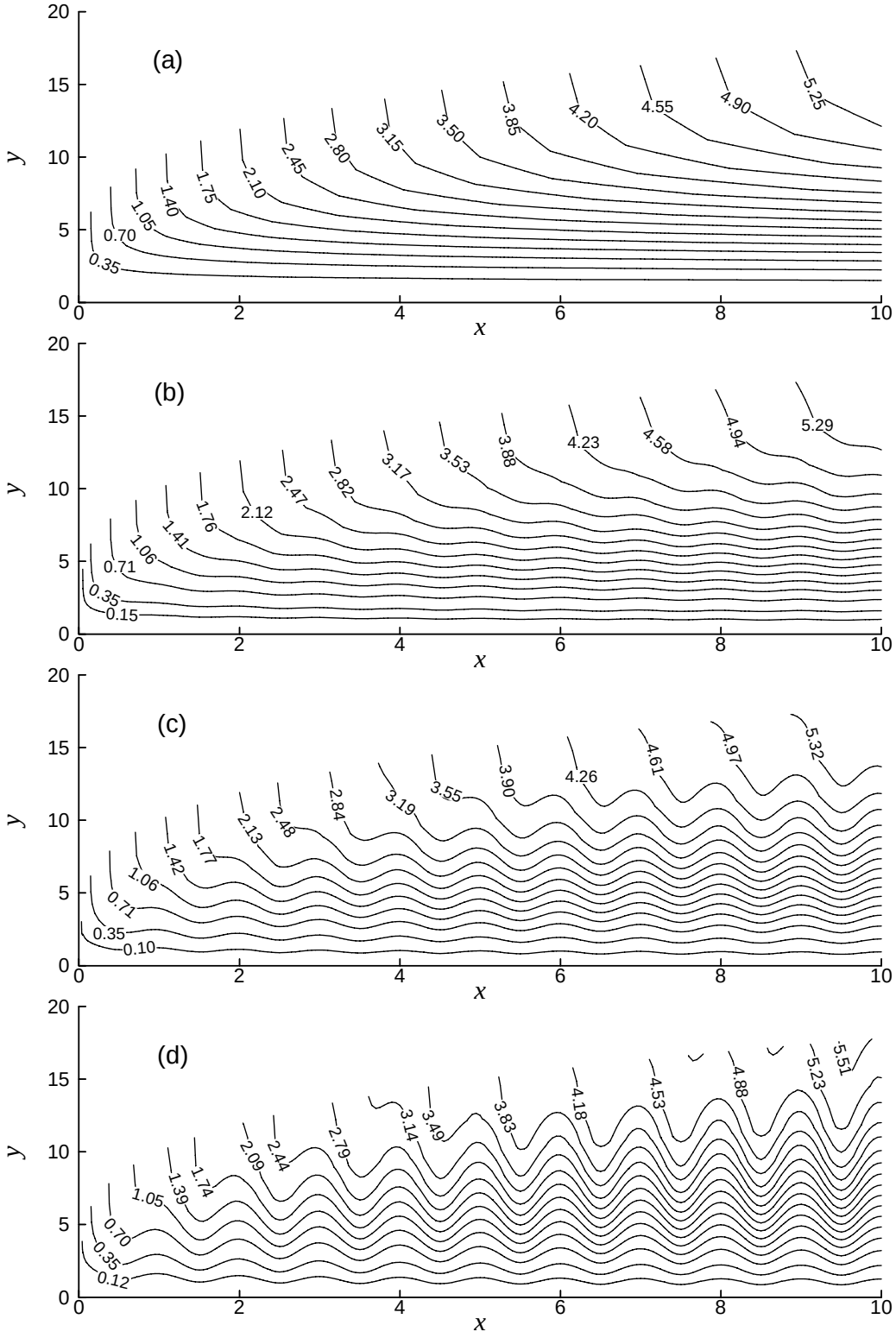

Figure 3.15: Streamlines for (a) $\alpha = 0.0$ (b) $\alpha = 0.1$ (c) $\alpha = 0.2$ (d) $\alpha = 0.3$ while $\varepsilon = 5.0$, $M = 0.5$ and Pr = 0.73.

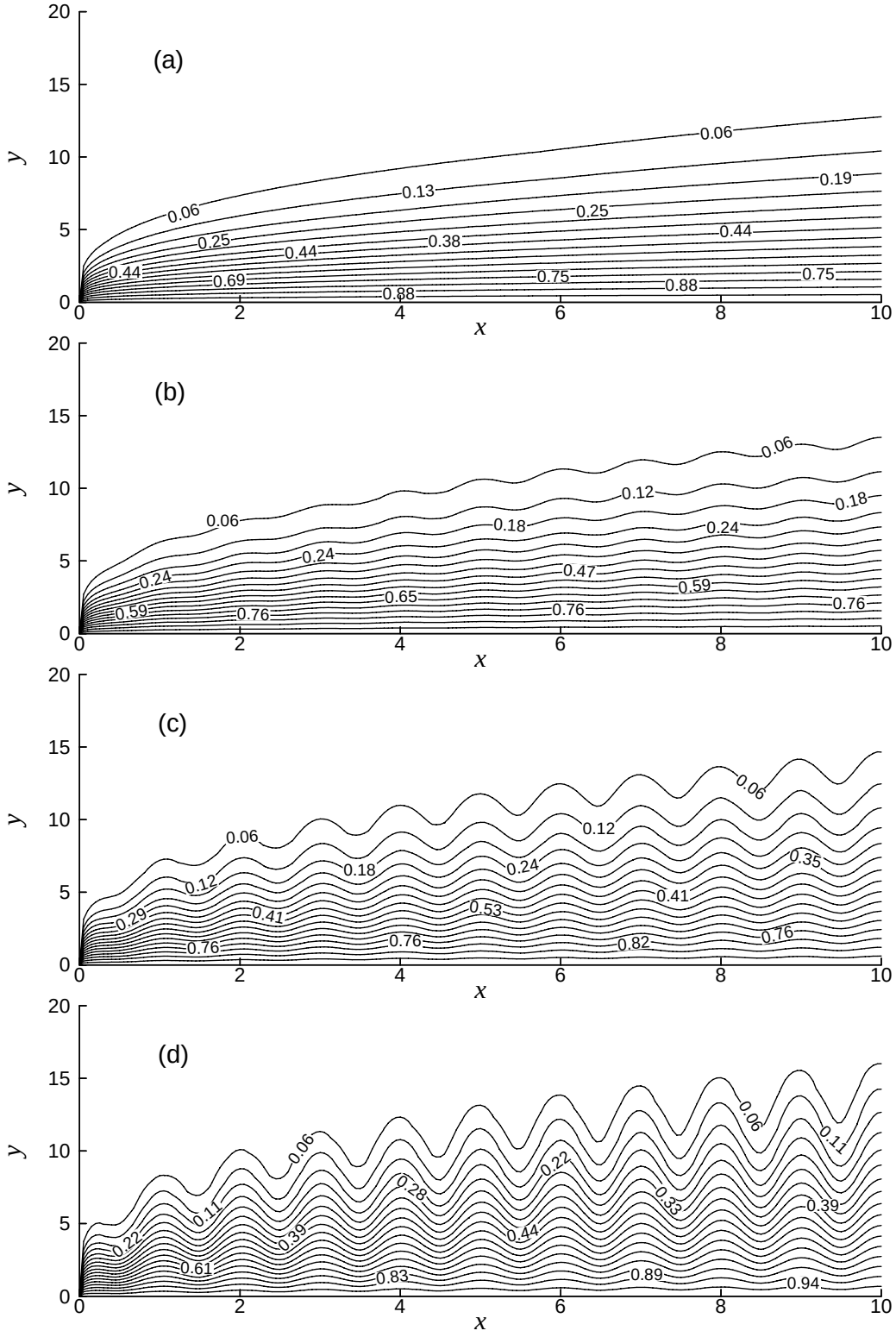

Figure 3.16: Isotherms for (a) $\alpha = 0.0$ (b) $\alpha = 0.1$ (c) $\alpha = 0.2$ (d) $\alpha = 0.3$ while $\varepsilon = 5.0$, $M = 0.5$ and Pr = 0.73.

The values of skin friction coefficient C_{fx} and the rate of heat transfer in terms of Nusselt number Nu_x have been presented in Table A1 for different values of Prandtl number (Pr = 0.73, 7.0, 100) while α = 0.3, magnetic parameter M = 0.5 and viscosity parameter ε = 5.0 which shown in appendix A. Here it is noted that the complete cycle of the wavy surface is from x = 0.0 to 2.0. The skin friction coefficient C_{fx} and the heat transfer rate increase for the first quarter of the cycle ($x \cong$ 0 to $x \cong$ 0.50) and decrease in the second quarter ($x \cong$ 0.50 to $x \cong$1.0). From $x \cong$ 1.0 to $x \cong$1.5 (i.e., third quarter) the skin friction coefficient C_{fx} again increases, whereas the last quarter ($x \cong$ 1.5 to $x \cong$ 2.0) it decreases. The skin friction coefficient C_{fx} and the rate of heat transfer Nu_x show similar characteristics throughout the domain. From this Table it can be found that the maximum values of local skin friction coefficient C_{fx} are 1.54688, 0.99193 and 0.53835 and the rate of heat transfer in terms of the local Nusselt number Nu_x are 0.25070, 0.48832 and 0.99839 for Pr = 0.73, 7.0 and 100.0 respectively which occur at x = 0.50. It is observed that the local skin friction coefficient C_{fx} decreases by approximately 65% and the rate of heat transfer in terms of the local Nusselt number Nu_x increases by approximately 75% as Pr increases from 0.73 to 100.0. It is also concluded that for air (Pr = 0.73) the rate of heat transfer is slow and the surface shear stress in terms of the skin friction coefficient is higher than that of water (Pr = 7.0). It is established that when Pr is small ($\Pr \leq 1$) then heat diffuses very quickly compared to the velocity (momentum). It means that the thickness of the thermal boundary layer is greater than that of the velocity boundary layer. In this case the temperature gradient as well as the heat transfer rate is slow.

Comparison of the skin friction coefficient C_{fx} and the local rate of heat transfer in terms of Nusselt number Nu_x against x for the variation of Prandtl number Pr with and without effects of magnetic field and temperature dependent viscosity with α = 0.3 are entered in Table A2 which shown in appendix A. Here it can be concluded that if the value of Pr increases the values of the skin friction coefficient C_{fx} decreases and the heat transfer rate increases for any values of viscosity parameter and magnetic parameter. It is also shown that if the effect of magnetic field increases, the values of the shear stress in terms of the skin friction coefficient decreases while it increases for the effect of temperature depedent viscosity and the rate of heat

transfer in terms of Nusselt number decreases for any values of viscosity and magnetic parameter.

(b) Viscosity is inversely proportional to linear function of temperature

Here the problem of variable viscosity inversely proportional to linear function of temperature on MHD natural convection flow of a viscous incompressible fluid along a vertical wavy surface with uniform surface temperature has been investigated. The governing equations (2.39) and (2.49) with the boundary condition given in equation (2.40) are solved numerically employing a very efficient implicit finite difference method together with the Keller-box scheme. Numerical values of the shear stress in terms of the skin friction coefficient and the rate of heat transfer in terms of the Nusselt number, the velocity, the temperature, the streamlines and the isotherms are presented graphically for different values of the viscosity parameter ε = 0.0 (constant viscosity) to 2.0, magnetic parameter ranging from M = 0.0 (non magnetic field) to 2.0, Prandtl number Pr = 0.73, 1.73, 3.0, 7.0, 15.5 which correspond to the air at 2100^0K, water at 100^0C, 60^0C, 20^0C and calcium chloride solution respectively and the amplitude-to-length ratio of the wavy surface ranging from α = 0.0 (flat plate) to 0.3. The effect of temperature depedent viscosity is very small which are depicted graphically in figures 3.17 - 3.24.

The influence of the temperature depedent viscosity (ε = 0.0, 0.5 and 1.0) on the surface shear stress in terms of the local skin friction C_{fx} and the rate of heat transfer in terms of the local Nusselt number Nu_x are illustrated graphically in figures 3.17(a) and 3.17(b) respectively when the values of α = 0.3, magnetic parameter M = 0.5 and Prandtl number Pr = 0.73. For increasing values of viscosity, the skin friction coefficient decreases slowly along the downstream direction of the surface against the axial distance of x. On the other hand, from figure 3.17(b) it is observed that the temperature gradient in terms of the rate of heat transfer increases along the wavy surface for increasing values of temperature depedent viscosity. Here it is concluded that for high viscous fluid with viscosity inversely proportional to linear function of temperature, the skin friction coefficient is slow and the corresponding rate of heat transfer is large. In figure 3.17(a), the maximum values of local skin friction

coefficient C_{fx} are 0.86640, 0.78213 and 0.77294 for ε = 0.0, 0.5 and 1.0 respectively which occurs at different values of x. It is seen that the local skin friction coefficient decreases by approximately 11% as the values of temperature depedent viscosity parameter increases from 0.0 to 1.0. Again figure 3.17(b) shows that the rate of heat transfer increases by approximately 8% due to the increased value of viscosity. Increasing values of viscosity lead to increase the amplitude of the heat transfer rate.

The effect of magnetic field (M = 0.0, 0.5, 1.0, 1.5, 2.0) on the surface shear stress in terms of the local skin friction C_{fx} and the rate of heat transfer in terms of the local Nusselt number Nu_x are depicted graphically in figures 3.18(a) and 3.18(b) respectively while the values of amplitude-to-length ratio of the wavy surface α = 0.3, viscosity parameter ε = 0.5 and Prandtl number Pr = 0.73. From figure 3.18(a), it is seen that an increase in the value of magnetic parameter leads to decrease the local skin friction coefficient. A similar situation is also observed from figure 3.18(b) in the case of local rate of heat transfer Nu_x at different position of x. The skin friction coefficient and the rate of heat transfer coefficient decrease by approximately 34% and 12% respectively as intensity of magnetic field increases from 0.0 to 2.0.

The surface shear stress in terms of the local skin friction coefficient C_{fx} and the rate of heat transfer in terms of the local Nusselt number Nu_x are displayed graphically in figures 3.19(a) and 3.19(b) respectively for the different values of Prandtl number (Pr = 0.73, 1.73, 3.0, 7.0 and 15.5) with other fixed controlling parameters amplitude-to-length ratio of the wavy surface α = 0.3, magnetic parameter M = 0.5 and viscosity parameter ε = 0.01. From figure 3.19(a), it is observed that the skin friction coefficient decreases significantly within the boundary layer due to increase values of Prandtl number Pr. The opposite result holds from figure 3.19(b) for the rate of heat transfer while Prandtl number Pr increases. The maximum values of local skin friction coefficient C_{fx} are 0.86331 and 0.51309 for Pr = 0.73 and 15.5 respectively which occurs at x = 0.50. The highest values of the rate of heat transfer in terms of the local Nusselt number Nu_x are 0.31856 and 0.85478 for Pr = 0.7 and 15.5 respectively which also occurs at x = 0.50. It is noted that the local skin friction coefficient C_{fx} decreases by approximately 41% and the rate of heat transfer in terms

of the local Nusselt number Nu_x increases by approximately 63% as Pr changes from 0.73 to 15.5.

Figures 3.20(a) and 3.20(b) demonstrate the effect of the variation of the amplitude-to-length ratio of the wavy surface (α = 0.0, 0.1, 0.2, 0.3) for Prandtl number Pr = 0.73, magnetic parameter M = 0.5 and viscosity parameter ε = 0.005. From both the figures it is clear that increase in the values of the amplitude-to-length ratio of the wavy surface leads to decrease the frictional force in terms of the skin friction coefficient and the heat transfer rate. The maximum values of the rate of heat transfer in terms of the local Nusselt number Nu_x are 0.35861 for α = 0.0 which occurs at the surface and 0.31840 for α = 0.3 which occurs at the axial position of x = 0.50. It is noted that the rate of heat transfer in terms of the local Nusselt number Nu_x decreases by approximately 12% as α increases from 0.0 to 0.3. As the surface waviness reduces the velocity force in each local point, the skin friction is also reduced.

The effects of temperature dependent viscosity (ε = 0.0, 0.5, 1.0, 1.5 and 2.0) on the velocity and the temperature within the boundary layer for the fluid having amplitude-to-length ratio of the wavy surface α = 0.3, magnetic parameter M = 0.5 and Prandtl number Pr = 0.73 are revealed in figure 3.21(a) and figure 3.21(b) respectively. From figure 3.21(a), it is seen that an increase in the viscosity is associated with a considerable increase in velocity. But for natural convection flow near the surface of the plate velocity increases and become maximum and then decreases and finally approaches to zero asymptotically. The highest values of velocity are 0.49107, 0.53378, 0.56908, 0.59709 and 0. 0.61730 for ε = 0.0, ε = 0.5, ε = 1.0, ε = 1.5 and ε = 2.0 respectively. The velocity of the fluid increases along η direction and reaches at utmost values which occurs between η = 0.73 to 1.43, then all the profiles steadily decrease, cross each other near the point η = 1.58 to 2.0 and finally approach to zero, the asymptotic value. It is observed that the velocity increases by approximately 21% when ε enhances from 0.0 to 2.0 near to the surface. On the other hand, an opposite situation is observed from figure 3.21(b) in the case of temperature field within the boundary layer with the increase values of temperature dependent viscosity parameter.

The effect of different values of intensity of magnetic field (M = 0.0, 0.5, 1.0, 1.5, 2.0) with Prandtl number Pr = 0.73, α = 0.3 and ε = 0.5 are depicted in figures 3.22(a) and 3.22(b) repectively. It is observed from figure 3.22(a) that the increase value of magnetic parameter leads to decrease the velocity up to the position of η = 4.4 after that position the velocity increase with the increase of intensity of magnetic field. It is also observed that the changes of velocity in the η direction reveals the typical velocity for natural convection boundary layer flow, i.e., the velocity is zero at the boundary wall then the velocity increases to the peak value as η increases and finally the velocity approaches to zero (the asymptotic value) but we see from this figure that all the velocity meet together at the position of η = 4.4 and cross the side. This is because of the velocity having lower peak values for higher values of magnetic parameter tend to decrease comparatively slower along η direction than velocity with higher peak values for lower values of magnetic parameter. Further from figure 3.22(b), it is seen that if intensity of magnetic field increases in the region $\eta \in$ [0, 10], the temperature near the surface is maximum and decreases away from the surface and finally approaches to zero.

The effect of variation of the temperature dependent viscosity on the development of streamlines and isotherms for Prandtl number Pr = 0.73, amplitude-to-length ratio of the wavy surface α = 0.3 and magnetic parameter M = 0.5 are presented in figures 3.23 and 3.24 respectively. The maximum values of ψ, that is, ψ_{max} are 6.46, 6.68, 6.78 and 6.81 for viscosity variation parameter ε = 0.0, 0.5, 1.0 and 2.0 respectively. From figure 3.23, it is seen that for the increased value of viscosity the flow rate in the boundary layer increase. From figure 3.24, it is observed that owing to the effect of temperature dependent viscosity the thermal boundary layer becomes thinner.

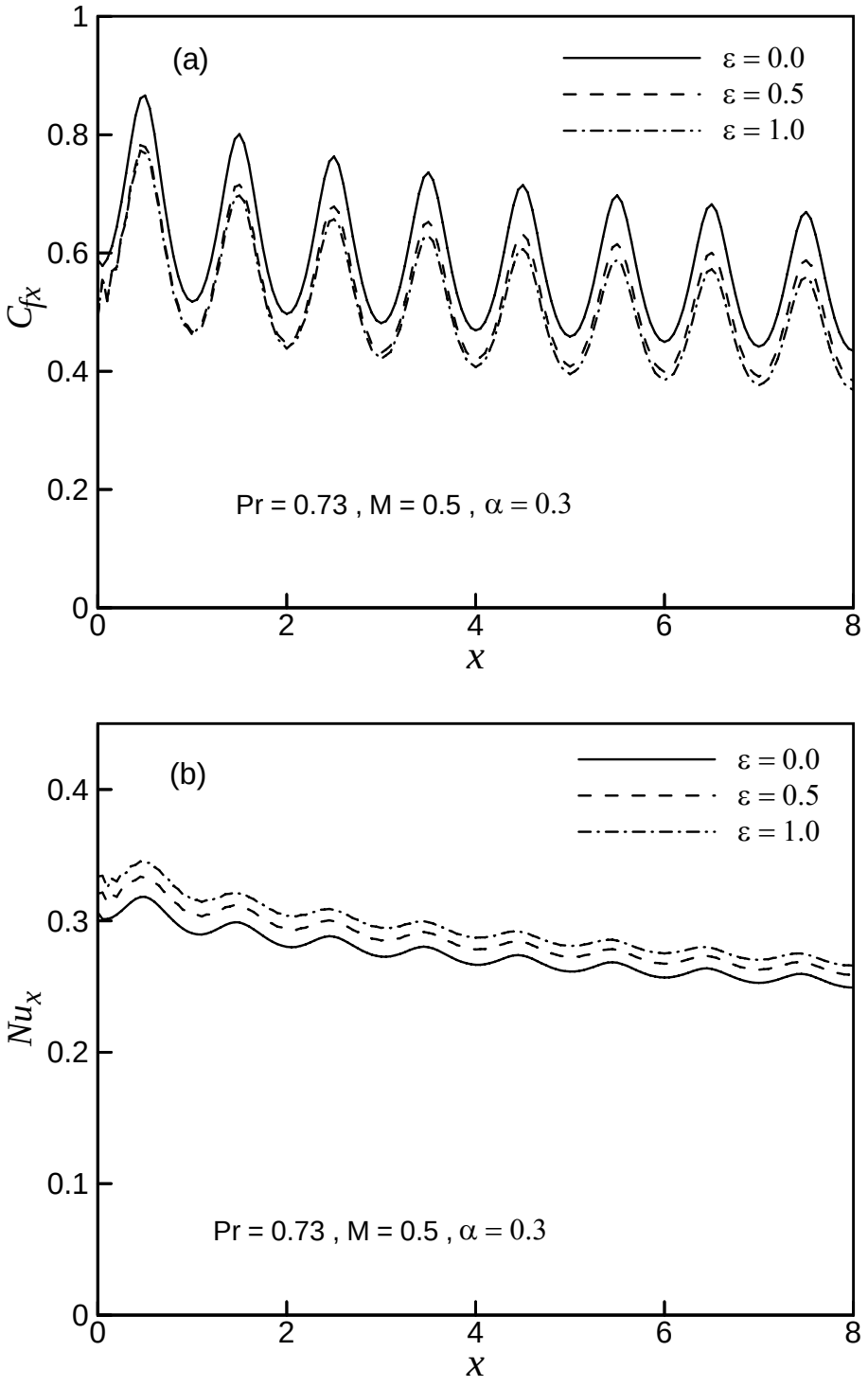

Figure 3.17: Variation of (a) skin friction coefficient C_{fx} and (b) rate of heat transfer Nu_x against dimensionless distance x for different values of viscosity parameter ε while α = 0.3, M = 0.5 and Pr = 0.73.

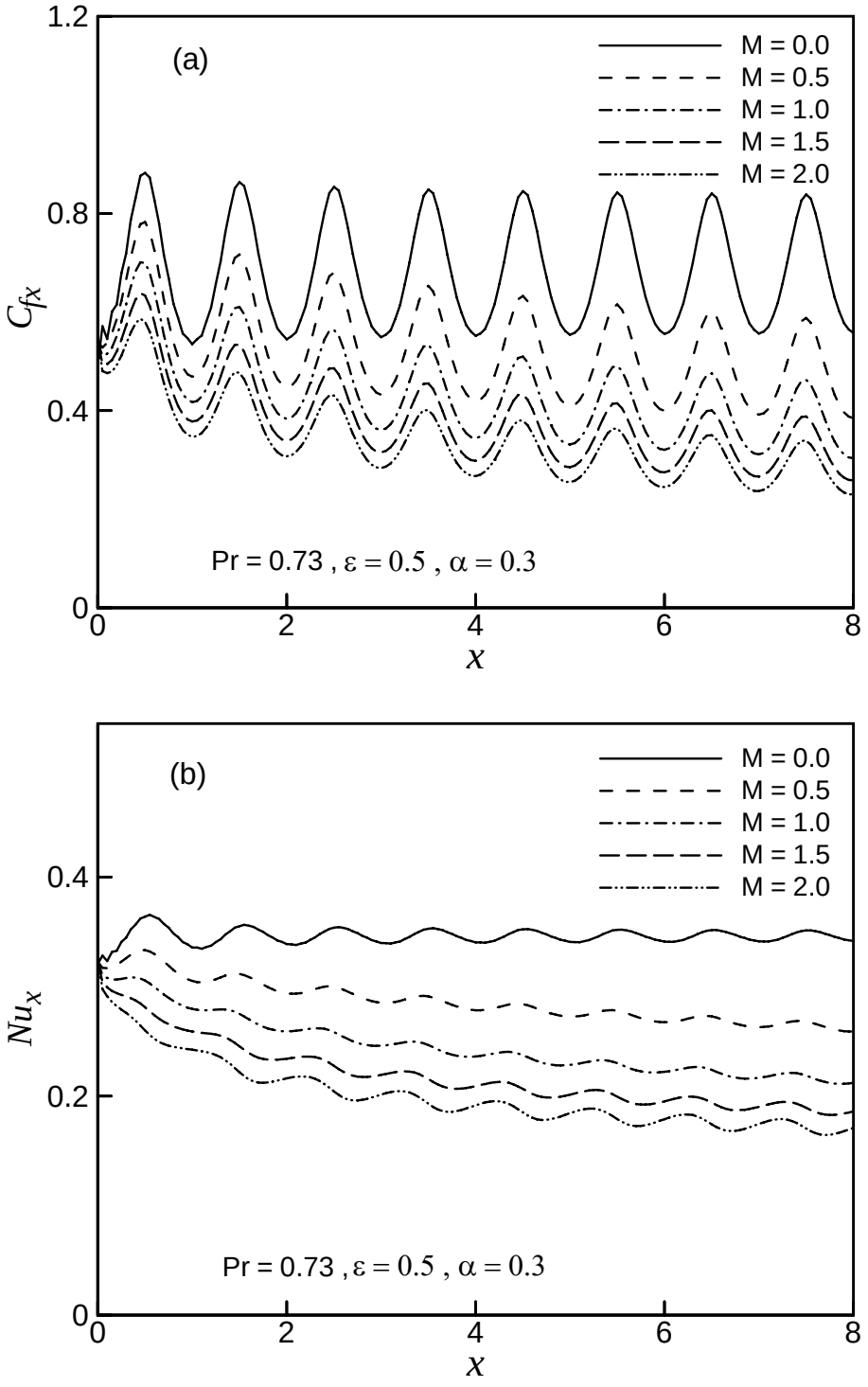

Figure 3.18: Variation of (a) skin friction coefficient C_{fx} and (b) rate of heat transfer Nu_x against dimensionless distance x for different values of magnetic parameter M with Pr = 0.73, α = 0.3 and ε = 0.5.

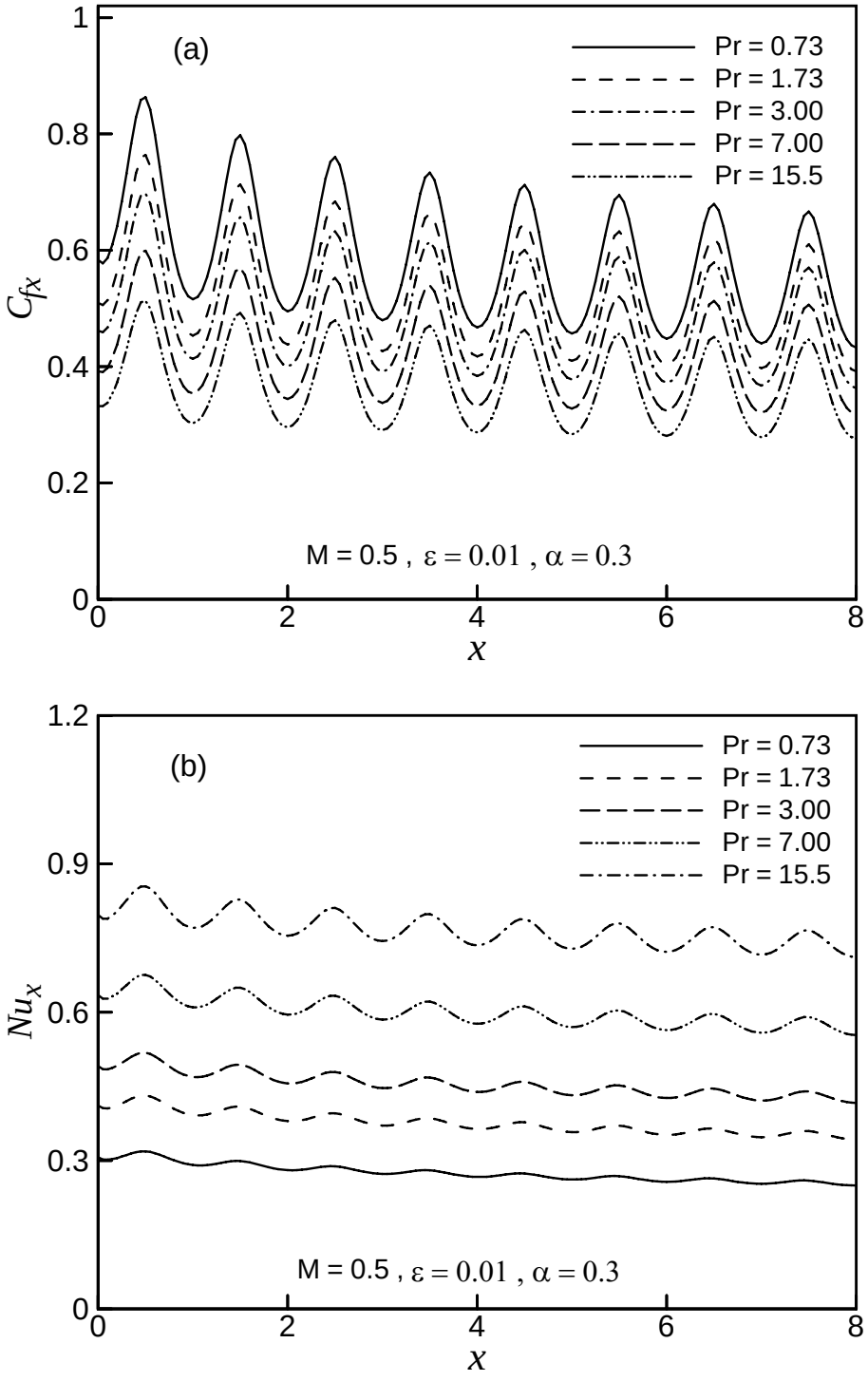

Figure 3.19: Variation of (a) skin friction coefficient C_{fx} and (b) rate of heat transfer Nu_x against dimensionless distance x for different values of Prandtl number Pr while $\alpha = 0.3$, $M = 0.5$ and $\varepsilon = 0.01$.

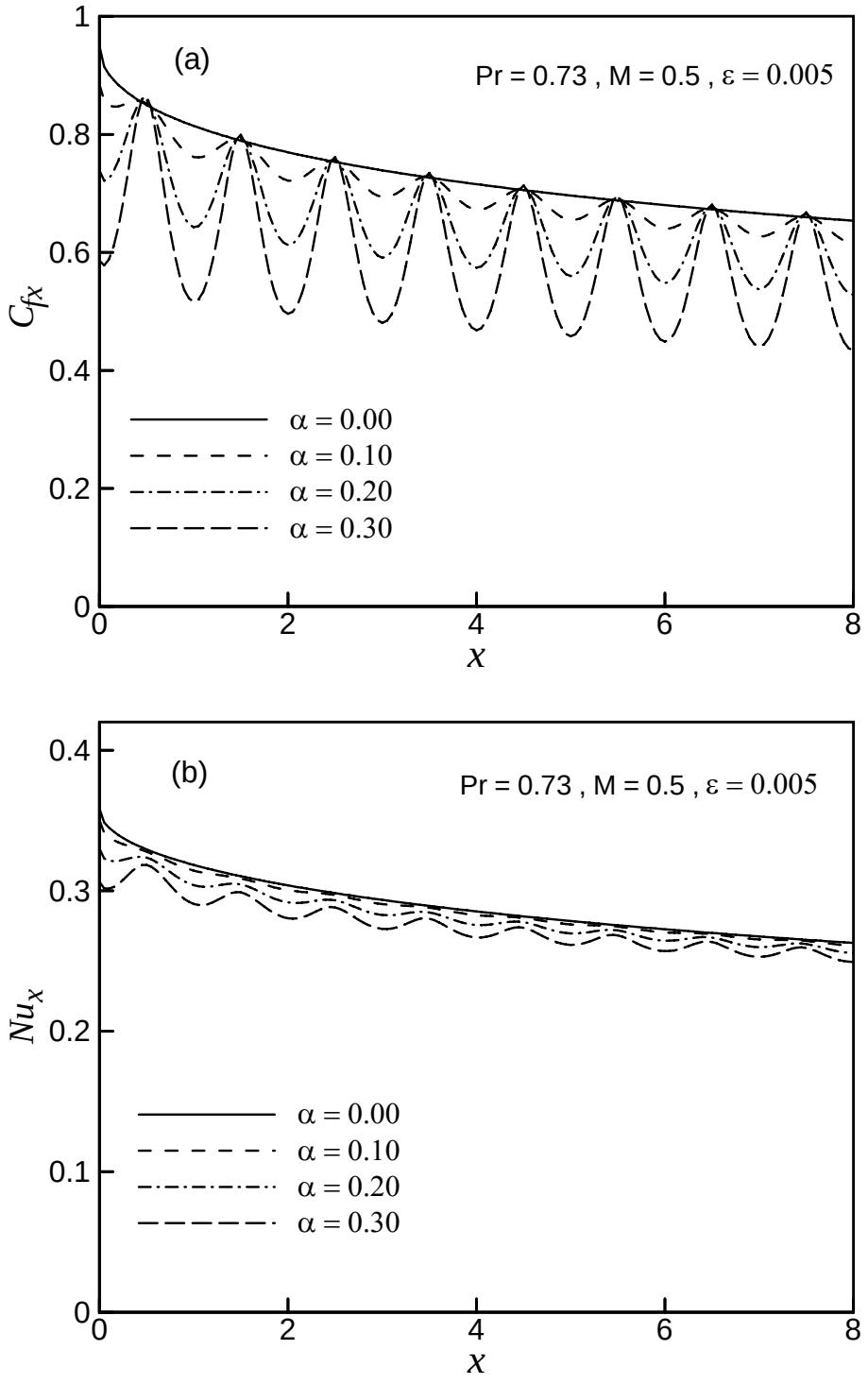

Figure 3.20: Variation of (a) skin friction coefficient C_{fx} and (b) rate of heat transfer Nu_x against dimensionless distance x for different values of α when Pr = 0.73, M = 0.5 and ε = 0.005.

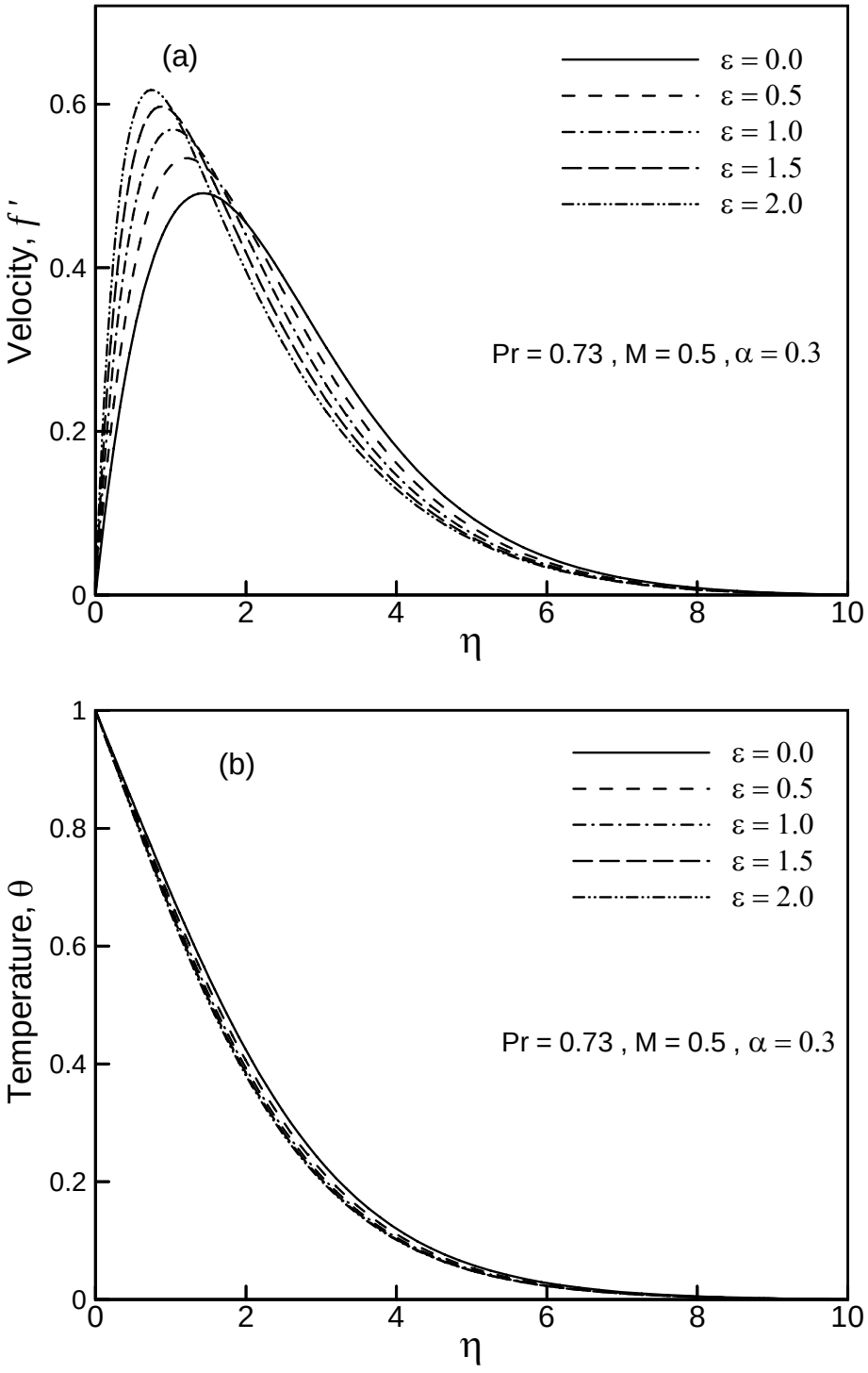

Figure 3.21: (a) Velocity profiles f' and (b) temperature distribution θ against dimensionless distance η for different values of viscosity parameter ε while $\alpha = 0.3$, $M = 0.5$ and Pr = 0.73.

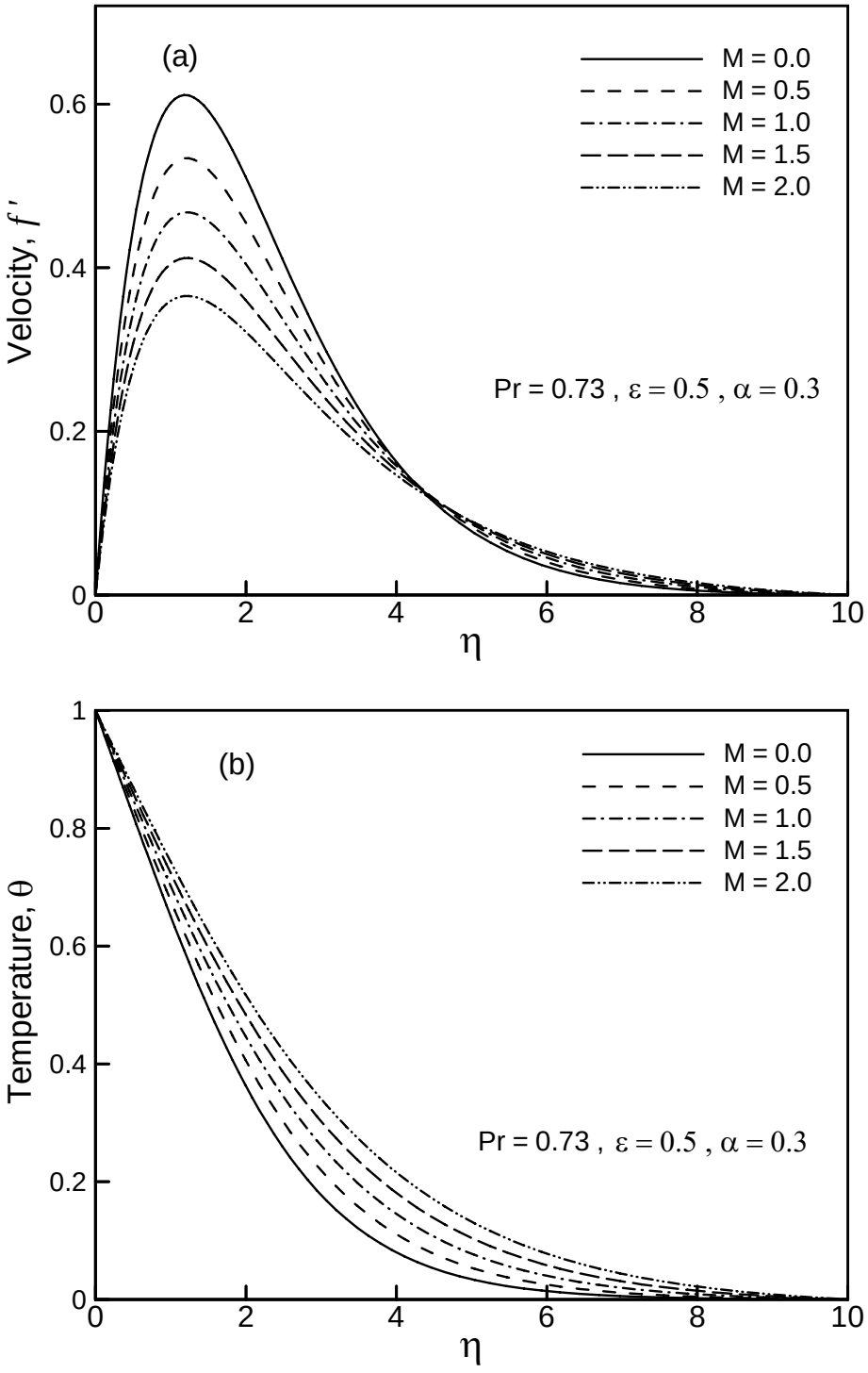

Figure 3.22: (a) Velocity profiles f' and (b) temperature distribution θ against dimensionless distance η for different values of magnetic parameter M with Pr = 0.73, α = 0.3 and ε = 0.5.

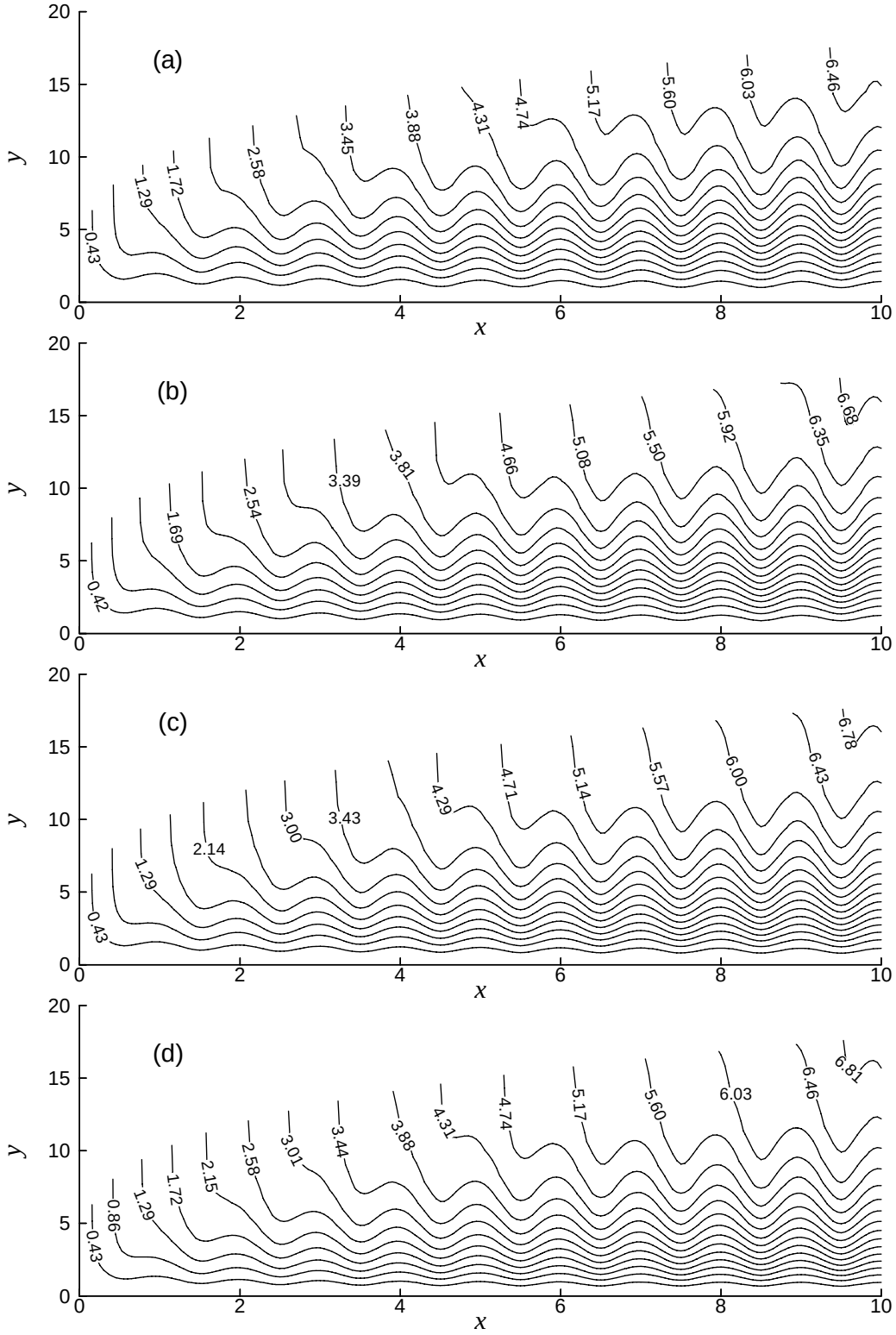

Figure 3.23: Streamlines for (a) $\varepsilon = 0.0$, (b) $\varepsilon = 0.5$ (c) $\varepsilon = 1.0$ and (d) $\varepsilon = 2.0$ while $M = 0.5$, $\alpha = 0.3$ and Pr = 0.73.

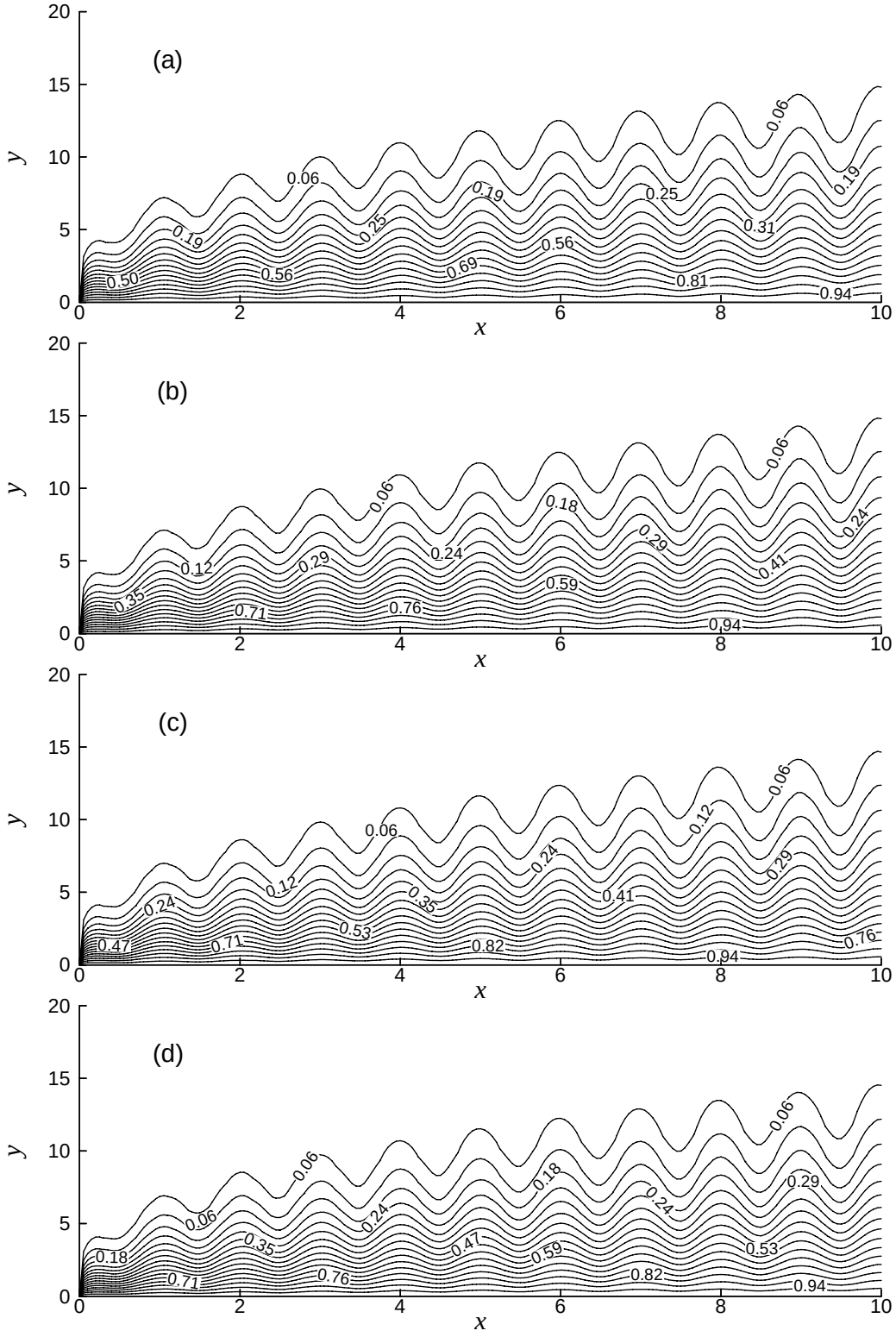

Figure 3.24: Isotherms for (a) ε = 0.0, (b) ε = 0.5 (c) ε = 1.0 and (d) ε = 2.0 while M = 0.5, α = 0.3 and Pr = 0.73.

3.3 Conclusions

The effects of the temperature dependent viscosity, the amplitude-to-length ratio of the wavy surface, the magnetic field and Prandtl number Pr on MHD natural convection flow of viscous incompressible fluid along a uniformly heated vertical wavy surface have been studied. From the present investigations the following conclusions may be drawn:

- When viscosity is linear function of temperature then the rate of heat transfer and the fluid velocity significantly reduce while the skin friction coefficient and the temperature increase for increasing values of viscosity parameter.
- The effect of increasing viscosity results in decreasing the local skin friction coefficient, the temperature and increasing the velocity, the local rate of heat transfer, over the whole boundary layer when viscosity considered inversely proportional to linear function of temperature.
- The skin friction coefficient, the velocity and the temperature decrease for increase of Prandtl number, over the whole boundary layer but the significant increase in the rate of heat transfer is observed.
- For higher values of Prandtl number, the velocity and thermal boundary layer strongly affected and become very thinner.
- Increased values of the intensity of magnetic field leads to decrease the skin friction coefficient, the rate of heat transfer and the velocity while the reverse phenomena occurs for the temperature.
- The flow rate decreases and the thermal boundary layer becomes thicker when the effect of magnetic field is considered.
- The rate of heat transfer and the skin friction coefficient decrease with the increase of amplitude-to-length ratio of the wavy surface, while the velocity and the temperature increase in the case of increasing the amplitude-to-length ratio of the wavy surface.
- The velocity and the thermal boundary layer become thicker slowly for the increasing value of the amplitude-to-length ratio of the wavy surface.

- The velocity of the fluid flow decreases quickly and the thermal boundary layer becomes thicker for increasing values of viscosity when it is considered as linear function of temperature and reverse phenomena occurs when viscosity is considered as inversely proportional to linear function of temperature.
- For temperature dependent viscosity, the viscosity variation parameter ε depend on the difference between the surface temperature and ambient temperature of the fluid. If the value of viscosity variation parameter ε is higher then this difference increases, this indicates that there will be more heat transfer from surface to the fluid within the boundary layer. In that why, temperature increases with the increasing value of viscosity. Temperature of the ambient fluid increases and temperature gradient at the surface decreases. So the rates of heat transfer decreases. Increasing viscosity decreases the velocity gradient normal to the wall. So the velocity of the fluid decreases quickly and fluid does not move freely. Fluid motion becomes slower. But when viscosity increased then the skin friction coefficient also increased because the skin friction coefficient is directly dependent on temperature dependent viscosity.
- The presence of the magnetic field acting along the horizontal direction retards the fluid velocity. For this a Lorentz force has been created within the flow region by the interaction between the applied magnetic field and flow field. This force acts against the direction of fluid flow and reduce the velocity and the skin friction coefficient. Due to interaction the temperature in the flow region increases and the temperature gradient at the wall as well as the heat transfer rate decreases. As a result the temperature profile gradually increases and thermal boundary layer grows thick.
- If the viscosity of the fluid is taken to be inversely proportional to linear function of temperature then velocity gradient normal to the wall increases. Velocity and the flow rate in the boundary layer increase. The skin friction coefficient directly depends on viscosity. When it is inversely proportional to linear function of temperature then the skin friction coefficient decreases for increasing value of viscosity. Viscosity also depends on the difference between the surface temperature and ambient temperature of the fluid. If this difference

increases then viscosity reduces the fluid temperature that causes thinner thermal boundary layer. Surface temperature as well as temperature gradient at the surface increases. Then the rates of heat transfer increase when viscosity is considered inversely proportional to linear function of temperature.

- The effect of viscosity is vary small when it is considered inversely proportional to linear function of temperature with other parameters. The values of viscosity considered in this case are all critical values.

CHAPTER 4

Effect of temperature dependent thermal conductivity on MHD natural convection flow

4.1 Introduction

The property of thermal conductivity changes significantly with temperature. It is essential to take into account the variation of thermal conductivity along a vertical wavy surface to obtain a better estimation of the flow and heat transfer behavior. Convective heat transfer has attracted the attention of engineers and scientists from many varying disciplines such as, chemical, civil, environmental, mechanical, aerospace, nuclear engineering, applied mathematics, geothermal physics, food science, etc. Flow and heat transfer from a wavy surface is often encountered in many engineering applications to enhance heat transfer such as micro-electronic devices, flat-plate solar collectors and flat-plate condensers in refrigerators, the molten core of the earth etc, electric machinery, cooling system of micro-electronic devices etc. In addition, roughened surfaces can be used in the cooling of electrical and nuclear components where the wall heat flux is known.

The present investigation is concerned with the effect of temperature dependent thermal conductivity on magnetohydrodynamic natural convection flow of viscous incompressible fluid along a uniformly heated vertical wavy surface. In formulating the equations governing the flow thermal conductivity of the fluid is considered to be linear function of temperature. The governing boundary layer equations (2.51) to (2.53) are first transformed into a non-dimensional form (2.56) to (2.58) using suitable set of dimensionless variables (2.55). The resulting nonlinear system of partial differential equations are mapped into the domain of a vertical flat plate and then solved numerically employing the implicit finite difference method, known as the Keller-box scheme. The numerical results of the surface shear stress in terms of skin friction coefficient and the rate of heat transfer in terms of local Nusselt number, the velocity and temperature profiles as well as the stream lines and the isotherms are shown graphically for a selection of parameters set consisting of thermal

conductivity parameter γ, magnetic parameter M, Prandtl number Pr and the amplitude-to-length ratio of the wavy surface α. Numerical results of the local skin friction coefficient and the rate of heat transfer for different values are presented in tabular form.

4.2 Results and discussion

There are four parameters of interest in the present problem, the effects of varying γ the temperature dependent thermal conductivity, the intensity of magnetic field, Prandtl number Pr and the amplitude-to-length ratio of the wavy surface on the surface shear stress in terms of local skin friction coefficient, the rate of heat transfer in terms of the local Nusselt number, the velocity profiles, the temperature profiles, the streamlines and the isotherms. Numerical values of local rate of heat transfer and shearing stress are calculated from equations (2.64) and (2.65) in terms of the Nusselt number Nu_x and skin friction coefficient C_{fx} respectively for a wide range of the axial distance x starting from the leading edge for different values of the aforementioned parameters γ, M, Pr and α. Numerical values of the skin friction coefficient C_{fx}, the rate of heat transfer in terms of the Nusselt number Nu_x, velocity profiles, temperature profiles, the streamlines and the isotherms are obtained for different values of thermal conductivity parameter $\gamma = 0.0$ (constant thermal conductivity) to 12.0, magnetic parameter ranging from $M = 0.0$ (non magnetic field) to 3.5, Prandtl number Pr = 0.73, 1.73, 4.24, 7.0, 9.45 and 13.5 which correspond to the air at 2100^0K, water at 100^0C, 40^0C, 20^0C, 10^0C and 0.01^0C respectively and the amplitude-to-length ratio of the wavy surface ranging from $\alpha = 0.0$ (flat plate) to 0.4 and these are shown graphically in figures 4.1- 4.15.

The effect for different values of temperature dependent thermal conductivity (γ = 0.0, 1.0, 4.0, 7.0, 12.0) on the skin friction coefficient and the heat transfer coefficient while Prandtl number Pr = 1.0, $\alpha = 0.3$ and $M = 0.8$ are shown in figures 4.1(a)-4.1(b) respectively. If the value of thermal conductivity parameter increases, the skin friction coefficient increases slowly and heat transfer coefficient increases monotonically along the upstream direction of the surface against x. The maximum values of the skin friction coefficient are recorded to be 0.78350, 0.84982, 0.93324, 0.96996 and 1.00 for γ = 0.0, 1.0, 4.0, 7.0, 12.0 and each of which occurs at same

point x = 0.50. However, the highest values of the rate of heat transfer are found to be 0.34186, 0.47389, 0.77061, 1.00287 and 1.34865 respectively. It occurs at the surface because thermal conductivity of solid is greater than that of fluid. Here it is observed that the skin friction coefficient and the rate of heat transfer coefficient increase by approximately 22% and 75% respectively when the value of thermal conductivity parameter changes from 0.0 to 12.0. The higher value of the thermal conductivity accelerates the fluid flow, increases the skin friction coefficient and also the heat transfer coefficient.

The variation of the local skin friction coefficient C_{fx} and local rate of heat transfer Nu_x for different values of Prandtl number (Pr = 0.73, 1.73, 4.24, 7.0, 9.45, 13.5) for γ = 5.0 and M = 0.8 are shown in figures 4.2(a)-4.2(b) respectively while α = 0.2. The influence of Prandtl number Pr, the surface shear stress in terms of local skin friction coefficient becomes slower in the downstream region. On the other hand, for increased values of Prandtl number the rate of heat transfer increases significantly against the axial distance of x. In this case the maximum values of local skin friction coefficient are 0.97199 and 0.67547 for Pr = 0.73 and 13.5 respectively which occurs at same point x = 0.45. Here it is observed that at x = 0.45 the skin friction coefficient decreases by approximately 31% due to the increased value of Pr. Again figure 4.2(b) shows that the maximum values of rate of heat transfer are 0.80666 and 2.28076 for Pr = 0.73 and 13.5 respectively and the heat transfer rate increases by approximately 65% as Pr changes from Pr = 0.73 to 13.5. Each of this occurs at the surface.

Figures 4.3(a)-4.3(b) show that the skin friction coefficient C_{fx} and the rate of heat transfer coefficient Nu_x decrease gradually from zero value at lower stagnation point along the x direction for the effect of magnetic field while Pr = 1.0, γ = 5.0 and α = 0.2. The maximum values of skin friction coefficient and the rate of heat transfer are recorded to be 1.14600, 0.88607 and 0.97925, 0.91644 for M = 0.0 and 3.5 respectively which occurs at the different position of x. It is noted that, the skin friction coefficient and the local Nusselt number decrease by approximately 23% and 6% respectively as the magnetic parameter M changes from 0.0 to 3.5.

The influence of the amplitude-to-length ratio of the wavy surface (α = 0.0, 0.2, 0.3, 0.4) leads to decrease the frictional force and the temperature gradient in terms of the heat transfer rate while Pr = 0.73, M = 0.8 and γ = 2.0 which are depicted in figures 4.4(a) and 4.4(b) respectively. The maximum values of the skin friction coefficient and the rate of heat transfer in terms of the local Nusselt number Nu_x are 1.12831 and 0.70567 respectively for α = 0.0 which occurs at the surface and 0.93936, 0.59409 respectively for α = 0.4 which occurs at the different position of x. It is seen that the skin friction coefficient and the rate of heat transfer decrease by approximately 17% and 16% respectively when the amplitude-to-length ratio of the wavy surface increases from 0.0 to 0.4.

The variation of temperature dependent thermal conductivity (γ = 0.0, 1.0, 4.0, 7.0,12.0) on the velocity $f'(x,\eta)$ and the temperature $\theta(x,\eta)$ within the boundary layer with other fixed parameters, α = 0.3, M = 0.8 and Pr = 1.0 are displayed in figure 4.5(a) and figure 4.5(b) respectively. As $\gamma = \gamma^*(T_w - T_\infty)$, so the increasing value of thermal conductivity parameter increases the temperature difference between the surface and ambient temperature of the fluid. Then heat is transferred quickly from surface to fluid within the boundary layer. For this reason both the velocity and temperature increase with the increasing value of thermal conductivity parameter. Moreover, the maximum values of velocity are found to be 0.41757, 0.48675, 0.59503, 0.65093 and 0.69985 for γ = 0.0, 1.0, 4.0, 7.0 and 12.0 respectively and each of which occurs at different position of η. It is observed that the velocity increases by approximately 40% as γ changes from 0 to 12.0.

Figure 4.6(a) and figure 4.6(b) deal with the effect of Prandtl number (Pr = 0.73, 1.73, 4.24, 7.0, 9.45, 13.5) when the values of amplitude-to-length ratio of the wavy surface α = 0.2, γ = 5.0 and M = 0.8 on the velocity $f'(x,\eta)$ and the temperature $\theta(x,\eta)$. When Prandtl number Pr increases then both the velocity and temperature decrease along the downstream direction against x, this is shown in figure 4.6. It is seen that the velocity decreases by approximately 55% when Pr increases from 0.73 to 13.5. Increasing values of Pr increases viscosity and decreases thermal action of the fluid. When viscosity increases then fluid does not move freely and finally velocity and temperature decrease.

The magnetic field acting along the horizontal direction retards the fluid velocity. The values of α = 0.2, γ = 5.0 and Pr = 1.0 are shown in figure 4.7(a). A Lorentz force is created by the interaction between the applied magnetic field and flow field. This force acts against the fluid flow and reduces the velocity. From figure 4.7(b), it is observed that the temperature within the boundary layer increases monotonically for increasing values of intensity of magnetic field from 0 to 3.5.

The effect of the temperature dependent thermal conductivity on the development of streamlines and isotherms are plotted in figures 4.8 and 4.9 respectively while Pr = 1.0, α = 0.3 and M = 0.8. It is found that for γ = 0.0 the value of ψ_{max} is 4.56, for γ = 4.0 ψ_{max} is 7.51, for γ = 7.0 ψ_{max} is 8.52 and ψ_{max} is 9.09 where γ = 10.0. So from figure 4.8, it is seen that the effect of temperature dependent thermal conductivity, the flow rate in the boundary layer strongly affected and leads to thicker velocity boundary layer. From figure 4.9, it is also observed that for the effect of thermal conductivity, the thermal boundary layer becomes thicker.

Figures 4.10 and 4.11 show the effect of Prandtl number on the formation of streamlines and isotherms respectively for the amplitude-to-length ratio of the wavy surface α = 0.2, M = 0.8 and γ = 5.0. It can be seen that for Pr equal to 0.73, 4.24, 9.45 and 13.5 the maximum values of ψ, that is, ψ_{max} are 8.71, 4.18, 2.71 and 2.19 respectively. So it is concluded that for higher values of Pr both the momentum and the thermal boundary layer become thinner.

The variation of the surface roughness on the streamlines and isotherms for the values of intensity of magnetic field equal to 0.0, 1.5, 2.5 and 3.5 are depicted in the figure 4.12 and figure 4.13 respectively while Pr = 1.0, α = 0.2 and γ = 5.0. From figure 4.13, it is observed that when the effect of magnetic field considered, the temperature of the fluid flow within the boundary layer becomes higher. On the other hand, the maximum values of ψ decreases monotonically while the values of intensity of magnetic field increases that depicts in figure 4.12. The maximum values of ψ, that is, ψ_{max} are 12.88, 5.41, 3.57 and 2.63 for M = 0.0, 1.5, 2.5 and 3.5 respectively.

The effect of variation of the surface roughness on the streamlines and isotherms for the values of the amplitude-to-length ratio of the wavy surface equal to 0.0, 0.2 and

0.3 are shown in the figure 4.14 and figure 4.15 respectively while Pr = 0.73, M = 0.8 and γ = 2.0. Figure 4.14 depicts that the maximum values of ψ increases slowly as the values of α increases. The maximum values of ψ, that is, ψ_{max} are 7.61, 7.72 and 8.02 for α = 0.0, 0.2 and 0.3 respectively. Figure 4.15 shows that for increasing values of the amplitude-to-length ratio of the wavy surface, the temperature of the fluid flow within the boundary layer becomes higher.

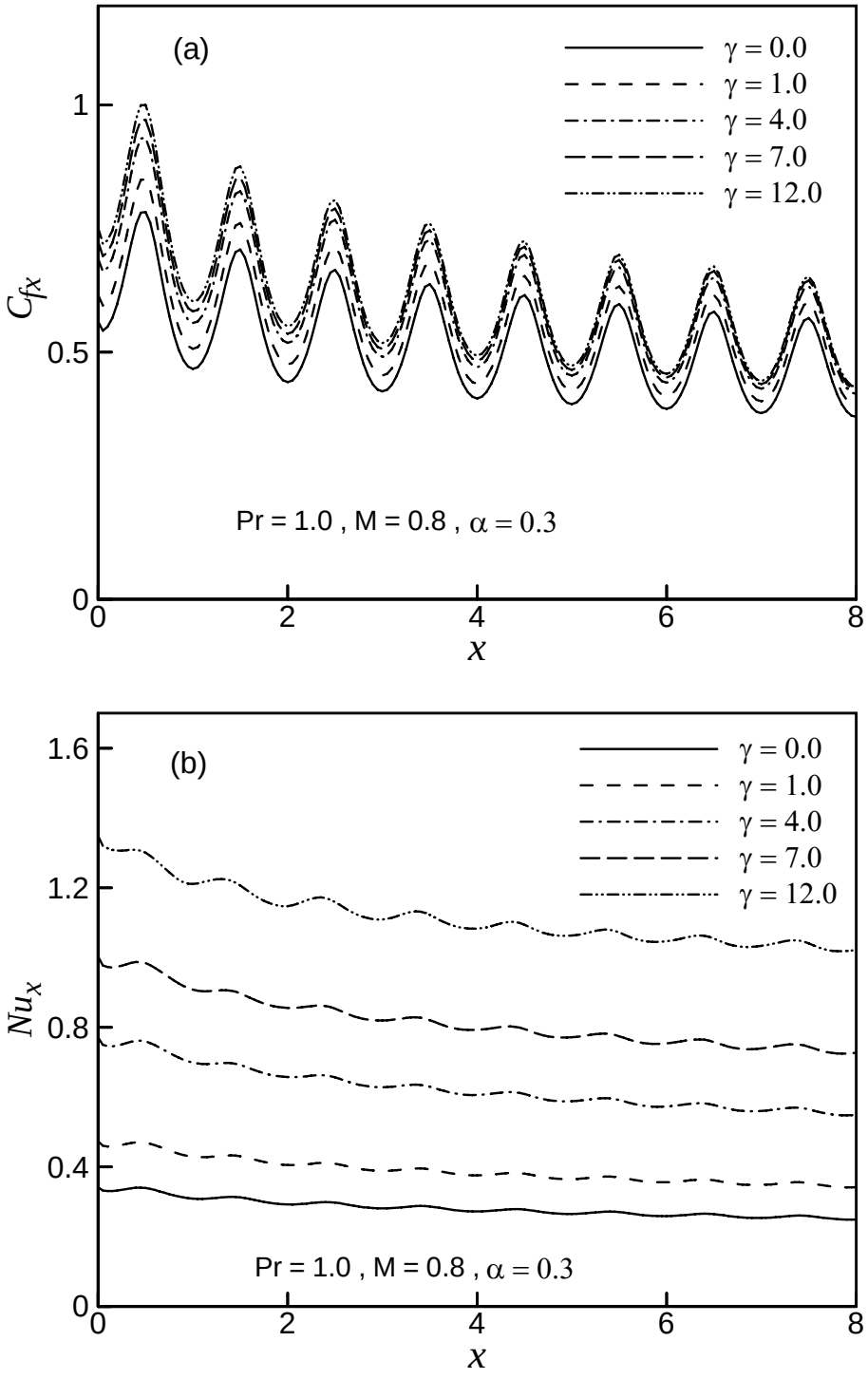

Figure 4.1: Variation of (a) skin friction coefficient C_{fx} and (b) rate of heat transfer Nu_x against dimensionless distance x for different values of thermal conductivity variation parameter γ while $\alpha = 0.3$, $M = 0.8$ and Pr = 1.0.

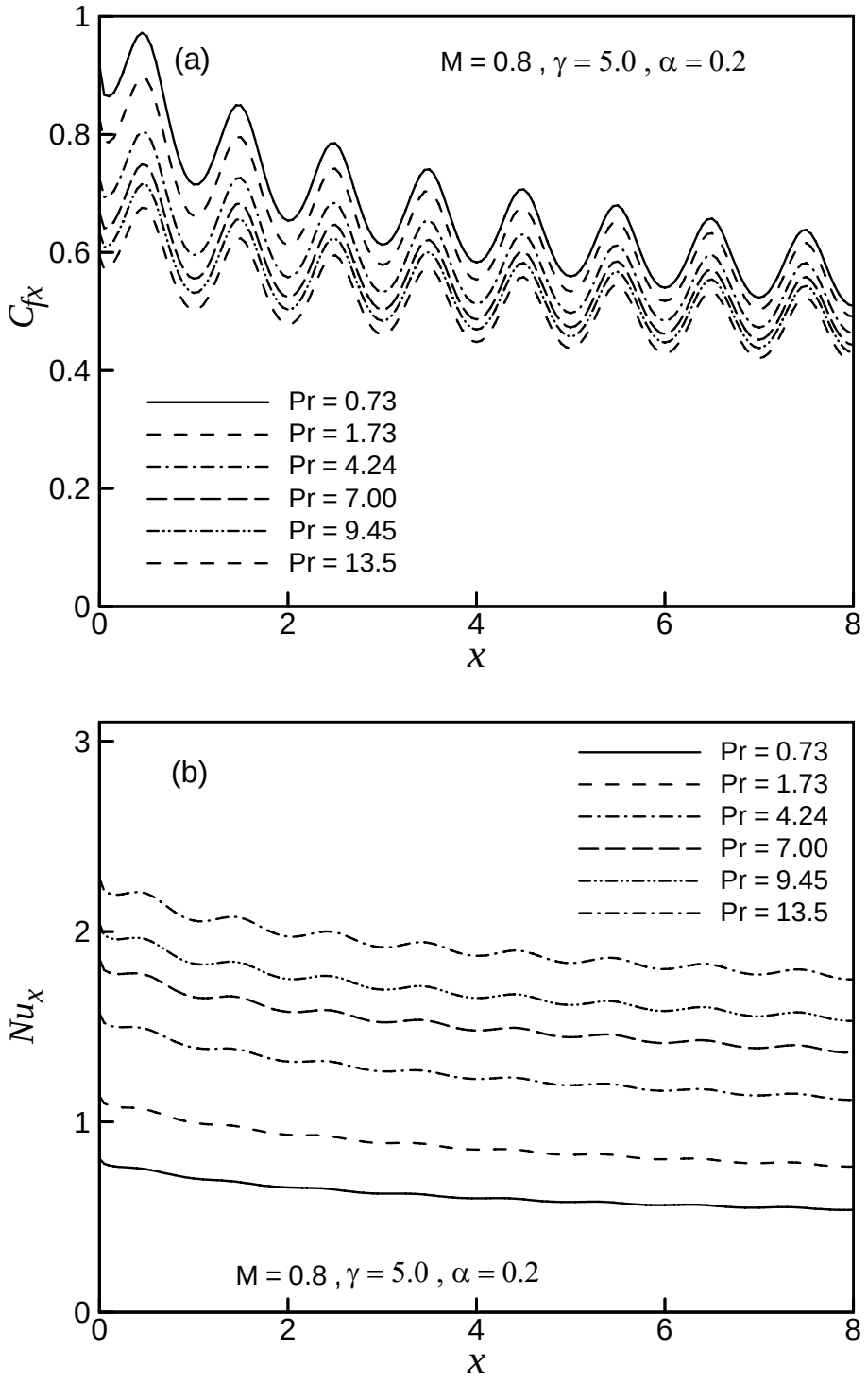

Figure 4.2: Variation of (a) skin friction coefficient C_{fx} and (b) rate of heat transfer Nu_x against dimensionless distance x for different values of Prandtl number Pr while $\alpha = 0.2$, $M = 0.8$ and $\gamma = 5.0$.

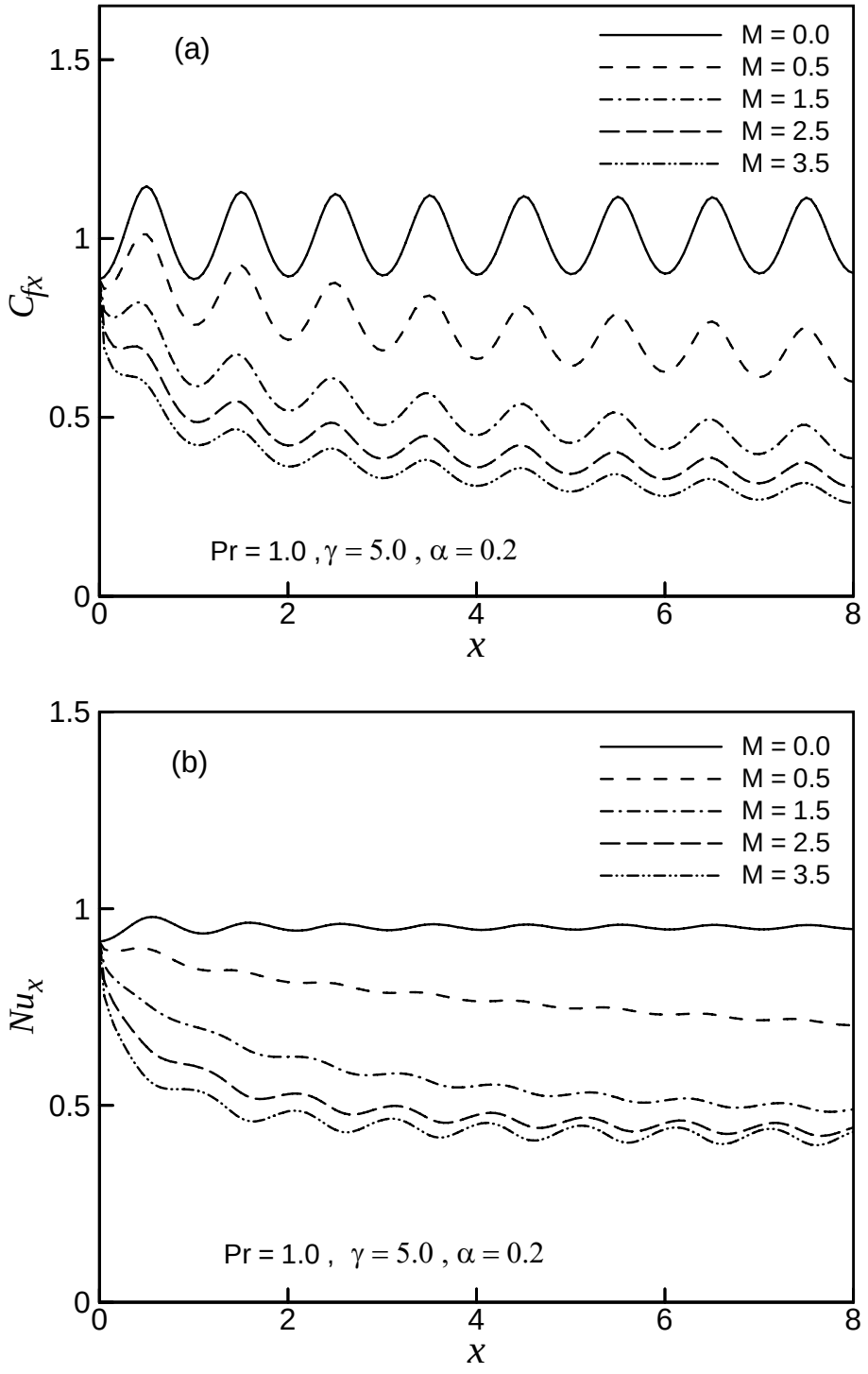

Figure 4.3: Variation of (a) skin friction coefficient C_{fx} and (b) rate of heat transfer Nu_x against dimensionless distance x for different values of magnetic parameter M with Pr = 1.0, $\alpha = 0.2$ and $\gamma = 5.0$.

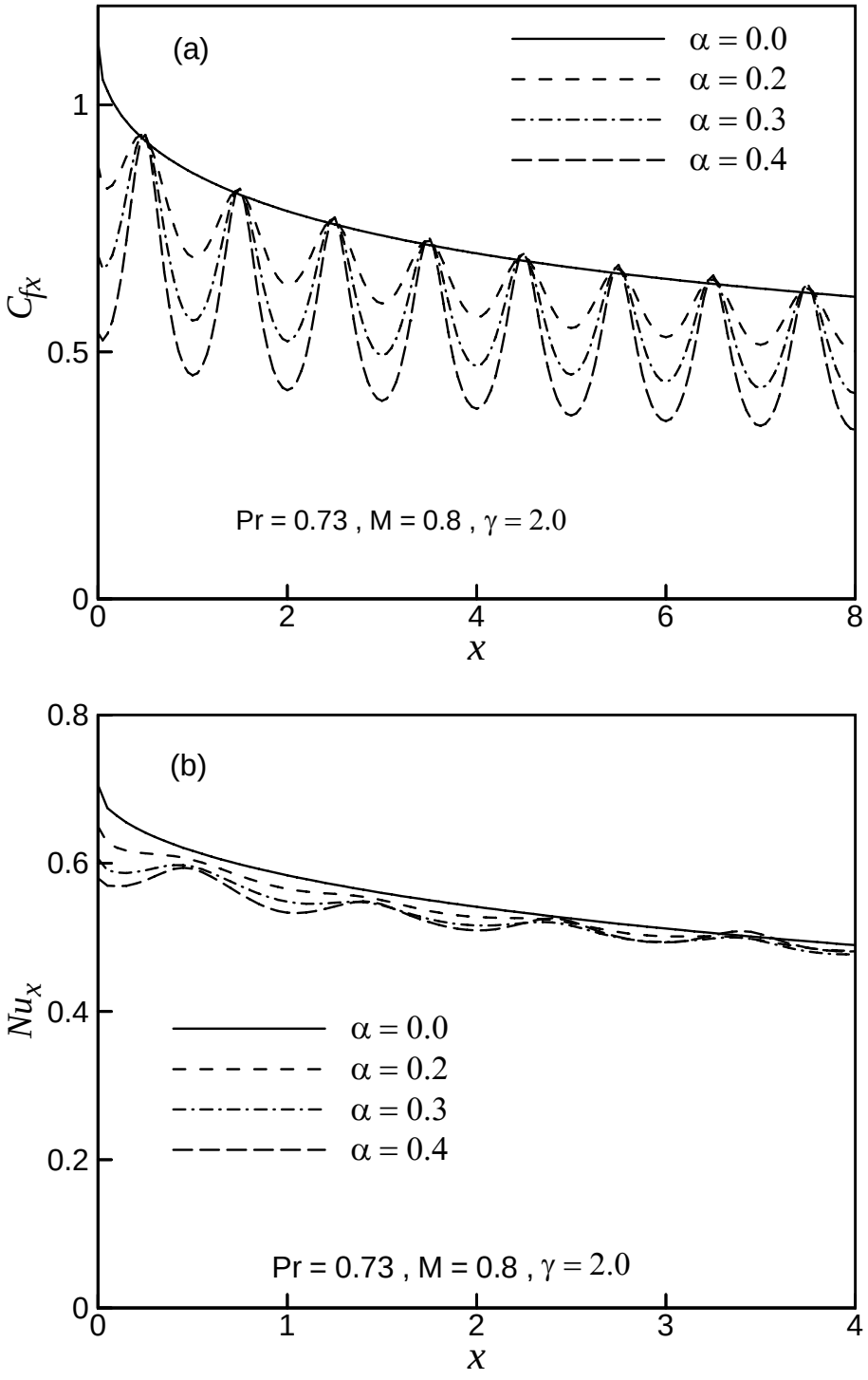

Figure 4.4: Variation of (a) skin friction coefficient C_{fx} and (b) rate of heat transfer Nu_x against dimensionless distance x for different values of amplitude-to-length ratio of the wavy surface α when Pr = 0.73, M = 0.8 and γ = 2.0.

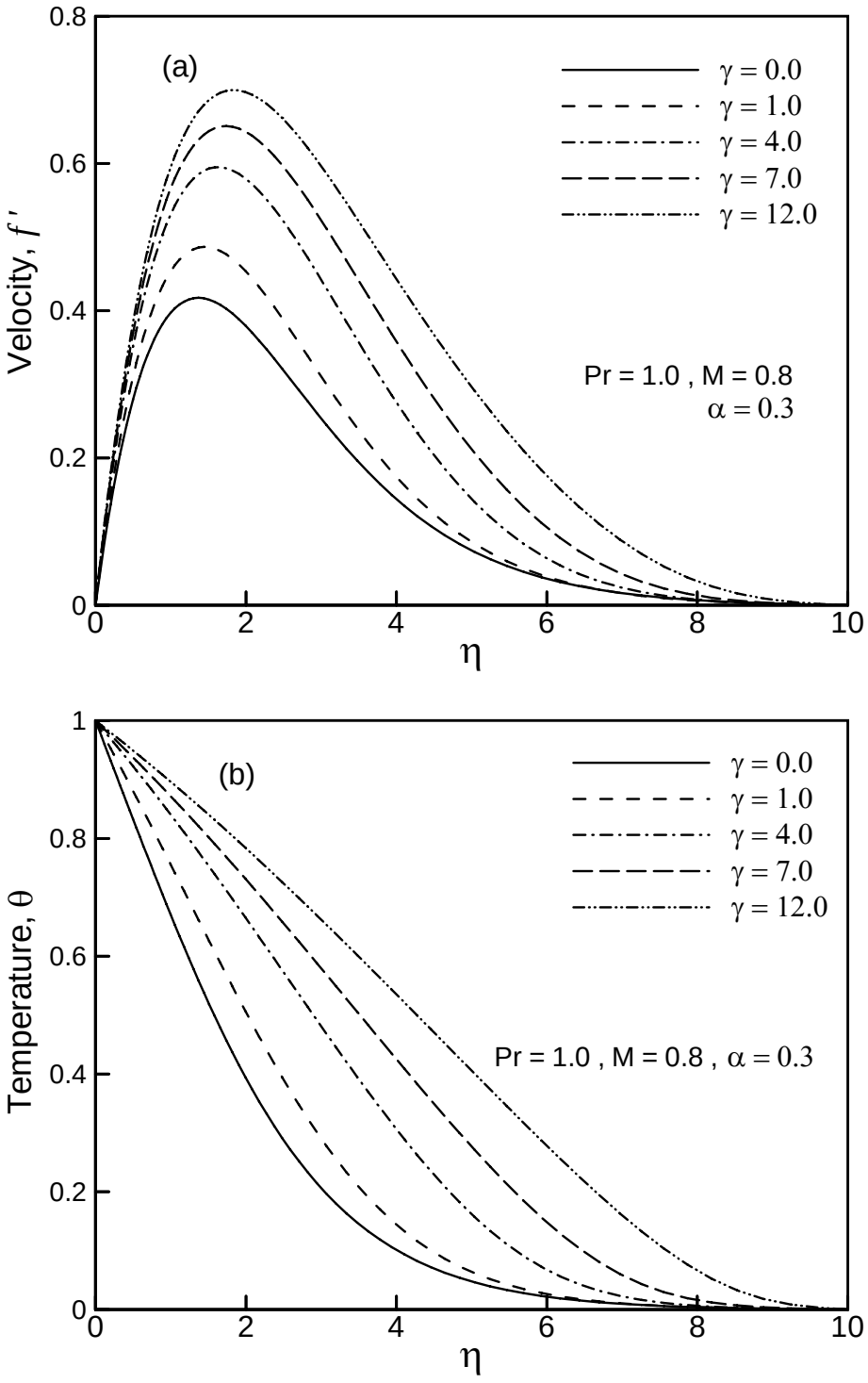

Figure 4.5: (a) Velocity profiles f' and (b) temperature distribution θ against dimensionless distance η for different values of γ while $\alpha = 0.3$, $M = 0.8$ and Pr = 1.0.

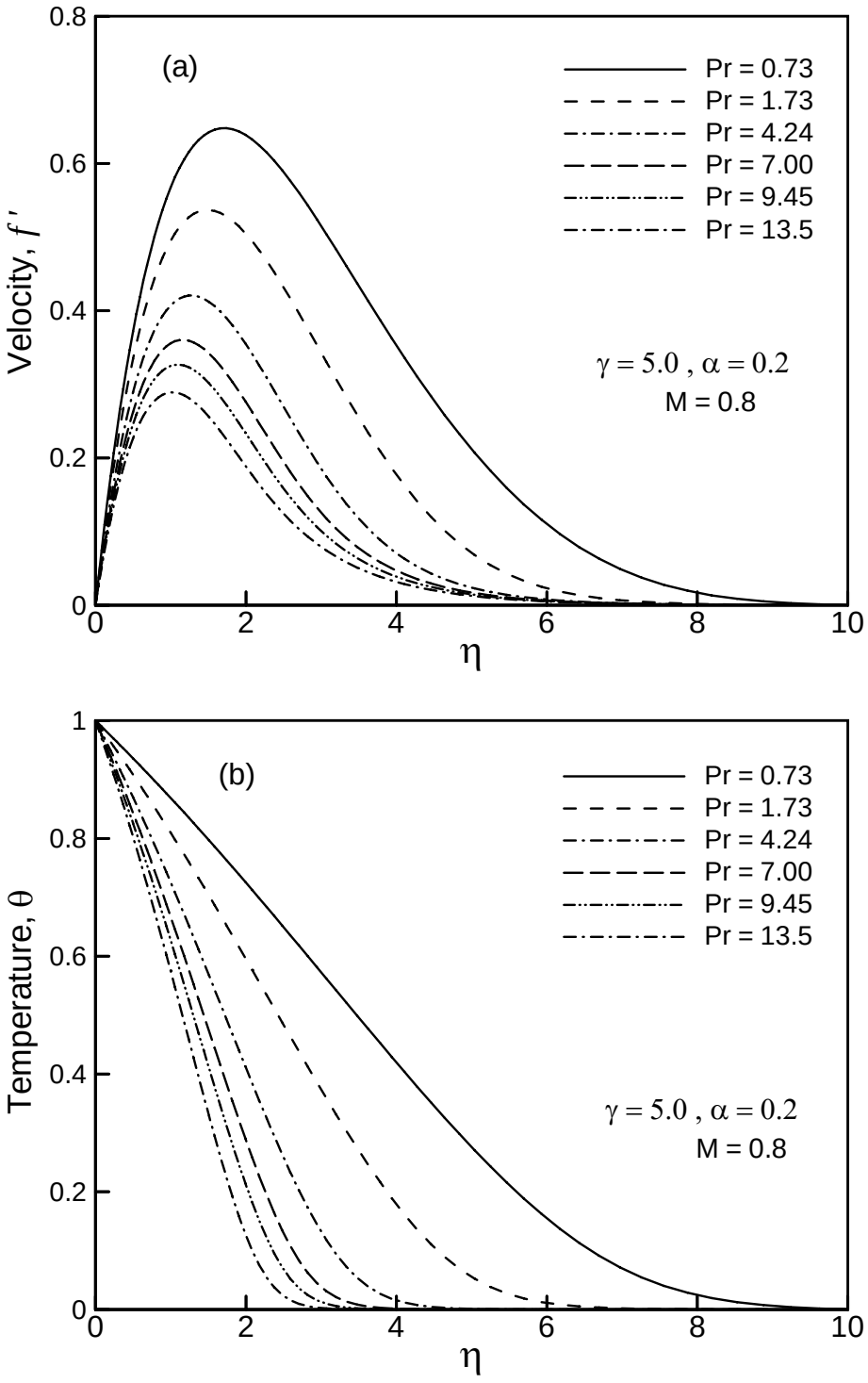

Figure 4.6: (a) Velocity profiles f' and (b) temperature distribution θ against dimensionless distance η for different values of Prandtl number Pr with $M = 0.8$, $\alpha = 0.2$ and $\gamma = 5.0$.

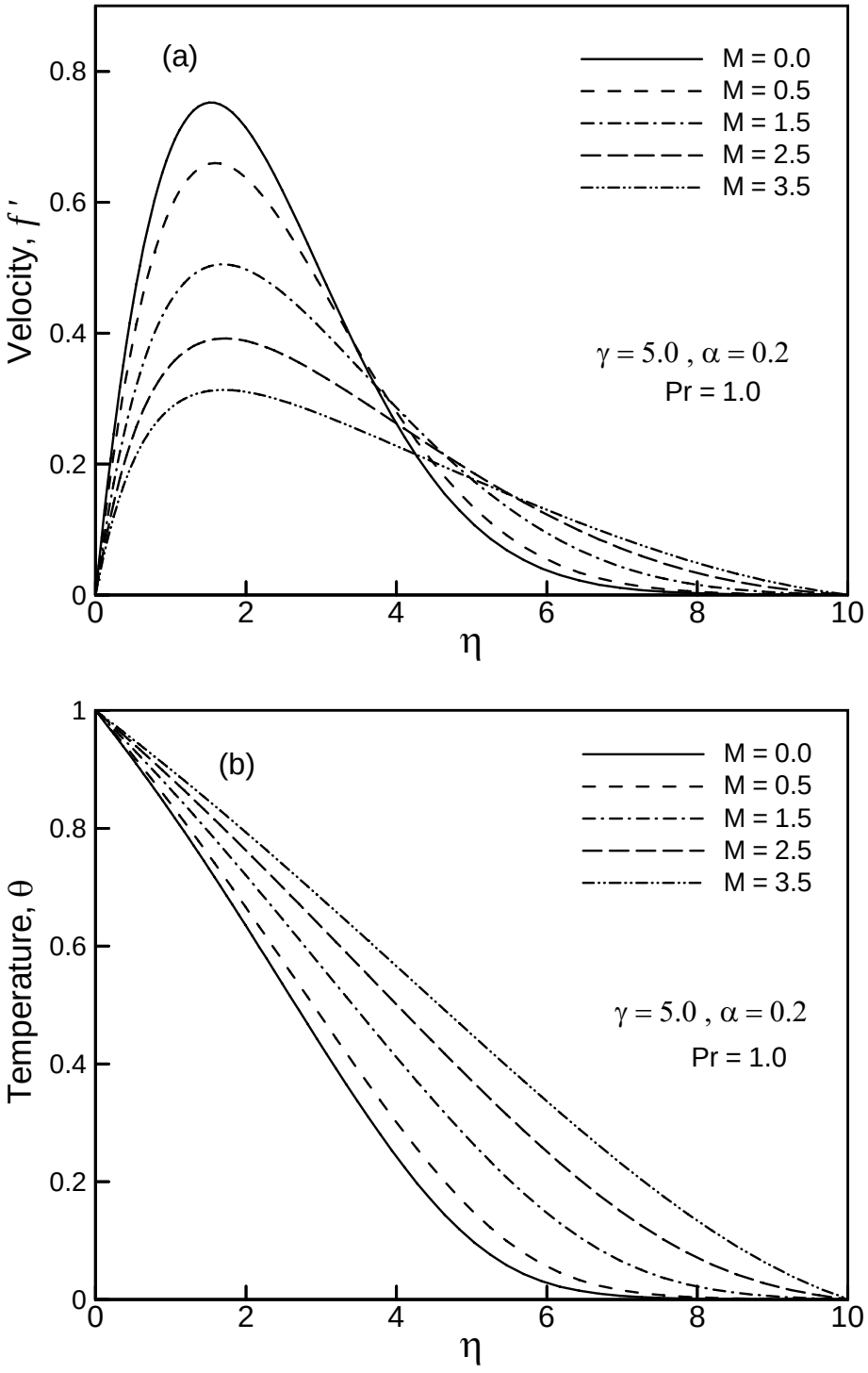

Figure 4.7: (a) Velocity profiles f' and (b) temperature distribution θ against dimensionless distance η for different values of magnetic parameter M with Pr = 1.0, $\alpha = 0.2$ and $\gamma = 5$.

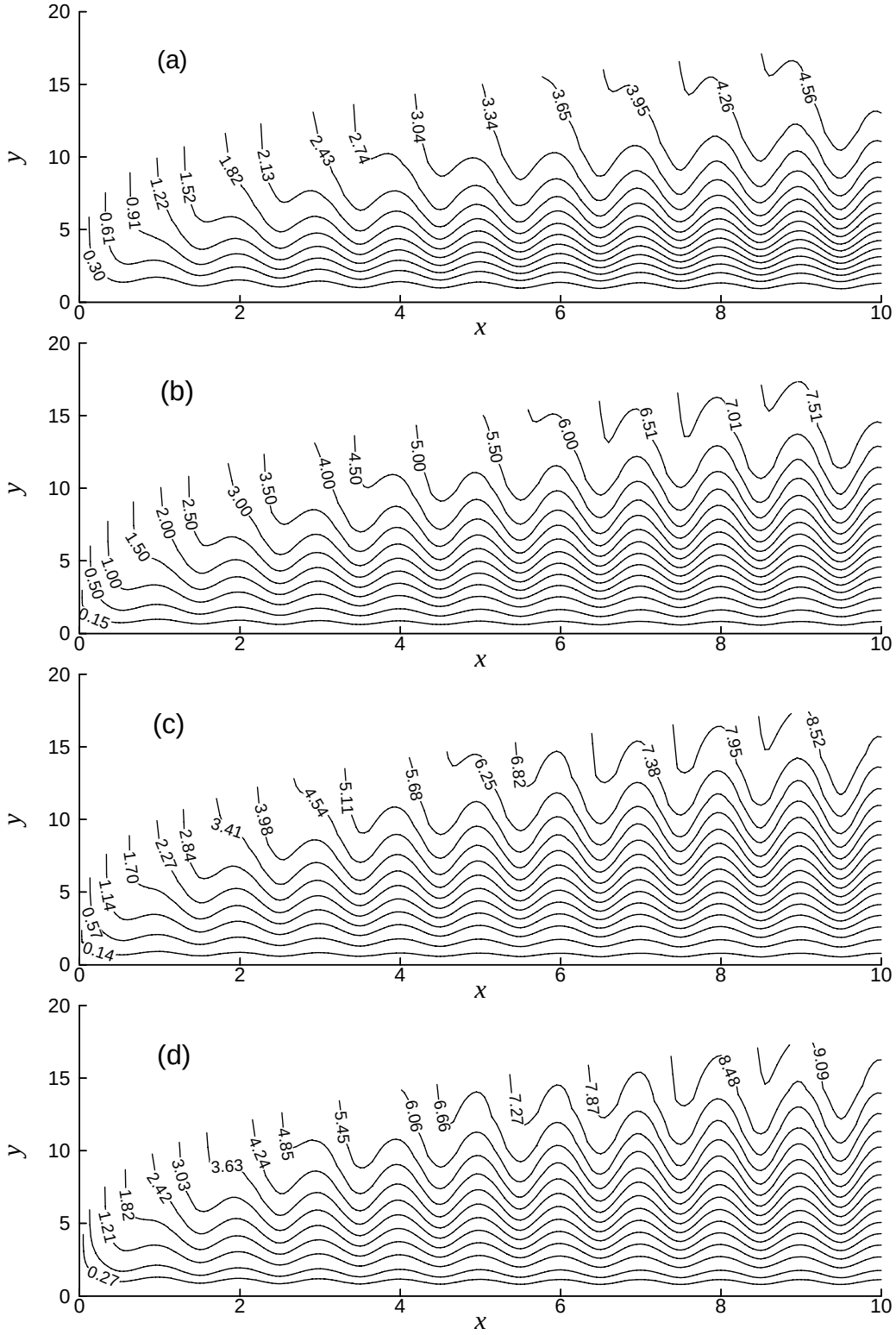

Figure 4.8: Streamlines for (a) γ = 0.0 (b) γ = 4.0 (c) γ = 7.0 (d) γ = 10.0 while Pr = 1.0, α = 0.3 and M = 0.8.

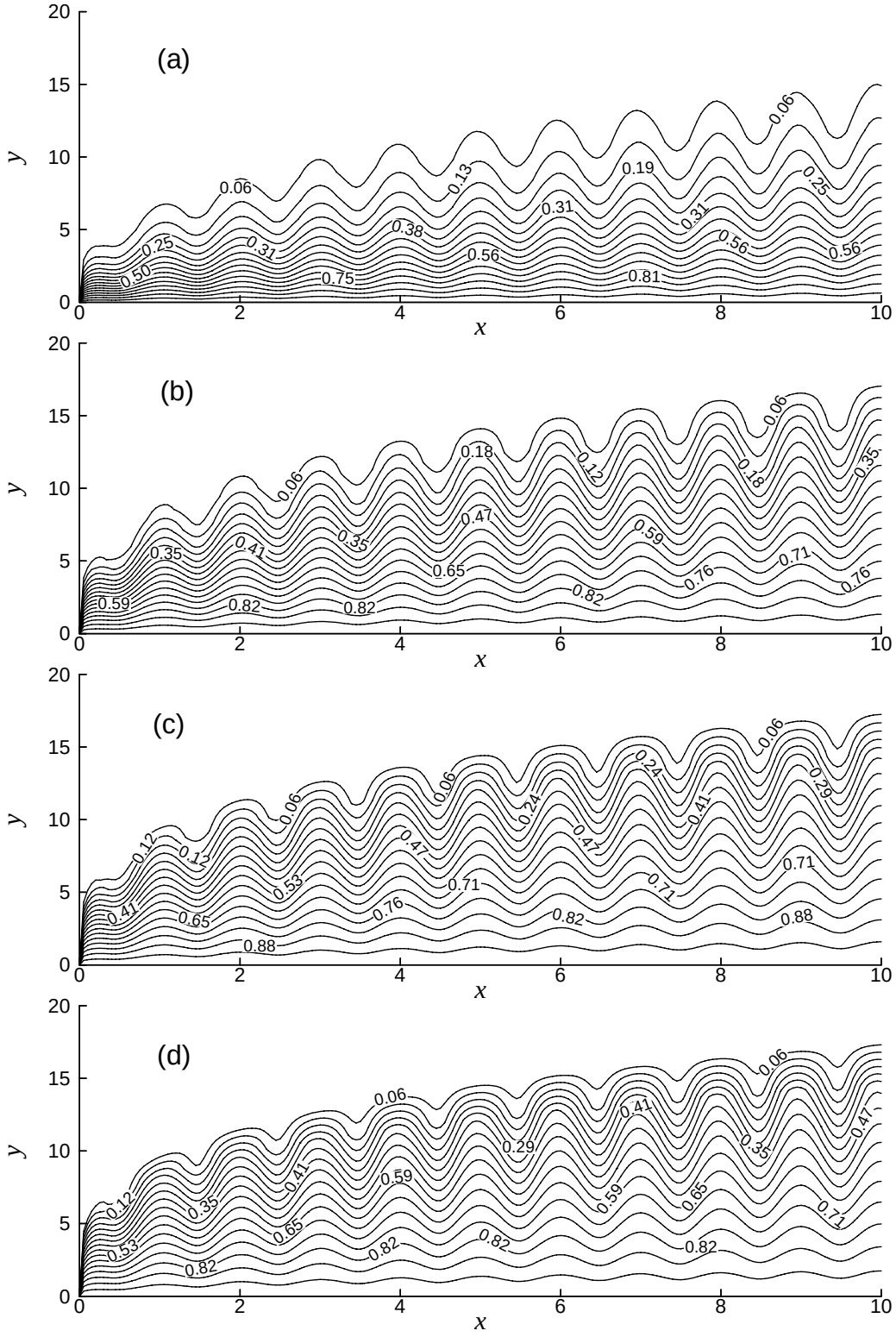

Figure 4.9: Isotherms for (a) γ = 0.0 (b) γ = 4.0 (c) γ = 7.0 (d) γ = 10.0 while Pr = 1.0, α = 0.3 and M = 0.8.

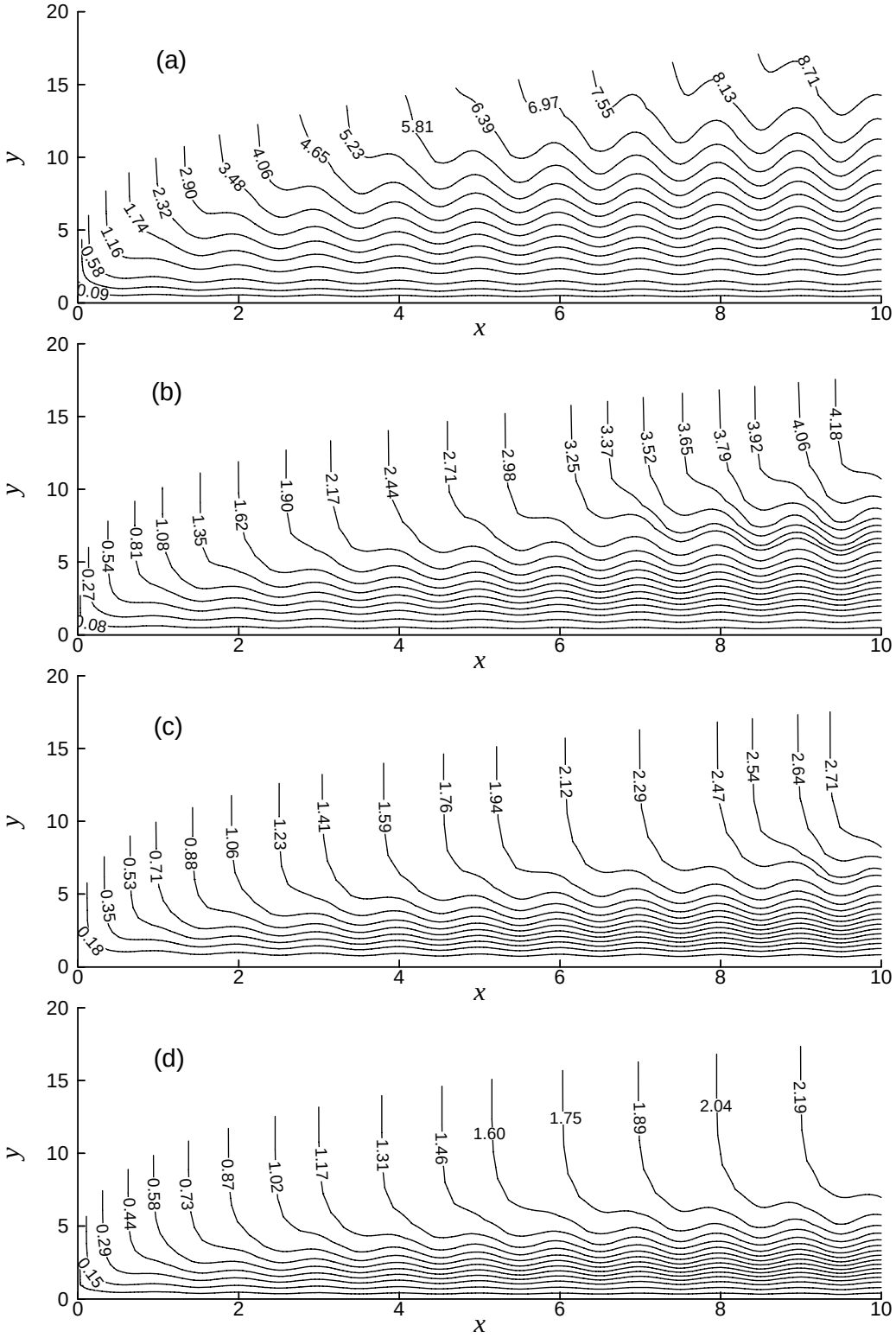

Figure 4.10: Streamlines for (a) Pr = 0.73 (b) Pr = 4.24 (c) Pr = 9.45 (d) Pr = 13.5 while $M = 0.8$, $\alpha = 0.2$ and $\gamma = 5.0$.

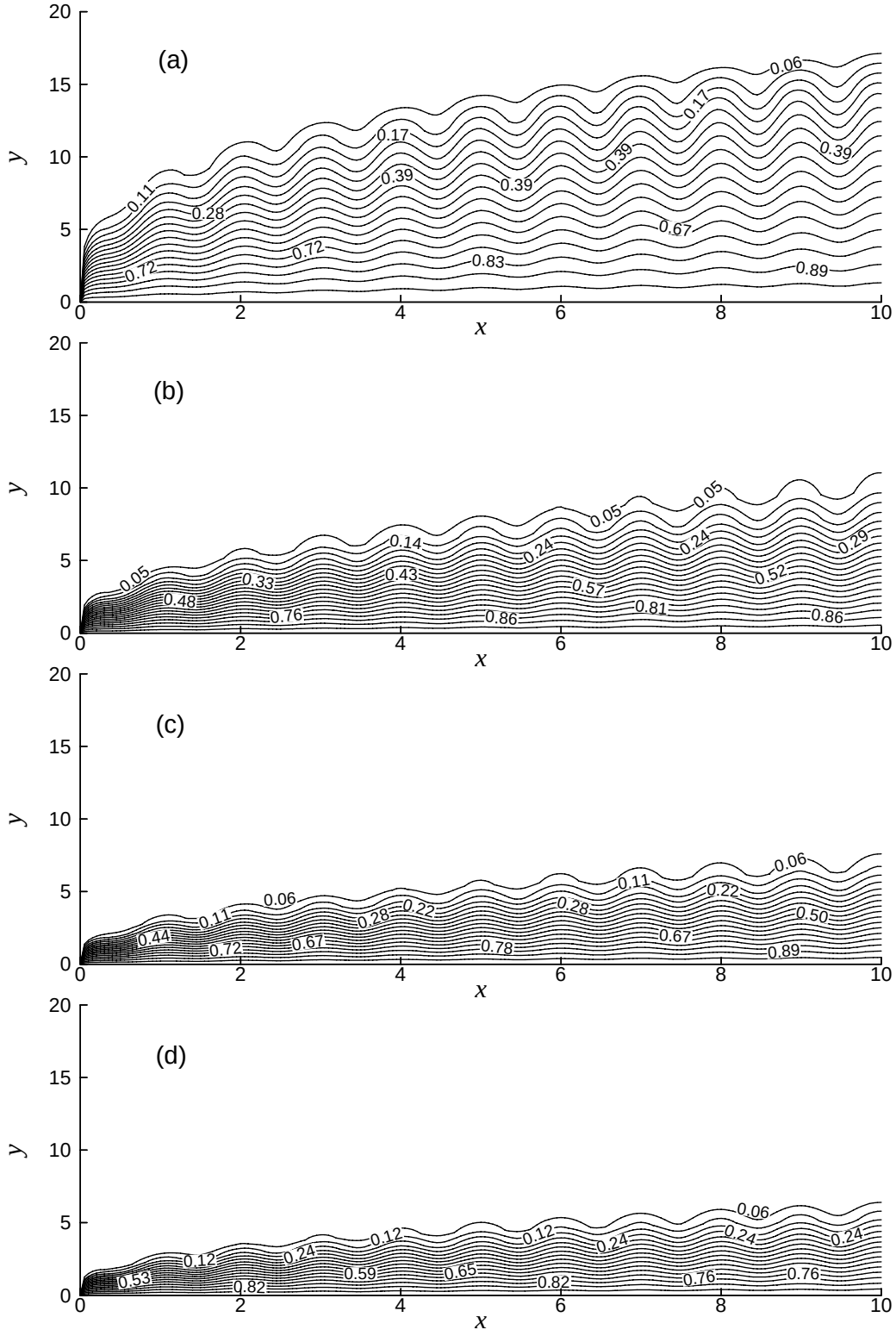

Figure 4.11: Isotherms for (a) Pr = 0.73 (b) Pr = 4.24 (c) Pr = 9.45 (d) Pr = 13.5 while $M = 0.8$, $\alpha = 0.2$ and $\gamma = 5.0$.

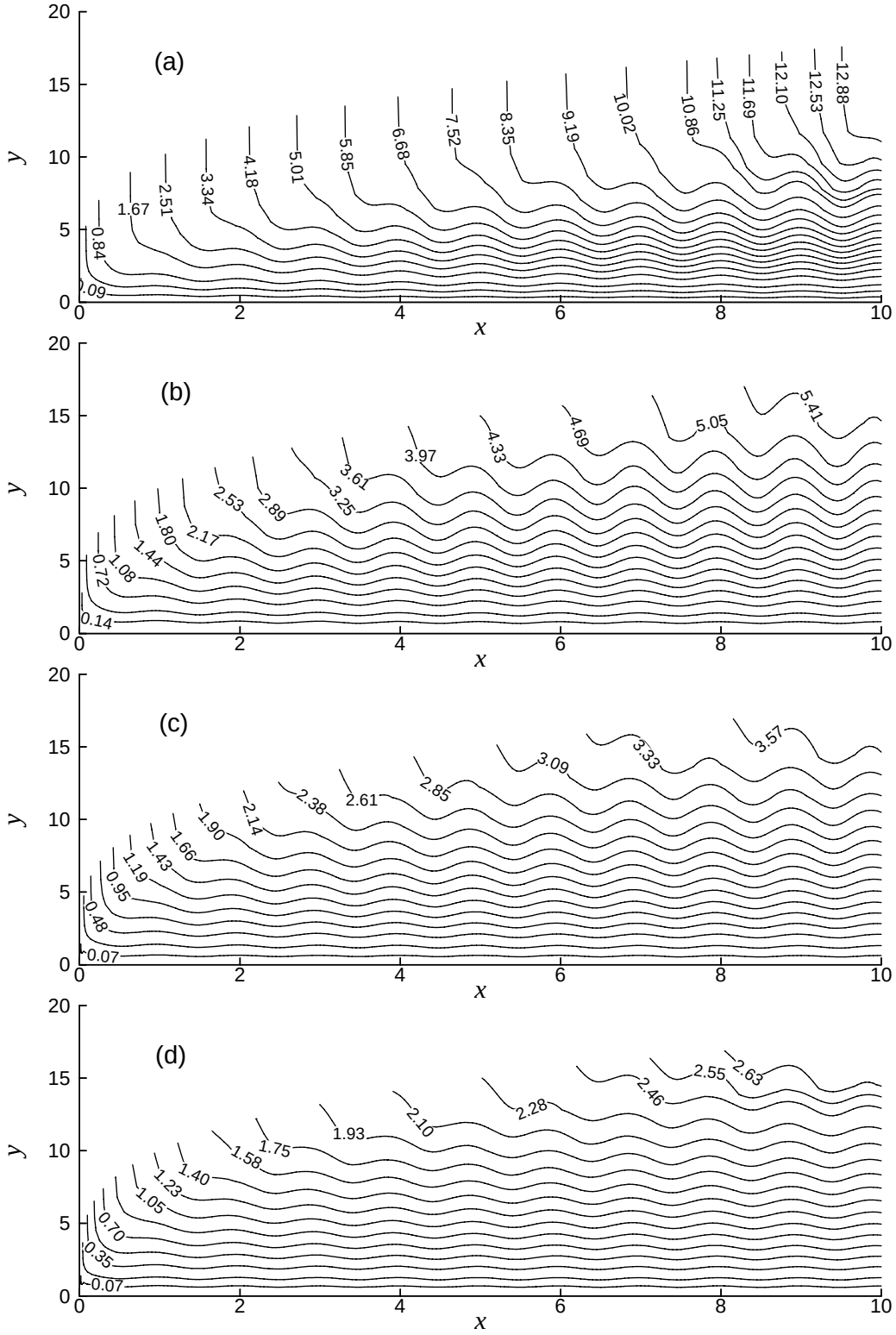

Figure 4.12: Streamlines for (a) M = 0.0 (b) M = 1.5 (c) M = 2.5 (d) M = 3.5 while Pr = 1.0, α = 0.2 and γ = 5.0.

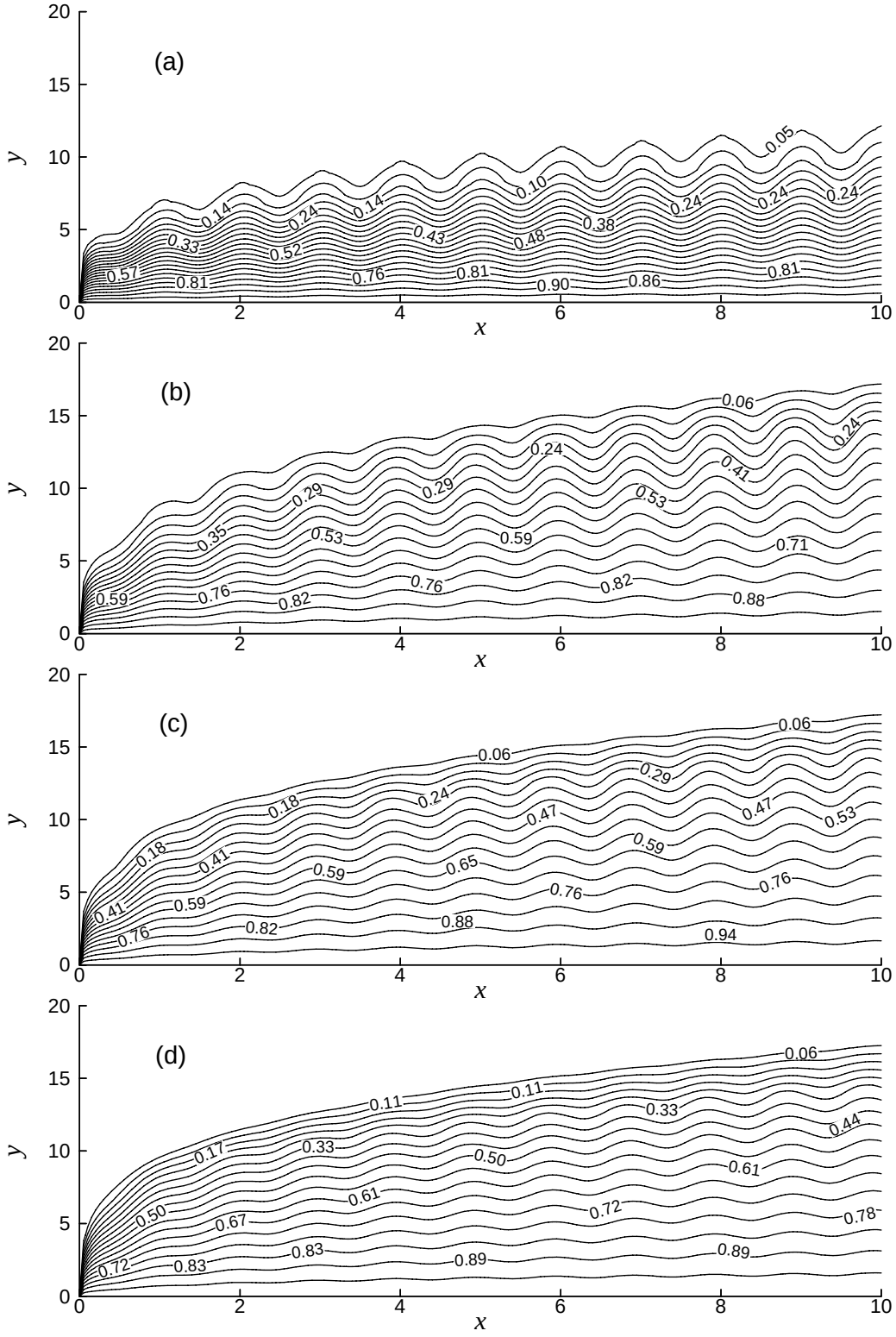

Figure 4.13: Isotherms for (a) M = 0.0 (b) M = 1.5 (c) M = 2.5 (d) M = 3.5 while Pr = 1.0, α = 0.2 and γ = 5.0.

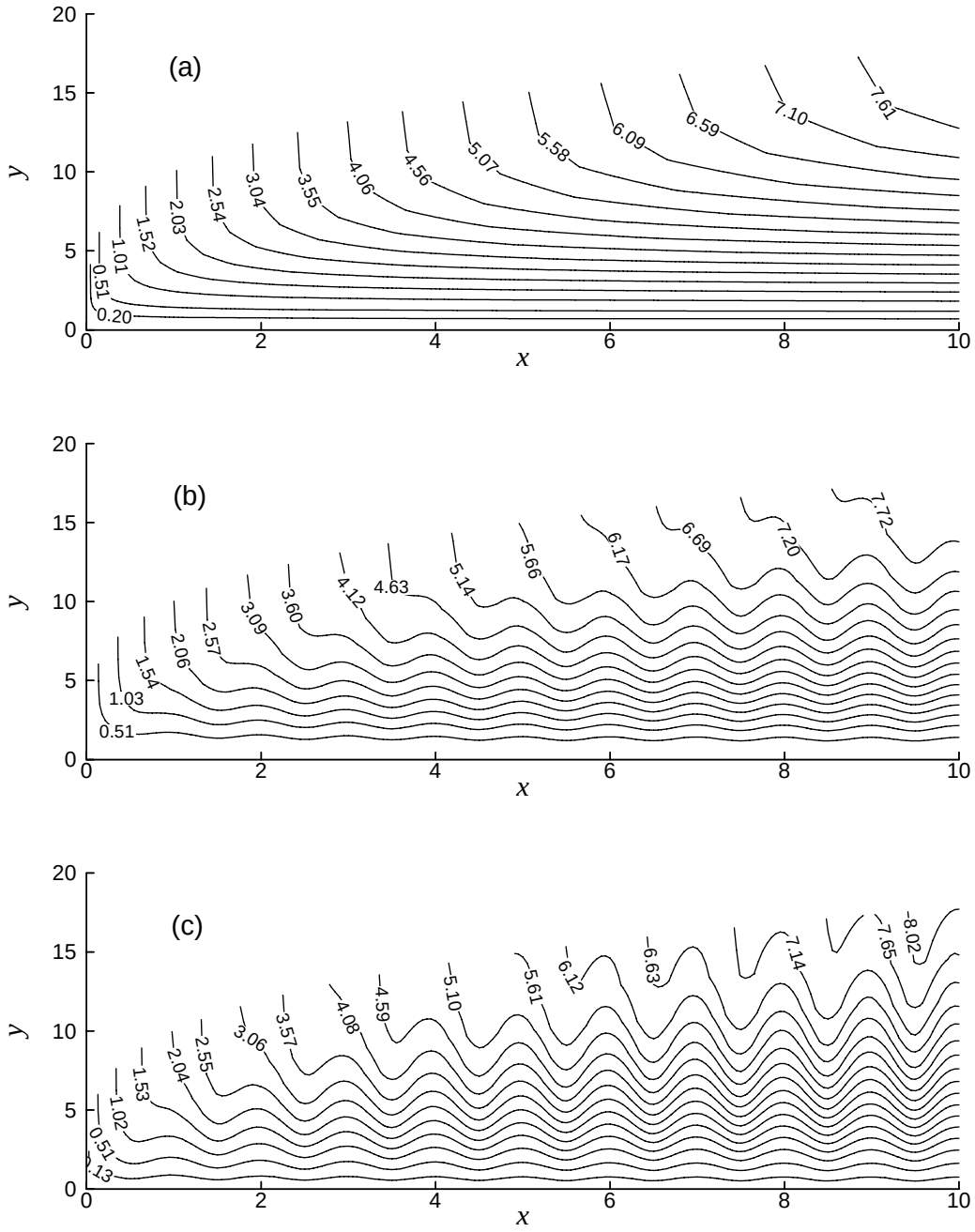

Figure 4.14: Streamlines for (a) α = 0.0 (b) α = 0.2 (c) α = 0.3 while γ = 2.0, Pr = 0.73 and M = 0.8.

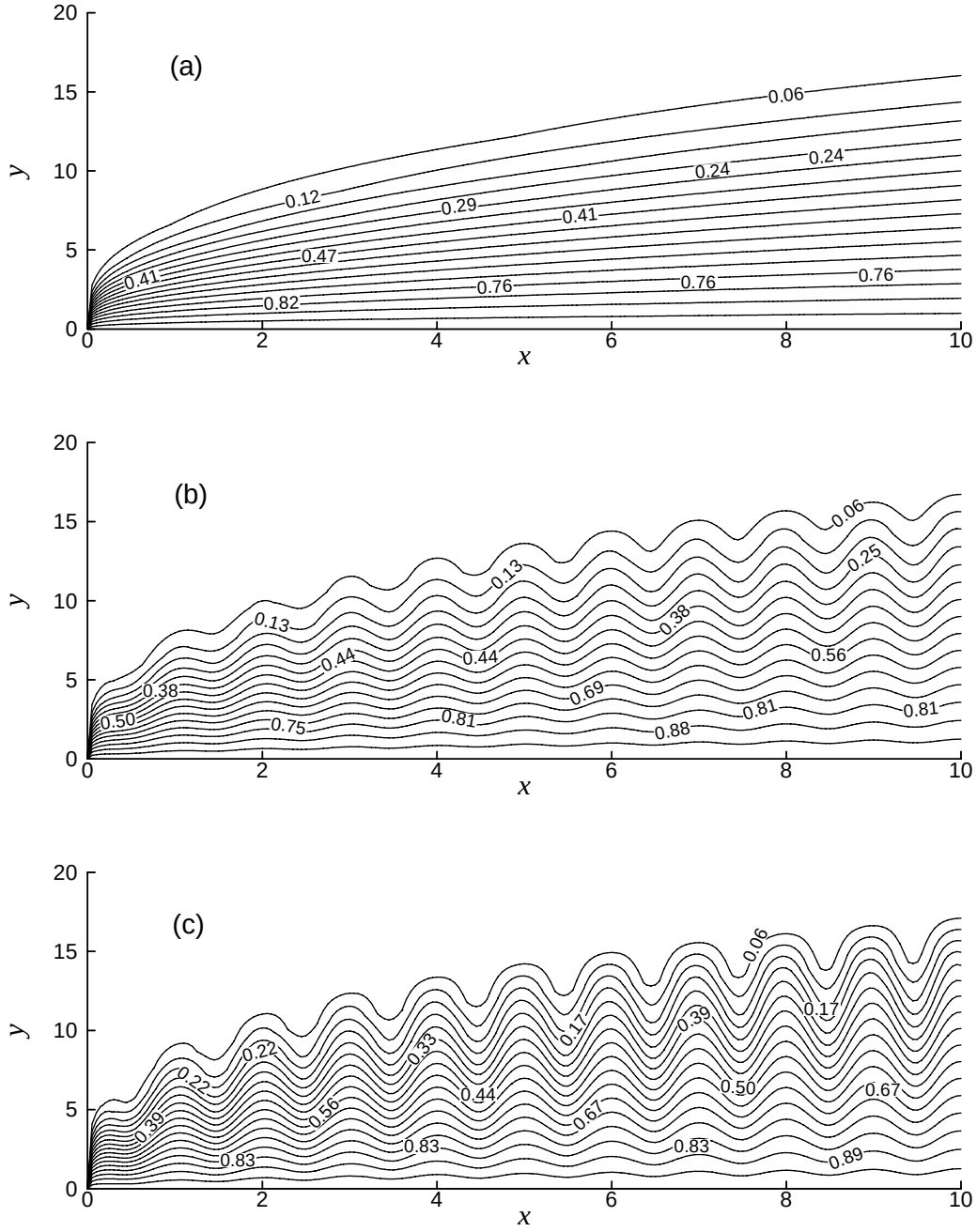

Figure 4.15: Isotherms for (a) $\alpha = 0.0$ (b) $\alpha = 0.2$ (c) $\alpha = 0.3$ while $\gamma = 2.0$, Pr = 0.73 and $M = 0.8$.

The values of skin friction coefficient C_{fx} and the rate of heat transfer in terms of Nusselt number Nu_x have been represented in Table A3 for the computational domain for variation of thermal conductivity parameter (γ = 0.0, 4.0, 10.0) while amplitude-to-length ratio of the wavy surface α = 0.3, M = 0.8 and Pr = 1.0 which shown in Appendix A. Here it is noted that the complete cycle of the wavy surface is from x = 0.0 to 2.0. The skin friction coefficient C_{fx} increases for the first quarter of the cycle ($x \cong 0$ to $x \cong 0.50$) and decreases in the second quarter ($x \cong 0.50$ to $x \cong 1.0$). From $x \cong 1.0$ to $\cong 1.5$ (i.e., third quarter) the skin friction coefficient again increases, whereas the fourth quarter ($x \cong 1.5$ to $x \cong 2.0$) it decreases. The skin friction coefficient and the rate of heat transfer show similar characteristics throughout the domain. However, the maximum values of local skin friction coefficient C_{fx} are recorded to be 0.78350, 0.93324 and 0.99073 for γ = 0.0, 4.0 and 10.0 respectively which occurs at x = 0.50. Moreover, the maximum values of the rate of heat transfer are recorded to be 0.34186, 0.77061 and 1.21257 for γ = 0.0, 4.0 and 10.0 respectively which occurs at the surface. The local skin friction coefficient C_{fx} and the rate of heat transfer in terms of Nusselt number Nu_x increase by approximately 21% and 72% respectively as γ increases from 0.0 to 10.0.

Skin friction coefficient C_{fx} and the local rate of heat transfer in terms of Nusselt number Nu_x against x for the variation of Prandtl number Pr, magnetic parameter M and thermal conductivity parameter γ with α = 0.2 are presented in Table A4 which shown in Appendix A. From this table it is concluded that if the value of Pr increases then the values of the skin-friction coefficient C_{fx} decreases and the rate of heat transfer in terms of Nusselt number Nu_x increases for any values of γ and M. However it is also seen that if the value of intensity of magnetic field increases the values of C_{fx} and Nu_x decreases while it increases of γ.

4.3 Conclusions

The problem of natural convection heat transfer of viscous incompressible fluid with temperature dependent thermal conductivity with magnetic field along a vertical wavy surface has been analyzed. Brief summaries of the major results are listed in the following:

- The effect of increasing temperature dependent thermal conductivity results in increasing the local skin friction coefficient, the local rate of heat transfer, the velocity and temperature as well as the streamlines and isotherms. When thermal conductivity is dependent on temperature then both the temperature and heat transfer rate increase.
- An increase in the values of Prandtl number Pr leads to decrease the velocity, temperature, the local skin friction coefficient and increases the local rate of heat transfer significantly. The velocity and thermal boundary layer also become thinner for large value of Prandtl number Pr.
- The effect of magnetic field is to decrease the skin friction coefficient and rate of heat transfer in terms of Nusselt number and the velocity over the whole boundary layer, but reverse case happens for the temperature. Increased values of intensity of magnetic field cause the velocity boundary layer thinner and thicker the thermal boundary layer.
- The skin friction coefficient and rate of heat transfer decrease for increased values of the amplitude-to-length ratio of the wavy surface over the whole boundary layer. The velocity, temperature increase and the momentum, the thermal boundary layer become thicker for the effect of amplitude-to-length ratio of the wavy surface.
- When thermal conductivity is dependent on temperature then thermal conductivity variation parameter γ depend on the difference between the surface temperature and ambient temperature of the fluid. This temperature difference increases with the increase of thermal conductivity. So increasing values of thermal conductivity variation parameter indicates that heat is transferred rapidly from surface to the fluid within the boundary layer. Then velocity and temperature increase for increasing values of temperature dependent thermal conductivity and also fluid mass is transferred. Thermal conductivity is a measure of ability of the fluid to conduct heat. Increasing velocity increases skin friction coefficient and flow rate in the boundary layer. The heat transfer rate also increases.

CHAPTER 5

Combined effect of temperature dependent viscosity and thermal conductivity on MHD natural convection flow

5.1 Introduction

Natural convection flow is often encountered in the study of the structure of stars and planets or in cooling of nuclear reactors. A considerable amount of research has been accomplished on the effects of electrically conducting fluids such as liquid metals, water mixed with a little acid and others in the presence of transverse magnetic field on the flow and heat transfer characteristics over various geometries. For the fluids, which are important in the theory of lubrication, the heat generated by the internal friction and the corresponding rise in temperature do affect the viscosity and thermal conductivity of the fluid and they can no longer be regarded as constant. Flow of electrically conducting fluid in the presence of magnetic field with combined effect of temperature dependent viscosity and thermal conductivity on MHD natural convection flow along a wavy surface problems are significant from the technical point of view.

In the present chapter, a steady two dimensional laminar flow of viscous incompressible fluid on MHD free convection flow with combined effect of temperature dependent viscosity and thermal conductivity along a uniformly heated vertical wavy surface has been investigated. Governing equations of the flow for both the viscosity and thermal conductivity of the fluid are considered to be linear function of temperature. Using the appropriate transformations given in equation (2.28) the governing equations (2.23), (2.24) and (2.53) with associated boundary conditions (2.26) are converted to non-dimensional boundary layer equations (2.66) to (2.68). These equations are solved numerically by employing the implicit finite difference method, known as the Keller-box scheme. The numerical results of the surface shear stress in terms of the skin friction coefficient C_{fx}, the rate of heat transfer in terms of Nusselt number Nu_x, the streamlines and the isotherms for viscosity parameter ε, thermal conductivity variation parameter γ, magnetic

parameter M are presented graphically while the amplitude-to-length ratio of the wavy surface $\alpha = 0.3$ and Prandtl number Pr = 7.0 (water).

5.2 Results and discussion

Numerical values of the skin friction coefficient C_{fx}, the rate of heat transfer in terms of the Nusselt number Nu_x, the streamlines and the isotherms are obtained for different values of the viscosity parameter ε = 0.0 (constant viscosity) to 30.0, the magnetic parameter M = 0.0 (non magnetic field) to 5.0 and thermal conductivity variation parameter γ ranging from 0.0 (constant thermal conductivity) to 15.0 and depicted in figures 5.1- 5.9.

Numerical values of the skin friction coefficient and the rate of heat transfer in terms of the local Nusselt number are depicted graphically in figures 5.1(a) and 5.1(b) respectively against the axial distance of x in the interval [0, 8] for the effect of temperature dependent viscosity (ε = 0.0, 5.0, 10.0, 20.0, 30.0) keeping all other controlling parameters amplitude-to-length ratio of the wavy surface α = 0.3, M = 1.0, γ = 4.0 and Pr = 7.0. Figure 5.1(a) indicates that increasing values of the viscosity parameter the skin friction coefficient increases monotonically along the upward direction of the surface and it is seen that the local skin friction coefficient increases by approximately 66% as ε changes from 0.0 to 30.0. The rate of heat transfer decreases by approximately 46% due to the increased value of viscosity parameter which is evident from figure 5.1(b).

The variation of temperature dependent thermal conductivity (γ = 0.0, 2.0, 6.0, 10.0, 15.0) on the skin friction coefficient and the heat transfer coefficient while Prandtl number Pr = 7.0, α = 0.3, ε = 5.0 and M = 0.8 are shown in figures 5.2(a)-5.2(b) respectively. For increasing value of γ the skin friction coefficient and heat transfer coefficient increase significantly along the upstream direction of the surface against the axial direction of x. It is observed that the skin friction coefficient and heat transfer rate increase by approximately 40% and 81% respectively when γ changes from 0.0 to 15.0.

The effect of magnetic field on the local skin friction coefficient C_{fx} and local rate of heat transfer Nu_x are illustrated in figures 5.3(a) and 5.3(b) respectively for Prandtl

number Pr = 7.0, α = 0.3, γ = 5.0 and viscosity parameter ε = 5.0. The skin friction coefficient and the rate of heat transfer coefficient decrease by approximately 34% and 12% respectively when the value of intensity of magnetic field increases from 0.0 to 5.0.

The effect of the temperature dependent viscosity on the development of streamlines and isotherms are plotted in figures 5.4 and 5.5 respectively for Pr = 7.0, α = 0.3, γ = 4.0 and M = 1.0. It is found that for ε = 0.0 the value of ψ_{max} is 2.86, for ε = 10.0 ψ_{max} is 2.49, for ε = 20.0 ψ_{max} is 2.29 and for ε = 30.0 ψ_{max} is 2.10. Hence from these figures it is seen that for the effect of viscosity, the flow rate in the boundary layer decreases and the thermal boundary layer becomes thicker monotonically.

Figures 5.6 and 5.7 show the effect of temperature dependent thermal conductivity on the formation of streamlines and isotherms respectively with other controlling parameters α = 0.3, M = 0.8, ε = 5.0 and Pr = 7.0. It can be noted that for γ equal to 0.0, 6.0, 10.0, and 15.0 the maximum values of ψ, that is, ψ_{max} are 1.62, 3.26, 4.06 and 4.58 respectively. So it can be concluded that for large value of thermal conductivity parameter both the momentum and the thermal boundary layer grow thicker.

The effect of different values of intensity of magnetic field equal to 0.0, 0.5, 3.0 and 5.0 on the streamlines and isotherms are illustrated in figures 5.8 and 5.9 respectively with other controlling parameters Prandtl number Pr = 7.0, α = 0.3, γ = 5.0 and ε = 5.0. Figure 5.8 depicts that the maximum values of ψ decreases quickly while the values of intensity of magnetic field increases. When M = 0.0 the value of ψ_{max} is 5.09, for M = 0.5 the value of ψ_{max} is 3.35, for M = 3.0 the value of ψ_{max} is 1.83 and for M = 5.0 the value of ψ_{max} is 1.35. On the other hand, temperature of the fluid flow increases significantly as the values of the intensity of magnetic field increase which is presented in figure 5.9.

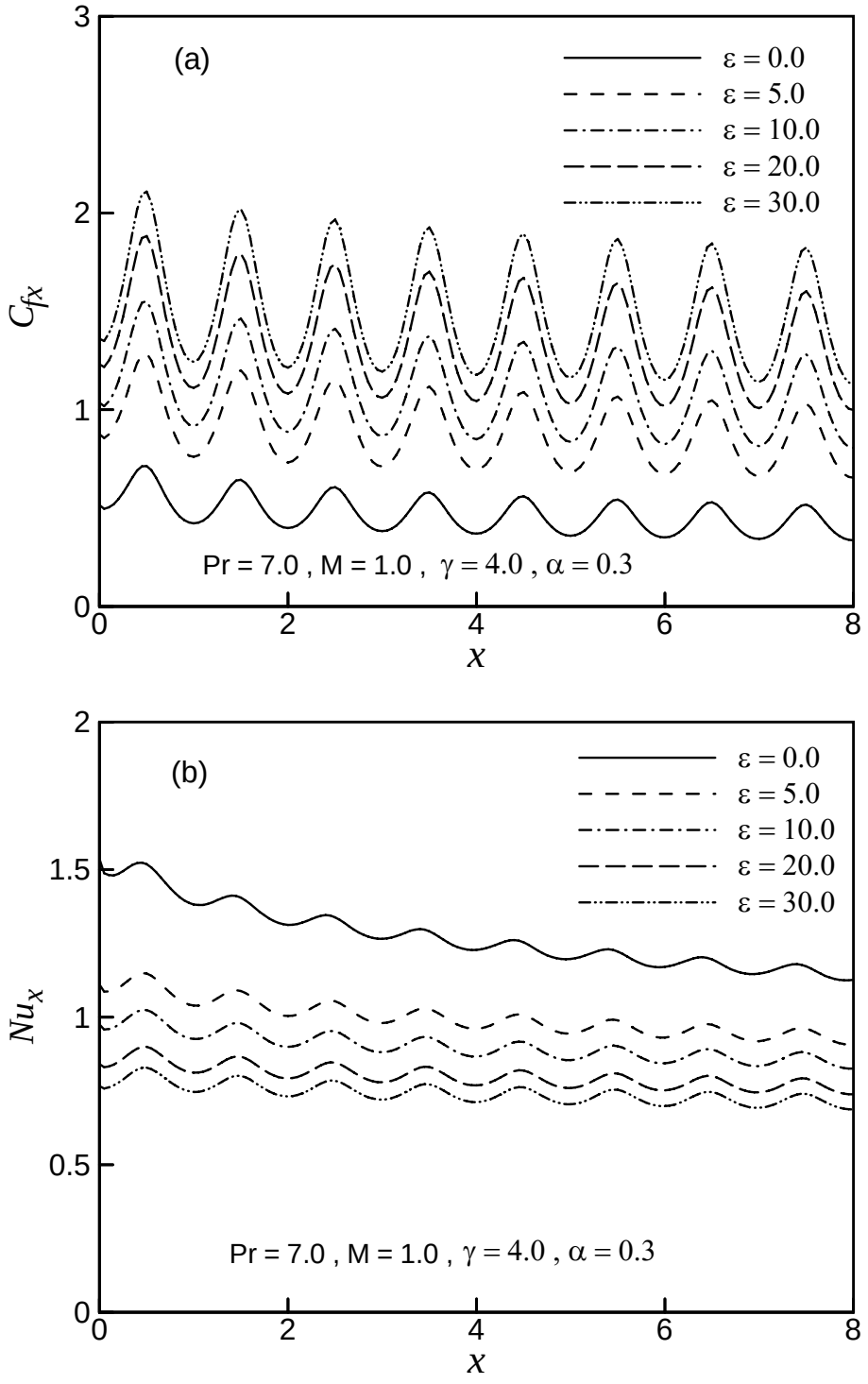

Figure 5.1: Variation of (a) skin friction coefficient C_{fx} and (b) rate of heat transfer Nu_x against dimensionless distance x for different values of viscosity parameter ε while Pr = 7.0, M = 1.0, γ = 4.0 and α = 0.3.

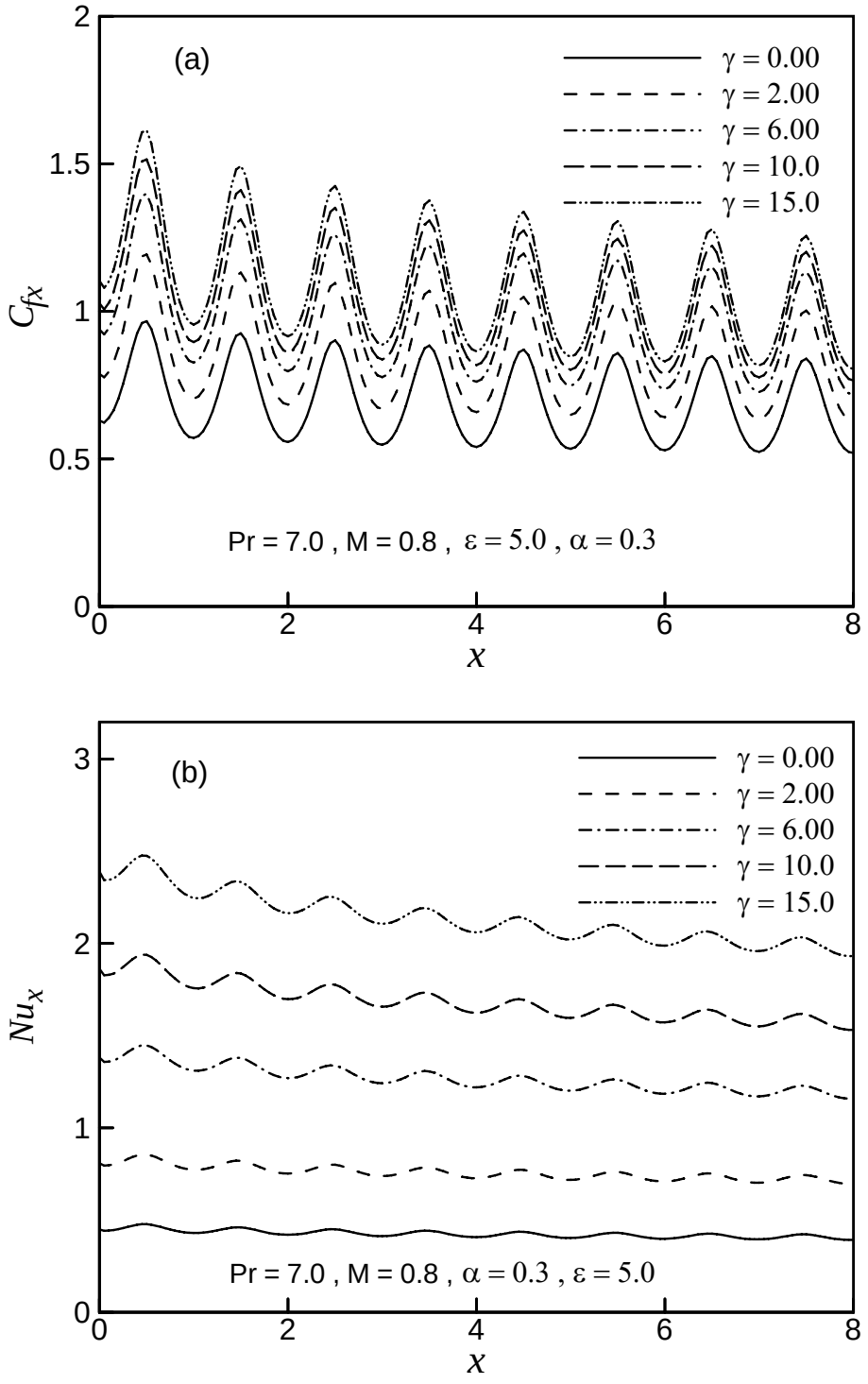

Figure 5.2: Variation of (a) skin friction coefficient C_{fx} and (b) rate of heat transfer Nu_x against dimensionless distance x for different values of γ while Pr = 7.0, M = 0.8, α = 0.3 and ε = 5.0.

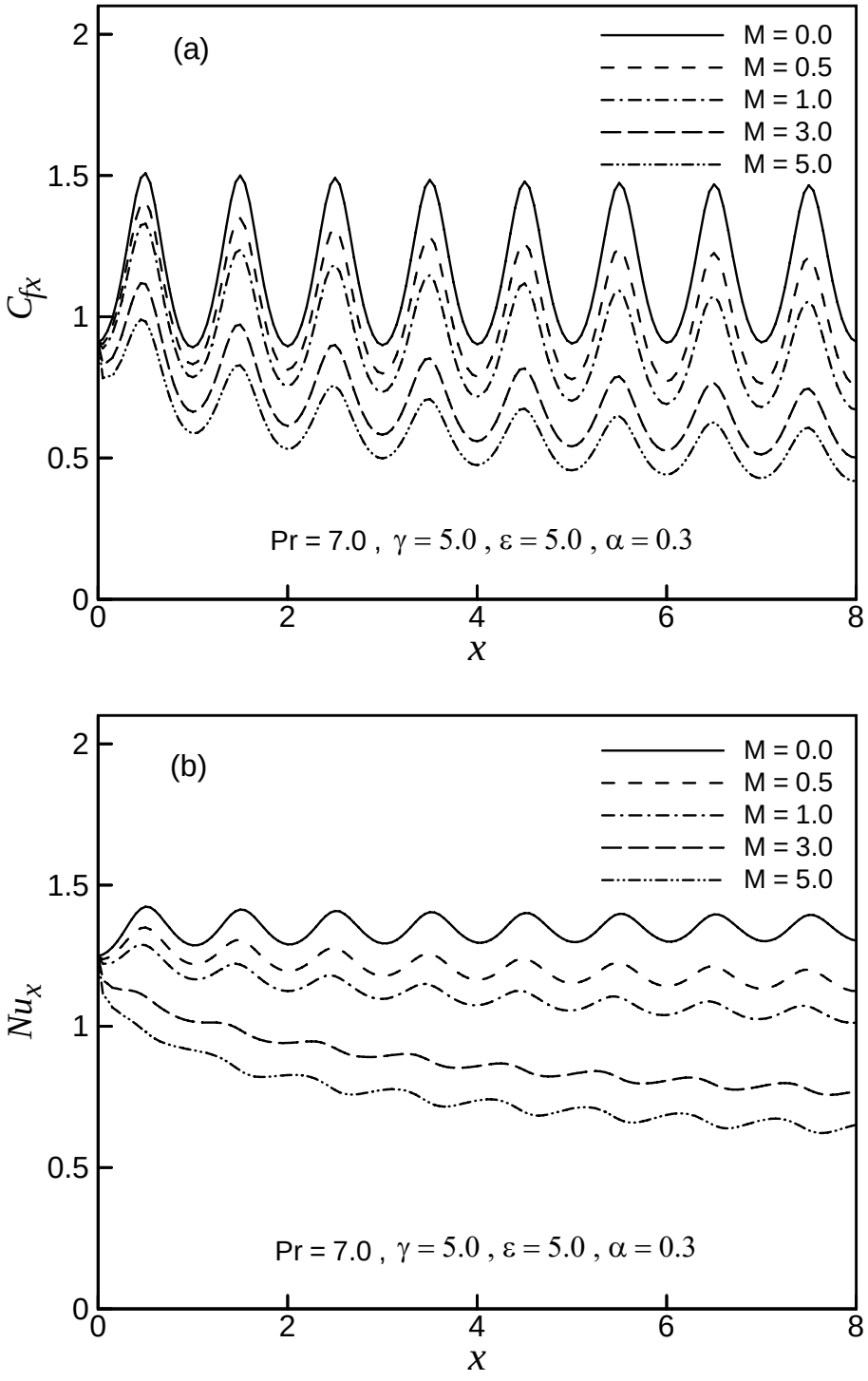

Figure 5.3: Variation of (a) skin friction coefficient C_{fx} and (b) rate of heat transfer Nu_x against dimensionless distance x for different values of magnetic parameter M with Prandtl number Pr = 7.0, γ = 5.0, ε = 5.0 and α = 0.3.

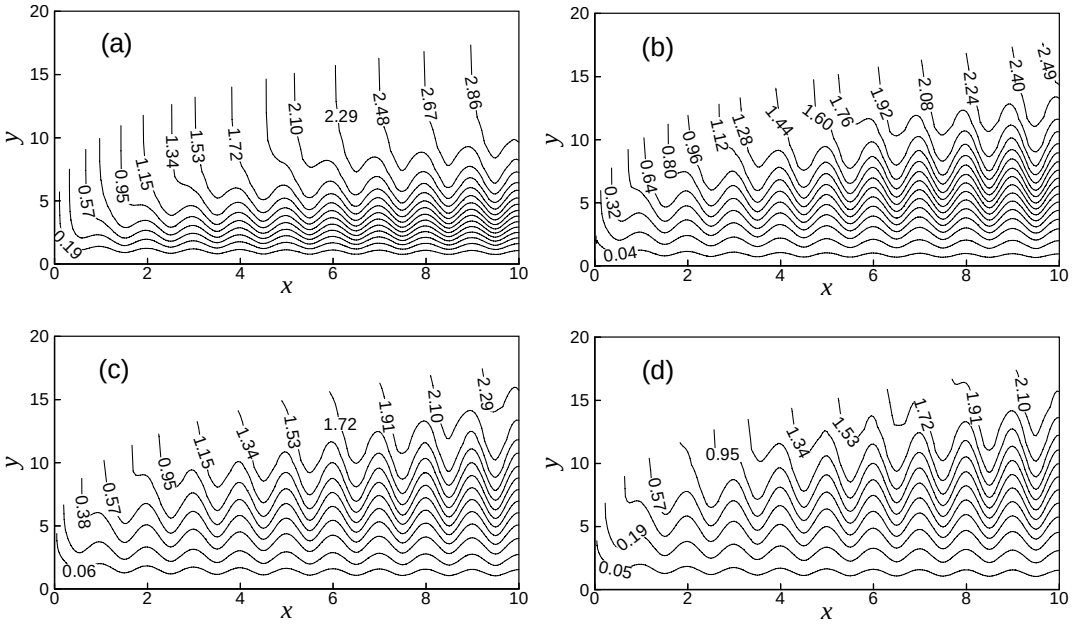

Figure 5.4: Streamlines for (a) ε = 0.0 (b) ε = 10.0 (c) ε = 20.0 (d) ε = 30.0 while Pr = 7.0, M = 1.0, γ = 4.0 and α = 0.3.

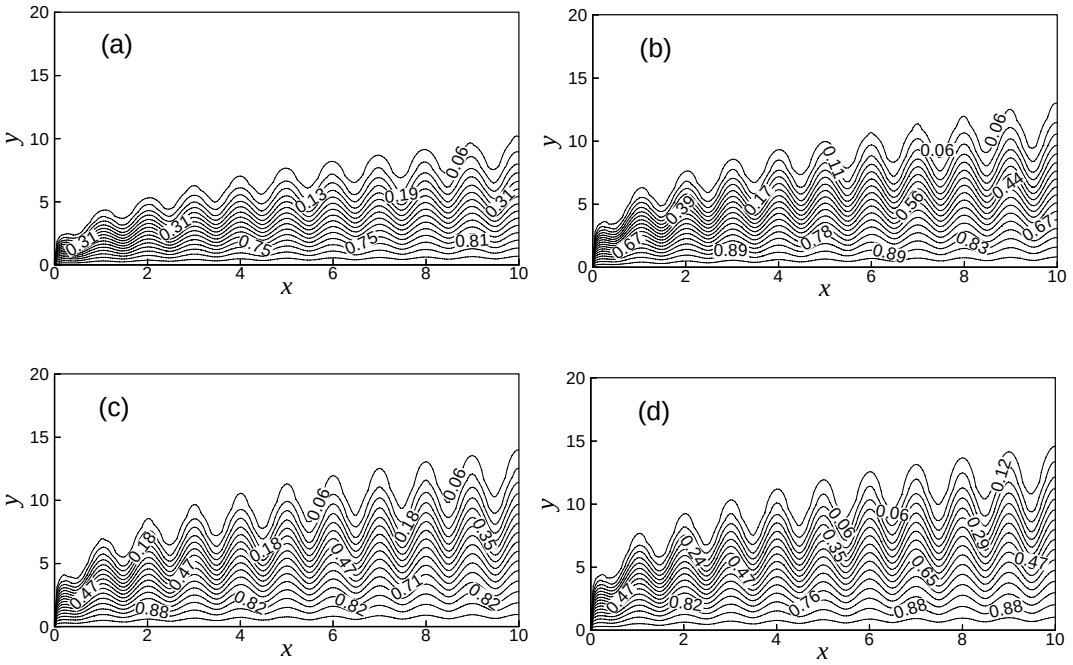

Figure 5.5: Isotherms for (a) ε = 0.0 (b) ε = 10.0 (c) ε = 20.0 (d) ε = 30.0 while Pr = 7.0, M = 1.0, γ = 4.0 and α = 0.3.

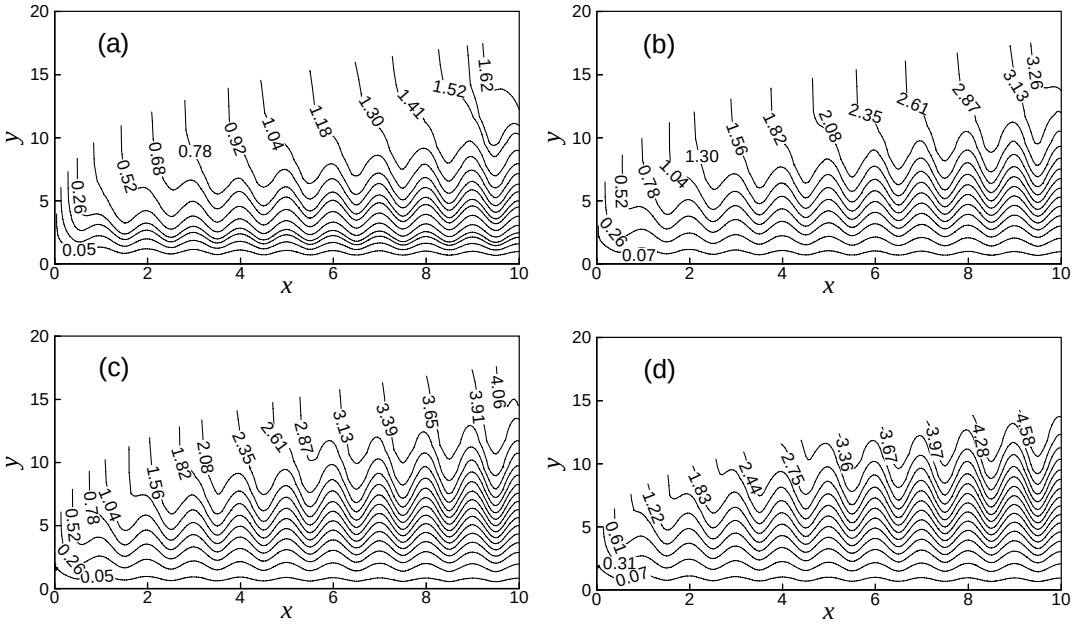

Figure 5.6: Streamlines for (a) $\gamma = 0.0$ (b) $\gamma = 6.0$ (c) $\gamma = 10.0$ (d) $\gamma = 15.0$ while Pr = 7.0, $M = 0.8$, $\alpha = 0.3$ and $\varepsilon = 5.0$.

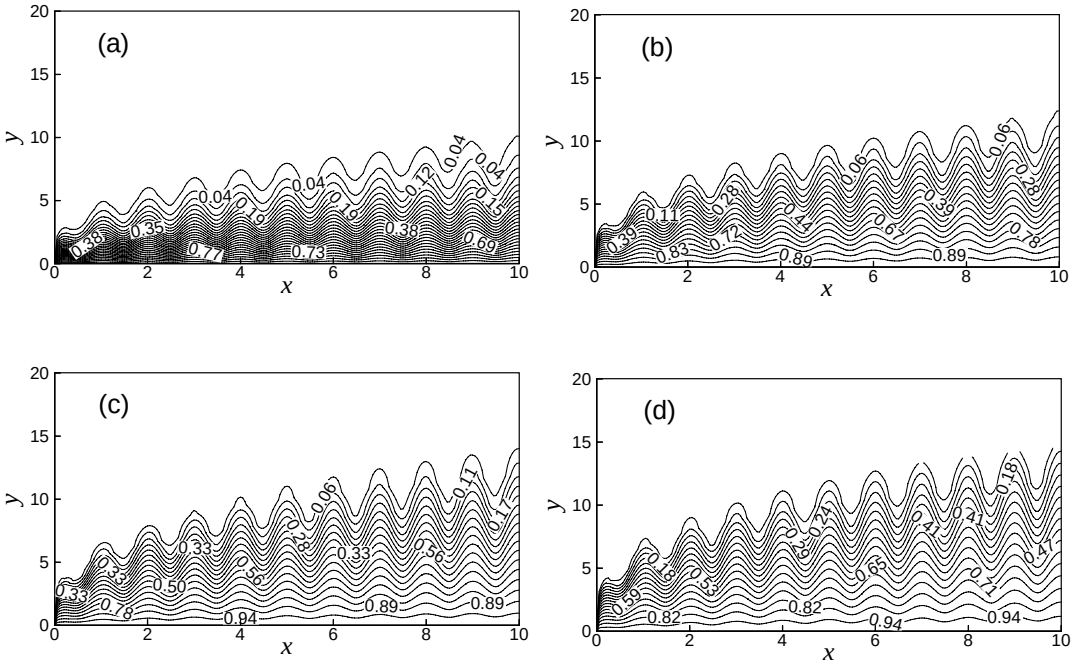

Figure 5.7: Isotherms for (a) $\gamma = 0.0$ (b) $\gamma = 6.0$ (c) $\gamma = 10.0$ (d) $\gamma = 15.0$ while Pr = 7.0, $M = 0.8$, $\alpha = 0.3$ and $\varepsilon = 5.0$.

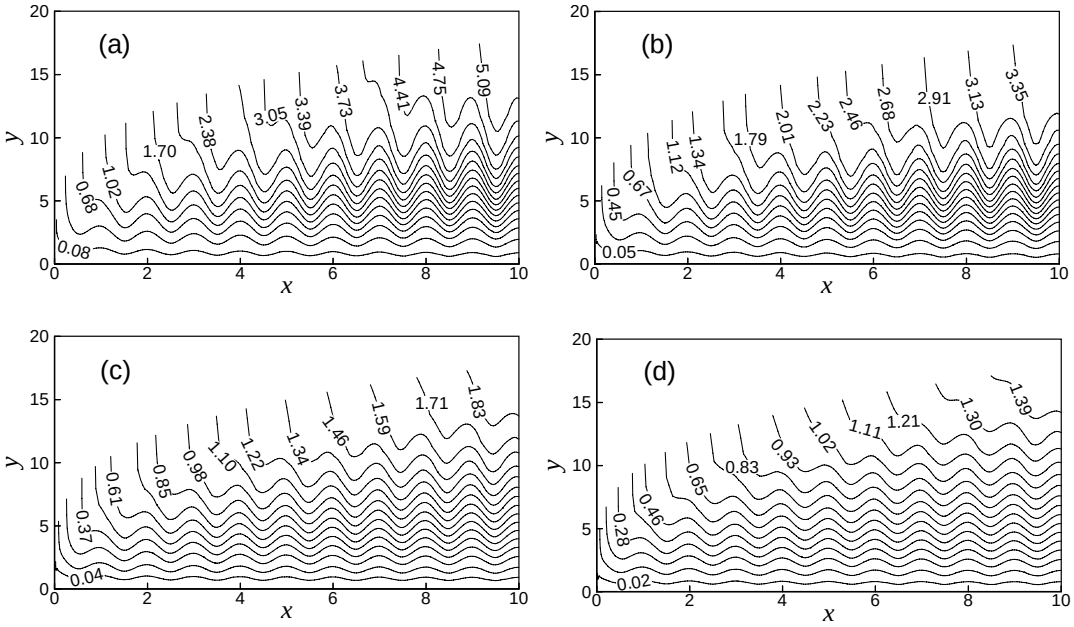

Figure 5.8: Streamlines for (a) M = 0.0 (b) M = 0.5 (c) M = 3.0 (d) M = 5.0 while Pr = 7.0, γ = 5.0, ε = 5.0 and α = 0.3.

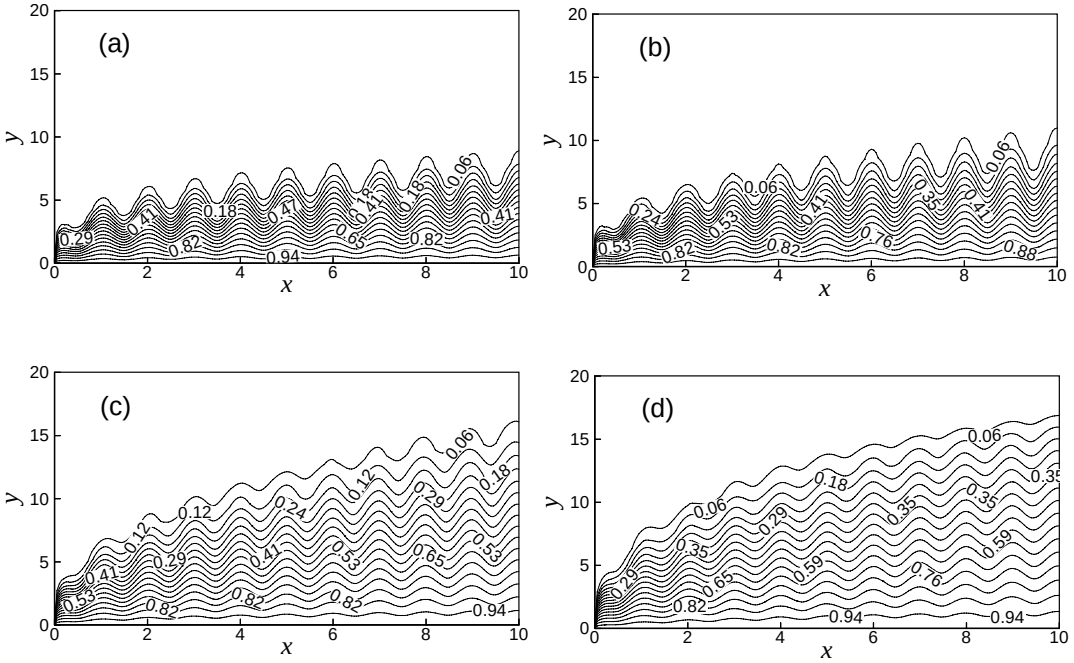

Figure 5.9: Isotherms for (a) M = 0.0 (b) M = 0.5 (c) M = 3.0 (d) M = 5.0 while Pr = 7.0, γ = 5.0, ε = 5.0 and α = 0.3.

5.3 Conclusions

The combined effect of temperature dependent viscosity and thermal conductivity on MHD natural convection flow of viscous incompressible fluid along a uniformly heated vertical wavy surface has been investigated. The conclusions are as follows:

- The effect of increasing temperature dependent viscosity results in increasing the local skin friction coefficient, the temperature and decreasing the velocity, the local rate of heat transfer over the whole boundary layer.
- An increase in the values of the intensity of magnetic field leads to decrease the skin friction coefficient, the local rate of heat transfer and the velocity of the fluid flow while the reverse phenomena occur for the temperature.
- It is found that the skin friction coefficient and heat transfer rate increase significantly for increasing values of temperature dependent thermal conductivity parameter.
- The velocity boundary layer becomes thinner and thicker the thermal boundary layer when the effect of temperature dependent viscosity is considered.
- For the effect of temperature dependent thermal conductivity both the velocity and thermal boundary layer grow thick.
- For higher value of the intensity of magnetic field the thermal boundary layer becomes thicker and thinner the velocity boundary layer.

CHAPTER 6

Effect of Joule heating on MHD natural convection flow

6.1 Introduction

When current flows in an electrical conductor such as wire, electrical energy is lost due to the resistance of the electrical conductor. This lost electrical energy is converted to thermal energy called Joule heating. This is because the electrical power loss equals the heat transfer. Joule heating or Ohmic heating in electronics and in physics refers to the increase in temperature of a conductor as a result of resistance to an electrical current flowing through it. But at an atomic level, Joule heating is the result of moving electrons colliding with atoms in a conductor, whereupon momentum is transferred to the atom, increasing its kinetic energy. When similar collisions cause a permanent structural change, rather than an elastic response, the result is known as electro migration. The increase in the kinetic energy of the ions manifests itself as heat and a rise in the temperature of the conductor. Hence energy is transferred from electrical power supply to the conductor and any materials with which it is in thermal contact.

The effects of Joule heating on MHD natural convection flow of viscous incompressible fluid with temperature dependent variable viscosity and thermal conductivity along a uniformly heated vertical wavy surface have been described in this chapter. The governing boundary layer equations are first transformed into a non-dimensional form using the appropriate transformations. The resulting nonlinear system of partial differential equations are mapped into the domain of a vertical flat plate and then solved numerically employing the implicit finite difference method, known as the Keller-box scheme. Numerical results are presented graphically by skin friction coefficient, the rate of heat transfer in terms of Nusselt number, the velocity and temperature profiles as well as the streamlines and the isotherms for a selection of parameters set consisting of Joule heating parameter J, viscosity parameter ε, thermal conductivity variation parameter γ, magnetic parameter M, the amplitude-to-length ratio of the wavy surface α and Prandtl number Pr. Numerical results of the

local skin friction coefficient C_{fx} and the rate of heat transfer Nu_x for Joule heating parameter J are also presented in tabular form.

This is the most general case among the cases considered in chapters 3 to 6. When the effect of temperature dependent thermal conductivity and Joule heating are ignored and the strength of magnetic field and temperature dependent viscosity are considered then the resulting cases are case-I and case-II. When the effect of magnetic field and temperature dependent thermal conductivity are considered and the effect of temperature dependent viscosity and Joule heating are ignored then it gives the case-III. When the effect of magnetic field and temperature dependent thermal conductivity, temperature dependent viscosity are considered and the effect of Joule heating is ignored case-IV is obtained.

6.2 Results and discussion

Numerical values of the shear stress in terms of the skin friction coefficients C_{fx} and the rate of heat transfer in terms of the Nusselt number Nu_x calculated from equations (2.44) and (2.64) for a wide range of the axial distance x starting from the leading edge. The velocity, the temperature profile, the streamlines and the isotherms are also obtained. These are shown graphically in figures 6.1-6.19 for different values of the aforementioned parameters of viscosity parameter ε = 0.0 (constant viscosity) to 20.0 and Joule heating parameter J = 0.0 (without Joule heating) to 2.0, thermal conductivity parameter γ = 0.0 (constant thermal conductivity) to 10.0, magnetic parameter M = 0.0 (non magnetic field) to 1.5, Prandtl number Pr = 0.73, 1.73, 3.0, 7.0 and 9.45 which correspond to the air at 2100^0K, water at 100^0C, 60^0C, 20^0C and 10^0C respectively and the amplitude-to-length ratio of the wavy surface α = 0.0 (flat plate) to 0.4. The skin friction coefficient C_{fx} and local rate of heat transfer Nu_x varies according to the slope of the wavy surface. This is due to the alignment of the buoyancy force $1/(1+\sigma_x^2)$, as shown in equation (2.38), which drives the flow tangentially to the wavy surface.

The effect of Joule heating on the local skin friction coefficient and the rate of heat transfer in terms of the local Nusselt number against x from the wavy surface while α = 0.3, M = 0.02, γ = 4.0, ε = 5.0 and Pr = 0.5 are illustrated in figures 6.1(a) and 6.1(b) respectively. Figure 6.1(a) shows that, the skin friction coefficient increases

slightly along the upstream direction of the surface. On the other hand, the heat transfer rate gradually decreases along the downstream direction of the surface. It can be shown from figure 6.1(b). The highest values of local skin friction coefficient are recorded to be 2.27275, 2.27366, 2.27550, 2.27733 and 2.27963 for J = 0.0, 0.02, 0.06, 0.10 and 0.15 respectively which occurs at same point of x = 0.5 shown in figure 6.1(a). The effect of Joule heating in fluid is very small. Thus the skin friction coefficient increases by only 0.30% when J changes from 0.0 to 0.15. The highest values of local rate of heat transfer are 0.56347, 0.56218, 0.55958, 0.55698 and 0.55372 for J = 0.0, 0.02, 0.06, 0.10 and 0.15 respectively which occur also at the same point of x = 0.5. Finally, it is seen that the rate of heat transfer decreases by 1.73% as the value of Joule heating parameter increases from 0.0 to 0.15.

The analysis of the effect of temperature dependent viscosity (ε = 0.0, 5.0, 10.0, 15.0 and 20.0) on the surface shear stress in terms of the local skin friction coefficient and the rate of heat transfer in terms of the local Nusselt number against x are exposed within the boundary layer with α = 0.3, M = 0.8, J = 0.02, γ = 5.0 and Pr = 1.0 in figure 6.2. This figure shows that an increase in the variable viscosity, the skin friction coefficient increases monotonically along the upstream direction of the surface and reduces the heat transfer rate. The decreasing heat transfer rate becomes slower in the downstream region against x. The maximum values of local skin friction coefficient are recorded to be 0.94844, 1.85317, 2.26859, 2.54961 and 2.76364 for ε = 0.0, 5.0, 10.0, 15.0 and 20.0 respectively which occurs at x = 0.50. Again the peak values of the rate of heat transfer are 0.85232 for ε = 0.0 which occurs at the surface and 0.70348, 0.65376, 0.62430 and 0.60373 for ε = 5.0, 10.0, 15.0 and 20.0 respectively which occurs at the same axial point of x = 0.45. It is observed that the local skin friction coefficient increases by approximately 65% and the rate of heat transfer devalues by approximately 29% as ε increases from 0.0 to 20.0.

The effect of variation of temperature dependent thermal conductivity (γ = 0.0, 2.0, 6.0, 10.0) on the skin friction coefficient and the heat transfer coefficient while Prandtl number Pr = 0.73, ε = 5.0, J = 0.02, α = 0.3 and M = 0.5 are displayed in figures 6.3(a) and 6.3(b) respectively. As the value of thermal conductivity increases,

the skin friction coefficient and heat transfer coefficient increase significantly along the upstream direction of the surface. The maximum values of the skin friction coefficient are recorded to be 1.54766, 1.84651, 2.06230 and 2.15417 for γ = 0.0, 2.0, 6.0 and 10.0 which occurs at x = 0.50. The skin friction coefficient increases by approximately 28% as the value of temperature dependent thermal conductivity parameter changes from 0 to 10.0 at x = 0.50. Again the highest values of heat transfer rate are recorded to be 0.25035, 0.43889, 0.72943 and 0.97869 respectively. That occurs at the different positions of x. The rate of heat transfer coefficient increases by approximately 74% when γ changes from 0 to 10.0.

The variation of the local skin friction coefficient C_{fx} and local rate of heat transfer Nu_x for different values of the intensity of magnetic field at different positions of x are illustrated in figure 6.4 for Pr = 0.7, α = 0.3, J = 0.02, γ = 5.0 and ε = 5.0. From figure 6.4 it is observed that an increase in the intensity of magnetic field (M = 0.0, 0.2, 0.6, 1.0, 1.5) leads to decrease the local skin friction coefficient C_{fx} and local rate of heat transfer Nu_x at different position of x. The maximum values of skin friction coefficient and the rate of heat transfer in terms of the local Nusselt number Nu_x are 2.25346 and 0.69817 for M = 0.0 which occurs at x = 0.50 and 1.70749 which occurs at x = 0.45 and 0.63160 which occurs at surface for M = 1.5 respectively. The skin friction coefficient and the rate of heat transfer coefficient decrease by approximately 24% and 10% respectively as intensity of magnetic field increases from 0.0 to 1.5.

The surface shear stress in terms of skin friction coefficient and local rate of heat transfer for influence of Prandtl number Pr while M = 0.2, γ = 4.0, ε = 5.0, α = 0.3 and J = 0.02 are displayed in figures 6.5(a) and 6.5(b) respectively. From figure 6.5(a), it is noted that the decreasing skin friction coefficient monotonically changes in the downstream region. On the other hand, increased values of Prandtl number Pr increase the rate of heat transfer in the upstream direction of the surface. Moreover, the maximum values of the skin friction coefficient are recorded to be 2.10123, 1.85016, 1.67411, 1.41363 and 1.32685 for Pr = 0.73, 1.73, 3.0, 7.0 and 9.45 respectively. Furthermore, maximum values of the rate of heat transfer Nu_x are 0.61615, 0.81031, 0.96284, 1.23774 and 1.34802 for Pr = 0.73, 1.73, 3.0, 7.0 and 9.45 respectively. In this case the local skin friction coefficient decreases by

approximately 37% and the rate of heat transfer increases by approximately 54% which occurs at the point x = 0.50 while Prandtl number Pr changes from 0.73 to 9.45.

The effect of amplitude-to-length ratio of the wavy surface (α = 0.0, 0.1, 0.2, 0.3, 0.4) leads to decrease the skin friction coefficient and the rate of heat transfer in terms of the local Nusselt number while Prandtl number Pr = 0.73, M = 0.2, J = 0.01, γ = 4.0 and ε = 5.0 are shown in figures 6.6(a) and 6.6(b) respectively. The pick values of skin friction coefficient and the rate of heat transfer in terms of the local Nusselt number Nu_x are 2.17998 and 0.64624 respectively for α = 0.0 which attains at the surface and 2.09955, 2.10851, 2.10078, 2.06092 and 0.63134, 0.61835, 0.61681, 0.62702 for α = 0.1, 0.2, 0.3 and 0.4 respectively which occurs at different position of x. It is shown that surface shear stress in terms of the frictional force and temperature gradient in terms of heat transfer rate decrease by 5.46% and 2.97% respectively when amplitude-to-length ratio of the wavy surface increases from 0.0 to 0.4. Because of increasing the surface waviness the velocity force as well as skin friction coefficient and the heat transfer rate decrease at the local points.

Figure 6.7(a) and figure 6.7(b) deal with the effect of Joule heating on the velocity $f'(x,\eta)$ and the temperature $\theta(x,\eta)$ within the boundary layer for different values of the controlling parameters thermal conductivity variation parameter γ = 4.0, viscosity parameter ε = 5.0, α = 0.3, magnetic parameter M = 0.02 and Prandtl number Pr = 0.5. From figure 6.7(a), it is revealed that the velocity $f'(x,\eta)$ increases very slowly with the increase of Joule heating parameter which indicates that Joule heating accelerates the fluid motion. Small increment is shown from figure 6.7(b) on the temperature $\theta(x,\eta)$ for increasing value of J. Moreover, the highest values of the velocity are 0.55037, 0.55053, 0.55425, 0.55813 and 0.56589 for J = 0.0, 0.02, 0.50, 1.0 and 2.0 respectively and each of which occurs at the same value of η = 3.06886. It is seen that the velocity increases by only 2.74% when the value of Joule heating parameter changes from 0.0 to 2.0.

Figure 6.8(a) demonstrates the velocity $f'(x,\eta)$ for variation of viscosity (ε = 0.0, 5.0, 10.0, 15.0, 20.0) with other fixed parameters Prandtl number Pr = 1.0, M = 0.8, J = 0.02, α = 0.3 and thermal conductivity variation parameter γ = 5.0 and the

corresponding temperature $\theta(x,\eta)$ is shown in figure 6.8(b). Increasing viscosity decreases the velocity gradient normal to the wall. That is why the velocity of the fluid reduces quickly with the increase of the temperature dependent viscosity, which is shown in figure 6.8(a). The maximum values of the velocity are 0.61747, 0.41457, 0.34402, 0.30133 and 0.27130 for ε = 0.0, 5.0, 10.0, 15.0 and 20.0 respectively. It is observed that the velocity decreases by approximately 56% as ε increases from 0.0 to 20.0 that occurs at the different position of η. On the other hand the temperature increases within the boundary layer with the increasing values of viscosity parameter. Viscosity is proportional to linear function of temperature. So the increasing value of viscoty parameter increases the temperature difference between the surface and ambient temperature of the fluid. Then heat is transferred rapidely from surface to fluid within the boundary layer.

The variation of the velocity $f'(x,\eta)$ and the temperature $\theta(x,\eta)$ for the effect of magnetic field (M = 0.0, 0.2, 0.6, 1.0, 1.5) while Pr = 0.7, J = 0.02, γ = 5.0, ε = 5.0 and α = 0.3 are shown in figure 6.9(a) and figure 6.9(b) respectively. It is observed from figure 6.9(a) that the increase of the intensity of magnetic field leads to decrease the velocity up to a position of η and finally increases with the increase of magnetic parameter M. This is because of the velocity having lower peak values for higher values of magnetic parameter along η direction. Further, from figure 6.9(b), the opposite result is seen for the temperature if intensity of magnetic field increases.

Figures 6.10 and 6.11 illustrate the effect of Joule heating on the development of streamlines and isotherms profile which are plotted for α = 0.3, Pr = 0.5, ε = 5.0, γ = 4.0 and M = 0.02. Joule heating is the heating effect of conductors carrying currents. So the velocity and thermal bundary layer become thicker with the increasing values of J. This happens, because the buoyancy force increases, including the flow rate increase within the boundary layer. The maximum values of ψ, that is, ψ_{max} are 13.22, 14.45, 15.28 and 16.31 for Joule heating parameter J = 0.0, 0.06, 0.10 and 0.15 respectively.

The effect for different values of temperature dependent viscosity parameter equal to 0.0, 5.0, 10.0 and 15.0 the streamlines and isotherms profile are shown in figures 6.12 and 6.13 respectively while Pr = 1.0, α = 0.3, J = 0.02, γ = 5.0 and M = 0.8.

From figure 6.12, it is noted that the maximum values of ψ decreases steadily while the values of viscosity parameter increases. The maximum values of ψ, that is, ψ_{max} are 8.14, 6.69, 5.88 and 5.29 for viscosity parameter ε = 0.0, 5.0, 10.0 and 15.0 respectively. It is observed from figure 6.13 that as the values of viscosity parameter increase the thermal boundary layer becomes thicker gradually. Finally, it is concluded that for the effect of temperature dependent viscosity the velocity of the fluid flow decreases and temperature of the fluid flow within the boundary layer increases.

The influence of temperature dependent thermal conductivity on the development of streamlines and isotherms are plotted in figures 6.14 and 6.15 respectively for Pr = 0.73, α = 0.3, J = 0.02, ε = 5.0 and M = 0.5. It can be seen that for γ equal to 0.0, 2.0, 6.0 and 10.0 the maximum values of ψ, that is, ψ_{max} are 5.41, 7.37, 9.05 and 9.68 respectively. So from figure 6.14, it is seen that for the effect of thermal conductivity, the flow rate in the boundary layer increases. From figure 6.15 the same result is also observed for the thermal boundary layer.

Figures 6.16 and 6.17 depict the variation on the streamlines and isotherms for the values of Prandtl number Pr equal to 0.73, 3.0, 7.0 and 9.45 while the amplitude-to-length ratio of the wavy surface α = 0.3, M = 0.2, J = 0.02, ε = 5.0 and γ = 4.0. It is found that for Pr = 0.73 the value of ψ_{max} is 10.76, for Pr = 3.0 ψ_{max} is 6.11, for Pr = 7.0 ψ_{max} is 3.99 and ψ_{max} is 3.42 where Pr = 9.45. So it can be concluded that for higher values of Pr lead to thinner both the velocity and thermal boundary layer.

Figure 6.18 and figure 6.19 display results for the effect of variation of the surface roughness on the formation of streamlines and isotherms respectively for the values of the amplitude-to-length ratio of the wavy surface equal to 0.0, 0.1 and 0.2 while Pr = 0.73, M = 0.2, J = 0.01, γ = 4.0 and ε = 5.0. It is observed from figure 6.18 that as the values of α increases the maximum values of ψ increases slightly. The maximum values of ψ, that is, ψ_{max} are 11.20, 11.28 and 11.69 for α = 0.0, 0.1 and 0.2 respectively. The velocity of the fluid flow increases slowly within the boundary layer. Figure 6.19 also shows the same results for increasing values of the amplitude-to-length ratio of the wavy surface. It means that thermal boundary layer becomes thicker slowly.

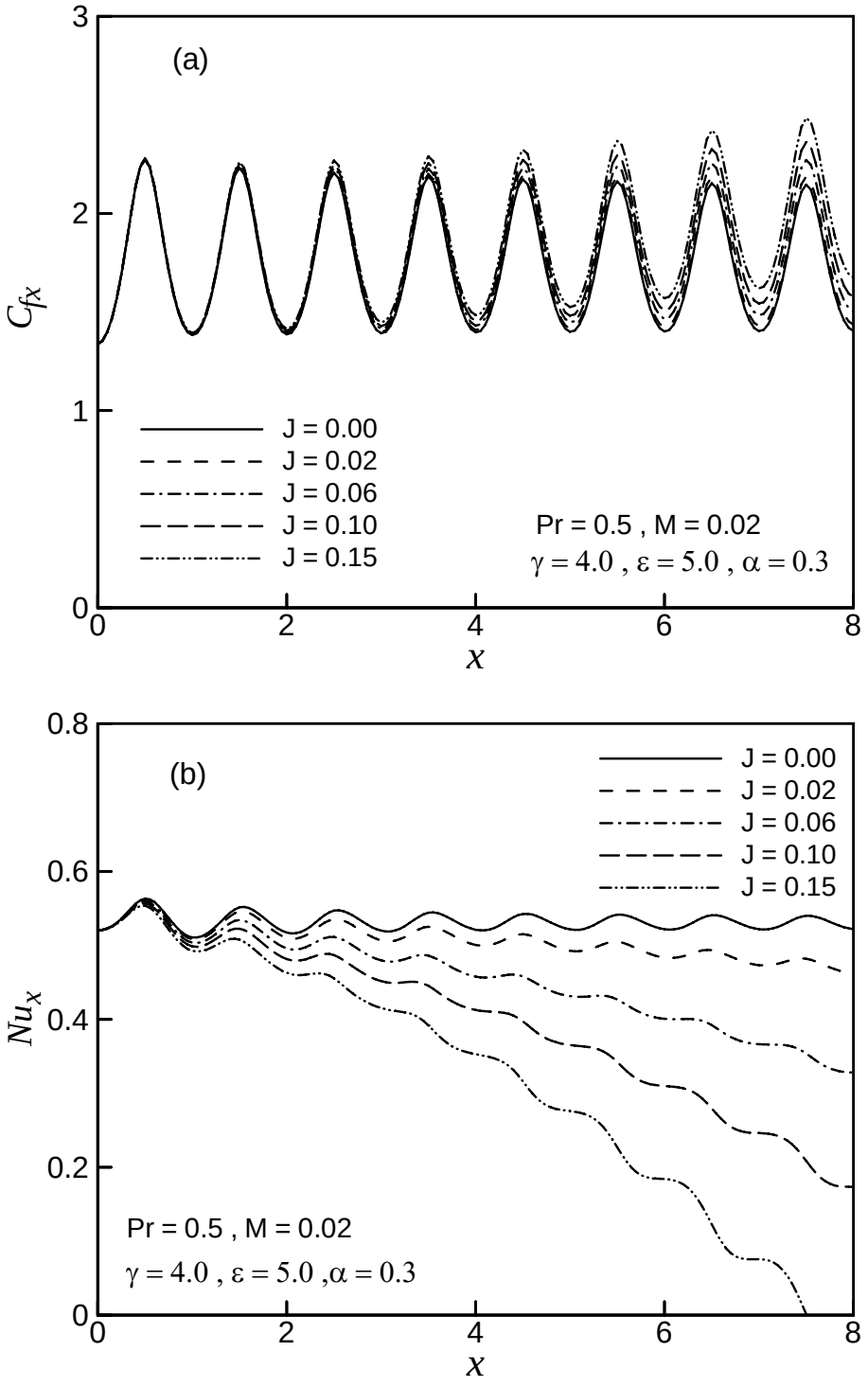

Figure 6.1: Variation of (a) skin friction coefficient C_{fx} and (b) rate of heat transfer Nu_x against dimensionless distance x for different values of J while Pr = 0.5, M = 0.02, γ = 4.0, ε = 5.0 and α = 0.3.

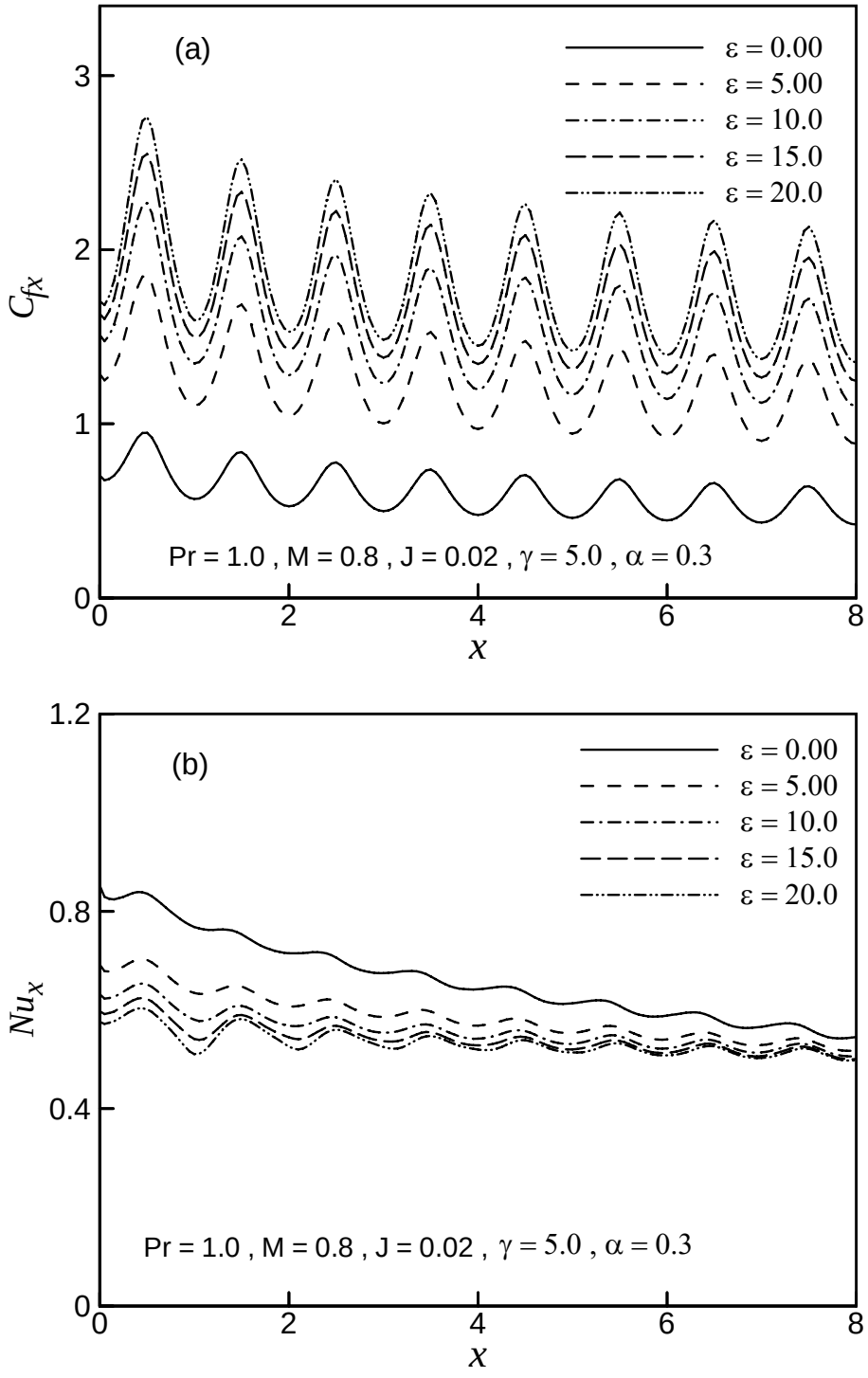

Figure 6.2: Variation of (a) skin friction coefficient C_{fx} and (b) rate of heat transfer Nu_x against dimensionless distance x for different values of viscosity parameter ε while $\alpha = 0.3$, $M = 0.8$, $J = 0.02$, $\gamma = 5.0$ and Pr = 1.0.

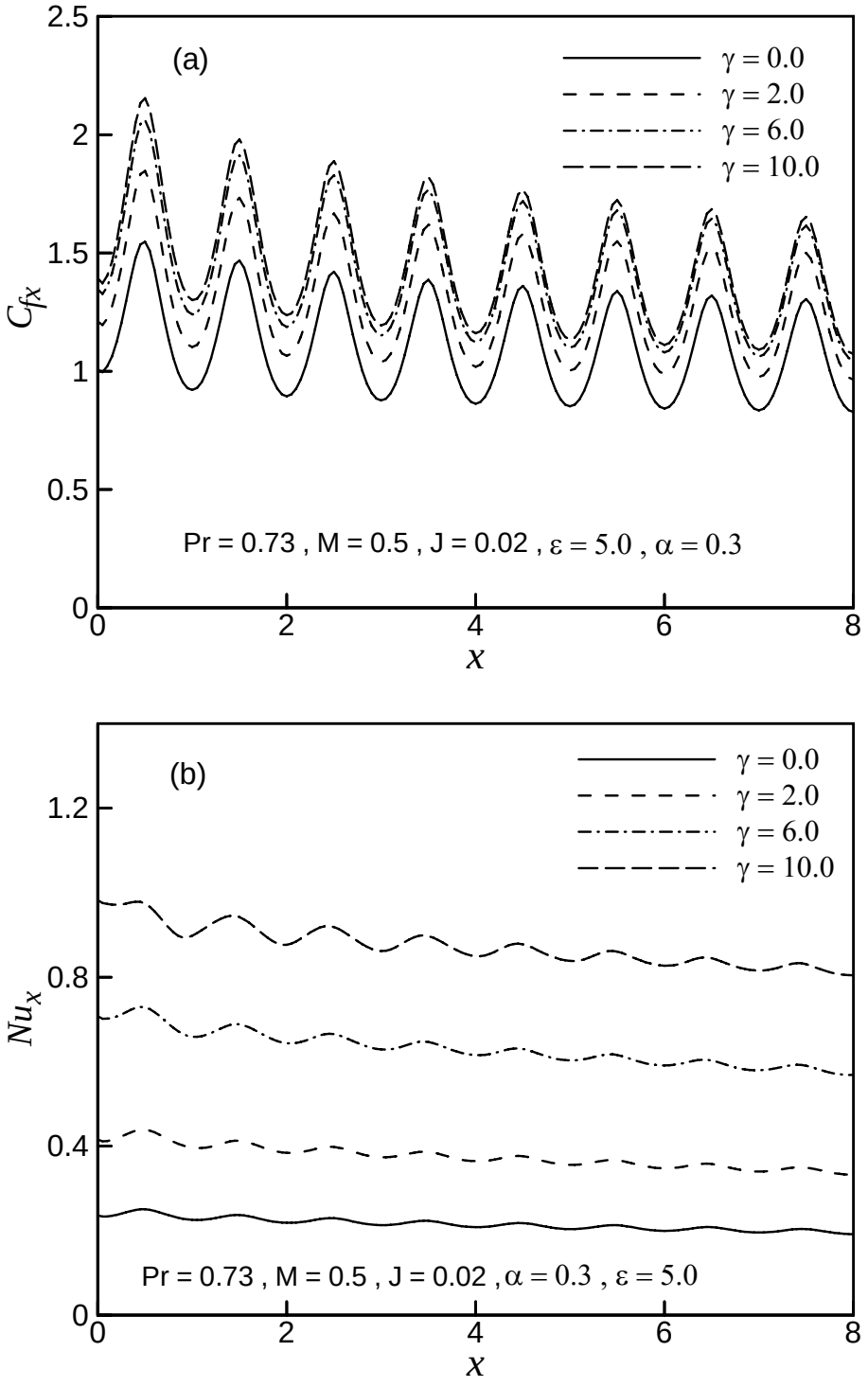

Figure 6.3: Variation of (a) skin friction coefficient C_{fx} and (b) rate of heat transfer Nu_x against dimensionless distance x for different values of thermal conductivity variation parameter γ while Pr = 0.73, M = 0.5, J = 0.02, α = 0.3 and ε = 5.0.

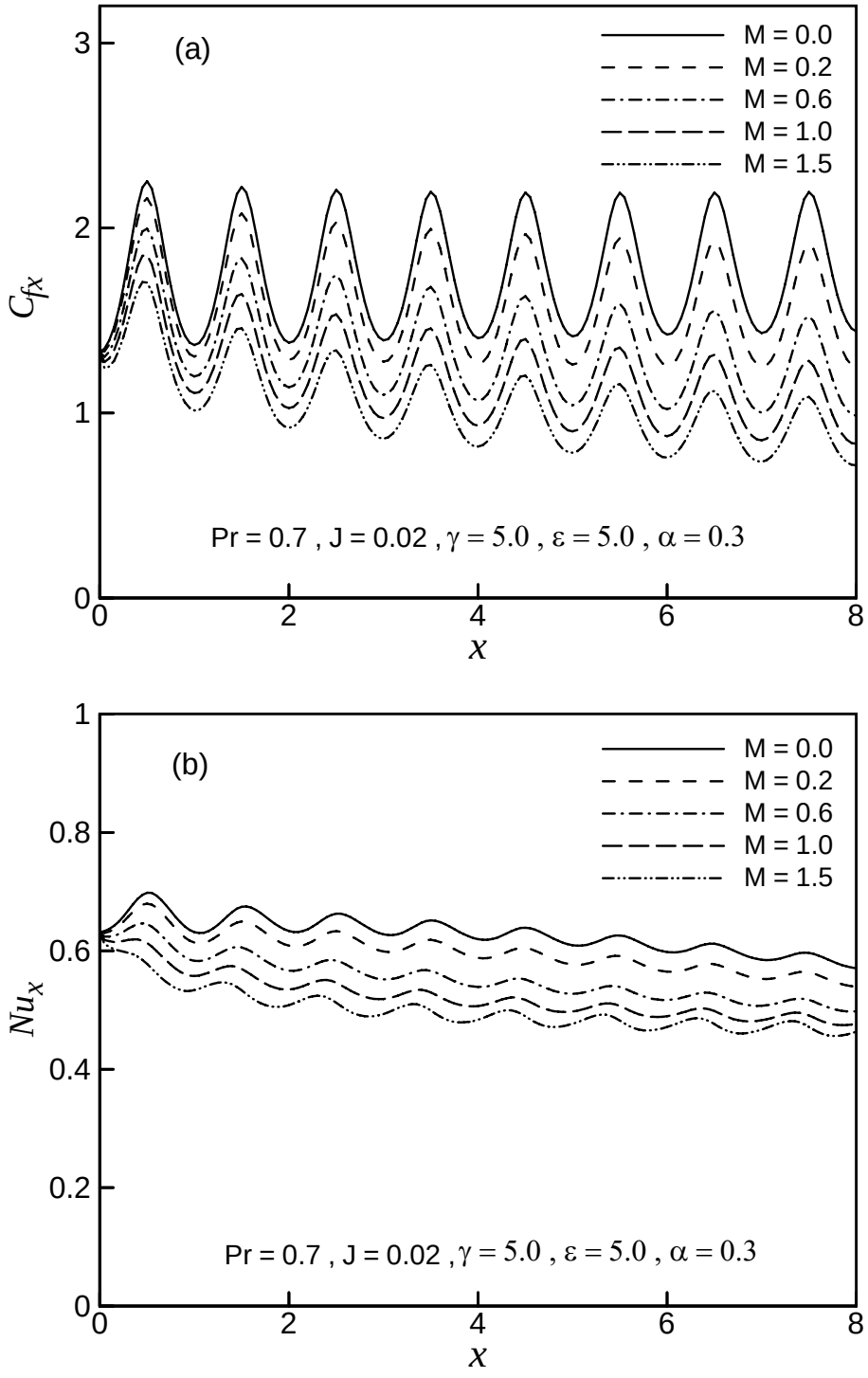

Figure 6.4: Variation of (a) skin friction coefficient C_{fx} and (b) rate of heat transfer Nu_x against dimensionless distance x for different values of M with Pr = 0.7, J = 0.02, γ = 5.0, ε = 5.0 and α = 0.3.

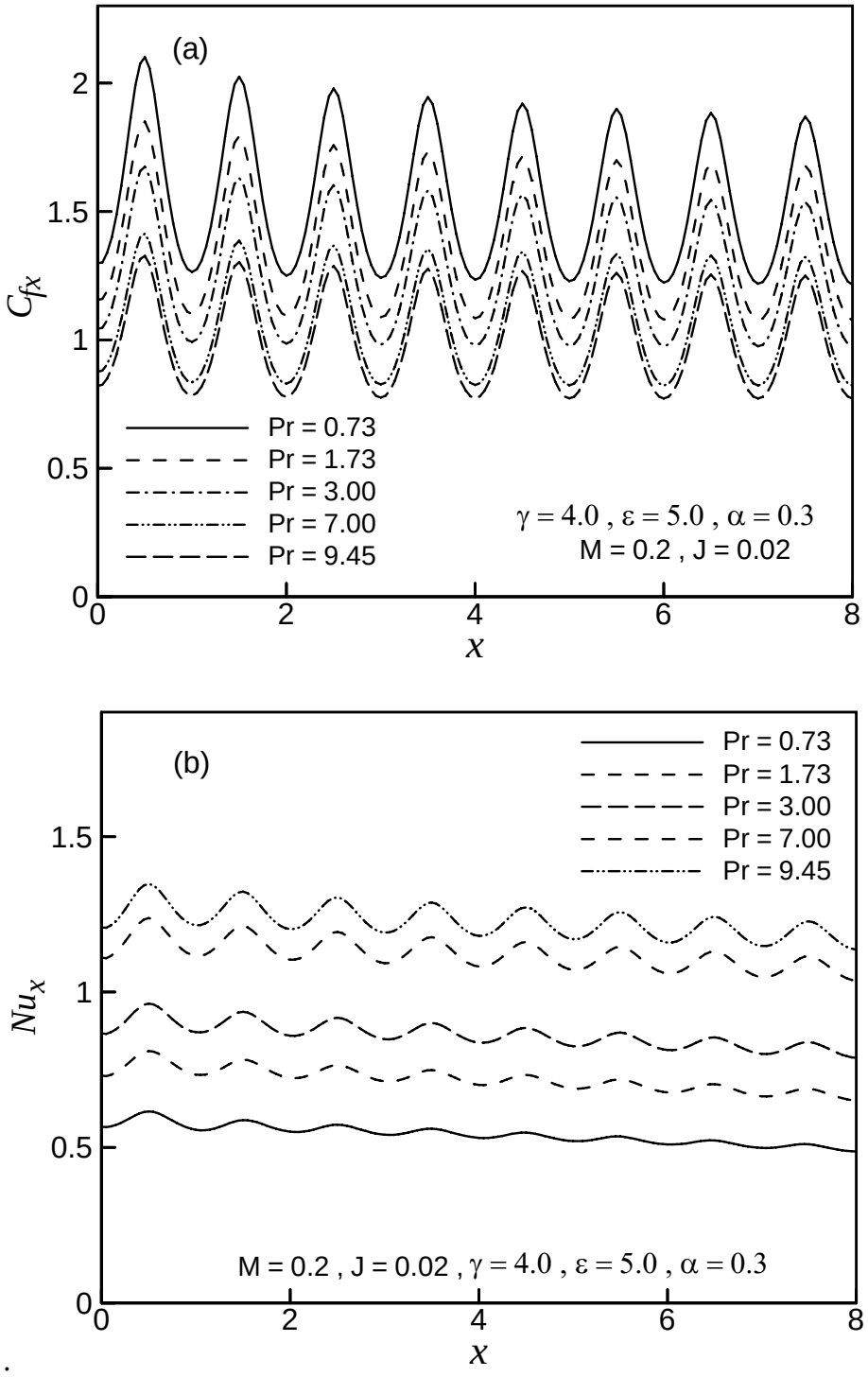

Figure 6.5: Variation of (a) skin friction coefficient C_{fx} and (b) rate of heat transfer Nu_x against dimensionless distance x for different values of Pr while $M = 0.2$, $J = 0.02$, $\gamma = 4.0$, $\varepsilon = 5.0$ and $\alpha = 0.3$.

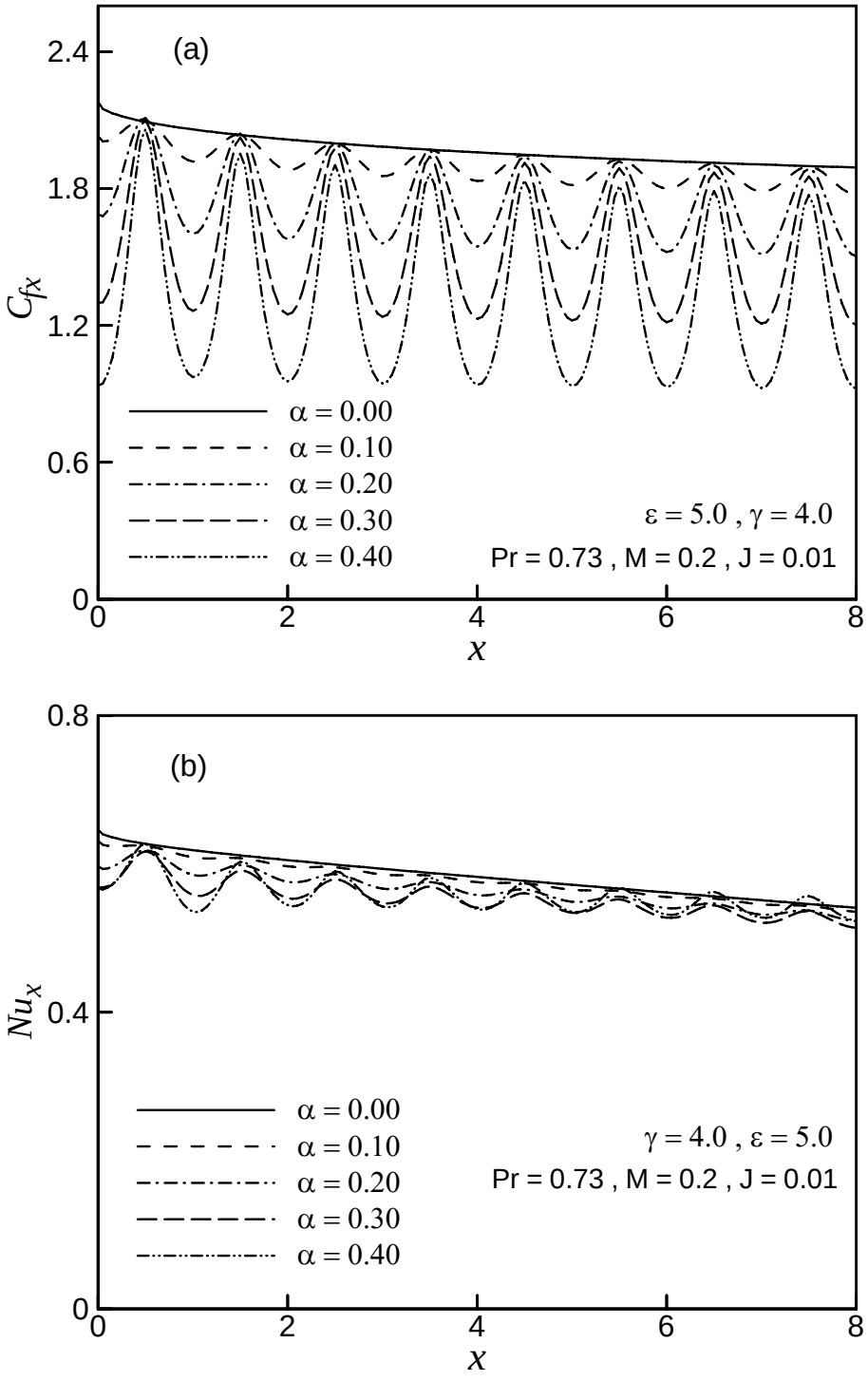

Figure 6.6: Variation of (a) skin friction coefficient C_{fx} and (b) rate of heat transfer Nu_x against dimensionless distance x for different values of α when $\gamma = 4.0$, $\varepsilon = 5.0$, Pr = 0.73, $M = 0.2$ and $J = 0.01$.

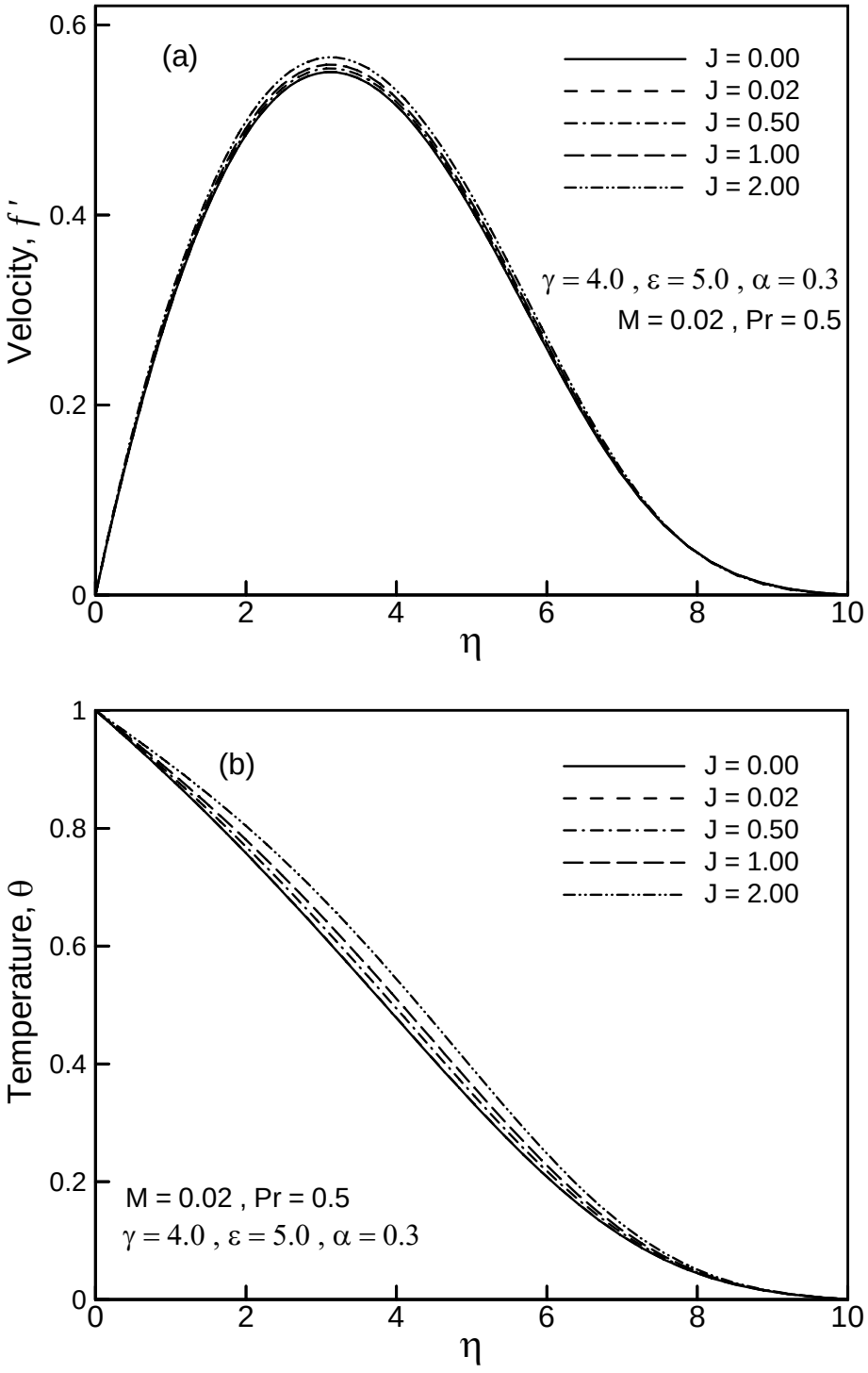

Figure 6.7: (a) Velocity profiles f' and (b) temperature distribution θ against dimensionless distance η for different values of J while Pr = 0.5, M = 0.02, γ = 4.0, ε = 5.0 and α = 0.3.

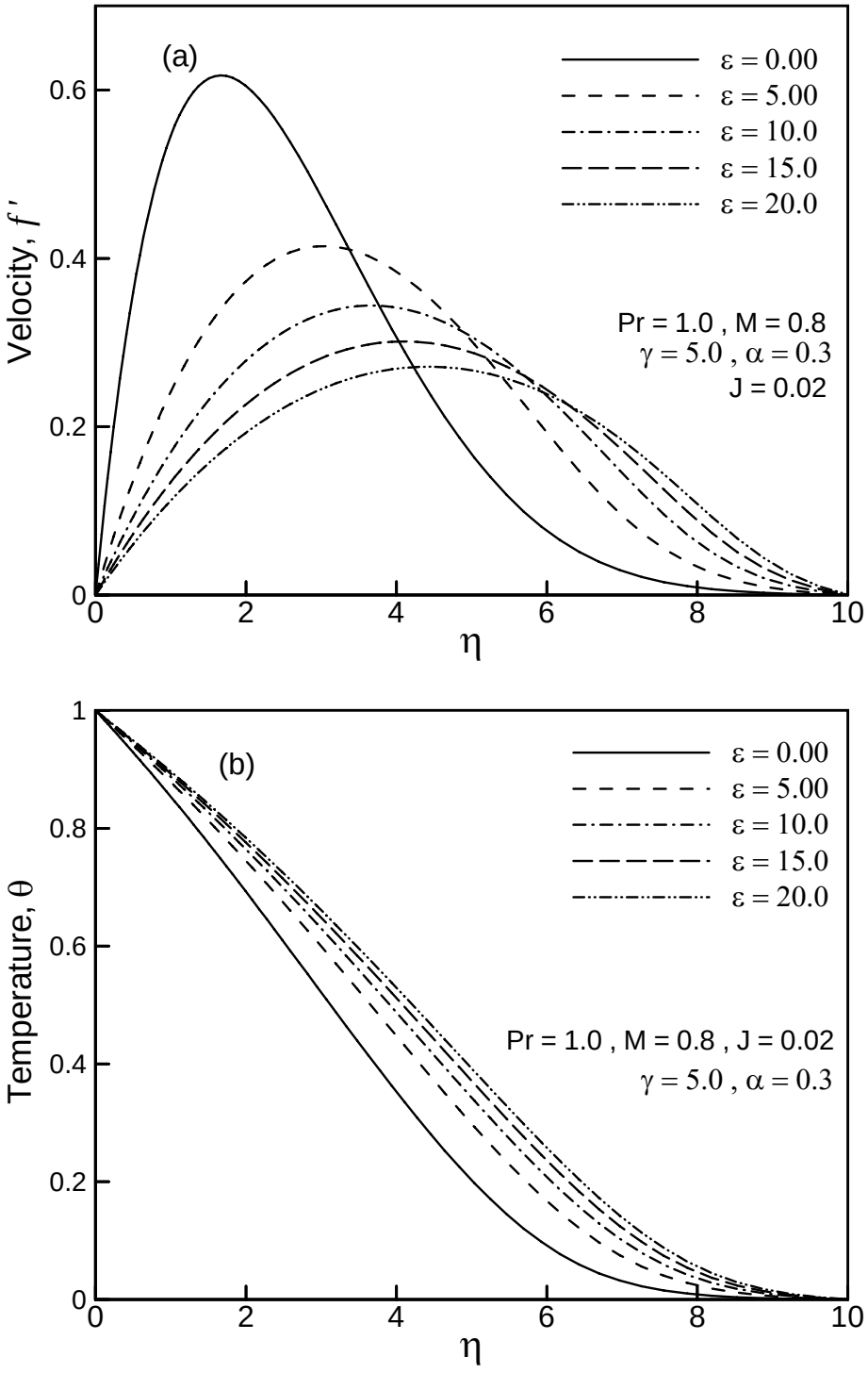

Figure 6.8: (a) Velocity profiles f' and (b) temperature distribution θ against dimensionless distance η for different values of ε while $\alpha = 0.3$, $M = 0.8$, $J = 0.02$, $\gamma = 5.0$ and Pr = 1.0.

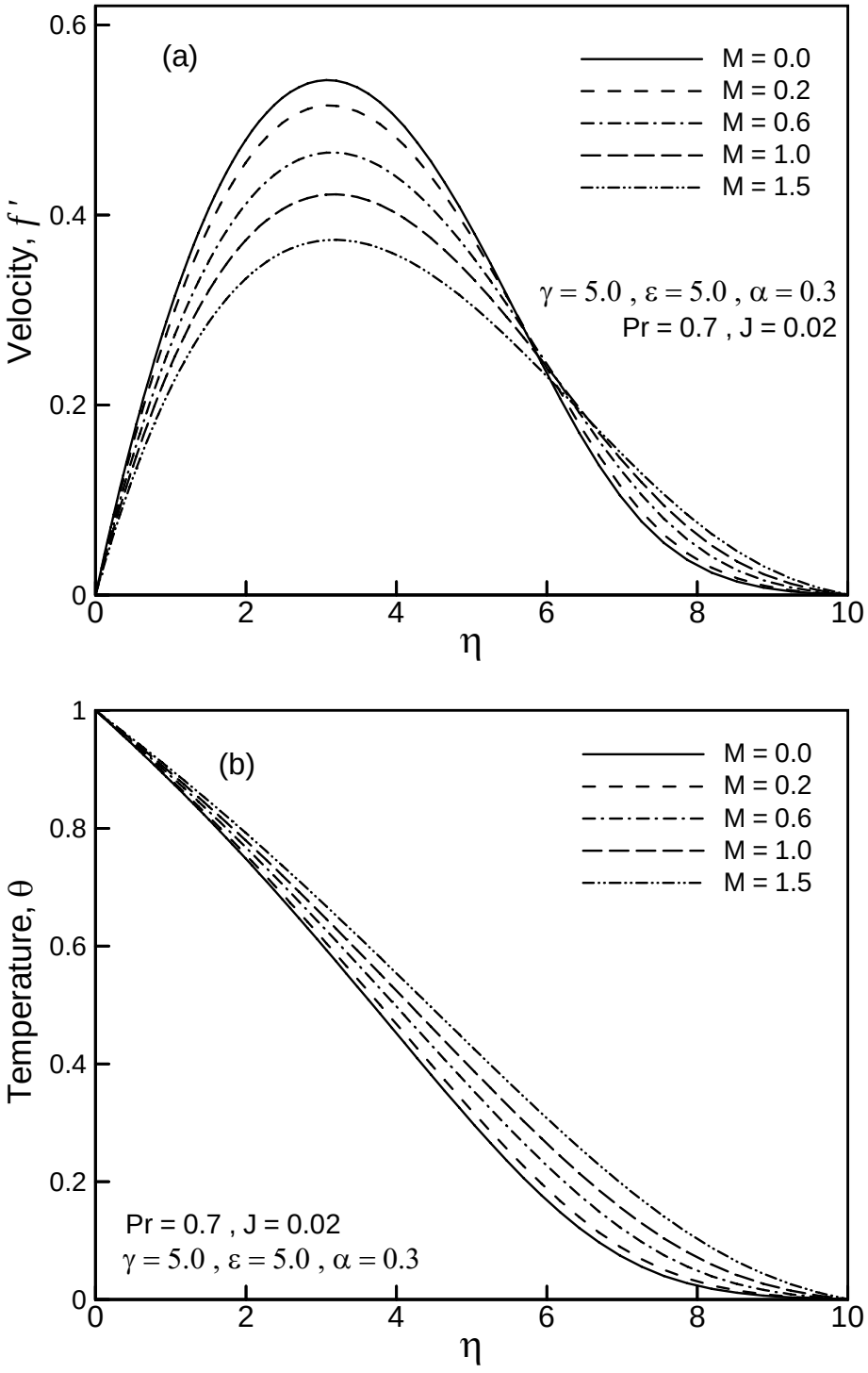

Figure 6.9: (a) Velocity profiles f' and (b) temperature distribution θ against dimensionless distance η for different values of M with Pr = 0.7, α = 0.3 and γ = 5.0, J = 0.02 and ε = 5.0.

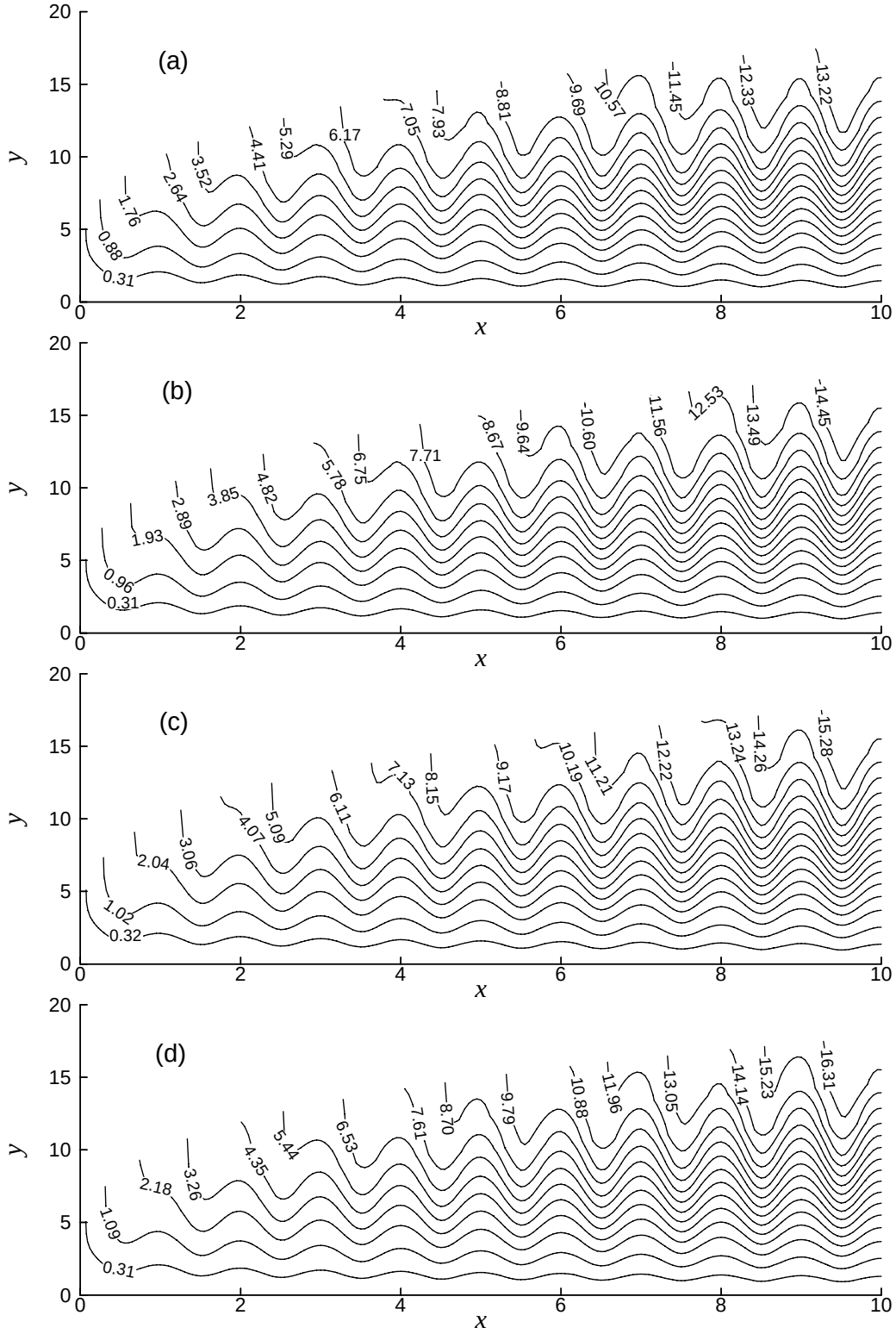

Figure 6.10: Streamlines for (a) J = 0.0 (b) J = 0.06 (c) J = 0.10 (d) J = 0.15 while α = 0.3, Pr = 0.5, ε = 5.0, γ = 4.0 and M = 0.02.

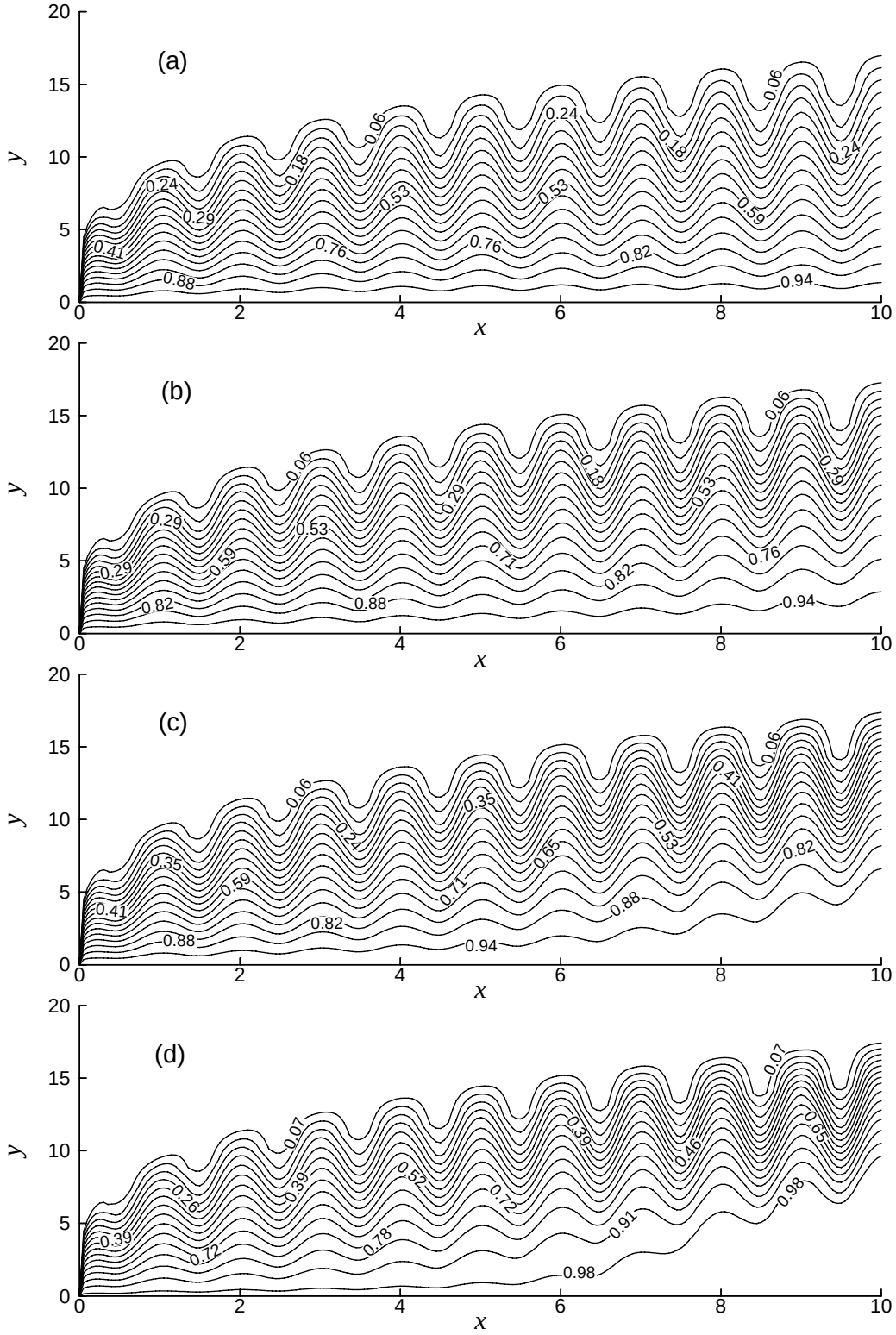

Figure 6.11: Isotherms for (a) J = 0.0 (b) J = 0.06 (c) J = 0.10 (d) J = 0.15 while α = 0.3, Pr = 0.5, ε = 5.0, γ = 4.0 and M = 0.02.

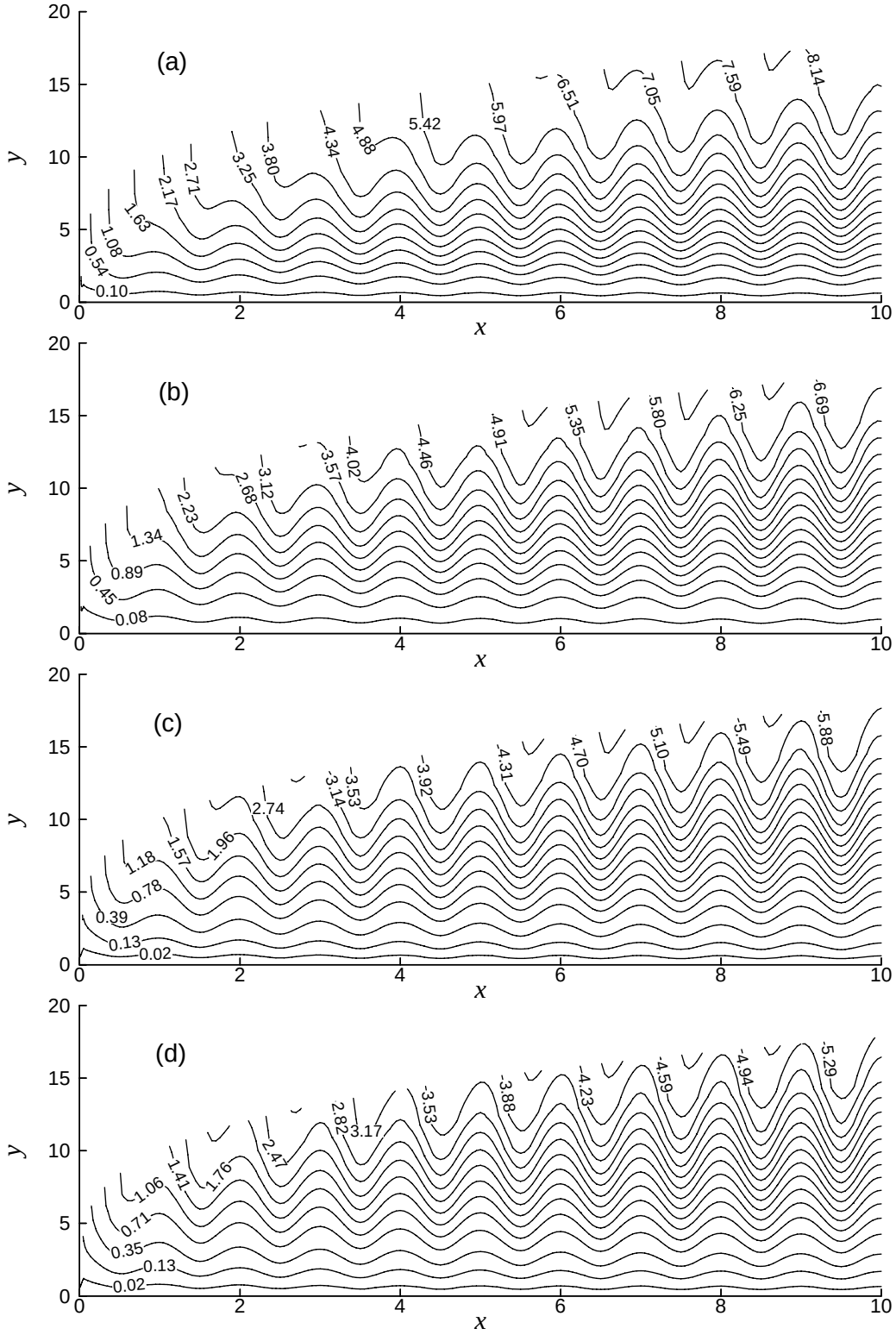

Figure 6.12: Streamlines for (a) $\varepsilon = 0.0$ (b) $\varepsilon = 5.0$ (c) $\varepsilon = 10.0$ (d) $\varepsilon = 15.0$ while Pr = 1.0, $\alpha = 0.3$, $J = 0.02$, $\gamma = 5.0$ and $M = 0.8$.

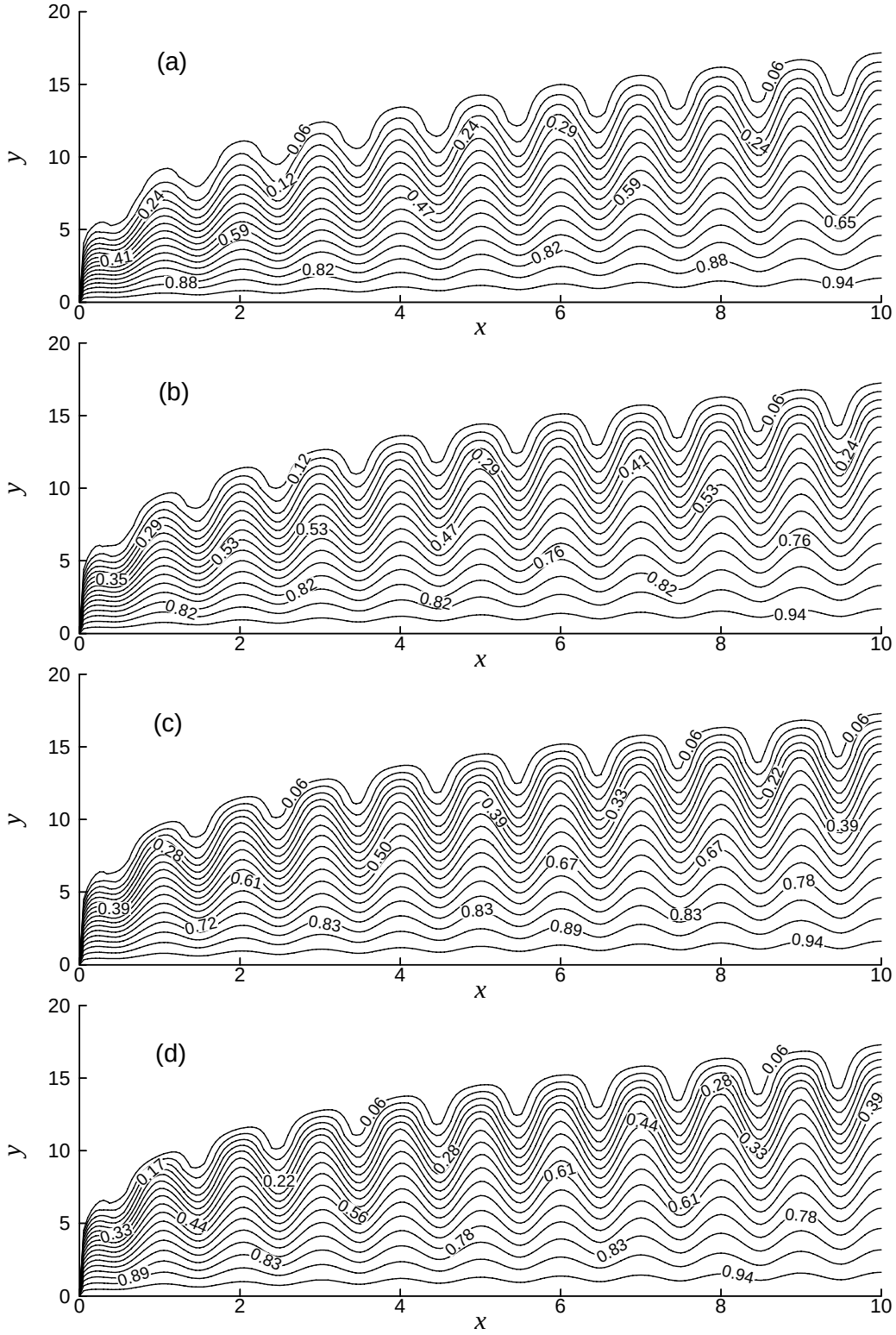

Figure 6.13: Isotherms for (a) ε = 0.0 (b) ε = 5.0 (c) ε = 10.0 (d) ε = 15.0 while Pr = 1.0, α = 0.3, J = 0.02, γ = 5.0 and M = 0.8.

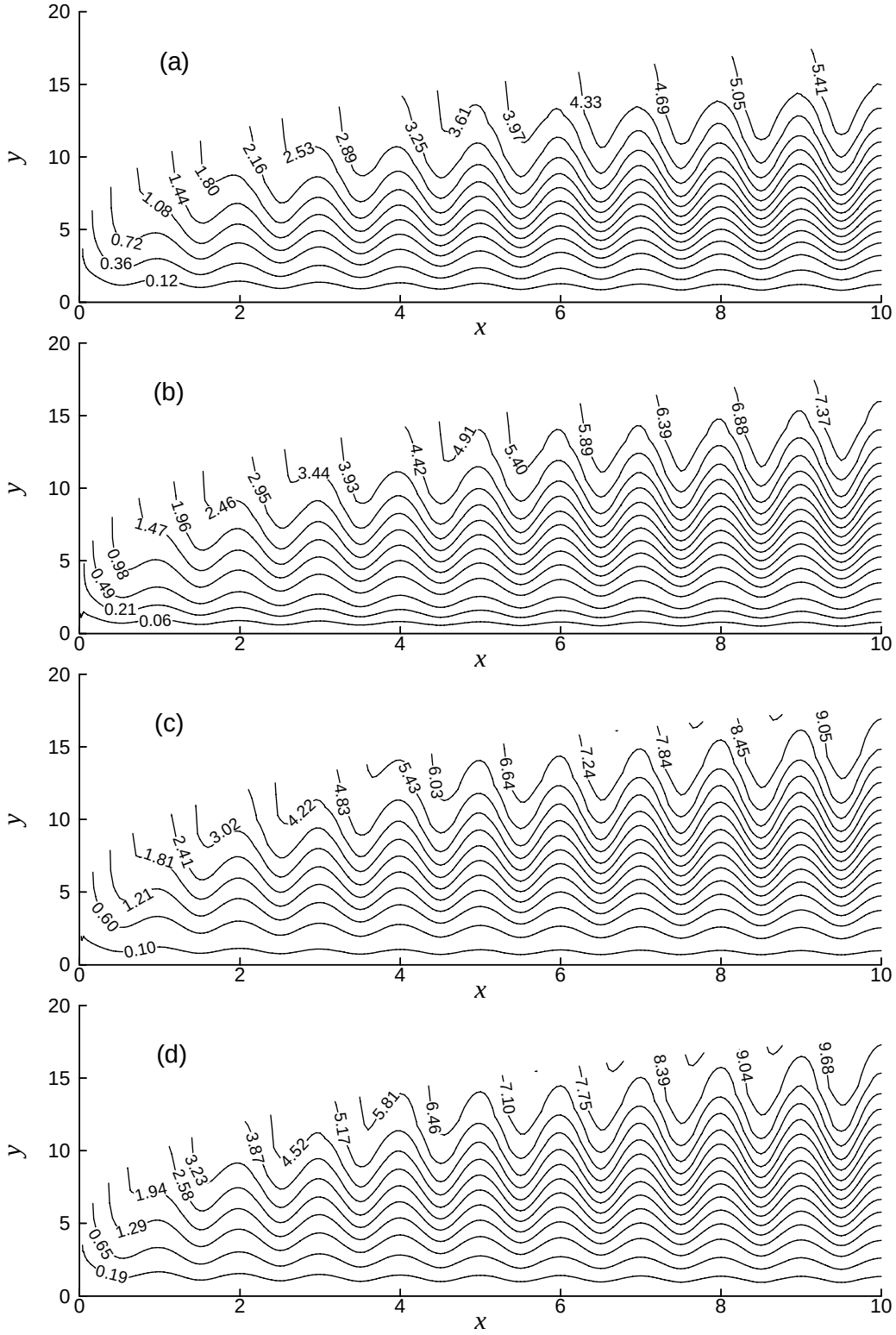

Figure 6.14: Streamlines for (a) $\gamma = 0.0$ (b) $\gamma = 2.0$ (c) $\gamma = 6.0$ (d) $\gamma = 10.0$ while Pr = 0.73, $\alpha = 0.3$, $J = 0.02$, $\varepsilon = 5.0$ and $M = 0.5$.

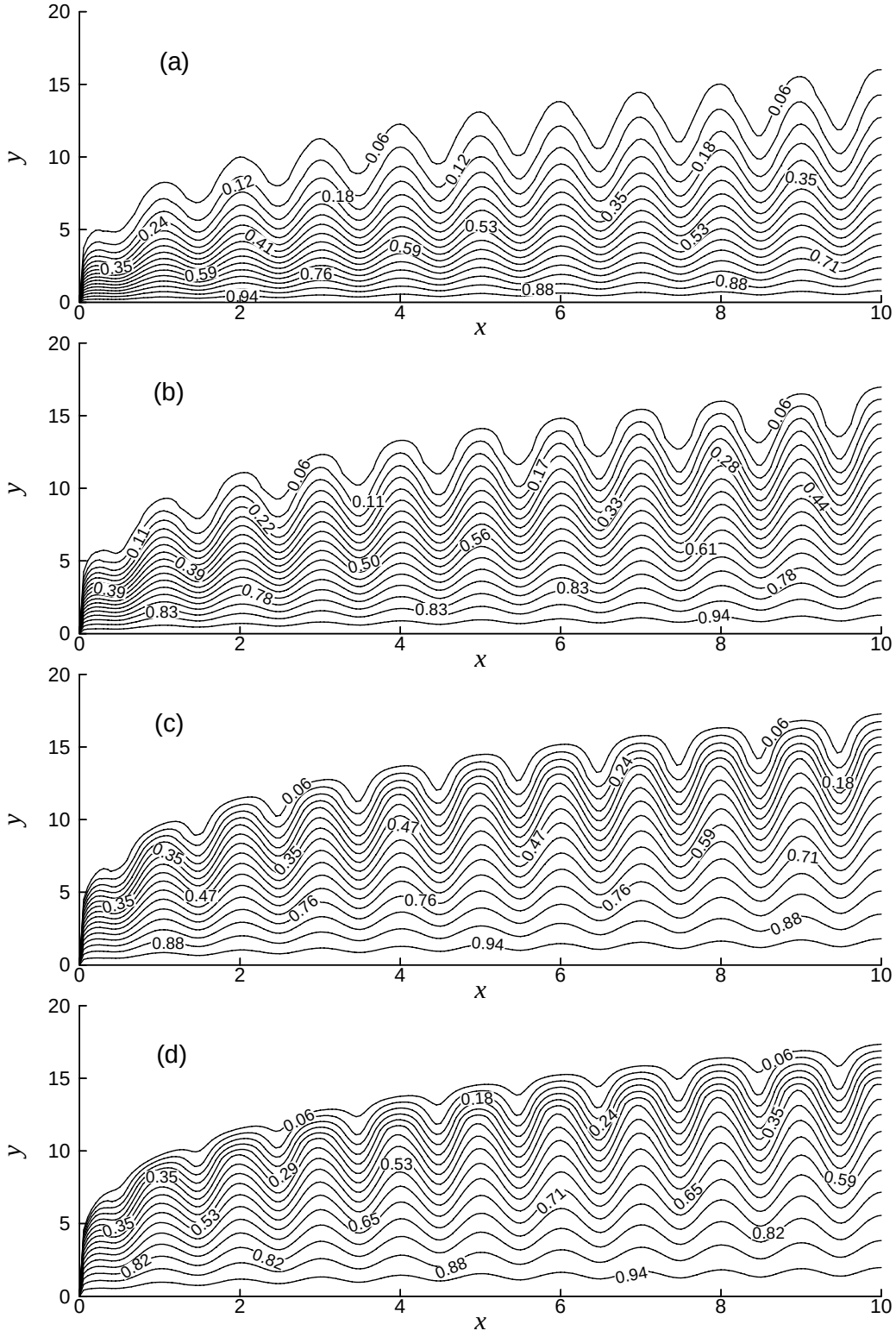

Figure 6.15: Isotherms for (a) $\gamma = 0.0$ (b) $\gamma = 2.0$ (c) $\gamma = 6.0$ (d) $\gamma = 10.0$ while Pr = 0.73, $\alpha = 0.3$, $J = 0.02$, $\varepsilon = 5.0$ and $M = 0.5$.

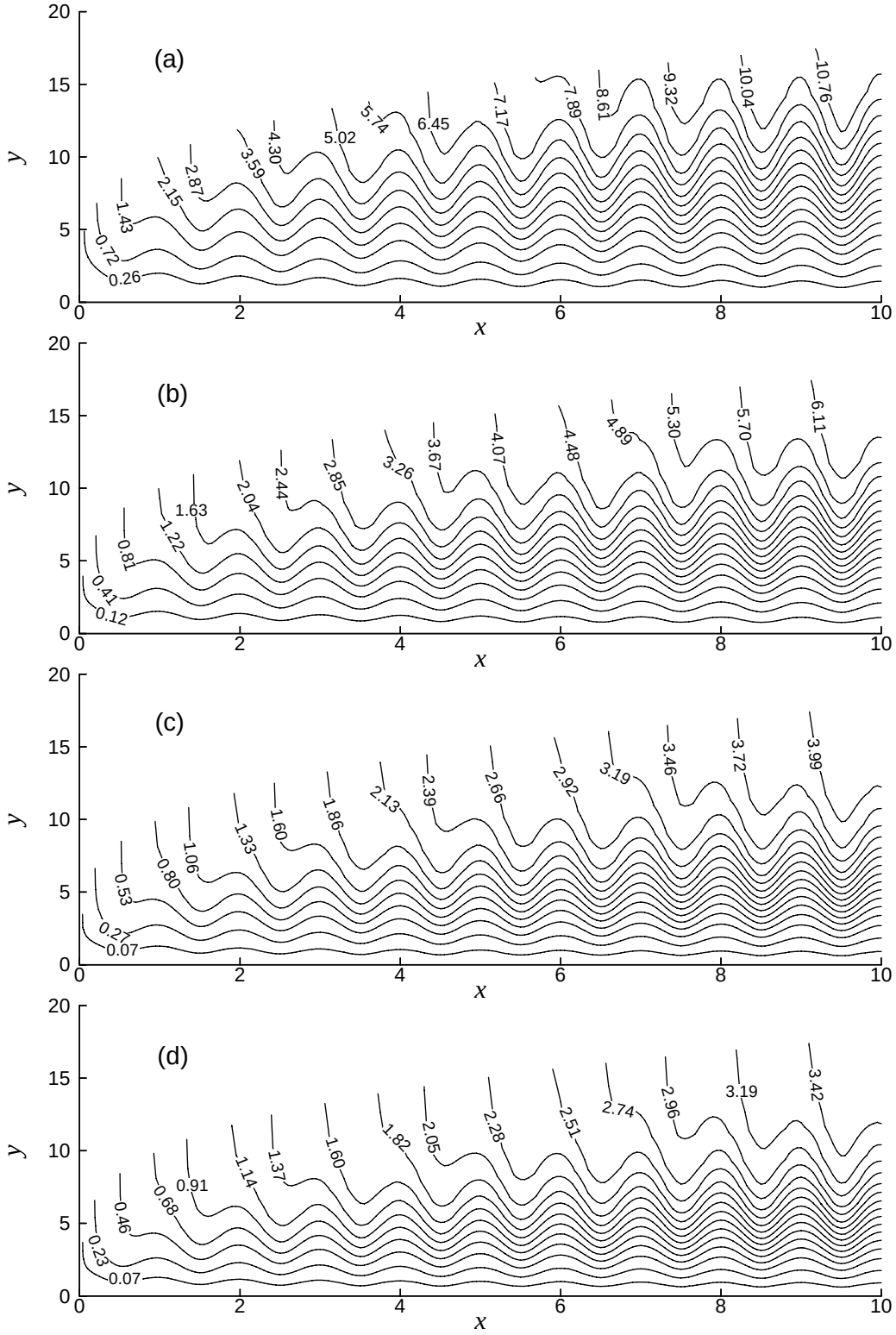

Figure 6.16: Streamlines for (a) Pr = 0.73 (b) Pr = 3.0 (c) Pr = 7.0 (d) Pr = 9.45 while $\varepsilon = 5.0$, $M = 0.2$, $J = 0.02$, $\gamma = 4.0$ and $\alpha = 0.3$.

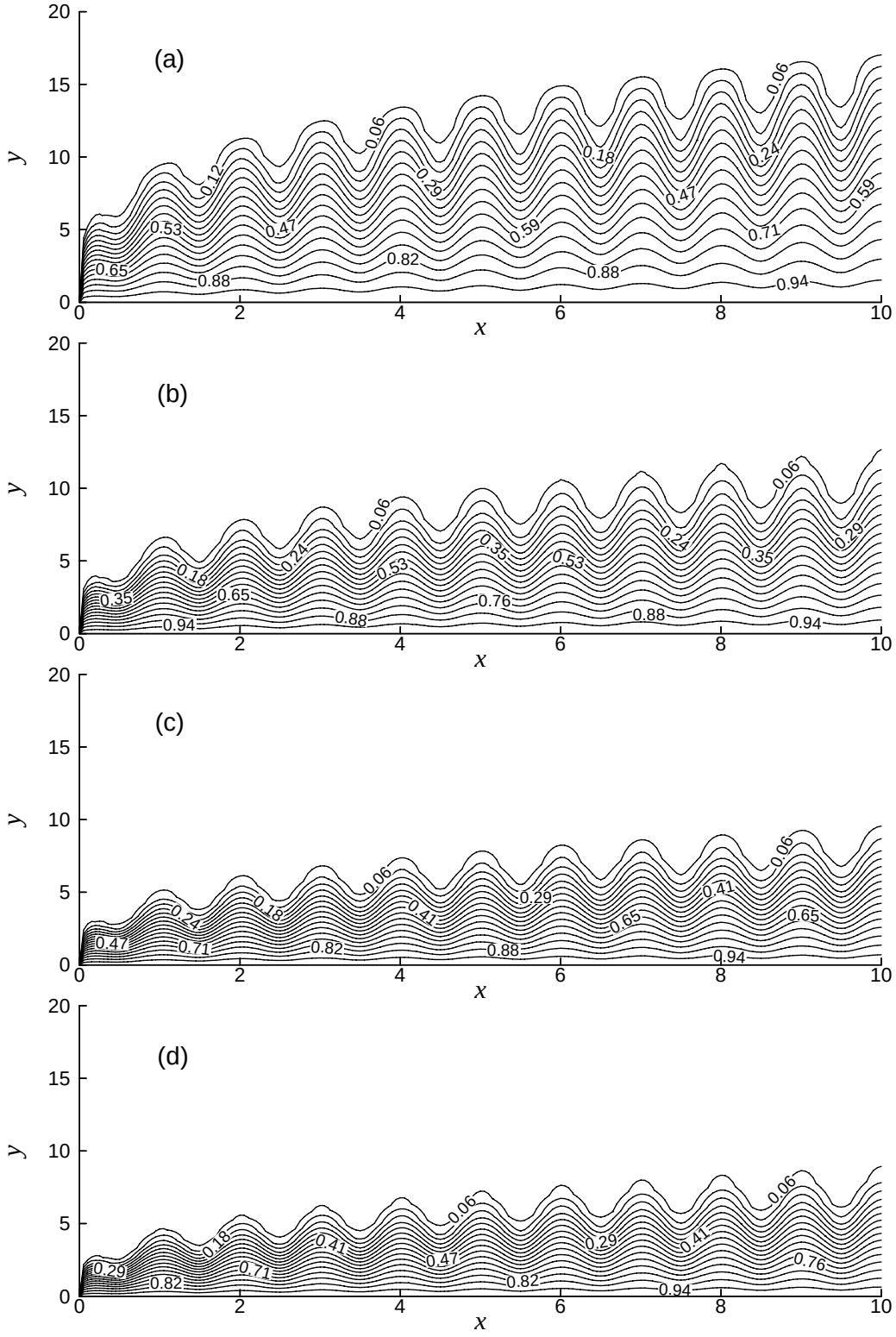

Figure 6.17: Isotherms for (a) Pr = 0.73 (b) Pr = 3.0 (c) Pr = 7.0 (d) Pr = 9.45 while $\varepsilon = 5.0$, $M = 0.2$, $J = 0.02$, $\gamma = 4.0$ and $\alpha = 0.3$.

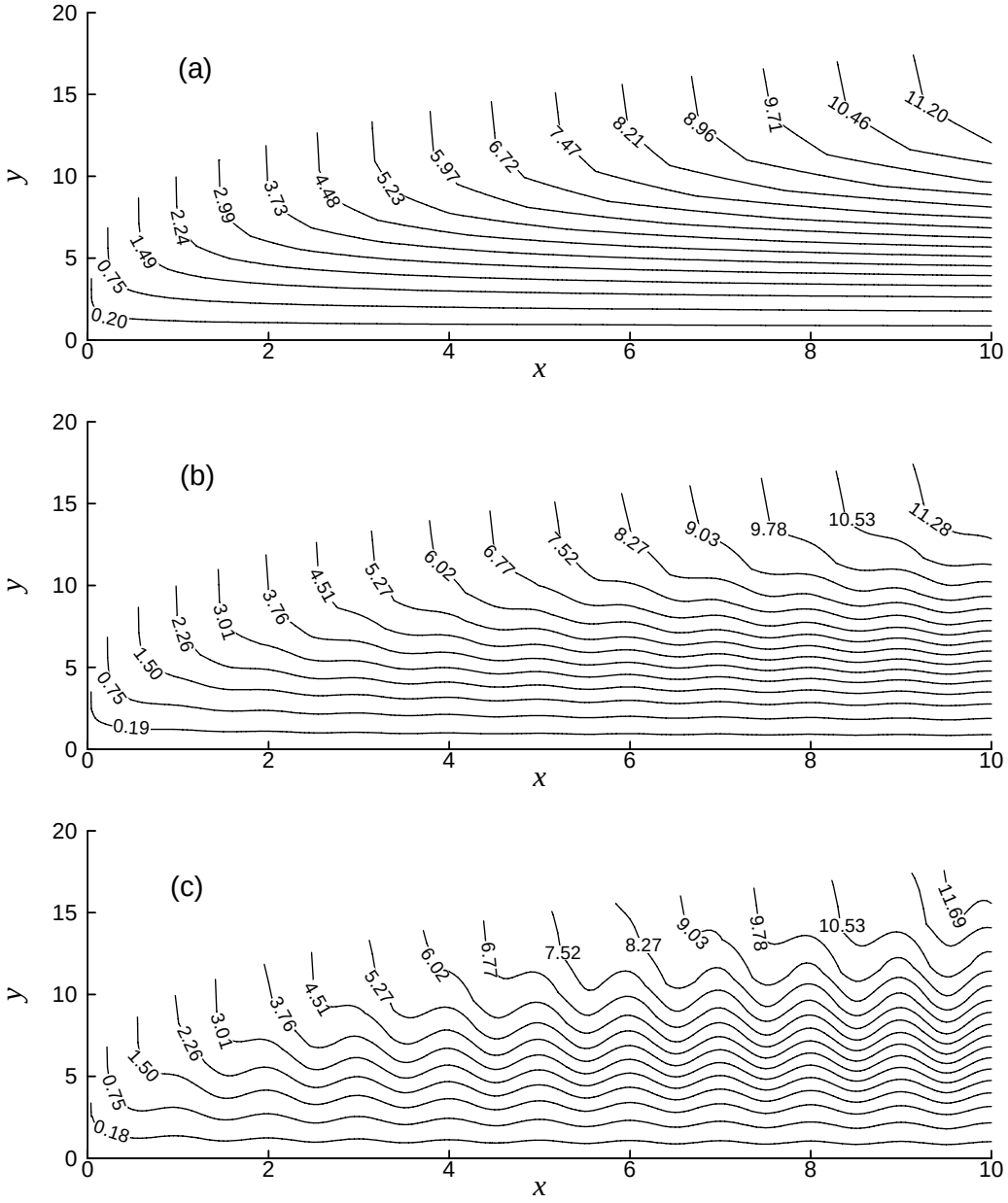

Figure 6.18: Streamlines for (a) α = 0.0 (b) α = 0.1 (c) α = 0.2 while Pr = 0.73, J = 0.01, ε = 5.0, M = 0.2 and γ = 4.0.

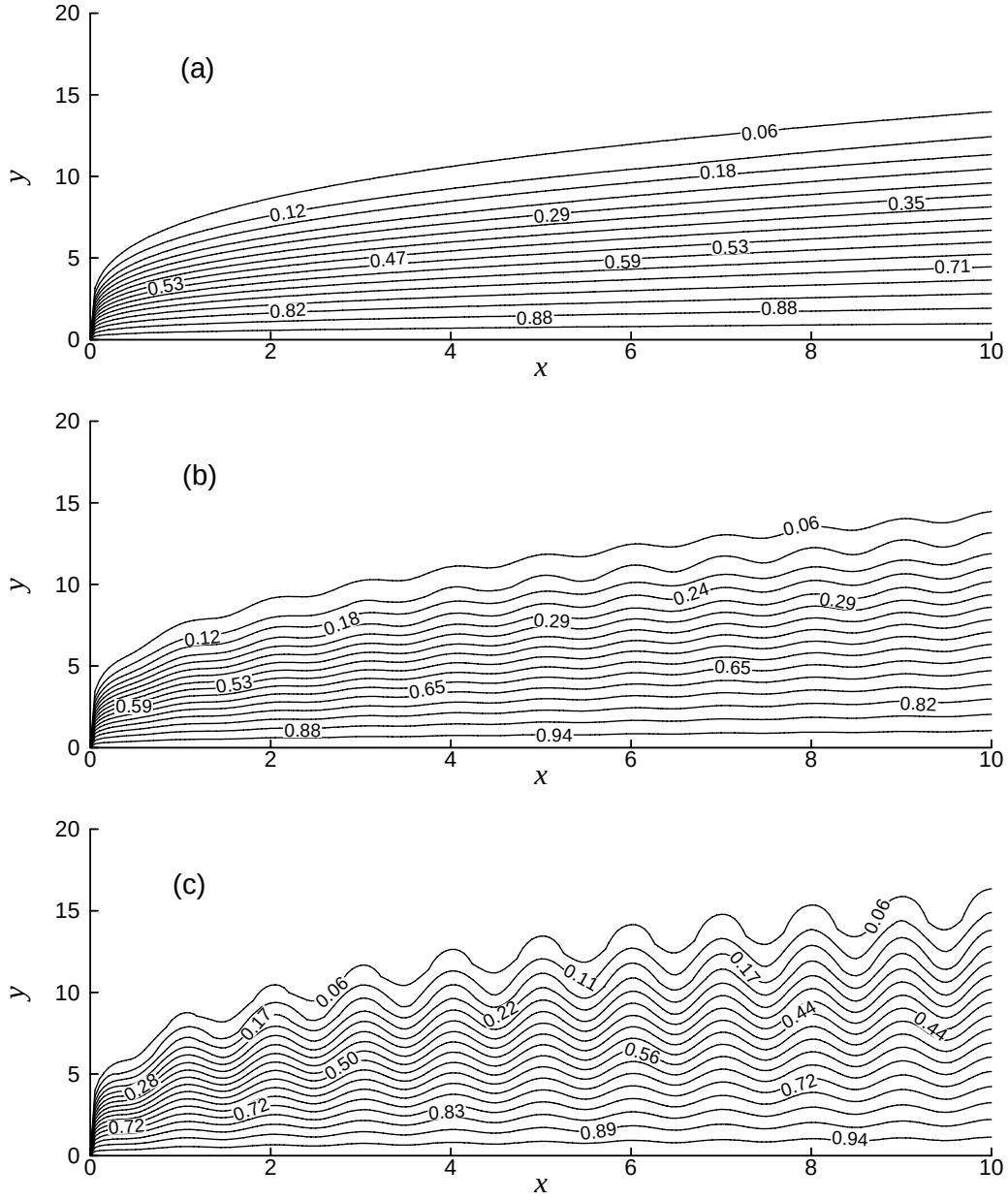

Figure 6.19: Isotherms for (a) $\alpha = 0.0$ (b) $\alpha = 0.1$ (c) $\alpha = 0.2$ while Pr = 0.73, $J = 0.01$, $\varepsilon = 5.0$, $M = 0.2$ and $\gamma = 4.0$.

The values of skin friction coefficient C_{fx} and the rate of heat transfer in terms of the local Nusselt number Nu_x for variation of Joule heating (J = 0.0, 0.06, 0.15) while the amplitude-to-length ratio of the wavy surface α = 0.3, magnetic parameter M = 0.02, thermal conductivity variation parameter γ = 4.0, viscosity variation parameter ε = 5.0 and Prandtl number Pr = 0.5 are entered in Table A5 which shown in appendix A. It is noted that the complete cycle of the wavy surface is from x = 0.0 to 2.0. The skin friction coefficient C_{fx} and the rate of heat transfer increase for the first quarter of the cycle ($x \cong 0$ to $x \cong 0.50$) and decrease in the second quarter ($x \cong 0.50$ to $x \cong 1.0$). From $x \cong 1.0$ to $\cong 1.5$ (i.e., third quarter) the skin friction coefficient C_{fx} again increases, where as the fourth quarter ($x \cong 1.5$ to $x \cong 2.0$) it decreases. The skin friction coefficient C_{fx} and the rate of heat transfer in terms of the local Nusselt number Nu_x show similar characteristics throughout the domain. The maximum values of local skin friction coefficient C_{fx} are recorded to be 2.27275, 2.27550 and 2.27963 for J = 0.0, 0.06 and 0.15 respectively and it is seen that the local skin friction coefficient C_{fx} increases by only 0.30%. The maximum values of the rate of heat transfer in terms of the local Nusselt number Nu_x are recorded to be 0.56347, 0.55958 and 0.55372 for J = 0.0, 0.06 and 0.15 respectively and the rate of heat transfer Nu_x decreases by 1.73% as J increases from 0.0 to 0.15. Both are occurs at the same value of x = 0.50.

6.3 Conclusions

A computational analysis of the effect of Joule heating on magnetic field natural convection flow with viscosity and thermal conductivity variation owing to temperature along a uniformly heated vertical wavy surface has been offered. The subsequent outcome may be drawn as:

- The local skin friction coefficient increases noticeably for the growing values of Joule heating parameter, temperature dependent viscosity parameter and temperature dependent thermal conductivity parameter and decreasing values of effect of magnetic field, Prandtl number Pr and the amplitude-to-length ratio of the wavy surface.
- An increase in the values of Joule heating parameter, temperature dependent viscosity parameter, amplitude-to-length ratio of the wavy surface and the

intensity of magnetic field lead to a significant decrease in the local rate of heat transfer. Moreover, the local rate of heat transfer increase due to increase of temperature dependent thermal conductivity and Prandtl number Pr.

- The rate of fluid flow within the boundary layer radically increases for increasing values of temperature dependent thermal conductivity and decrease for increasing values of temperature dependent viscosity, the intensity of magnetic field and Prandtl number Pr.
- The temperature of the fluid flow within the boundary layer rises considerably for the increasing values of temperature dependent viscosity, temperature dependent thermal conductivity, the effect of magnetic field and decreasing values of Prandtl number.
- The velocity and temperature increase slightly for Joule heating and the amplitude-to-length ratio of the wavy surface.
- The velocity and thermal boundary layer expand for increasing values of Joule heating parameter and the amplitude-to-length ratio of the wavy surface.

CHAPTER 7

Comparison

7.1 Introduction

The comparisons of the numerical results of the skin friction coefficient, the rate of heat transfer, the velocity, the temperature as well as the streamlines and the isotherms for the effect of temperature dependent viscosity, thermal conductivity, magnetic field and Joule heating are presented graphically and also in tabular form. The comparisons of the present numerical results of the velocity, the temperature, the skin friction coefficient and the rate of heat transfer are also represented in tabular form and graphically with those obtaintd by Hossain et al. (2002) and Alam et al. (1997). The present results are excellent agreement with the solutions of Hossain et al. (2002) and Alam et al. (1997) which are shown in this chapter.

7.2 Comparison of streamlines and isotherms for the effect of temperature dependent viscosity and magnetic field

Figure 7.1 illustrates the effect of temperature dependent viscosity and magnetic field, on the development of streamlines which are plotted for the amplitude-to-length ratio of the wavy surface α = 0.3 and Prandtl number Pr = 0.73. When ε = 0 and M = 0, where the viscosity is independent of temperature and in absence of magnetic field as shown in figure 7.1(a). In this case ψ_{max} is 9.25. In figure 7.1(b) it is seen that an increase in the value of M causes the effects of the wavy surface to be attenuated and the boundary layer becomes thinner where ψ_{max} is 6.20. In this case viscosity of fluid is constant. The magnetic field acting along the horizontal direction retards the fluid velocity. For this there creates a Lorentz force by the interaction between the applied magnetic field and flow field. This force acts against the fluid flow and reduces the velocity. However when the value of viscosity increases similar thing happens and the maximum value of ψ, that is ψ_{max} is 8.08 which is found in figure 7.1(c). The combined effects of viscosity and magnetic field are shown in figure 7.1(d). In this case the maximum value of ψ is 5.23 decreases comparatively in presence of magnetic field and temperature dependent viscosity.

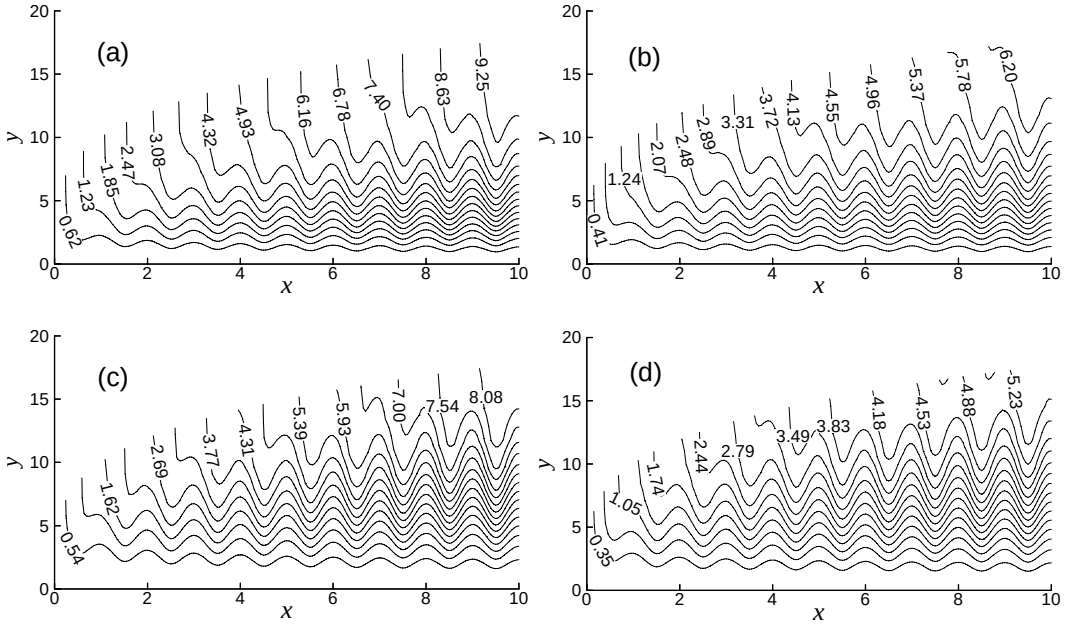

Figure 7.1: Streamlines for (a) ε = 0.0, M = 0.0 (b) ε = 0.0, M = 0.5 (c) ε = 5.0, M = 0.0 (d) ε = 5.0, M = 0.5 while Pr = 0.73 and α = 0.3.

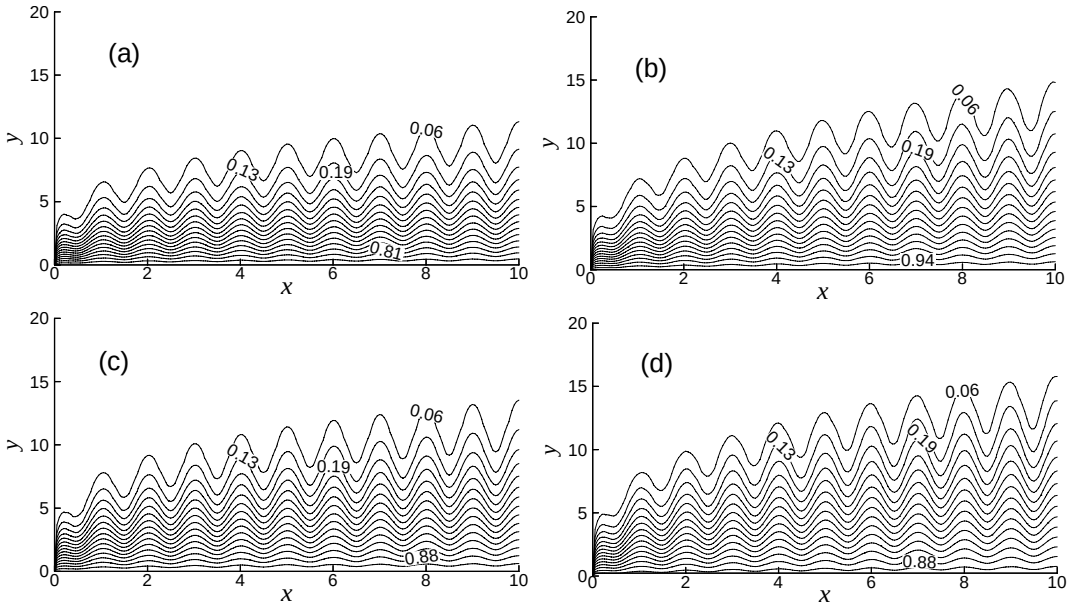

Figure 7.2: Isotherms for (a) ε = 0.0, M = 0.0 (b) ε = 0.0, M = 0.5 (c) ε = 5.0, M = 0.0 (d) ε = 5.0, M = 0.5 while Pr = 0.73 and α = 0.3.

The influence of the temperature dependent viscosity and magnetic field on the isotherms for α = 0.3 and Pr = 0.73 are displayed in figure 7.2. As mentioned before,

owing to the presence of temperature dependent viscosity and magnetic field ($\varepsilon > 0$ and $M > 0$) the temperature of the fluid increases where the thermal boundary layer grows thick. In the downstream region the temperature of the fluid flow is negligible in this case. For constant viscosity and in absence of magnetic field, it is observed that the opposite phenomenon happens.

7.3 Comparison of streamlines and isotherms for the effect of thermal conductivity and magnetic field

The effect of temperature dependent thermal conductivity and magnetic field, on the development of streamlines which are displayed in figure 7.3 for the amplitude-to-length ratio of the wavy surface $\alpha = 0.2$ and Prandtl number Pr = 0.73. When $\gamma = 0$ and $M = 0$ where the thermal conductivity is independent of temperature and in absence of magnetic field is shown in figure 7.3(a). In this case the maximum value of ψ i.e. ψ_{max} is 9.10. In figure 7.3(b) it is noted that an increase in the value of thermal conductivity, thicker the velocity boundary layer. In this case the maximum value of ψ is 11.53. Because the increasing value of γ increase the temperature difference between the surface and outside the boundary layer. Then heat is transferred rapidly from surface to fluid within the boundary layer. That is why both velocity and temperature of the fluid flow increase with the increasing value of γ. On the other hand, when the value of M increase the boundary layer becomes thinner and the value of ψ_{max} is 5.05 which is observed in figure 7.3(c). The magnetic field acting along the horizontal direction retards the fluid velocity. Applied magnetic field creates a Lorentz force by the interaction between magnetic field and flow field, this force acts against the fluid flow and reduces the velocity. The combined effects of temperature dependent thermal conductivity and magnetic field are shown in figure 7.3(d). In this case the maximum value of ψ i.e. ψ_{max} is 7.03. Under any circumstances the value of ψ increases for the effect of temperature dependent thermal conductivity and the value of ψ decreases in presence of magnetic field.

The variation of temperature dependent thermal conductivity and the intensity of magnetic field on the isotherms for $\alpha = 0.2$ and Pr = 0.73 are depicted in figure 7.4. The effect of temperature dependent thermal conductivity and magnetic field ($\gamma > 0$ and $M > 0$) the thermal state of the fluid increases, causing the thermal boundary

layer grows thick. On the other hand for constant thermal conductivity and in absence of magnetic field, it is noted that the opposite result obtained.

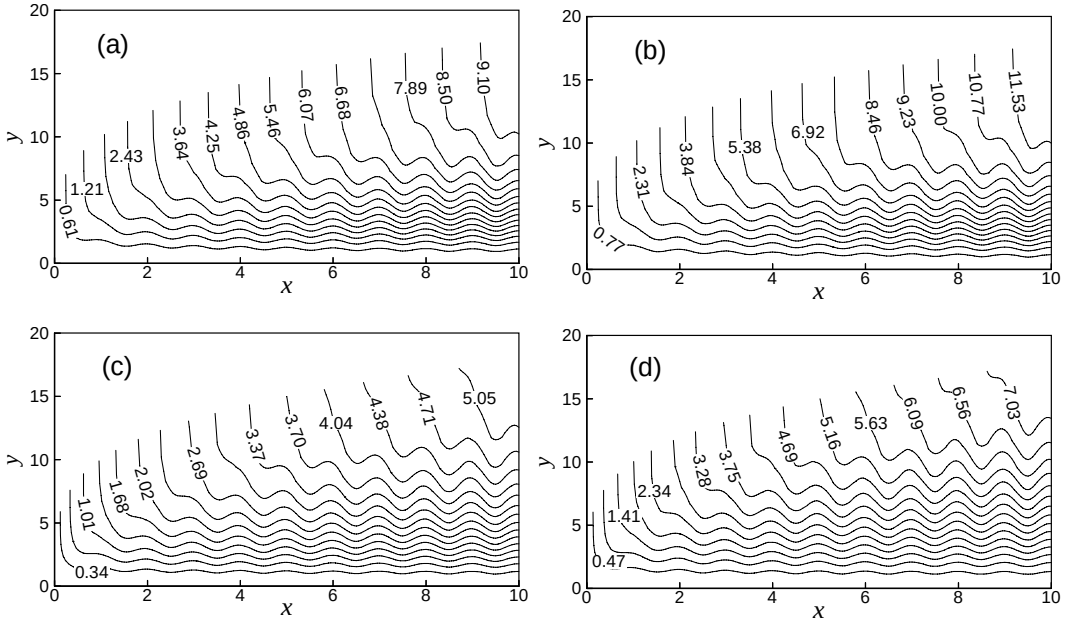

Figure 7.3: Streamlines for (a) γ = 0.0, M = 0.0 (b) γ = 2.0, M = 0.0 (c) γ = 0.0, M = 0.8 and (d) γ = 2.0, M = 0.8 while Pr = 0.73 and α = 0.2.

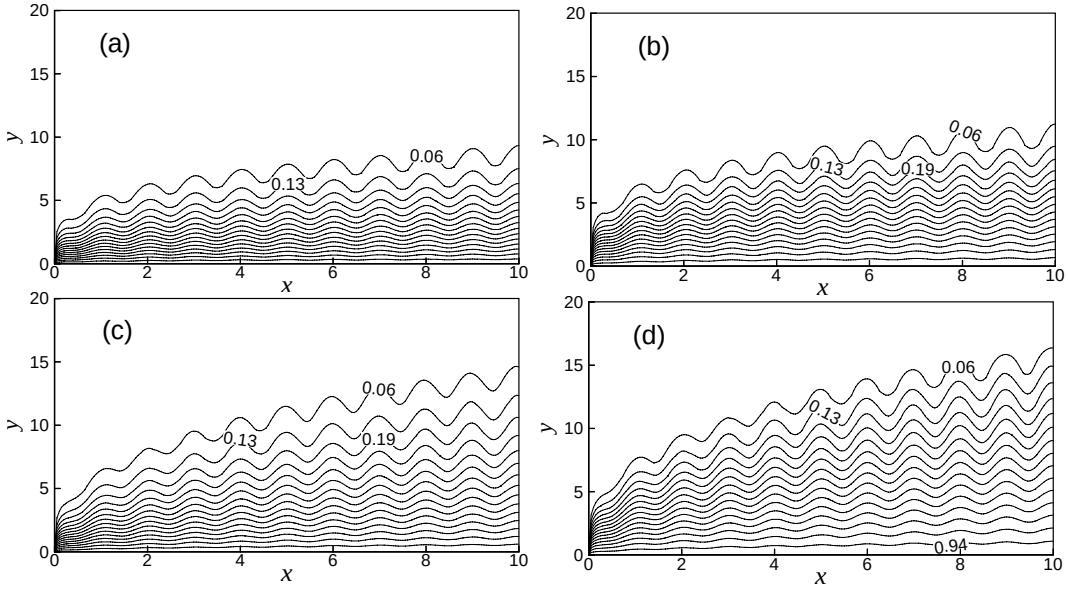

Figure 7.4: Isotherms for (a) γ = 0.0, M = 0.0 (b) γ = 2.0, M = 0.0 (c) γ = 0.0, M = 0.8 and (d) γ = 2.0, M = 0.8 while Pr = 0.73 and α = 0.2.

7.4 Comparison of effect of Joule heating

The comparison of the effect of viscosity when linear function of temperature on the velocity within the boundary layer with other controlling parameters Pr = 1.0, M = 0.8, γ = 5.0 and α = 0.3 having the effect of Joule heating (J = 0.0 and J = 0.02) are shown in figure 7.5 and 7.6 respectively. In figure 7.5, the maximum values of velocity are 0.61724, 0.41442, 0.34390, 0.29913 and 0.27122 due to the values of ε = 0.0, 5.0, 10.0, 15.0 and 20.0 respectively. Each of which occurs at different position of η. Velocity decreases by 56.05% when the value of viscosity changes from 0.0 to 20.0. From figure 7.6 it is observed that the maximum values of velocity are 0.61747, 0.41457, 0.34402, 0.30133 and 0.27130 for ε = 0.0, 5.0, 10.0, 15.0 and 20.0 respectively in the presence of Joule heating (J = 0.02). In this case velocity decreases by 56.063%, which is greater than 56.05% in the absence of Joule heating (J = 0.0).

Figures 7.7 and 7.8 illustrate the comparison of the effect of thermal conductivity against η on the velocity with other controlling parameters Pr = 0.73, M = 0.5, ε = 5.0 and α = 0.3 with and without effect of Joule heating. The maximum values of velocity are obtained 0.31975, 0.40816, 0.48793 and 0.52353 from figure 7.7 due to the values of γ = 0.0, 2.0, 6.0 and 10.0 respectively. Velocity increases by 38.92% in the absence of Joule heating (J = 0.0). The maximum values of velocity are 0.31981, 0.40832, 0.48808 and 0.52366 for γ = 0.0, 2.0, 6.0 and 10.0 respectively and each of which occurs at different position of η. Velocity increases by 38.93% in the case of using Joule heating (J = 0.02) when thermal conductivity parameter γ increases from 0 to 10.0.

From figures 7.5 to 7.8, it is also observed that when the effect of Joule heating (J = 0.02) is considered then some variations are obtained significantly. This is because Joule heating is the heating effect of conductors carrying currents. So velocity of the fluid flow increases.

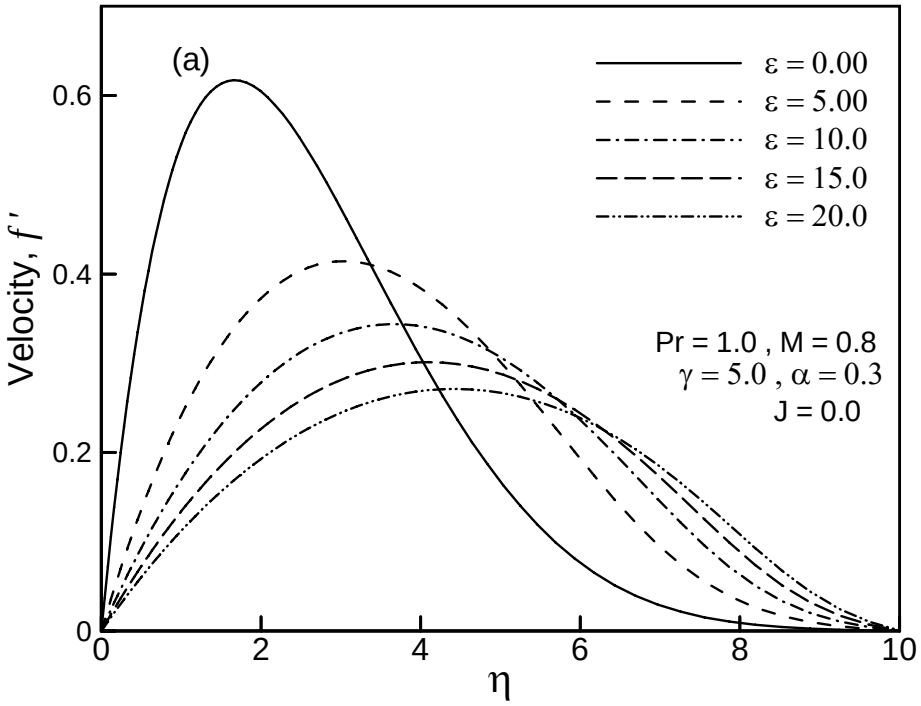

Figure 7.5: Velocity profiles f' against dimensionless distance η for different values of ε while $\alpha = 0.3$, $M = 0.8$, $J = 0.0$, $\gamma = 5.0$ and Pr = 1.0.

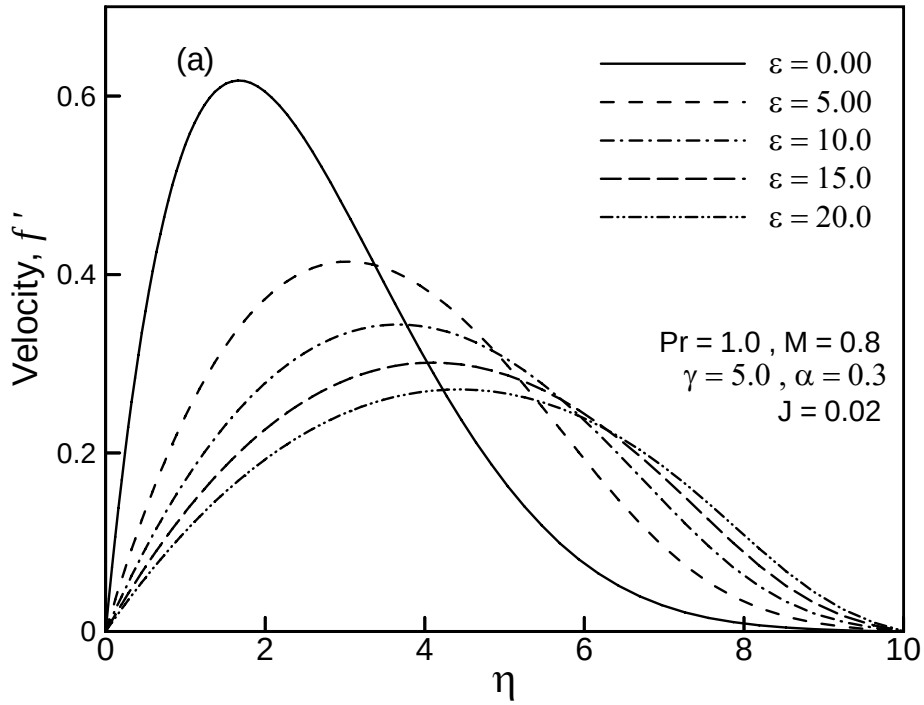

Figure 7.6: Velocity profiles f' against dimensionless distance η for different values of ε while $\alpha = 0.3$, $M = 0.8$, $J = 0.02$, $\gamma = 5.0$ and Pr = 1.0.

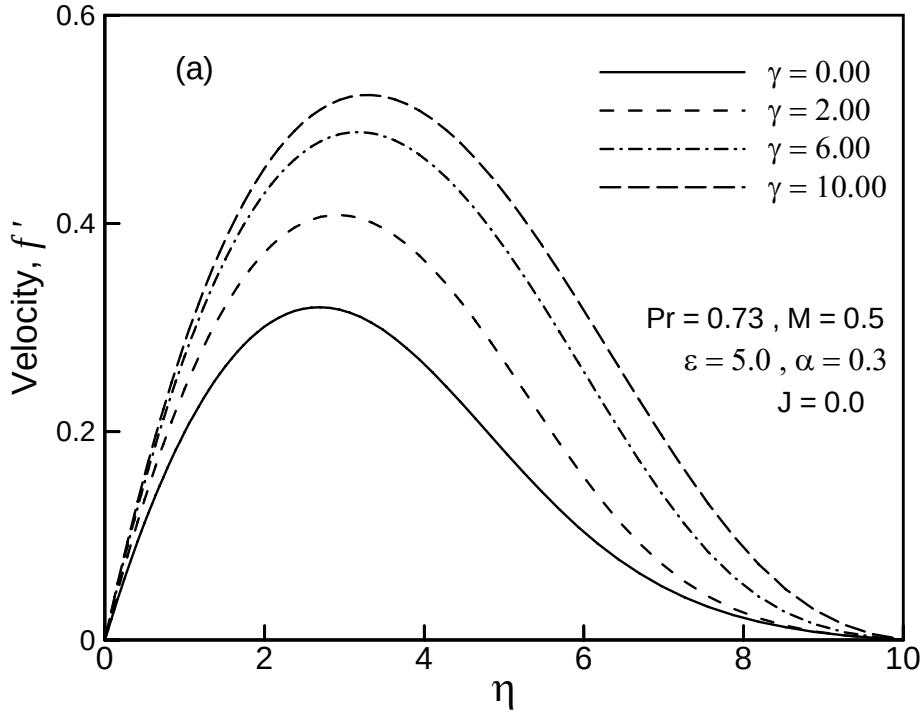

Figure 7.7: Velocity profiles f' against dimensionless distance η for different values of γ while α = 0.3, M = 0.5, J = 0.0, ε = 5.0 and Pr = 0.73.

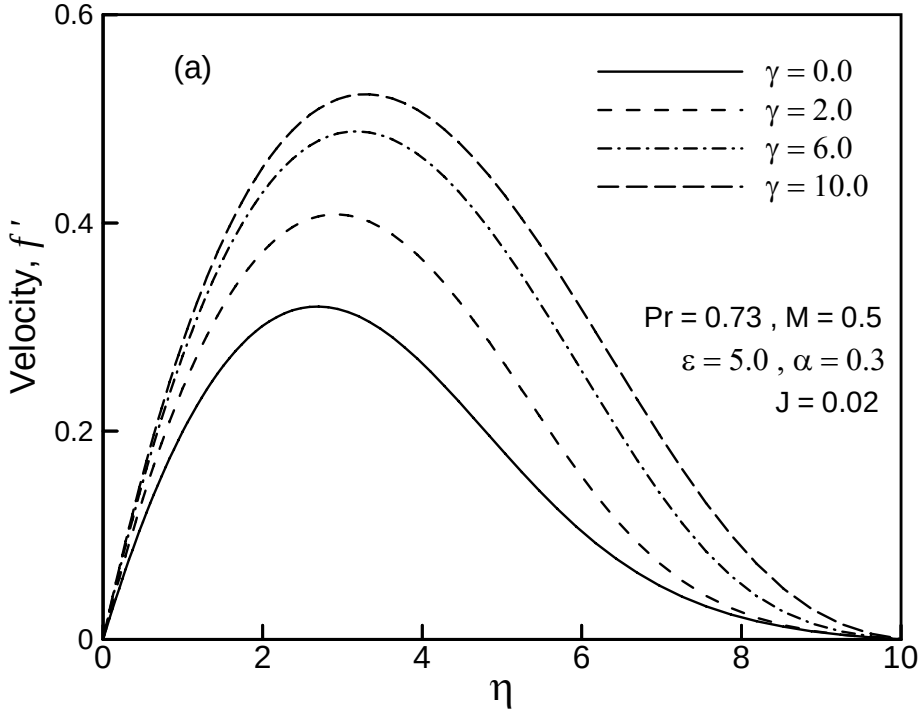

Figure 7.8: Velocity profiles f' against dimensionless distance η for different values of γ while α = 0.3, M = 0.5, J = 0.02, ε = 5.0 and Pr = 0.73.

Table 7.1: Comparison of skin friction coefficient C_{fx} against x for the variation of viscosity parameter ε with other fixed controlling values M = 0.5, Pr = 0.73 and α = 0.3.

x	Skin friction coefficient C_{fx} (Linear function of temperature)			Skin friction coefficient C_{fx} (Inversely proportional to linear function of temperature)	
	ε = 0.0	ε = 5.0	ε = 60.0	ε = 0.5	ε = 1.0
0.00	0.58858	1.00692	1.56895	0.49331	0.48914
0.50	0.86640	1.54688	2.85371	0.77939	0.76874
1.00	0.51748	0.91916	1.61053	0.46576	0.46115
1.50	0.80079	1.46536	2.67869	0.71506	0.69689
2.00	0.49685	0.89141	1.56602	0.44594	0.43838
2.50	0.76312	1.41516	2.62220	0.67851	0.65706
3.00	0.48145	0.87162	1.53839	0.43070	0.42089
3.50	0.73610	1.37827	2.58088	0.65233	0.62862
4.00	0.46905	0.85588	1.52144	0.41834	0.40681
4.50	0.71486	1.34874	2.54667	0.63176	0.60634
5.00	0.45861	0.84266	1.50983	0.40794	0.39503
5.50	0.69730	1.32400	2.51747	0.61476	0.58798
6.00	0.44957	0.83118	1.50076	0.39895	0.38491
6.50	0.68230	1.30269	2.49216	0.60027	0.57236
7.00	0.44161	0.82099	1.49299	0.39103	0.37606
7.50	0.66921	1.28394	2.46993	0.58763	0.55878
8.00	0.43448	0.81181	1.48594	0.38397	0.36819
8.50	0.65758	1.26718	2.45017	0.57643	0.54677
9.00	0.42803	0.80343	1.47937	0.37759	0.36112
9.50	0.64713	1.25202	2.43238	0.56638	0.53603
10.0	0.42214	0.79572	1.47314	0.37179	0.35470

Table 7.1 represents the values of skin friction coefficient C_{fx} for the computational domain for the variation of viscosity (ε = 5.0, 60.0) when linear function and (ε = 0.5, 1.0) when inversely proportional to linear function of temperature with other fixed controlling values amplitude-to-length ratio of the wavy surface α = 0.3, magnetic parameter M = 0.5 and Prandtl number Pr = 0.73. Here it is found that the

complete cycle of the wavy surface from x = 0.0 to 10.0. Skin friction coefficient C_{fx} increases when viscosity linear function of temperature and reverse results found when viscosity inversely proportional to linear function of temperature. The maximum values of local skin friction coefficient C_{fx} are recorded to be 0.86640, 1.54688 and 2.85371 for ε = 0.0, 5.0 and 60.0 respectively when viscosity is taken to be linear function of temperature which occurs at x = 0.50 and it is seen that the local skin friction coefficient C_{fx} increases by approximately 70% when ε changes from 0.0 to 60.0. On the other hand the maximum values of local skin friction coefficient C_{fx} are recorded to be 0.86640, 0.77939 and 0.76874 for ε = 0.0, 0.5 and 1.0 respectively which occurs also at the same point x = 0.50 when viscosity inversely proportional to linear function of temperature considered. It is observed that the local skin friction coefficient C_{fx} decreases by approximately 12% as ε increases from 0.0 to 1.0.

The values of the rate of heat transfer in terms of the local Nusselt number Nu_x for the variation of viscosity (ε = 5.0, 60.0) when linear function of temperature and (ε = 0.5, 1.0) when inversely proportional to linear function of temperature with other fixed controlling values amplitude-to-length ratio of the wavy surface α = 0.3, magnetic parameter M = 0.5 and Prandtl number Pr = 0.73 are represented in Table 7.2. Here it is observed that the rate of heat transfer in terms of the local Nusselt number Nu_x show the complete cycle of the wavy surface throughout the domain from x = 0.0 to 10.0. However the maximum values of local rate of heat transfer are recorded to be 0.31824, 0.25070 and 0.17193 for ε = 0.0, 5.0 and 60.0 respectively when viscosity is a linear function of temperature and the rate of heat transfer in terms of the local Nusselt number Nu_x decreases by approximately 46% as ε increases from 0.0 to 60.0. Moreover the maximum values of local rate of heat transfer are recorded to be 0.31824, 0.33285 and 0.34435 for ε = 0.0, 0.5 and 1.0 respectively which occurs at x = 0.50 when viscosity inversely proportional to linear function of temperature. It is noted that the rate of heat transfer in terms of the local Nusselt number Nu_x increases by approximately 8% as ε increases from 0.0 to 1.0.

Table 7.2: Comparison of rate of heat transfer in terms of Nusselt number Nu_x against x for the viscosity parameter ε with other fixed controlling values $M = 0.5$, Pr = 0.73 and $\alpha = 0.3$.

x		Rate of heat transfer Nu_x (Linear function of temperature)		Rate of heat transfer Nu_x (Inversely proportional to linear function of temperature)	
	$\varepsilon = 0.0$	$\varepsilon = 5.0$	$\varepsilon = 60.0$	$\varepsilon = 0.5$	$\varepsilon = 1.0$
0.00	0.30648	0.23573	0.16031	0.32074	0.33388
0.50	0.31824	0.25070	0.17193	0.33285	0.34435
1.00	0.29051	0.22614	0.14091	0.30458	0.31590
1.50	0.29874	0.23824	0.17258	0.31133	0.32076
2.00	0.28028	0.22026	0.14807	0.29343	0.30383
2.50	0.28803	0.23206	0.16838	0.29965	0.30827
3.00	0.27275	0.21597	0.15088	0.28504	0.29461
3.50	0.28001	0.22742	0.16620	0.29088	0.29888
4.00	0.26662	0.21259	0.15165	0.27820	0.28712
4.50	0.27357	0.22366	0.16528	0.28382	0.29130
5.00	0.26141	0.20978	0.15173	0.27238	0.28074
5.50	0.26814	0.22048	0.16489	0.27785	0.28489
6.00	0.25687	0.20736	0.15159	0.26731	0.27520
6.50	0.26342	0.21774	0.16465	0.27267	0.27932
7.00	0.25285	0.20523	0.15139	0.26282	0.27030
7.50	0.25925	0.21533	0.16441	0.26808	0.27439
8.00	0.24924	0.20332	0.15119	0.25878	0.26590
8.50	0.25551	0.21317	0.16413	0.26396	0.26996
9.00	0.24597	0.20158	0.15099	0.25512	0.26191
9.50	0.25212	0.21123	0.16382	0.26022	0.26594
10.0	0.24297	0.20000	0.15081	0.25177	0.25825

In table 7.3, the numerical values of skin friction coefficient C_{fx} against x for different values of viscosity (with and without effect of J) with other fixed controlling values $M = 0.8$, Pr = 1.0, $\gamma = 5.0$ and $\alpha = 0.3$ are shown. It is observed from this table that the values of skin friction coefficient C_{fx} at different position of x for $\varepsilon = 0.0$, 5.0, 10.0 and 20.0 are smaller when Joule heating is not used ($J = 0.0$)

than that of using Joule heating (J = 0.02). The skin friction coefficient C_{fx} increases is around 65.68% as ε changes from 0.0 to 20.0 at the axial position of x = 0.50 when there is no effect of Joule heating. But applying the effect of Joule heating (J = 0.02) the skin friction coefficient C_{fx} increases is around 65.691% as ε changes from 0.0 to 20.0 at the same axial position of x.

Table 7.3: Comparison of skin friction coefficient C_{fx} against x for the variation of viscosity parameter (ε = 0.0, 5.0, 10.0, 20.0) with and without effect of Joule heating parameter J with other fixed parameters M = 0.8, Pr = 1.0, γ = 5.0 and α = 0.3.

x	Skin friction coefficient C_{fx}							
	ε = 0.0		ε = 5.0		ε = 10.0		ε = 20.0	
	J = 0.0	J= 0.02	J = 0.0	J= 0.02	J = 0.0	J= 0.02	J = 0.0	J= 0.02
0.00	0.70328	0.70328	1.28671	1.28671	1.51106	1.51106	1.70544	1.70544
0.50	0.94819	0.94844	1.85247	1.85317	2.26779	2.26859	2.76283	2.76364
1.00	0.56820	0.56856	1.10422	1.10514	1.34618	1.34721	1.59428	1.59513
1.50	0.83657	0.83743	1.68208	1.68443	2.07328	2.07588	2.51554	2.51783
2.00	0.52608	0.52695	1.04200	1.04420	1.27656	1.27897	1.52639	1.52843
2.50	0.77671	0.77821	1.58741	1.59154	1.96675	1.97130	2.40154	2.40556
3.00	0.49705	0.49841	0.99865	1.00216	1.22849	1.23232	1.48001	1.48328
3.50	0.73512	0.73725	1.52028	1.52616	1.89094	1.89744	2.32015	2.32594
4.00	0.47498	0.47680	0.96512	0.96992	1.19115	1.19638	1.44361	1.44813
4.50	0.70332	0.70604	1.46782	1.47539	1.83167	1.84006	2.25606	2.26359
5.00	0.45725	0.45951	0.93772	0.94375	1.16053	1.16711	1.41318	1.41896
5.50	0.67767	0.68094	1.42474	1.43391	1.78286	1.79307	2.20316	2.21239
6.00	0.44251	0.44516	0.91452	0.92172	1.13455	1.14244	1.38688	1.39390
6.50	0.65627	0.66005	1.38823	1.39893	1.74134	1.75329	2.15811	2.16901
7.00	0.42993	0.43296	0.89439	0.90270	1.11198	1.12113	1.36369	1.37192
7.50	0.63797	0.64222	1.35661	1.36876	1.70522	1.71884	2.11889	2.13141
8.00	0.41901	0.42238	0.87662	0.88600	1.09204	1.10239	1.34294	1.35235
8.50	0.62204	0.62673	1.32877	1.34229	1.67327	1.68850	2.08415	2.09826
9.00	0.40937	0.41306	0.86073	0.87111	1.07417	1.08569	1.32417	1.33473
9.50	0.60797	0.61306	1.30392	1.31876	1.64465	1.66142	2.05298	2.06863
10.0	0.40078	0.40476	0.84636	0.85771	1.05799	1.07063	1.30705	1.31873

Table 7.4: Comparison of rate of heat transfer Nu_x against x for the variation of thermal conductivity parameter (γ = 0.0, 2.0, 6.0, 10.0) with and without effect of Joule heating parameter J with other fixed controlling values M = 0.5, Pr = 0.73, ε = 5.0 and α = 0.3.

x	Rate of heat transfer Nu_x							
	γ = 0.0		γ = 2.0		γ = 6.0		γ = 10.0	
	J = 0.0	J= 0.02	J = 0.0	J= 0.02	J = 0.0	J= 0.02	J = 0.0	J= 0.02
0.00	0.23573	0.23573	0.41570	0.41570	0.70763	0.70763	0.98251	0.98251
0.50	0.25070	0.25035	0.43968	0.43889	0.72996	0.72840	0.97633	0.97420
1.00	0.22614	0.22549	0.39765	0.39625	0.66149	0.65879	0.90160	0.89805
1.50	0.23824	0.23684	0.41571	0.41254	0.69442	0.68831	0.95044	0.94232
2.00	0.22026	0.21848	0.38807	0.38423	0.65078	0.64358	0.88605	0.87668
2.50	0.23206	0.22932	0.40423	0.39811	0.67679	0.66519	0.93390	0.91882
3.00	0.21597	0.21285	0.38039	0.37361	0.64126	0.62875	0.87776	0.86169
3.50	0.22742	0.22315	0.39581	0.38636	0.66405	0.64644	0.91993	0.89736
4.00	0.21259	0.20797	0.37428	0.36423	0.63369	0.61539	0.87290	0.84969
4.50	0.22366	0.21771	0.38903	0.37598	0.65418	0.63022	0.90827	0.87789
5.00	0.20978	0.20354	0.36917	0.35559	0.62730	0.60287	0.86898	0.83838
5.50	0.22048	0.21275	0.38337	0.36649	0.64633	0.61580	0.89891	0.86052
6.00	0.20736	0.19940	0.36476	0.34747	0.62173	0.59095	0.86531	0.82712
6.50	0.21774	0.20813	0.37850	0.35762	0.63992	0.60264	0.89147	0.84497
7.00	0.20523	0.19546	0.36090	0.33972	0.61684	0.57953	0.86177	0.81589
7.50	0.21533	0.20375	0.37424	0.34920	0.63455	0.59039	0.88550	0.83082
8.00	0.20332	0.19166	0.35745	0.33223	0.61251	0.56854	0.85841	0.80474
8.50	0.21317	0.19956	0.37046	0.34112	0.62994	0.57880	0.88063	0.81774
9.00	0.20158	0.18797	0.35434	0.32496	0.60867	0.55793	0.85525	0.79374
9.50	0.21123	0.19550	0.36706	0.33331	0.62591	0.56770	0.87657	0.80547
10.0	0.20000	0.18436	0.35152	0.31786	0.60523	0.54765	0.85232	0.78293

The numerical values of rate of heat transfer Nu_x against x for the variation of thermal conductivity parameter (with and without effect of J) with other fixed parameters M = 0.5, Pr = 0.73, ε = 5.0 and α = 0.3 are shown in table 7.4. It is noted from this table that the values of rate of heat transfer Nu_x for γ = 0.0, 2.0, 6.0 and 10.0 are higher at different position of x when Joule heating is not considered (J = 0.0) than that of using Joule heating (J = 0.02). At the axial position of x = 0.50 the rate of heat transfer Nu_x increases is around 74.32% as γ changes from 0.0 to 10.0 when there is

no effect of Joule heating. But in presence of Joule heating (J = 0.02) the rate of heat transfer Nu_x increases is around 74.26% as γ changes from 0.0 to 10.0 at the same axial position x.

Table 7.5: Comparison of velocity and temperature against η for the variation of magnetic parameter (M = 0.0, 1.5) with and without effect of Joule heating parameter J with other fixed controlling values γ = 5.0, Pr = 0.73, ε = 5.0 and α = 0.3.

η	M = 0.0		M = 1.5		M = 0.0		M = 1.5	
	Velocity				Temperature			
	J= 0.0	J= 0.02	J= 0.0	J= 0.02	J= 0.0	J= 0.02	J= 0.0	J= 0.02
0.0400	0.0144	0.01454	0.0111	0.01115	0.9953	0.99541	0.9960	0.99614
0.4543	0.1521	0.15289	0.1136	0.11404	0.9460	0.94689	0.9548	0.95547
1.0553	0.3131	0.31476	0.2259	0.22686	0.8710	0.87306	0.8926	0.89413
1.5094	0.4050	0.40732	0.2864	0.28765	0.8113	0.81432	0.8436	0.84582
2.0826	0.4858	0.48881	0.3374	0.33905	0.7321	0.73642	0.7792	0.78240
3.0688	0.5379	0.54198	0.3711	0.37353	0.5868	0.59350	0.6626	0.66748
4.1055	0.4878	0.49317	0.3508	0.35395	0.4265	0.43562	0.5342	0.54071
5.0387	0.3737	0.38021	0.2987	0.30254	0.2853	0.29569	0.4168	0.42460
6.1740	0.2001	0.20704	0.2114	0.21571	0.1387	0.14837	0.2787	0.28720
7.2582	0.0729	0.07738	0.1240	0.12796	0.049	0.05566	0.1617	0.16943
8.1919	0.0217	0.02339	0.0614	0.06418	0.0155	0.01798	0.0821	0.08775
9.2436	0.0034	0.00372	0.0163	0.01721	0.0028	0.00330	0.0234	0.02572

The comparison of velocity and temperature against η for the variation of the strength of magnetic field (M = 0.0, 1.5) with and without effect of Joule heating with other fixed controlling values γ = 5.0, Pr = 0.73, ε = 5.0 and α = 0.3 is depicted in Table 7.5. When Joule heating (J = 0.0) is ignored with different values of magnetic parameter M (M = 0.0, 1.5) then the velocity and temperature are smaller than that of using Joule heating, J = 0.02. From Table 7.5 it is clearly seen that Joule heating dominates the magnetic field.

Table 7.6: Comparison of the present numerical results of skin friction coefficient, $f''(x,0)$ and the heat transfer, $-\theta'(x,0)$ with Hossain et al. (2002) for the variation of Prandtl number Pr while $M = 0.0$, $\gamma = 0.0$, $J = 0.0$ and $\varepsilon = 0.0$ with $\alpha = 0.1$.

Pr	$f''(x,0)$		$-\theta'(x,0)$	
	Hossain et al. (2002)	Present work	Hossain et al. (2002)	Present work
1.0	0.908	0.91084	0.401	0.39914
10.0	0.591	0.59482	0.825	0.82315
25.0	0.485	0.48910	1.066	1.06405
50.0	0.485	0.41880	1.066	1.28351
100.0	0.352	0.35690	1.542	1.54198

A comparison of the present numerical results of the skin friction coefficient $f''(x,0)$ and the rate of heat transfer $-\theta'(x,0)$ with the results obtained by Hossain et al. (2002) is depicted in Table 7.6. Here, the magnetic parameter M, viscosity variation parameter ε, thermal conductivity parameter γ and Joule heating parameter J are ignored while different values of Prandtl number Pr = (1.0, 10, 25.0, 50.0 and 100.0) are chosen. From Table 7.6, it is clearly seen that the present results are excellent agreement with the solution of Hossain et al. (2002).

The influence of the magnetic parameter M, on velocity and the temperature are illustrated in figures 7.9 and 7.10 respectively with Pr = 1.0, $\alpha = 0.1$, $\gamma = 0.0$, $J = 0.0$, $\varepsilon = 0.0$ and the local Nusselt number are illustrated in figures 7.11 and 7.12 respectively with Pr = 1.0, $\alpha = 0.0$, $\gamma = 0.0$, $J = 0.0$ and $\varepsilon = 0.0$. The results for constant viscosity ($\varepsilon = 0.0$), constant thermal conductivity ($\gamma = 0.0$), without Joule heating ($J = 0.0$) and a fluid having Pr = 1.0 are compared with those of Alam et al. (1997) and a very good agreement is found.

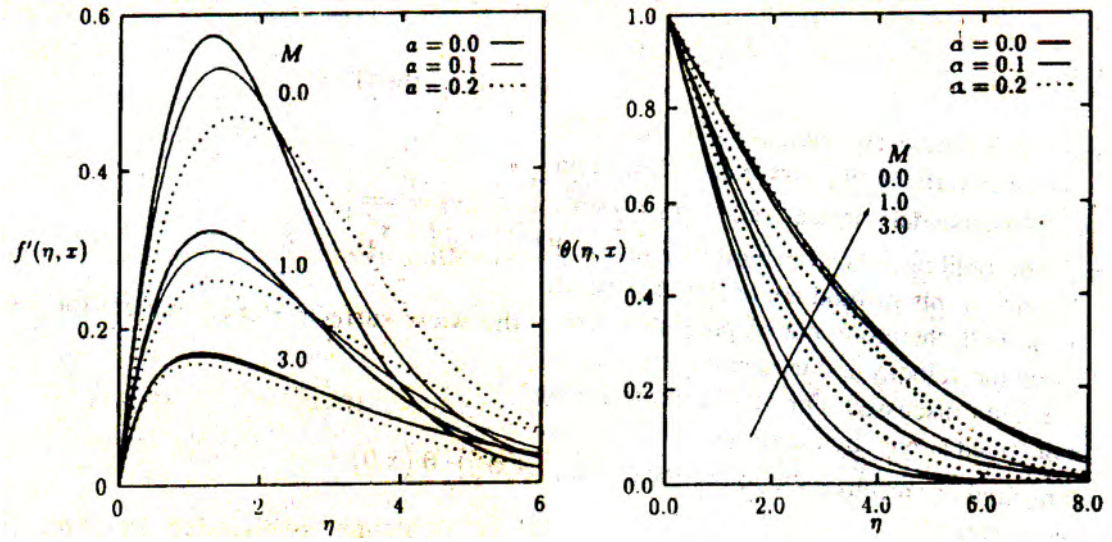

(a) (b)

Figure 7.9: (a) Velocity profiles and (b) temperature profiles for different values of M with Pr = 1.0, α = 0.1, γ = 0.0, J = 0.0 and ε = 0.0 (Alam et al. (1997)).

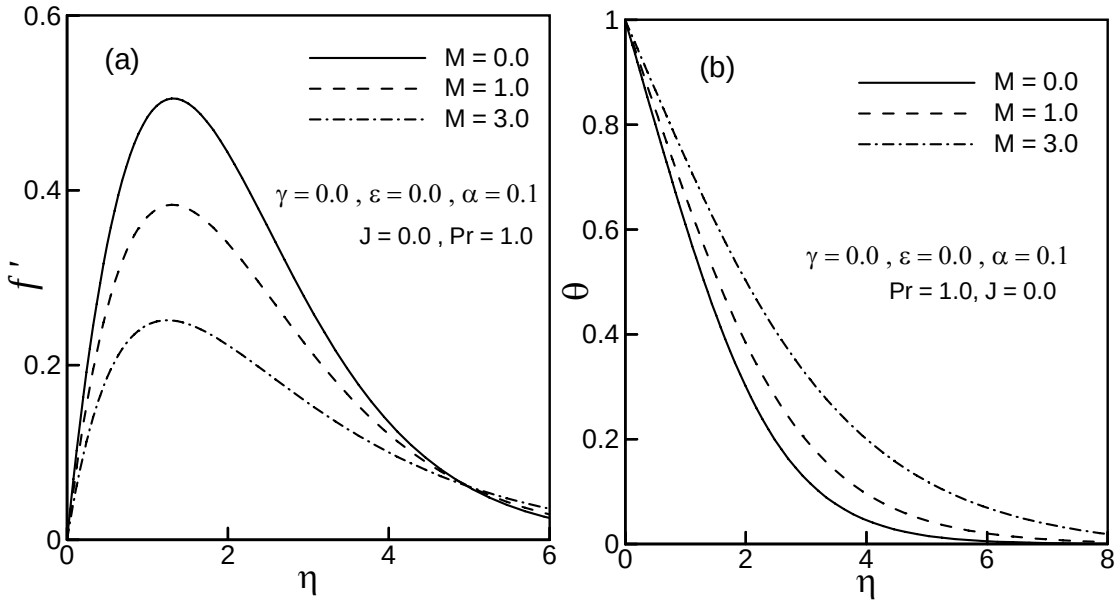

Figure 7.10: (a) Velocity profiles and (b) temperature distribution for different values of magnetic parameter M with Pr = 1.0, α = 0.1, γ = 0.0, J = 0.0 and ε = 0.0 (present work).

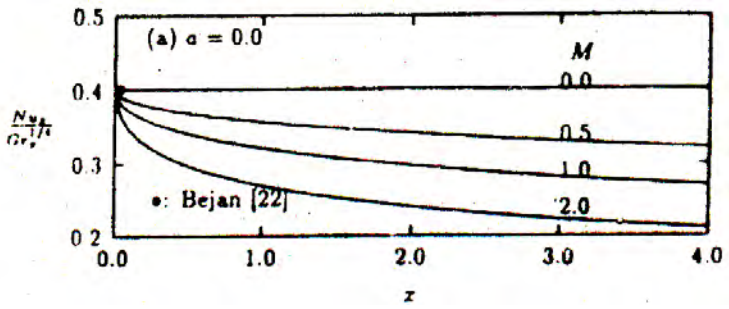

Figure 7.11: Local Nusselt number for different values of magnetic parameter M with Pr = 1.0, $\alpha = 0.0$, $\gamma = 0.0$, $J = 0.0$ and $\varepsilon = 0.0$ (Alam et al. (1997)).

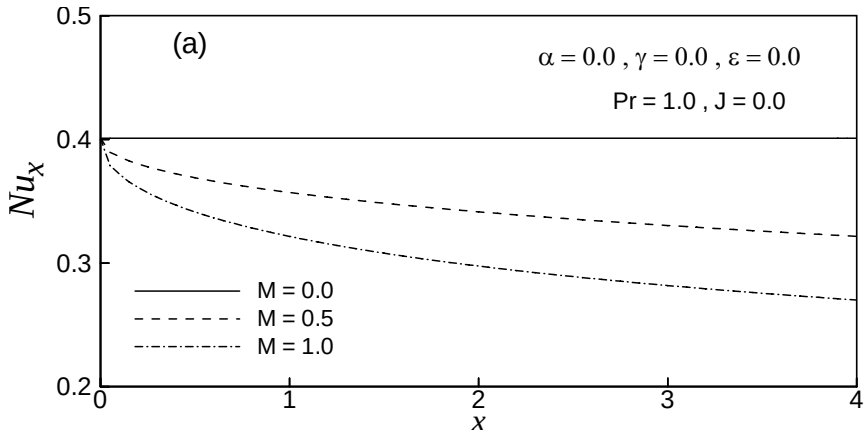

Figure 7.12: Local Nusselt number for different values of magnetic parameter M with Pr = 1.0, $\alpha = 0.0$, $\gamma = 0.0$, $J = 0.0$ and $\varepsilon = 0.0$ (present work).

CHAPTER 8
Conclusions

8.1 General

The main objective of this work is to study the magnetohydrodynamic two-dimensional incompressible laminar and natural convection flow with temperature dependent physical properties along a vertical wavy surface. The governing boundary layer equations are first transformed into a non-dimensional form using the appropriate transformations. The resulting nonlinear system of partial differential equations are mapped into the domain of a vertical flat plate and then solved numerically employing the implicit finite difference method, known as the Keller-box scheme. The description so far may be summarized as follows.

8.2 Summary of the major outcome

In chapter 3, magnetohydrodynamic natural convection boundary layer flow of viscous incompressible fluid with temperature dependent viscosity (linear function and inversely proportional to linear function of temperature) along a vertical wavy surface has been considered. In this chapter the large value of viscosity variation parameter (ε = 60.0) is taken to be a linear function of temperature. Viscosity variation parameter ε is also considered greater than 200 and then the numerical results are also obtained but the maximum value of velocity not at the leading edge of x-axis. In this case the velocity becomes an irregular shape. Skin friction coefficient highly increases and surface becomes more roughness. It is well known that when viscosity is constant then both of the skin friction coefficient and velocity increase or decrease because there is a linear relationship between the surface shear stress in terms of the skin friction coefficient and the velocity gradient. But the present work indicates that when viscosity is dependent on temperature then opposite results are obtained. In the case of viscosity as a linear function of temperature then skin friction coefficient increases and velocity decreases. In this chapter, it is also noted that when skin friction coefficient decreases then velocity increases in the case of viscosity as an inversely proportional to linear function of temperature. Skin friction coefficient and velocity are directly dependent on temperature dependent viscosity. The effect of viscosity is vary small and it is also observed that for each

parameter, if the value of viscosity is greater than the value taken then it does not converge with other controlling parameters when it is considered inversely proportional to linear function of temperature. In that case figures of skin friction coefficient, the rate of heat transfer in terms of the Nusselt number Nu_x, the velocity, the temperature, the streamlines and the isotherms will not be better than that are shown in this chapter in case II. It is concluded that temperature dependent viscosity dominates the other parameters.

In chapter 4, the effect of temperature dependent thermal conductivity on magnetohydrodynamic natural convection flow of viscous incompressible fluid along a uniformly heated vertical wavy surface has been considered. The results indicated that both the flow and heat transfer strongly depend on the temperature dependent thermal conductivity. The rate of heat transfer in terms of local Nusselt number Nu_x increases in this case. The velocity and temperature as well as the streamlines and the isotherms patterns are also increase. When temperature increases then the rate of heat transfer in terms of local Nusselt number Nu_x decreases or vice versa as thermal conductivity constant, which is shown in another chapters. When temperature dependent thermal conductivity considered then both the temperature and heat transfer rate increase. Temperature and the rate of heat transfer in terms of local Nusselt number are directly dependent on temperature dependent thermal conductivity.

In chapter 5, a steady two-dimensional laminar flow of viscous incompressible fluid on MHD free convection flow with combined effects of temperature dependent viscosity and thermal conductivity along a uniformly heated vertical wavy surface have been studied. Here maximum value of intensity of magnetic field is 5.0, which is greater than any other values of intensity of magnetic field considered in any other chapter. It means that temperature dependent viscosity and thermal conductivity dominate the magnetic field.

In chapter 6, Joule heating effect on MHD natural convection flow with viscosity and thermal conductivity variation owing to temperature along a uniformly heated vertical wavy surface has been analyzed. The results noted that both the flow and heat transfer strongly depend on the Joule heating. In this chapter results also show

that the effects of all other parameters are comparatively small when Joule heating is considered. It is also observed that if Joule heating parameter J is greater than 0.02 then the numerical results do not exists for all parameters and do not converge with other controlling parameters. In this chapter, the highest value of magnetic parameter M = 1.5, Joule heating parameter J = 2.0, viscosity parameter ε = 20.0, thermal conductivity variation parameter γ = 10.0 and Prandtl number Pr = 9.45 are all critical values. For the same value of viscosity parameter ε = 5.0, the skin friction coefficient in Table 7.4 against x = 0.5 are 1.85247 and 1.85317 respectively. The variation of skin friction coefficient at x = 0.5 in chapter 5 and chapter 6 occurred only for Joule heating. Therefore, it is clearly noted that Joule heating dominates the viscosity. Also, the other cases such as thermal conductivity, magnetic field and Prandtl number analysis can be shown in a similar way. Finally it is concluded that Joule heating dominates the magnetic field, viscosity, thermal conductivity and also Prandtl number.

The comparisons of the numerical results for the skin friction coefficient and the rate of heat transfer for the two cases of viscosity (linear function and inversely proportional to linear function of temperature) are shown in tabular form in Table 7.1 and Table 7.2. From these two tables it is noted that numerical results of the skin friction coefficient increases and the rate of heat transfer decreases for increasing values of ε when viscosity dependent on linear function of temperature and the reverse results are obtained when viscosity dependent on inversely proportional to linear function of temperature which shown in chapter 7. In this chapter tt is also concluded that when the effect of Joule heating is considered then some variations are obtained significantly. Comparisons with previously reported investigations are also performed and the results show excellent agreement.

For the effect of magnetic field the skin friction coefficient, the rate of heat transfer, the velocity gradually decrease where the velocity boundary layer grows thin but the temperature increases and the thermal boundary layer becomes thicker which are displayed in chapter 3, chapter 4, chapter 5 and chapter 6.

The skin friction coefficient, velocity and temperature as well as streamlines and isotherms are all decreasing and the rate of heat transfer in terms of local Nusselt

number Nu_x increasing for the increasing values of Prandtl number Pr described in chapters 3, 4 and 6. The results also indicate that when Prandtl number Pr is very large (Pr = 100) then the velocity and thermal boundary layer become very thinner and skin friction highly decreases and the heat transfer rate rapidely increases which are displayed in chapter 3. It is also observed from chapter 3, 4 and 6 that the maximum value of Pr is different. The maximum value of Pr is 100 when temperature dependent viscosity is considered which are shown in chapter 3. Chapter 4 and 6, the maximum value of Pr 13.5 while $\alpha = 0.2$, $M = 0.8$ and $\gamma = 5.0$ and 9.45 while $M = 0.2$, $J = 0.02$, $\gamma = 4.0$, $\varepsilon = 5.0$ and $\alpha = 0.3$ respectively. It is concluded that temperature dependent viscosity, thermal conductivity and Joule heating dominate the Prandtl number.

It is depicted from chapter 3, chapter 4 and chapter 6 that for the effect of amplitude-to-length ratio of the wavy surface, the skin friction coefficient and the rate of heat transfer decrease but the velocity and temperature increase. Increasing velocity increases skin friction coefficient. But the opposite result observed in this case. This is because the increasing values of the amplitude-to-length ratio of the wavy surface, surface becomes more roughened and velocity force decreases at the local points.

8.3 Extension of this work

The present work may be extended for consideration of following cases:

- Temperature dependent physical properties like viscosity, thermal conductivity and Prandtl number with different physics like heat generation/absorption, viscous dissipation, radiation effect, stress work and pressure work may be considered.
- Considering non-uniform surface temperature, porous medium and unsteady flow this work can be extended.
- Mixed and forced convection can also be considered through including the governing equation of concentration conservation.
- The study can be extended for turbulent flow using different fluids like, Newtonian or non-Newtonian fluid, micro polar fluid and different thermal boundary conditions such as heat flux or radiation.
- Considering critical behavior of the flow may extend this problem.

References

Ahmed N. and Zaidi H. N., (2004): “Magnetic effect on overback convection through vertical stratum”, Proceeding 2nd BSME-ASME International Conference on Thermal Engineering, pp. 157–166.

Ahmed M. U., (2008): “MHD free convection flow along a heated vertical wavy surface with heat generation”, M.Phil Thesis, Department of Mathematics, Bangladesh University of Engineering and Technology (BUET), Dhaka, Bangladesh.

Alam K. C. A., Hossain M. A. and Rees D. A. S., (1997): “Magnetohydrodynamic free convection along a vertical wavy surface”, Internat. J. Appl. Mech. Engrg. Vol. 1, pp. 555–566.

Alam M. M., Alim M. A. and Chowdhury M. M. K., (2007): “Viscous dissipation effects on MHD natural convection flow over a sphere in the presence of heat generation”, Nonlinear Analysis: Modelling and Control, Vol. 12, pp. 447-459.

Alim M. A., Alam M. and Mamun A. A., (2007): “Joule heating effect on the coupling of conduction with MHD free convection flow from a vertical flat plate”, Nonlinear Analysis: Modelling and Control, Vol. 12(3), pp. 307-316.

Alim M. A., Alam M., Mamun A. A. and Hossain M. B., (2008): “Combined effect of viscous dissipation & Joule heating on the coupling of conduction & free convection along a vertical flat plate”, Int. Comm. Heat and Mass Transfer, Vol. 35(3), pp. 338-346.

Al-Nimr M. A. and Hader M. A., (1999): “MHD free convection flow in open-ended vertical porous channels”, Chemical Engineering Science, Vol. 54(12), pp. 1883-1889.

Arunachalam M. and Rajappa N. R., (1978): “Thermal boundary layer in liquid metals with variable thermal conductivity”, Appl. Sci. Res., Vol. 34, pp. 179-187.

Bhavnani S. H. and Bergles A. E., (1991): “Natural convection heat transfer from sinusoidal wavy surfaces”, Waerme Stoffuebertragung/Thermo Fluid Dynam., Vol. 26, pp. 341–349.

Cebeci T. and Bradshaw P., (1984): “Physical and Computational Aspects of Convective Heat Transfer”, Springer, New York.

Cengel Y. A., (2007): “Heat and Mass Transfer”, McGraw-Hill Companies, New York.

Chaim T. C., (1998): “Heat transfer in a fluid with variable thermal conductivity over a linearly stretching sheet”, Acta Mechanica, Vol. 129, pp. 63-72.

Charraudeau J., (1975): “Influence de gradients de properties physiques en convection force application au cas du tube”, Int. J. Heat and Mass Transfer, Vol. 18, pp. 87-95.

Chen C. K. and Wang C. C., (2000): “Transient analysis of force convection along a wavy surface in micropolar fluids”, AIAA J. Thermophys. Heat Transfer, Vol. 14, pp. 340–347.

Cheng C. Y., (2000): “Natural convection heat and mass transfer near a vertical wavy surface with constant wall temperature and concentration in a porous medium”, Int. Comm. Heat and Mass Transfer, Vol. 27, No. 8, pp. 1143–1154.

Cheng C. Y., (2000): “Natural convection heat and mass transfer near a wavy cone with constant wall temperature and concentration in a porous medium”, Mech. Res. Commun., Vol. 27, pp. 613–620.

Cheng C. Y., (2006): “The effect of temperature dependent viscosity on natural convection heat transfer from a horizontal isothermal cylinder of elliptic cross section”, Int. Comm. Heat and Mass Transfe, Vol. 33, pp. 1021–1028.

Chiu C.-P. and Chou H.-M., (1993): “Free convection in the boundary layer flow of a micropolar fluid along a vertical wavy surface”, Acta Mechanica, Vol. 101, pp. 161–174.

Chiu C.-P. and Chou H.-M., (1994): “Transient analysis of natural convection along a vertical wavy surface in micropolar fluids”, Int. J. Eng. Science, Vol. 32, pp. 19–33.

Chowdhury M. K. and Islam M. N., (2000): “MHD free convection flow of visco-elastic fluid past an infinite porous plate”, Heat and Mass Transfer, Vol. 36(5), pp. 439-447.

Cramer K. R. and Pai S. I., (1974): “Magnetofluid Dynamics for Engineering and Applied Physicists”, McGraw-Hill, New York, pp. 164-172.

Damseh R., Al-Odat M. Q. and Al-Nimr M. A., (2008): “Entropy generation during fluid flow in a channel under the effect of transverse magnetic field”, Heat and Mass Transfer, Vol. 44(8), pp. 897-904.

El-Amin M. F., (2003): “Combined effect of viscous dissipation and Joule heating on MHD forced convection over a non isothermal horizontal cylinder embedded in a fluid saturated porous medium”, Journal of Magnetism and Magnetic Materials, Vol. 263, pp. 337-343.

Elbashbeshy E. M. A, (2000): “Free convection flow with variable viscosity and thermal diffusivity along a vertical plate in the presence of magnetic field”, Int. J. Eng. Science, Vol. 38(2), pp. 207-213.

Ferziger J. and Peric M., (1996): “Computational Methods for Fluid Dynamics”, Springer, Berlin.

Gebhart B. and Pera L., (1971): “The nature of vertical natural convection flows resulting from the combined buoyancy effects of thermal and mass diffusion”, Int. J. Heat and Mass Transfer, Vol. 14, pp. 2025–2050.

Gray J., Kassory D. R. and Tadjeran H., (1982): “The effect of significant viscosity variation on convective heat transport in water–saturated porous media”, J. Fluid Mech., Vol. 117, pp. 233-249.

Hadjadj A. and Kyal M. E., (1999): “Effect of two sinusoidal protuberances on natural convection in a vertical annulus”, Numer. Heat Transfer, Vol. 36, pp. 273–289.

Hady F. M., Bakier A. Y. and Gorla R. S. R., (1996): “Mixed convection boundary layer flow on a continuous flat plate with variable viscosity”, Int. J. Heat and Mass Transfer, Vol. 31, pp. 169-172.

Hossain M. A. and Ahmed M., (1990): “MHD forced and free convection boundary layer flow near the leading edge”, Int. J. Heat and Mass Transfer, Vol. 33, No.3, pp. 571-575.

Hossain M. A., (1992): “The viscous and Joule heating effects on MHD free convection flow with variable plate temperature”, Int. J. Heat and Mass Transfer, Vol. 35(12), pp. 3485-3487.

Hossain M. A. and Pop I., (1996): “Magnetohydrodynamic boundary layer flow and heat transfer on a continuous moving wavy surface”, Arch. Mech., Vol. 48, pp. 813–823.

Hossain M. A., Alam K. C. A. and Rees D. A. S., (1997): “MHD forced and free convection boundary layer flow along a vertical porous plate”, Applied Mechanics and Engineering, Vol. 2, No. 1, pp. 33-51.

Hossain M. A., Das S. K. and Pop I., (1998): “Heat transfer response of MHD free convection flow along a vertical plate to surface temperature oscillation”, Int. J. of Non-Linear Mechanics, Vol. 33, No. 3, pp. 541–553.

Hossain M. A. and Rees D. A. S., (1999): “Combined heat and mass transfer in natural convection flow from a vertical wavy surface”, Acta Mechanica, Vol. 136, pp. 133–141.

Hossain M. A. and Munir M. S., (2000): “Mixed convection flow from a vertical flat plate with temperature dependent viscosity”, Int. J. Thermal Sciences, Vol. 39, pp. 173-183.

Hossain M. A. and Munir M. S., (2001): “Natural convection flow of a viscous fluid about a truncated cone with temperature dependent viscosity and thermal conductivity”, Int. J. Nume. Met. For Heat Fluid Flow, Vol. 11, pp. 494-510.

Hossain M. A., Munir M. S. and Rees D. A. S., (2000): “Flow of viscous incompressible fluid with temperature dependent viscosity and thermal conductivity past a permeable wedge with uniform surface heat flux”, Int. J. Thermal Sciences, Vol. 39, pp. 635-644.

Hossain M. A. and Wilson M., (2001): “Unsteady flow of viscous incompressible fluid with temperature dependent viscosity due to a rotating disc in presence of transverse magnetic field and heat transfer”, Int. J. Thermal Sciences, Vol. 40, pp. 11-20.

Hossain M. A., Kabir S. and Rees D. A. S., (2002): “Natural convection of fluid with temperature dependent viscosity from heated vertical wavy surface”, Z. Angew. Math. Phys., Vol. 53, pp. 48–57.

Hossain M. A., Khanafer K. and Vafai K., (2001): “The effect of radiation on the free convection flow of fluid with variable viscosity from a porous vertical plate”, Int. J. Thermal Sciences, Vol. 40, pp. 115-124.

Ingham D. B., (1978): “Free convection boundary layer on an isothermal horizontal cylinder”, Z. Angew. Math. Phys., Vol. 29, pp. 871–883.

Jang J. H., Yan W. M. and Liu H. C., (2003): “Natural convection heat and mass transfer along a vertical wavy surface”, Int. J. Heat and Mass Transfer, Vol. 46, pp. 1075–1083.

Jang J. H. and Yan W. M., (2004a): “Mixed convection heat and mass transfer along a vertical wavy surface”, Int. J. Heat and Mass Transfer, Vol. 47, pp. 419–428.

Jang J. H. and Yan W. M., (2004b): “Transient analysis of heat and mass transfer by natural convection over a vertical wavy surface”, Int. J. Heat and Mass Transfer, Vol. 47, pp. 3695–3705.

Kafoussius N. G. and Rees D. A. S., (1995): “Numerical study of the combined free and forced convective laminar boundary layer flow past a vertical isothermal flat plate with temperature dependent viscosity”, Acta Mechanica, Vol. 127, pp. 39-50.

Kafoussius N. G. and Williams E. M., (1995): “The effect of temperature dependent viscosity on the free convective laminar boundary layer flow past a vertical isothermal flat plate”, Acta Mechanica, Vol. 110, pp. 123-137.

Kays W. M., (1966): “Convective Heat and Mass Transfer”, McGraw-Hill, New York, pp. 362.

Keller H. B. (1978): “Numerical methods in boundary layer theory”, Annual Review of Fluid Mechanics, Vol. 10, pp. 417–433.

Kim E., (1997): “Natural convection along a wavy vertical plate to non-Newtonian fluids”, Int. J. Heat and Mass Transfer, Vol. 40, pp. 3069–3078.

Kuiken H. K., (1970): “Magneto-hydrodynamic free convection in a strong cross field”, J. Fluid Mech., Vol. 4, pp. 21-38.

Kumari M., Pop I. and Takhar H. S., (1997): “Free-convection boundary-layer flow of a non-Newtonian fluid along a vertical wavy surface”, Int. J. Heat Fluid Flow, Vol. 18, pp. 625–631.

Kumar B. V. R., Murthy P. V. S. N. and Singh P., (1998): “Free convection heat transfer from an isothermal wavy surface in a porous enclosure”, Int. J. Numer. Methods Fluids, Vol. 28, pp. 633–661.

Kumar B. V. R., (2000): “A study of free convection induced by a vertical wavy surface with heat flux in a porous enclosure”, Numer. Heat Transfer, Vol. 37, pp. 493–510.

Kumar B. V. R. and Shalini, (2004): “Non-Darcy free convection induced by a vertical wavy surface in a thermally stratified porous medium”, Int. J. Heat and Mass Transfer, Vol. 47, pp. 2353–2363.

Mahmud S., Das P. K. and Islam A. K. M. S., (2001): “Numerical prediction of fluid flows and heat transfer in a wavy pipe”, Int. J. Thermal Fluid Science, Vol. 10, pp. 133–138.

Mahmud S., Das P. K., Hyder N. and Islam A. K. M. S., (2002): “Free convection in an enclosure with vertical wavy walls”, Int. J. Thermal Sciences, Vol. 41, pp. 440–446.

Mamun M. M., Rahman A. and Rahman L T., (2005): “Natural convection flow from an isothermal sphere with temperature dependent thermal conductivity”, Journal of Naval Architecture and Marine Engineering, Vol. 2, pp. 53-64.

Mamun A. A., Azim N. H. M. A. and Maleque M. A., (2007): “Combined effect of conduction and viscous dissipation on MHD free convection flow along a vertical flat plate”, Journal of Naval Architecture and Marine Engineering, Vol. 4, No. 2, pp. 87-98.

Mehta K. N. and Sood S., (1992): “Transient free convection flow with temperature dependent viscosity in a fluid saturated porous media”, Int. J. Eng. Science, Vol. 30, pp. 1083-1087.

Mehta K. N. and Sood S., (1993): “Effect of temperature dependent viscosity on the free convective flow across an impermeable partition”, Int. J. Eng. Science, Vol. 31, pp. 1093-1103.

Mendez F. and Trevino C., (2000): “The conjugate conduction-natural convection heat transfer along a thin vertical plate with non-uniform internal heat generation”, Int. J. Heat and Mass Transfer, Vol. 43, pp. 2739–2748.

Molla M. M., Hossain M. A. and Yao L. S., (2004): “Natural convection flow along a vertical wavy surface with uniform surface temperature in presence of heat generation/absorption”, Int. J. Thermal Sciences, Vol. 43, pp. 157-163.

Molla M. M., Hossain M. A. and Gorla R. S. R., (2005): “Natural convection flow from an isothermal horizontal circular cylinder with temperature dependent viscosity”, Heat and Mass Transfer, Vol. 41, pp. 594-598.

Molla M. M., Taher M. A., Chowdhury M. M. K. and Hossain M. A., (2006): “Magnetohydrodynamic natural convection flow on a sphere with uniform heat flux in presence of heat generation”, Acta Mechanica, Vol. 186, pp. 75-86.

Moulic S. G. and Yao L. S., (1989): “Mixed convection along wavy surface”, ASME J. Heat Transfer, Vol. 111, pp. 974–979.

Moulic S. G. and Yao L. S., (1989): “Natural convection along a wavy surface with uniform heat flux”, ASME J. Heat Transfer, Vol. 111, pp. 1106–1108.

Munir M. S., Hossain M. A. and Pop I., (2001): “Natural convection of a viscous fluid with viscosity inversely proportional to linear function of temperature from a vertical wavy cone”, Int. J. Thermal Sciences, Vol. 40, pp. 366–371.

Munir M. S., Hossain M. A. and Pop I., (2001): “Natural convection with variable viscosity and thermal conductivity from a vertical wavy cone”, Int. J. Thermal Sciences, Vol. 40, pp. 437–443.

Murthy P. V. S. N., Kumar B. V. R. and Singh P., (1997): “Natural convection heat transfer from a horizontal wavy surface in a porous enclosure”, Numer. Heat Transfer, Part A Vol. 31, pp. 207–221.

Nasrin R. and Alim M. A., (2009): “MHD free convection flow along a vertical flat plate with thermal conductivity and viscosity depending on temperature”, Journal of Naval Architecture and Marine Engineering, Vol. 6, No. 2, pp. 72 – 83.

Necati Ö. M., (1985): “Heat Transfer”, New York, International Edition.

Palani G. and Kim K. Y., (2009): “Numerical study on a vertical plate with variable viscosity and thermal conductivity”, Arch Appl. Mech., Vol. 80, pp. 711-725.

Parveen N. and Chowdhury M. M. K., (2009): “Stability analysis of the laminar boundary layer flow”**,** GANIT- Journal of Bangladesh Mathematical Society, (ISSN 1606-3694) Vol. 29, pp. 23-34.

Parveen N. and Alim M. A., (2010a): “Natural convection of fluid with variable thermal conductivity along a uniformly heated vertical wavy surface”, Proceeding 13ACFM Asian Congress of Fluid Mechanics, Paper ID 264, pp. 839-842.

Parveen N. and Alim M. A., (2010b): “Effect of temperature dependent viscosity inversely proportional to linear function of temperature on magnetohydrodynamic natural convection flow along a vertical wavy surface”, Proceeding MARTEC-2010 International Conference on Marine Technology, Paper No. MARTEC-166, pp.329-334.

Parveen N. and Alim M. A., (2011a): “Joule heating effect on magnetohydrodynamic natural convection flow of fluid with temperature dependent viscosity inversely proportional to linear function of temperature along a vertical wavy surface”, Proceeding 3rd International Conference on Water and Flood Management, ICWFM-2011, Paper No. ICWFM –123, pp. 17-24.

Parveen N. and Alim M. A., (2011b): “Effect of temperature dependent thermal conductivity on magnetohydrodynamic natural convection flow along a vertical wavy surface”, International Journal of Energy & Technology, Vol. 3 (9), pp. 1–9.

Parveen N. and Alim M. A., (2011c): “Effect of temperature-dependent variable viscosity on magnetohydrodynamic natural convection flow along a vertical wavy surface”, International Scholarly Research Network Mechanical Engineering, Vol. 2011, Article ID 505673, pp. 1-10.

Parveen N. and Alim M. A., (2011d): “Joule heating effect on magnetohydrodynamic natural convection flow along a vertical wavy surface with viscosity dependent on temperature”, International Journal of Energy & Technology, Vol. 3 (1), pp. 1–11.

Patankar C. V., (1980): “Numerical Heat Transfer and Fluid Flow”, Hemisphere/McGraw-Hill, New York.

Pop I., Romania C. S. and Ohio N. C., (1996): “Laminar boundary layer flow of power-law fluids over wavy surfaces”, Acta Mechanica, Vol. 115, pp. 55–65.

Pozzi A. and Lupo M., (1988): “The coupling of conduction with laminar convection along a flat plate”, Int. J. Heat and Mass Transfer, Vol. 31, No. 9, pp.1807-1814.

Rahman S. U., (2000): “Natural convection along vertical wavy surfaces: an experimental study”, Chem. Eng. J., Vol. 84, pp. 587–591.

Rahman M. M., Mamun A. A., Azim M. A. and Alim M. A., (2008): “Effects of temperature dependent thermal conductivity on magnetohydrodynamic free

convection flow along a vertical flat plate with heat conduction", Nonlinear Analysis: Modelling and Control, Vol. 13 (4), pp. 513-524.

Rahman M. M. and Alim M. A., (2009): "Numerical study of magnetohydrodynamic free convective heat transfer flow along a vertical plate with temperature dependent thermal conductivity", Journal of Naval Architecture and Marine Engineering, Vol. 6, No. 1, pp. 16-29.

Raisinghania M. D., (2003): "Fluid Dynamics", S. Chand and Company Ltd., New Delhi.

Raptis A. and Kafoussius N. G., (1982): "Magnetohydrodynamic free convection flow and mass transfer through a porous medium bounded by an infinite vertical porous plate with constant heat flux", Canadian Journal of Physics, Vol. 60, No. 12, pp.1725-1729.

Rees D. A. S. and Pop I., (1994): "A note on free convection along a vertical wavy surface in a porous medium", ASME J. Heat Transfer, Vol. 116, pp. 505–508.

Rees D. A. S. and Pop I., (1994): "Free convection induced by a horizontal wavy surface in a porous medium", Fluid Dyn. Res., Vol. 14, pp. 151–166.

Rees D. A. S. and Pop I., (1995): "Free convection induced by a vertical wavy surface with uniform heat flux in a porous medium", J. Heat Transfer, Vol. 117, pp. 547–550.

Saidi C., Legay F. and Pruent B., (1987): "Laminar flow past a sinusoidal cavity", Int. J. Heat and Mass Transfer, Vol. 30, pp. 649–660.

Sparrow E. M. and Cess R. D., (1961): "The effect of magnetic field on free convection heat transfer", Int. J. Heat and Mass Transfer, Vol. 3, pp. 267-274.

Tashtoush B. and Al-Odat M., (2004): "Magnetic field effect on heat and fluid flow over a wavy surface with a variable heat flux", J. Magn. Magn. Mater, Vol. 268, pp. 357–363.

Wang C. C. and Chen C. K., (2001): "Transient force and free convection along a vertical wavy surface in micropolar fluid", Int. J. Heat and Mass Transfer, Vol. 44, pp. 3241–3251.

Wang C. C. and Chen C. K., (2002): "Forced convection in a wavy wall channel", Int. J. Heat and Mass Transfer, Vol. 45, pp. 2587–2595.

Wilks G., (1976): "Magneto-hydrodynamic free convection about a semi-infinite vertical plate in a strong cross field", J. App. Math. Phy., Vol. 27, pp. 621-631.

Yang Y.-T., Chen C. K. and Lin M.-T., (1996): “Natural convection of non-Newtonian fluids along a wavy vertical plate including the magnetic field effect”, Int. J. Heat and Mass Transfer, Vol. 39, pp. 2831–2842.

Yao L.S., (1983): “Natural convection along a vertical wavy surface”, ASME J. Heat Transfer, Vol. 105, pp. 465–468.

Yao L. S., (1988): “A note on Prandtl’s transposition theorem”, ASME J. Heat Transfer, Vol. 110, pp. 503–507.

Yao L. S., (2006): “Natural convection along a vertical complex wavy surface”, Int. J. Heat and Mass Transfer, Vol. 49, pp. 281–286.

Appendix

Implicit Finite Difference Method (IFDM)

It is assumed that $f_j^{n-1}, u_j^{n-1}, v_j^{n-1}, g_j^{n-1}, p_j^{n-1}$, for $0 \le j \le J$ are known. Then equations (2.79) to (2.90) form a system of (5*J*+5) non linear equations for the solutions of the (5*J*+5) unknowns $\left(f_j^n, u_j^n, v_j^n, g_j^n, p_j^n\right)$, j = 0, 1, 2, 3,……*J*. These non-linear systems of algebraic equations are to be linearized by Newton's Quassy linearization method. The iterates $\left(f_j^i, u_j^i, v_j^i, g_j^i, p_j^i\right)$, i = 0, 1, 2, 3……*N* are defined with initial values equal those at the previous *x*-station (which is usually the best initial available). For the higher iterates the following forms can be written

$$f_j^{(i+1)} = f_j^i + \delta f_j^i \tag{A1}$$

$$u_j^{(i+1)} = u_j^i + \delta u_j^i \tag{A2}$$

$$v_j^{(i+1)} = v_j^i + \delta v_j^i \tag{A3}$$

$$g_j^{(i+1)} = g_j^i + \delta g_j^i \tag{A4}$$

$$p_j^{(i+1)} = p_j^i + \delta p_j^i \tag{A5}$$

Now by substituting the right hand sides of the above equations in place of f_j^n, u_j^n, v_j^n and g_j^n in equations (2.83)-(2.85) and in equations (2.90) and (2.92) dropping the terms that are quadratic in $\delta f_j^i, \delta u_j^i, \delta v_j^i$ and δp_j^i, then take the following linear system of algebraic form

$$\frac{f_j^{(i)} - f_{j-1}^{(i)}}{h_j} + \frac{\delta f_j^{(i)} - \delta f_{j-1}^{(i)}}{h_j} = u_{j-\frac{1}{2}}^{(i)} + \delta u_{j-\frac{1}{2}}^{(i)} = \frac{1}{2}\left\{u_j^{(i)} + \delta u_j^{(i)} + u_{j-1}^{(i)} + \delta u_{j-1}^{(i)}\right\}$$

$$f_j^{(i)} + \delta f_j^{(i)} - f_{j-1}^{(i)} - \delta f_{j-1}^{(i)} = \frac{h_j}{2}\left\{u_j^{(i)} + \delta u_j^{(i)} + u_{j-1}^{(i)} + \delta u_{j-1}^{(i)}\right\}$$

$$\delta f_j^{(i)} - \delta f_{j-1}^{(i)} - \frac{h_j}{2}\left(\delta u_j^{(i)} + \delta u_{j-1}^{(i)}\right) = (r_1)_j \tag{A6}$$

$$\delta u_j^{(i)} - \delta u_{j-1}^{(i)} - \frac{h_j}{2}\left(\delta v_j^{(i)} + \delta v_{j-1}^{(i)}\right) = (r_4)_j \tag{A7}$$

$$\delta g_j^{(i)} - \delta g_{j-1}^{(i)} - \frac{h_j}{2}\left(\delta p_j^{(i)} + \delta p_{j-1}^{(i)}\right) = (r_5)_j \tag{A8}$$

where, $(r_1)_j = f_{j-1}^{(i)} - f_j^{(i)} + h_j u_{j-1/2}^{(i)}$

$(r_4)_j = u_{j-1}^{(i)} - u_j^{(i)} + h_j v_{j-1/2}^{(i)}$

$(r_5)_j = g_{j-1}^{(i)} - g_j^{(i)} + h_j p_{j-1/2}^{(i)}$

Then equation (2.90) becomes,

$$\begin{aligned}
&(P_1T)_{j-1/2}^{n} h_j^{-1}\left(v_j^{(i)} + \delta v_j^{(i)} - v_{j-1}^{(i)} - \delta v_{j-1}^{(i)}\right) + \left\{(P_2)_{j-1/2}^{n} + \alpha_n\right\}\left\{(fv)_{j-1/2}^{(i)} + \delta(fv)_{j-1/2}^{(i)}\right\} \\
&- \left\{(P_3)_{j-1/2}^{n} + \alpha_n\right\}\left\{(u^2)_{j-1/2}^{(i)} + \delta(u^2)_{j-1/2}^{(i)}\right\} + (P_4)_{j-1/2}^{n}\left\{g_{j-1/2}^{(i)} + \delta g_{j-1/2}^{(i)}\right\} \\
&- (P_5)_{j-1/2}^{n}\left\{(u)_{j-1/2}^{(i)} + \delta(u)_{j-1/2}^{(i)}\right\} + (P_6)_{j-1/2}^{n}\left\{(pv)_{j-1/2}^{(i)} + \delta(pv)_{j-1/2}^{(i)}\right\} \\
&+ \alpha_n\left\{f_{j-1/2}^{(i)} + \delta f_{j-1/2}^{(i)}\right\} v_{j-1/2}^{n-1} - \alpha_n\left(v_{j-1/2}^{(i)} + \delta v_{j-1/2}^{(i)}\right) f_{j-1/2}^{n-1} = R_{j-1/2}^{n-1}
\end{aligned}$$

$$\begin{aligned}
&(P_1T)_{j-1/2}^{n} h_j^{-1}\left(v_j^{(i)} + \delta v_j^{(i)} - v_{j-1}^{(i)} - \delta v_{j-1}^{(i)}\right) \\
&+ \left\{(P_2)_{j-1/2}^{n} + \alpha_n\right\}\left\{(fv)_{j-1/2}^{(i)} + \frac{1}{2}\left(f_j^{(i)}\delta v_j^{(i)} + v_j^{(i)}\delta f_j^{(i)} + f_{j-1}^{(i)}\delta v_{j-1}^{(i)} + v_{j-1}^{(i)}\delta f_{j-1}^{(i)}\right)\right\} \\
&- \left\{(P_3)_{j-1/2}^{n} + \alpha_n\right\}\left\{(u^2)_{j-1/2}^{(i)} + u_j^{(i)}\delta u_j^{(i)} + u_{j-1}^{(i)}\delta u_{j-1}^{(i)}\right\} \\
&+ (P_4)_{j-1/2}^{n}\left\{g_{j-1/2}^{(i)} + \frac{1}{2}\left(\delta g_j^{(i)} + \delta g_{j-1}^{(i)}\right)\right\} - (P_5)_{j-1/2}^{n}\left\{(u)_{j-1/2}^{(i)} + \frac{1}{2}\left(\delta(u)_j^{(i)} + \delta(u)_{j-1}^{(i)}\right)\right\} \\
&+ (P_6)_{j-1/2}^{n}\left\{(pv)_{j-1/2}^{(i)} + \frac{1}{2}\left(p_j^{(i)}\delta v_j^{(i)} + v_j^{(i)}\delta p_j^{(i)} + p_{j-1}^{(i)}\delta v_{j-1}^{(i)} + v_{j-1}^{(i)}\delta p_{j-1}^{(i)}\right)\right\} \\
&+ \alpha_n\left\{f_{j-1/2}^{(i)} + \frac{1}{2}\left(\delta f_j^{(i)} + \delta f_{j-1}^{(i)}\right)\right\} v_{j-1/2}^{n-1} \\
&- \alpha_n\left(v_{j-1/2}^{(i)} + \frac{1}{2}\left(\delta v_j^{(i)} + \delta v_{j-1}^{(i)}\right)\right) f_{j-1/2}^{n-1} = R_{j-1/2}^{n-1}
\end{aligned}$$

$$\begin{aligned}
&\Rightarrow (s_1)_j \delta v_j^{(i)} + (s_2)_j \delta v_{j-1}^{(i)} + (s_3)_j \delta f_j^{(i)} + (s_4)_j \delta f_{j-1}^{(i)} + (s_5)_j \delta u_j^{(i)} \\
&+ (s_6)_j \delta u_{j-1}^{(i)} + (s_7)_j \delta g_j^{(i)} + (s_8)_j \delta g_{j-1}^{(i)} + (s_9)_j \delta p_j^{(i)} + (s_{10})_j \delta p_{j-1}^{(i)} = (r_2)_j
\end{aligned} \tag{A9}$$

$$
\begin{aligned}
(r_2)_j \;=\; & R^{n-1}_{j-1/2} - (P_1T)^n_{j-1/2} h_j^{-1}\left(v_j^{(i)} - v_{j-1}^{(i)}\right) - \left\{(P_2)^n_{j-1/2} + \alpha_n\right\}(fv)^{(i)}_{j-1/2} \\
& + \left\{(P_3)^n_{j-1/2} + \alpha_n\right\}\left(u^2\right)^{(i)}_{j-1/2} - (P_4)^n_{j-1/2}\, g^{(i)}_{j-1/2} + (P_5)^n_{j-1/2}\, u^{(i)}_{j-1/2} \\
& - (P_6)^n_{j-1/2}(pv)^{(i)}_{j-1/2} - \alpha_n\left(f^{(i)}_{j-1/2} v^{n-1}_{j-1/2} - v^{(i)}_{j-1/2} f^{n-1}_{j-1/2}\right)
\end{aligned} \tag{A10}
$$

Thus the coefficients of momentum equation are:

$$(s_1)_j = h_j^{-1}(P_1T)^n_{j-1/2} + \frac{(P_2)^n_{j-1/2} + \alpha_n}{2} f_j^{(i)} + \frac{1}{2}(P_6)^n_{j-1/2}\, p_j^{(i)} - \frac{\alpha_n}{2} f^{n-1}_{j-1/2} \tag{A11}$$

$$(s_2)_j = -h_j^{-1}(P_1T)^n_{j-1/2} + \frac{(P_2)^n_{j-1/2} + \alpha_n}{2} f_{j-1}^{(i)} + \frac{1}{2}(P_6)^n_{j-1/2}\, p_{j-1}^{(i)} - \frac{\alpha_n}{2} f^{n-1}_{j-1/2} \tag{A12}$$

$$(s_3)_j = \frac{(P_2)^n_{j-1/2} + \alpha_n}{2} v_j^{(i)} + \frac{\alpha_n}{2} v^{n-1}_{j-1/2} \tag{A13}$$

$$(s_4)_j = \frac{(P_2)^n_{j-1/2} + \alpha_n}{2} v_{j-1}^{(i)} + \frac{\alpha_n}{2} v^{n-1}_{j-1/2} \tag{A14}$$

$$(s_5)_j = -\left\{(P_3)^n_{j-1/2} + \alpha_n\right\} u_j^{(i)} - \frac{(P_5)^n_{j-1/2}}{2} \tag{A15}$$

$$(s_6)_j = -\left\{(P_3)^n_{j-1/2} + \alpha_n\right\} u_{j-1}^{(i)} - \frac{(P_5)^n_{j-1/2}}{2} \tag{A16}$$

$$(s_7)_j = \frac{(P_4)^n_{j-1/2}}{2} \tag{A17}$$

$$(s_8)_j = \frac{(P_4)^n_{j-1/2}}{2} \tag{A18}$$

$$(s_9)_j = \frac{(P_6)^n_{j-1/2}}{2} v_j^{(i)} \tag{A19}$$

$$(s_{10})_j = \frac{(P_6)^n_{j-1/2}}{2} v_{j-1}^{(i)} \tag{A20}$$

Similarly by using the equations (A1) to (A5), then the equation (2.95) can be written as

$$\frac{1}{\mathrm{Pr}} h_j^{-1} (P_1)_{j-1/2}^n \left(p_j^{(i)} + \delta\, p_j^{(i)} - p_{j-1}^{(i)} - \delta p_{j-1}^{(i)} \right) + \left\{ (P_2)_{j-1/2}^n + \alpha_n \right\} \left\{ (fp)_{j-1/2}^{(i)} + \delta (fp)_{j-1/2}^{(i)} \right\}$$
$$- \alpha_n \left\{ (ug)_{j-1/2}^{(i)} + \delta (ug)_{j-1/2}^{(i)} \right\} + \alpha_n \left\{ \left(u_{j-1/2}^{(i)} + \delta\, u_{j-1/2}^{(i)} \right) g_{j-1/2}^{n-1} - u_{j-1/2}^{n-1} \left(g_{j-1/2}^{(i)} + \delta\, g_{j-1/2}^{(i)} \right) \right\}$$
$$- \alpha_n \left\{ \left(p_{j-1/2}^{(i)} + \delta\, p_{j-1/2}^{(i)} \right) f_{j-1/2}^{n-1} - p_{j-1/2}^{n-1} \left(f_{j-1/2}^{(i)} + \delta\, f_{j-1/2}^{(i)} \right) \right\} = T_{j-1/2}^{n-1}$$

$$\Rightarrow \frac{1}{\mathrm{Pr}} h_j^{-1} (P_1)_{j-1/2}^n \left(p_j^{(i)} + \delta\, p_j^{(i)} - p_{j-1}^{(i)} - \delta p_{j-1}^{(i)} \right)$$
$$+ \left\{ (P_2)_{j-1/2}^n + \alpha_n \right\} \left\{ (fp)_{j-1/2}^{(i)} + \frac{1}{2} \left\{ \delta (fp)_j^{(i)} + \delta (fp)_{j-1}^{(i)} \right\} \right\}$$
$$- \alpha_n \left\{ (ug)_{j-1/2}^{(i)} + \frac{1}{2} \left\{ \delta (ug)_j^{(i)} + \delta (ug)_{j-1}^{(i)} \right\} \right\} + \alpha_n \left\{ u_{j-1/2}^{(i)} + \frac{1}{2} \left(\delta\, u_j^{(i)} + \delta\, u_{j-1}^{(i)} \right) \right\} g_{j-1/2}^{n-1}$$
$$- \alpha_n \left\{ g_{j-1/2}^{(i)} + \frac{1}{2} \left(\delta\, g_j^{(i)} + \delta\, g_{j-1}^{(i)} \right) \right\} u_{j-1/2}^{n-1}$$
$$- \alpha_n \left\{ p_{j-1/2}^{(i)} + \frac{1}{2} \left(\delta\, p_j^{(i)} + \delta\, p_{j-1}^{(i)} \right) \right\} f_{j-1/2}^{n-1} + \alpha_n \left\{ f_{j-1/2}^{(i)} + \frac{1}{2} \left(\delta\, f_j^{(i)} + \delta\, f_{j-1}^{(i)} \right) \right\} p_{j-1/2}^{n-1} = T_{j-1/2}^{n-1}$$

$$(t_1)_j\, \delta\, p_j^{(i)} + (t_2)_j \delta\, p_{j-1}^{(i)} + (t_3)_j\, \delta\, f_j^{(i)} + (t_4)_j \delta\, f_{j-1}^{(i)} + (t_5)_j\, \delta\, u_j^{(i)}$$
$$+ (t_6)_j\, \delta\, u_{j-1}^{(i)} + (t_7)_j \delta\, g_j^{(i)} + (t_8)_j \delta\, g_{j-1}^{(i)} + (t_9)_j \delta\, v_j^{(i)} + (t_{10})_j \delta\, v_{j-1}^{(i)} = (r_3)_j \quad \text{(A21)}$$

$$\Rightarrow (r_3)_j = T_{j-1/2}^{n-1} - \frac{1}{\mathrm{Pr}} h_j^{-1} (P_1)_{j-1/2}^n \left(p_j^{(i)} - p_{j-1}^{(i)} \right) - \left\{ (P_2)_{j-1/2}^n + \alpha_n \right\} (fp)_{j-1/2}^{(i)}$$
$$+ \alpha_n (ug)_{j-1/2}^{(i)} + \alpha_n \left(g_{j-1/2}^{(i)} u_{j-1/2}^{n-1} - g_{j-1/2}^{n-1} u_{j-1/2}^{(i)} \right) + \alpha_n \left(p_{j-1/2}^{(i)} f_{j-1/2}^{n-1} - p_{j-1/2}^{n-1} f_{j-1/2}^{(i)} \right) \quad \text{(A22)}$$

The coefficients of energy equation are:

$$(t_1)_j = \frac{1}{\mathrm{Pr}} h_j^{-1} (P_1)_{j-1/2}^n + \frac{(P_2)_{j-1/2}^n + \alpha_n}{2} f_j^{(i)} - \frac{\alpha_n}{2} f_{j-1/2}^{n-1} \quad \text{(A23)}$$

$$(t_2)_j = -\frac{1}{\mathrm{Pr}} h_j^{-1} (P_1)_{j-1/2}^n + \frac{(P_2)_{j-1/2}^n + \alpha_n}{2} f_{j-1}^{(i)} - \frac{\alpha_n}{2} f_{j-1/2}^{n-1} \quad \text{(A24)}$$

$$(t_3)_j = \frac{(P_2)_{j-1/2}^n + \alpha_n}{2} p_j^{(i)} + \frac{\alpha_n}{2} p_{j-1/2}^{n-1} \quad \text{(A25)}$$

$$(t_4)_j = \frac{(P_2)_{j-1/2}^n + \alpha_n}{2} p_{j-1}^{(i)} + \frac{\alpha_n}{2} p_{j-1/2}^{n-1} \quad \text{(A26)}$$

$$(t_5)_j = -\frac{\alpha_n}{2} g_j^{(i)} + \frac{\alpha_n}{2} g_{j-1/2}^{n-1} \tag{A27}$$

$$(t_6)_j = -\frac{\alpha_n}{2} g_{j-1}^{(i)} + \frac{\alpha_n}{2} g_{j-1/2}^{n-1} \tag{A28}$$

$$(t_7)_j = -\frac{\alpha_n}{2} u_j^{(i)} - \frac{\alpha_n}{2} u_{j-1/2}^{n-1} \tag{A29}$$

$$(t_8)_j = -\frac{\alpha_n}{2} u_{j-1}^{(i)} - \frac{\alpha_n}{2} u_{j-1/2}^{n-1} \tag{A30}$$

$$(t_9)_j = 0 \tag{A31}$$

$$(t_{10})_j = 0 \tag{A32}$$

The boundary conditions (2.96) becomes

$$\begin{aligned} &\delta f_0^n = 0, \qquad \delta u_0^n = 0, \ \delta g_0^n = 0 \\ &\delta u_j^n = 0, \qquad \delta g_j^n = 0 \end{aligned} \tag{A33}$$

which just express the requirement for the boundary conditions to remain during the iteration process. Now the system of linear equations (A6)-(A9) and (A21) together with the boundary conditions (A33) can be written in matrix or vector form, where the coefficient matrix has a block tri-diagonal structure. The whole procedure, namely reduction to first order followed by central difference approximations, Newton's Quasi-linearization method and the block Thomas algorithm, is well known as the Keller-box method.

Table A1: Skin friction coefficient C_{fx} and the rate of heat transfer in terms of Nusselt number Nu_x for different values of Prandtl number (Pr = 0.73, 7.0, 100) while $\alpha = 0.3$, $M = 0.5$ and $\varepsilon = 5.0$.

x	Skin friction coefficient C_{fx}			Rate of heat transfer Nu_x		
	Pr = 0.73	Pr = 7.0	Pr = 100	Pr = 0.73	Pr = 7.0	Pr = 100
0.00	1.00692	0.62979	0.33300	0.23573	0.44871	0.89761
0.50	1.54688	0.99193	0.53835	0.25070	0.48832	0.99839
1.00	0.91916	0.58519	0.31729	0.22614	0.43981	0.89799
1.50	1.46536	0.96150	0.53097	0.23824	0.47574	0.98663
2.00	0.89141	0.57531	0.31483	0.22026	0.43248	0.89106
2.50	1.41516	0.94320	0.52651	0.23206	0.46783	0.97934
3.00	0.87162	0.56829	0.31308	0.21597	0.42731	0.88625
3.50	1.37827	0.92949	0.52314	0.22742	0.46194	0.97390
4.00	0.85588	0.56271	0.31170	0.21259	0.42319	0.88244
4.50	1.34874	0.91835	0.52038	0.22366	0.45712	0.96945
5.00	0.84266	0.55804	0.31053	0.20978	0.41974	0.87924
5.50	1.32400	0.90888	0.51801	0.22048	0.45302	0.96564
6.00	0.83118	0.55398	0.30951	0.20736	0.41674	0.87646
6.50	1.30269	0.90061	0.51593	0.21774	0.44942	0.96228
7.00	0.82099	0.55038	0.30860	0.20523	0.41405	0.87398
7.50	1.28394	0.89325	0.51405	0.21533	0.44620	0.95927
8.00	0.81181	0.54713	0.30777	0.20332	0.41163	0.87174
8.50	1.26718	0.88659	0.51234	0.21317	0.44327	0.95652
9.00	0.80343	0.54417	0.30701	0.20158	0.40941	0.86968

Table A2: Comparison of skin friction coefficient C_{fx} and the rate of heat transfer in terms of Nusselt number Nu_x against x for the variation of Prandtl number Pr with and without effects of magnetic parameter M and viscosity parameter ε while $\alpha = 0.3$.

Pr	$\varepsilon = 0.0$, $M = 0.0$		$\varepsilon = 0.0$, $M = 0.5$		$\varepsilon = 5.0$, $M = 0.0$		$\varepsilon = 5.0$, $M = 0.5$	
	C_{fx}	Nu_x	C_{fx}	Nu_x	C_{fx}	Nu_x	C_{fx}	Nu_x
0.7	0.97482	0.34175	0.87097	0.31346	1.69448	0.26456	1.55731	0.24755
1.74	0.84656	0.46767	0.76566	0.43181	1.42192	0.34631	1.32449	0.32597
3.0	0.76895	0.55765	0.70032	0.51737	1.26523	0.40490	1.18768	0.38310
7.0	0.65372	0.72178	0.60129	0.67456	1.04514	0.51175	0.99193	0.48832

Table A3: Skin friction coefficient C_{fx} and the rate of heat transfer in terms of Nusselt number Nu_x for variation of thermal conductivity parameter (γ = 0.0, 4.0, 10.0) while α = 0.3, M = 0.8 and Pr = 1.0.

x	Skin friction coefficient C_{fx}			Rate of heat transfer Nu_x		
	γ = 0.0	γ = 4.0	γ = 10.0	γ = 0.0	γ = 4.0	γ = 10.0
0.00	0.56194	0.68937	0.74304	0.34186	0.77061	1.21257
0.50	0.78350	0.93324	0.99073	0.33933	0.75934	1.17930
1.00	0.46597	0.55867	0.59607	0.30903	0.69889	1.09245
1.50	0.70729	0.82527	0.86863	0.31277	0.69200	1.08479
2.00	0.43912	0.51847	0.54747	0.29235	0.65746	1.03332
2.50	0.66610	0.76742	0.80223	0.29760	0.65660	1.03746
3.00	0.42049	0.49063	0.51455	0.28100	0.62832	0.99521
3.50	0.63730	0.72719	0.75638	0.28653	0.62992	1.00142
4.00	0.40622	0.46942	0.48972	0.27222	0.60615	0.96803
4.50	0.61508	0.69640	0.72146	0.27781	0.60882	0.97364
5.00	0.39463	0.45236	0.46994	0.26501	0.58815	0.94689
5.50	0.59702	0.67154	0.69342	0.27062	0.59160	0.95201
6.00	0.38487	0.43814	0.45360	0.25891	0.57309	0.92976
6.50	0.58180	0.65077	0.67013	0.26451	0.57716	0.93487
7.00	0.37644	0.42599	0.43976	0.25362	0.56024	0.91558
7.50	0.56868	0.63298	0.65031	0.25919	0.56483	0.92104
8.00	0.36902	0.41542	0.42780	0.24896	0.54915	0.90372
8.50	0.55716	0.61748	0.63313	0.25450	0.55414	0.90969
9.00	0.36241	0.40609	0.41731	0.24481	0.53947	0.89371

Table A4: Skin friction coefficient C_{fx} and the rate of heat transfer in terms of Nusselt number Nu_x against x for the variation of Prandtl number Pr, magnetic parameter M and thermal conductivity parameter γ with α = 0.2.

Pr	M = 0.0, γ = 0.0		M = 0.0, γ = 2.0		M = 0.8, γ = 0.0		M = 0.8, γ = 2.0	
	C_{fx}	Nu_x	C_{fx}	Nu_x	C_{fx}	Nu_x	C_{fx}	Nu_x
0.73	0.96181	0.35267	1.10027	0.59707	0.81128	0.32999	0.91383	0.55883
1.73	0.83837	0.47511	0.97802	0.82424	0.72029	0.44434	0.82894	0.77102
4.24	0.71227	0.63141	0.84609	1.11656	0.62331	0.59015	0.73142	1.04404
7.00	0.64567	0.73367	0.77363	1.30780	0.57038	0.68546	0.67555	1.22245

Table A5: Skin friction coefficient C_{fx} and the rate of heat transfer in terms of Nusselt number Nu_x for variation of Joule heating parameter (J = 0.0, 0.06, 0.15) with other fixed controlling parameters α = 0.3, M = 0.02, γ = 4.0, ε = 5.0 and Pr = 0.5.

x	Skin friction coefficient C_{fx}			Rate of heat transfer Nu_x		
	J = 0.0	J = 0.06	J = 0.15	J = 0.0	J = 0.06	J = 0.15
0.00	1.33816	1.33816	1.33816	0.52014	0.52015	0.52015
0.50	2.27275	2.27550	2.27963	0.56347	0.55958	0.55372
1.00	1.38357	1.38770	1.39395	0.51095	0.50376	0.49284
1.50	2.23131	2.24309	2.26100	0.55161	0.53438	0.50794
2.00	1.38659	1.39829	1.41620	0.51747	0.49615	0.46302
2.50	2.20677	2.23119	2.26890	0.54714	0.51157	0.45559
3.00	1.39261	1.41435	1.44818	0.52008	0.47983	0.41539
3.50	2.18803	2.22784	2.29044	0.54430	0.48620	0.39196
4.00	1.39718	1.43103	1.48473	0.52130	0.45793	0.35296
4.50	2.17388	2.23152	2.32402	0.54261	0.45810	0.31626
5.00	1.40019	1.44797	1.52539	0.52181	0.43143	0.27603
5.50	2.16285	2.24064	2.36825	0.54159	0.42690	0.22707
6.00	1.40216	1.46556	1.57060	0.52200	0.40084	0.18399
6.50	2.15384	2.25402	2.42220	0.54085	0.39224	0.12276
7.00	1.40351	1.48412	1.62086	0.52210	0.36636	0.07566
7.50	2.14618	2.27093	2.48546	0.54025	0.35389	0.00154
8.00	1.40444	1.50386	1.67657	0.52218	0.32799	-0.05059
8.50	2.13948	2.29098	2.55794	0.53970	0.31166	-0.13852
9.00	1.40510	1.52488	1.73810	0.52225	0.28562	-0.19670
9.50	2.13353	2.31392	2.63974	0.53920	0.26538	-0.29953
10.0	1.40556	1.54728	1.80579	0.52232	0.23908	-0.36483